PONTIFICIA UNIVERSIDAD CATÓLICA DEL PERÚ

Escuela de Posgrado

Estudio del proceso de cristalización y polimorfismo de la manteca de cacao en la cadena de fabricación de chocolate oscuro a partir de cacao (*Theobroma cacao* L.) variedad Criollo

Tesis para obtener el grado académico de Doctor en Ingeniería

que presenta:

Efraín Manuelito Castro Alayo

Asesor:

Fiorella Patricia Cardenas Toro

Lima, 2022

DEDICATORIA

A mi esposa, Shenifer, por su apoyo constante en todo lo que me propongo. Continuamos juntos en la lucha por lograr nuestras metas.

A mi hija Lucía, esperando que este trabajo sea un ejemplo de esfuerzo y dedicación para lograr lo que se proponga en la vida.

A mis padres Vicente y Susana, a quienes agradeceré eternamente por formarme como persona y profesional.

AGRADECIMIENTO

A Dios y la Virgen María por darme la oportunidad de despertar cada día para poder compartir con mi familia y amigos.

A la Dra. Fiorella Patricia Cárdenas Toro por todo el apoyo brindado a lo largo del proceso de desarrollo del presente trabajo. Su asesoramiento fue esencial para diseñar los experimentos con criterio científico y obtener resultados factibles de ser publicados. Espero que más allá de esta tesis sigamos trabajando juntos por lo que nos apasiona: la ingeniería.

Al Dr. Juan Tejedo, por su apoyo incondicional y las facilidades brindadas para el entrenamiento en la metodología de Microscopía Confocal Raman en la Universidad Pablo de Olavide – Sevila, España. Seguimos siendo amigos y continuamos en la búsqueda de nuevas investigaciones como parte de un excelente equipo.

A la Dra. Ana Paula Zaderenko, especialista en Microscopía Confocal Raman, sus conocimientos y amplia experiencia fueron fundamentales para la identificación y caracterización de las muestras estudiadas.

A Ilse Cayo, Llisela Torrejón, Marleni Medina, César Balcázar, Lucas Muñóz, Alexa Pajuelo y Yordana Chacón; quienes apoyaron en la obtención de los resultados experimentales y gestión de las actividades que llevaron a la exitosa culminación de la presente tesis. Su apoyo fue muy importante para el cumplimiento de los objetivos.

RESUMEN

El objetivo general de la presente tesis fue estudiar el proceso de cristalización y polimorfismo de la manteca de cacao (MC) en la cadena de fabricación de chocolate oscuro a partir de cacao (*Theobroma cacao* L.) variedad Criollo. La revisión de la literatura demostró que en la cadena de fabricación de chocolates, la fermentación del cacao es la etapa más importante porque genera el perfil aromático; pero, puede influir en la cristalización y polimorfismo de la MC y por tanto en la cadena de fabricación del chocolate, hipótesis que fue establecida a partir del análisis bibliométrico. Para la evaluación de la cristalización, polimorfismo y miscibilidad de la MC se usó Calorimetría Diferencial de Barrido (DSC) y Microscopía Confocal Raman (CRM). Durante la fermentación espontánea se pudo notar que el cacao alcanzó su temperatura más alta (45,35 °C) a los siete días, periodo durante el cual pudo determinarse los parámetros cinéticos de cristalización de la MC en el interior del grano usando DSC y la teoría de Avrami. Se encontró que durante el proceso de fermentación se produjeron núcleos de cristales metaestables (β_1' y β_2') de MC, los cuales crecieron de manera espontánea o esporádica, en forma de plato, varillas o agujas. La técnica multivariada k-means identificó patrones que dividieron la fermentación en dos etapas: en la primera (0 – 3 días), la MC cristalizó en 15,78 minutos y en la segunda (4 – 7 días) cristalizó en 17,88 minutos, por ello se propuso un proceso de fermentación de solo tres días para cacao Criollo. Para la fabricación de chocolate fue necesario implementar una etapa previa que consistió en analizar la miscibilidad de la MC con aceite de coco (CNO) y aceite de sacha inchi (SIO). Entonces, se preparó equivalentes de manteca de cacao (CBE) mezclando la MC con cada uno de los aceites vegetales en diferentes concentraciones. Los espectros Raman mostraron que SIO se diferenció de CNO y MC por su alta proporción de insaturación, evidenciado por la alta intensidad del pico a 1662,7 cm^{-1}. Los picos a 1745,4 cm^{-1} y 1733,8 cm^{-1} en la MC evidenciaron la existencia de las formas β_2' y β_1'. Las imágenes químicas Raman y la técnica Resolución de Curva Multivariada-Mínimos Cuadrados Alternantes generaron mapas de distribución e histogramas para determinar cualitativamente la miscibilidad del aceite vegetal con la MC, mientras que con

i

Rstudio se calculó la desviación estándar relativa para determinar la miscibilidad de manera cuantitativa. Ambas técnicas mostraron que mezclar MC con CNO en proporciones de 55/45 y MC con SIO en proporciones de 65/35 pueden generar CBE con alta miscibilidad, la cual se reduce al incrementar la proporción de MC. La cinética de cristalización isotérmica develó que SIO cristaliza a temperaturas inferiores a cero grados y al igual que CNO, sus propiedades térmicas se modificaron cuando fueron mezclados con la MC para formar su correspondiente CBE. CNO cristalizó más rápido que la MC, pero al mezclarse con ésta, su velocidad de cristalización y entalpía de fusión se redujeron. Finalmente, estos CBEs fueron utilizados en combinación con el régimen de temperado para producir dos tipos de chocolates oscuros (Ch-SIO y Ch-CNO), evaluando su cinética de cristalización, polimorfismo, propiedades físicas y térmicas del producto final. La velocidad de cristalización de la MC incrementó como consecuencia de los CBE y temperado, obteniendo una cristalización más rápida en el Ch-SIO (7,08 ± 0,15 min) que en el Ch-CNO (7,25 ± 0,18 min). Ambos factores produjeron chocolates con altos porcentajes de forma β_2 (92,56 ± 1,49% en Ch-SIO y 90,3 ± 1,18% en Ch-CNO) que superan los valores establecidos en literatura. La presencia de esta forma polimórfica fue corroborada con los bajos valores del índice de blancura (27,55 ± 0,22 – 28,73 ± 0,54). Las propiedades físicas y térmicas de los chocolates cambiaron dentro de valores aceptables.

Palabras clave: Chocolate oscuro, Cinética, Cristalización, Espectroscopía confocal Raman, Manteca de cacao, Polimorfismo.

ABSTRACT

The general objective of this thesis was to study the process of crystallization and polymorphism of cocoa butter (CB) in the manufacturing chain of dark chocolate from cocoa (*Theobroma cacao* L.) Criollo variety. The literature review showed that in the chocolate manufacturing chain, cocoa fermentation is the most important stage because it generates the aromatic profile; but, it can influence the crystallization and polymorphism of CB and the chocolate manufacturing chain, a hypothesis that was established from the bibliometric analysis. Differential Scanning Calorimetry (DSC) and Confocal Raman Microscopy (CRM) were used for the evaluation of CB crystallization, polymorphism and miscibility. During the spontaneous fermentation it was possible to notice that the cocoa reached its highest temperature (45.35 °C) after seven days, a period during which the kinetic parameters of CB crystallization inside the bean could be determined using DSC and Avrami's theory. It was found that during the fermentation process nuclei of metastable crystals (β_1' y β_2') of CB were produced, which grew spontaneously or sporadically, in the form of plates, rods or needles. The multivariate k-means technique identified patterns that divided the fermentation into two stages: in the first (0-3 days), the cocoa butter crystallized in 15.78 minutes and in the second (4-7 days) it crystallized in 17. 88 minutes, for this reason a fermentation process of only three days for Criollo cocoa was proposed. For the manufacture of chocolate, it was necessary to implement a previous stage that consisted of analyzing the miscibility of cocoa butter with coconut oil (CNO) and sacha inchi oil (SIO). Then, cocoa butter equivalents (CBE) were prepared by mixing the CM with each of the vegetable oils at different concentrations. Raman spectra showed that SIO differed from CNO and CB by its high proportion of unsaturation, evidenced by the high intensity of the peak at 1662.7 cm^{-1}. The peaks at 1745.4 cm^{-1} and 1733.8 cm^{-1} in the CB evidenced the existence of the β_2' and β_1' forms. Raman chemical images and the Multivariate Curve Resolution-Alternating Least Squares technique generated distribution maps and histograms to determine qualitatively the miscibility of vegetable oil with CB, while with Rstudio the relative standard deviation was calculated to determine the miscibility quantitatively. Both techniques showed that mixing CB with CNO in proportions of 55/45 and CB with SIO in proportions of 65/35 can

generate CBE with high miscibility, which is reduced by increasing the proportion of CB. Isothermal crystallization kinetics revealed that SIO crystallizes at temperatures below zero degrees and, like CNO, its thermal properties were modified when mixed with CB to form its corresponding CBE. CNO crystallized faster than CB, but when mixed with it, its rate of crystallization and melting enthalpy were reduced. Finally, these CBEs were used in combination with the tempering regimen to produce two types of dark chocolates (Ch-SIO and Ch-CNO), evaluating the crystallization kinetics, polymorphism, physical and thermal properties of the final product. The crystallization rate of CB increased as a consequence of the CBE and tempering, obtaining a faster crystallization in the Ch-SIO (7.08 ± 0.15 min) than in the Ch-CNO (7.25 ± 0.18min). Both factors produced chocolates with high percentages of β_2 form (92.56 ± 1.49% in Ch-SIO and 90.3 ± 1.18% in Ch-CNO) that exceed the values established in the literature. The presence of this polymorphic form was corroborated by the low values of the whiteness index (27.55 ± 0.22 – 28.73 ± 0.54). The physical and thermal properties of the chocolates changed within acceptable values.

Keywords: Dark chocolate, Kinetics, Crystallization, confocal Raman spectroscopy, Cocoa butter, Polymorphism.

ÍNDICE

ÍNDICE DE TABLAS

ÍNDICE DE FIGURAS

ÍNDICE DE ANEXOS

LISTA DE ABREVIATURAS

MC	Manteca de cacao
CNO	Coconut oil
SIO	Sacha inchi oil
DSC	Differential Scanning Calorimetry
CRM	Confocal Raman Microscopy
MCR–ALS	Multivariate Curve Resolution–Alternating Least Squares
CB	Cocoa butter
CBE	Cocoa butter equivalent
Ch-SIO	Chocolate con aceite de sacha inchi
Ch-CNO	Chocolate con aceite de coco
AOAC	Association of Official Agricultural Chemists
mEq NaOH	Miliequivalentes de hidróxido de sodio
POP	1,3-dipalmitoyl-2-oleoylglycerol
POS	*rac*-palmitoil-stearoil-2-oleoil-glicerol
SOS	1,3-distearoil-2-oleoilglicerol
Ppb	Partes por billon
µg/kg	Microgramos por kilo
TAG	Triacilglicerol
LAB	Lactic acid bacteria
AAB	Acetic acid bacteria
TMP	Tetramethyl pyrazine
TrMP	Trimethyl pyrazine
APROCAM	Asociación de Productores Cafetaleros y Cacaoteros de Amazonas
HPLC	High Performance Liquid Chromatography
JAOCS	Journal of the American Oil Chemists´ Society
AMC	Análisis Múltiple de Correspondencias
XRD	X-ray diffraction
RSD	Relative standard deviation
FWHM	Full width at half máximum
CRI	Chemical Raman imaging

CB/CNO	CBE que contiene CB y CNO
CB/SIO	CBE que contiene CB y SIO
IOCCC	International Office of Cocoa, Chocolate, and Sugar Confectionery

INTRODUCCIÓN

El cacao (*Theobroma cacao* L.) y el chocolate, son conocidos como alimentos de lujo (Castro-Alayo et al., 2019). El chocolate representa el 0,17% del total de comercio mundial, habiendo sido comercializado por un total de USD 28,6 mil millones en el 2020 (OEC, 2022). Los granos de cacao son convertidos en chocolate a través de una cadena compleja de procesos que involucra fermentación, secado, tostado y temperado (Santos et al., 2020; Caligiani et al., 2016). La fermentación es considerada uno de los más importantes procesos de poscosecha (Michel et al., 2021) que impacta en la calidad total del grano de cacao y es un paso esencial en la formación de compuestos aromáticos en la fabricación de chocolate (Assi-Clair et al., 2019; Hernández et al., 2019). Para los fabricantes de chocolate, el grado de fermentación de los granos es el principal criterio de calidad (Caligiani et al., 2016).

Existen tres reconocidas variedades genéticas de cacao: Forastero, Criollo y Trinitario; además de una cuarta variedad de origen ecuatoriano conocida como Nacional (Afoakwa et al., 2011). El mercado mundial divide el cacao en dos categorías: "fino de aroma" (Criollo y Trinitario) y "ordinario" (Forastero). La variedad Nacional son considerados Forasteros pero producen cacao fino (ICCO, 2017). Se considera a la variedad Criollo como la más fina debido a su descripción aromática frutal y floral (Ascrizzi et al., 2017), debido a la presencia de 3-metilbutanal (afrutado), 1,3-butanodiol (floral), linalol (floral), 2-fenil etil acetato (frutal) (TGSC, 2021), medidas en concentraciones traza como ppb o µg/kg. Las exportaciones mundiales de cacao fino son pequeñas (12% del cacao total exportado), siendo Ecuador, República Dominicana y Perú los países que exportan el 90% del volumen mundial de cacao fino (ICCO, 2017).

El aroma del chocolate es influenciado no solo por el origen y variedad del cacao sino también por las operaciones de poscosecha y proceso de fabricación (Santander Muñoz et al., 2020; Aprotosoaie et al., 2016; Afoakwa et al., 2008). Se cree que los compuestos aromáticos que se producen durante la fermentación del cacao migran hacia el interior del grano, donde permanecen y llegan a formar parte de la calidad aromática del chocolate (Ascrizzi et al., 2017: Afoakwa et al., 2008). Por ello, para obtener granos de cacao con características

aromáticas deseables, se está tratando de mejorar el proceso de fermentación mediante el uso de cultivos iniciadores (Tabla 1) (Chagas Junior et al., 2021).

Tabla 1. Rol de cultivos iniciadores en la fermentación de cacao (Chagas Junior et al., 2021).

Cultivo iniciador	Resultados
Saccharomyces cerevisiae + *Torulaspora delbrueckii*	Altos niveles de compuestos volátiles y bajos tiempos de fermentación
Saccharomyces cerevisiae + *Lactobacillus plantarum* + *Acetobacter aceti*	Producción de alcoholes y degradación de compuestos fenólicos. Mejores resultados sensoriales
Candida parapsilosis + *Torulaspora delbrueckii* + *Pichia kluyveri*	Reducción de acidéz, cambios en la concentración de azúcares y aminoácidos

El chocolate es un material blando y complejo, caracterizado por partículas sólidas (cacao en polvo, partículas sólidas de leche y cristales de azúcar) dispersas en una matriz de grasa cristalizada compuesta principalmente por manteca de cacao (MC) (Ewens et al., 2021; Liendo et al., 1997). La MC es un lípido sólido polimórfico, cuya estructura cristalina determina la calidad final del chocolate (Liu et al., 2022; Yao et al., 2020; Sasaki et al., 2012). Está compuesta por triacilgliceroles (TAGs) (Servent et al., 2018), de los cuales, 1,3-dipalmitoil-2-oleoil-glicerol (POP), *rac*-palmitoil-stearoil-2-oleoil-glicerol (POS) y 1,3-distearoil-2-oleoilglicerol (SOS) representan 80-95% (Watanabe et al., 2020; Teixeira et al., 2018; Sasaki et al., 2012; Bresson et al., 2011) y definen la característica física de la MC (Sirbu et al., 2018). Esta composición cambia de acuerdo con las variedades de cacao y lugar de cutivo, por ejemplo, cuando el cultivo de cacao está más cerca al ecuador, su grasa será más dura (Ostrowska-Ligęza et al., 2021). En el trabajo realizado por Ostrowska-Ligęza et al. (2021), se encontró que el contenido de ácidos grasos insaturados fue 62% en cacao Criollo de Perú y 64% en cacao Forastero de Ecuador, esta composición también influyó en el perfil de fusión de la MC de ambas variedades.

La MC posee polimorfismo (Norazlina et al., 2020), es decir que puede cristalizar en seis formas polimórficas diferentes (formas I-VI o también conocidas como γ, α, β'_2, β'_1, β_2 y β_1) de acuerdo al aumento de su estabilidad y sus puntos de fusión (Tabla 2) (Declerck et al., 2021; Pirouzian et al., 2020; Devos et al., 2020; Dahlenborg et al., 2015; Toro-Vázquez et al., 2012). La forma β_2 (V) se promueve industrialmente, debido a sus características únicas de

textura, brillo, fusión y sensación en la boca (J. Chen et al., 2021; Pirouzian et al., 2020; Devos et al., 2020; Bayés-García et al., 2019; Prosapio & Norton, 2019; Fernandes et al., 2013; Toro-Vázquez et al., 2012; Beckett, 2009).

Tabla 2. Temperaturas de fusión y rango de temperarutas de fusión de las diferentes poliformas de la MC de acuerdo con diferentes autores (Beckett, 2009).

Declerk (2021)	Windhab and Zeng (1998), Melting range	Wille and Lutton (1966)
sub-α (13–18 °C)	γ (13–18 °C)	I (17,3 °C)
α (17,1–24 °C)	α (18–22,5 °C)	II (23,3 °C)
β_2' (22,4–28 °C)	III (22,5–27 °C)	III (25,5 °C)
β_1' (21–33 °C)	β_{IV} (27–29 °C)	IV (27,5 °C)
β_2 (30–34,5 °C)	β_V (29–33,5 °C)	V (33,8 °C)
β_1 (33,5–36,3 °C)	β_{Vi} (33,5–37,5 °C)	VI (36,3 °C)

La cristalización es la transición de fase de la MC del estado líquido al estado sólido (Campos & Marangoni, 2012), es un proceso de dos etapas que generalmente comienza con la nucleación (pre cristalización) que se realiza en la etapa de temperado y el crecimiento de los TAG de mayor fusión que luego actúan como una plantilla para promover la cristalización de los TAG dominantes (Davis & Dimick, 1989; Loisel et al., 1998; Sonwai et al., 2017; Afoakwa et al., 2009). La cristalización se completa durante el almacenamiento, cuando el nivel de cristales de la forma β_2 aumenta hasta 60-80% (Pirouzian et al., 2020). Para optimizar la cristalización, se requiere que la MC en el chocolate cristalice en la forma β_2 lo más rápido posible (Devos et al., 2020) por lo que la velocidad de cristalización es un factor crítico en la elaboración del chocolate (Pirouzian et al., 2020) para obtener el rango de fusión y brillo deseados, así como para evitar defectos de calidad debido a la floración de grasa (Declerck et al., 2021). Esta velocidad es calculada mediante la ecuación de Avrami durante el estudio de la cinética de cristalización (Jin et al., 2019) (ver sección 3.3.6). Adicionalmente, Smith et al. (2008) señaló que el control de la cristalización es crucial para el color, la textura, el perfil de fusión y otras características de calidad. Dentro de esta compleja microestructura, los cristales de MC son determinantes para las características sensoriales como la liberación de sabor, sensación en la boca y propiedades de fusión (Bayés-García et al., 2019; Yao et al., 2020), debido a ello, la cristalización de la MC juega un papel importante en la obtención de un

chocolate de alta calidad (Fernandes et al., 2013) y puede ser influenciada por el manejo del grano de cacao después de la cosecha, ya que la composición de TAG y los perfiles menores de lípidos van cambiando (Lechter, 2012).

El proceso de fermentación viene siendo estudiado durante años para entender los cambios químicos del grano de cacao, pero algunos temas concernientes a esos cambios en la MC aún no están claros (Servent et al., 2018). Existe escasa información disponible con respecto al efecto de la fermentación en el comportamiento de la MC, sin embargo, desde el punto de vista químico algunos autores sugirieron que la fermentación puede afectar la cantidad de ácidos grasos libres y el tipo de fosfolípidos (Marty-Terrade & Marangoni, 2012), lo cual afectaría la cristalización de la MC. Bayés-García et al. (2019) establecieron que los cambios enzimáticos durante la fermentación implican modificaciones estructurales como la re deposición de lípidos dentro de las células, que pueden modificar el comportamiento de cristalización de la MC al modificarse sus temperaturas de cristalización. Así mismo, Sirbu et al. (2018) encontró pequeñas variaciones en el perfil de TAG de granos de cacao de distintos orígenes a lo largo de la fermentación. Los cambios de temperatura que se dan durante la fermentación pueden provocar diversos estados polimórficos en función del tiempo de duración del proceso, lo cual afectaría la cristalización.

La elaboración de chocolate incluye una compleja etapa de temperado para dirigir la cristalización de la MC hacia la formación de redes con polimorfismo específico (J. Chen et al., 2021), los esfuerzos de investigación sobre la cristalización de la MC se han centrado en optimizar la presencia de la forma β_2 (Sonwai et al., 2017) porque garantiza la textura, brillo, fusión en boca, propiedades térmicas y reología del chocolate. Debido a que las propiedades importantes del chocolate, también dependen en gran medida de la disposición molecular interna (polimorfo) (Ewens et al., 2021), resulta necesario conocer la cristalización y el polimorfismo de la MC durante el procesamiento (Afoakwa et al., 2009).

Las empresas de confitería se esfuerzan en desarrollar nuevas recetas de chocolate para mejorar su perfil nutricional (por ejemplo, reduciendo la cantidad de grasas saturadas) y contrarrestar el aumento del precio de la MC (Ewens et al., 2021; Biswas et al., 2017). Por ello, se han desarrollado diferentes estrategias para mejorar los chocolates, una de ellas es usar grasas alternativas

a la MC para reemplazarla o para ser mezcladas y utilizadas en la elaboración de chocolate (Watanabe et al., 2020; Pirouzian et al., 2020); al mezclarlas, la compatibilidad molecular entre los TAGs nativos de la MC se modifica afectando la cinética de cristalización y polimorfismo, como consecuencia, las propiedades físicas y funcionales del sistema cristalizado son diferentes a los observados en la MC pura (Toro-Vázquez et al., 2012). Diferentes estrategias de reformulación pueden afectar dramáticamente el comportamiento termodinámico y cinético de cristalización de la MC; por lo tanto, afecta las propiedades estructurales y sensoriales del chocolate (Ewens et al., 2021). Cualquier grasa tiene un gran impacto en la cinética de cristalización de la MC (Pirouzian et al., 2020; Svanberg et al., 2011). Entonces, monitorear el efecto de las estrategias de reformulación sobre la cristalización de la MC es esencial para obtener productos de alta calidad (Ewens et al., 2021).

Un chocolate de calidad requiere de un buen grano de cacao y un proceso eficiente. Fabricantes, científicos, productores, etc, coinciden en que un chocolate de calidad reúne los atributos de aroma, sabor y textura; por ello, la cadena de fabricación (desde la fermentación del grano hasta la elaboración de chocolate) debe alinearse hacia el logro de este objetivo. Investigadores coinciden en que la fermentación es uno de los procesos más importantes en la poscosecha de cacao (Michel et al., 2021), pero la información existente solo aborda la producción de aromas, precursores arométicos, polifenoles, capacidad antioxidante, entre otros. La fermentación también podría modificar la composición química de la MC, afectando su comportamiento de cristalización, polimorfismo y miscibilidad con otros aceites y grasas vegetales, factores que influirán en la calidad del producto final. No se conocen las propiedades térmicas, cristalización y polimorfismo de la MC durante la fermentación del grano de cacao, ni en qué medida éstas propiedades son modificadas hasta que se convierte en chocolate, entonces no existe patrones de cristalización de la MC en su estado original durante la fermentación del grano de cacao, lo cual está llevando a establecer estrategias de reformulación equivocadas y procesos de cristalización no controlados.

Estudios como los realizados por Y. Chen et al. (2022) y H. Chen et al. (2022) han demostrado que el uso de diversos ingredientes en las recetas de chocolates cambian sus propiedades de calidad, las cuales podrían ser influenciadas por la

cinética de cristalización y polimorfismo de la MC durante la etapa de temperado. La industria del chocolate necesita mejorar sus formulaciones para fabricar productos de calidad, sanos y de bajo costo; en ese sentido, actualmente se viene estudiando la posibilidad de reemplazar la MC, en ciertos porcentajes o en su totalidad, con aceites o grasas vegetales que sean física y químicamente miscibles con la MC para que puedan fusionarse y formar un solo componente que proporcione al chocolate características de calidad semejantes a las que son otorgadas por la MC. La regulación europea solo permite el uso de grasas y aceites vegetales, además de la MC, hasta 5% del peso total del chocolate, los permitidos son: Illipe, palma, sal, shea, kokum gurgi y pepa de mango. Por ello, se viene investigando nuevas alternativas a las ya existentes. Las cristalización de aceites vegetales utilizados actualmente, ha sido estudiada solamente durante el proceso del temperado del chocolate sin tener en cuenta un patrón inicial de cristalización ya sea como MC pura o durante la fermentación de cacao, de esta manera se desconoce el proceso durante toda la cadena de producción de chocolate. Podemos afirmar que la cristalización de la MC aún no ha sido estudiada durante el proceso de fermentación espontánea del grano de cacao Criollo y la fabricación de chocolate oscuro, por tanto, no existe conocimiento sobre este tema y por ello se propone la presente tesis.

La tesis está organizada en cinco capítulos, iniciando con una revisión general del tema de fermentación de cacao Criollo y posteriormente el estudio bibliométrico realizado al tema de cristalización y polimorfismo de la MC. El tercer capítulo trata sobre la cinética de cristalización y polimorfismo de la MC durante la fermentación espontánea de cacao Criollo. El cuarto capítulo aborda el estudio de la miscibilidad de la MC con aceites vegetales extraidos de plantas que son cultivadas en Perú y finalmente, e quinto capítulo aborda el estudio de la cinética de cristalización y polimorfismo de la MC durante la elaboración de chocolate oscuro y el efecto de nuevos CBE sobre las características físicas, térmicas de este producto.

01/E044-2018-01-BM y del proyecto N° 16808-2016/Proyecto-Cacao del Programa Nacional de Innovación Agraria.

1. Objetivos

1.1. Objetivo general.

Estudiar el proceso de cristalización y polimorfismo de la manteca de cacao en la cadena de fabricación de chocolate oscuro a partir de cacao (*Theobroma cacao* L.) variedad Criollo, específicamente en las etapas de fermentación y temperado.

1.2. Objetivos específicos.

a. Caracterizar la cinética de cristalización, polimorfismo y punto de fusión de la manteca de cacao Criollo durante el proceso de fermentación.
b. Evaluar la miscibilidad de la manteca de cacao Criollo con aceites vegetales.
c. Caracterizar la cinética de cristalización, polimorfismo y punto de fusión de la manteca de cacao Criollo en presencia de aceites vegetales durante el proceso de temperado de chocolate.

2. Organización de la tesis.

2.1. Capítulo I. Revisión del tema de fermentación de cacao Criollo.

Este estudio de revisión reafirma la importancia del proceso de fermentación espontánea de cacao Criollo; ya que permite y crea las condiciones para la generación de los principales compuestos volátiles aromáticos responsables del aroma característico de los chocolates finos. Sin embargo, las referencias consultadas no presentaron evidencia del efecto que tiene la fermentación sobre la manteca de cacao y sus propiedades, aun sabiendo que es el componente principal del chocolate.

El desarrollo de este capítulo permitió publicar el artículo titulado "Formation of aromatic compounds precursors during fermentation of Criollo and Forastero cocoa" en la revista Heliyon (DOI: 10.1016/j.heliyon.2019.e01157) con índice H = 46 y ubicada en el cuartil 1 (Q1).

2.2. Capítulo II. Análisis bibliométrico.

Describe las principales conclusiones del estudio bibliométrico que refuerzan la justificación para la realización del estudio sobre cristalización y polimorfismo de la MC durante la fermentación. Se consideró necesario estudiar la MC durante las principales etapas de la cadena de fabricación de chocolates oscuros porque no existe evidencia sobre ello.

2.3. Capítulo III. Estudio de la cinética de cristalización, polimorfismo y punto de fusión de la manteca de cacao Criollo durante el proceso de fermentación.

Se hizo el seguimiento de los principales parámetros de la fermentación espontánea, mostrando que, hasta el séptimo día de fermentación, los granos de cacao pueden llegar hasta los 45,35 °C de temperatura. Usando Calorimetría Diferencial de Barrido (DSC) se pudo observar el comportamiento de cristalización isotérmica de la MC en su estado puro (Tabla A1), del estándar de triglicérido 1,3-dipalmitoyl-2-oleoylglycerol (componente de la MC) (Tabla A2) y de la MC en el interior del grano durante los días de fermentación (Tabla A3); posteriormente, el ajuste de los datos calorimétricos a la ecuación de Avrami permitió determinar los parámetros cinéticos de cristalización de la MC (índice de Avrami, velocidad de cristalización, tiempo medio de cristalización y tiempo de inducción) (Tabla A4). Durante todo el proceso de fermentación se produjeron núcleos de cristales de MC que crecieron espontánea o esporádicamente en forma de plato, varillas o agujas, estos cristales fueron metaestables de comportamiento polimórfico β_1' y β_2'. Usando la técnica multivariada k-means para identificación de patrones (Tabla A5), se logró distinguir que el proceso de fermentación espontánea del cacao Criollo puede dividirse en dos etapas: una primera etapa de cristalización rápida desde el inicio de la fermentación hasta el tercer día en donde la MC cristalizó en 15,78 minutos y una segunda etapa de cristalización lenta, desde el cuarto hasta el séptimo día, en la cual la MC cristalizó en 17,88 minutos. Con estos resultados se propuso que, basándonos en la cristalización de la MC, el proceso de fermentación debe realizarse en tres días.

El desarrollo de este objetivo permitió publicar el artículo titulado "Kinetics Crystallization and Polymorphism of Cocoa Butter Throughout the Spontaneous Fermentation Process" en la revista Foods (DOI: 10.3390/foods11121769) con índice H = 53 y ubicada en el cuartil 1 (Q1).

2.4. Capítulo IV. Evaluación de la miscibilidad de la manteca de cacao Criollo con aceites vegetales.

En este objetivo se estudió la miscibilidad de la MC con dos aceites vegetales provenientes de plantas que crecen en el Perú, como son aceite de coco y aceite de sacha inchi. Se preparó CBE mezclando la MC con cada uno de los aceites en diferentes concentraciones y se usó Microscopía Confocal Raman para obtener imágenes químicas (Figura A1, A2, Tabla A6) e identificar diferencias químicas entre cada aceite y la MC a través de sus espectros Raman, así también se evaluó la miscibilidad de estos aceites con la MC. Los espectros mostraron que el aceite de sacha inchi se diferenció de los otros dos por su alta proporción de ácido oleico, evidenciado por la alta intensidad del pico a 1662,7 cm^{-1}. También se pudo evidenciar la presencia de los picos a 1745,4 cm^{-1} y 1733,8 cm^{-1} en la MC que son representativos de las formas β_2' y β_1'. El mapeo Raman de los CBE y la técnica de Resolución de Curva Multivariada con Mínimos Cuadrado Alternantes permitió generar mapas químicos para determinar la miscibilidad del aceite vegetal con la MC obteniendo su mapa de distribución, histograma y desviación estándar relativa. Los resultados mostraron que mezclar MC con aceite de coco en proporciones de 55/45 y MC con aceite de sacha inchi en proporciones de 65/35 pueden generar CBE con alta miscibilidad, pero esta miscibilidad se reduce en la medida en que se incrementa la proporción de MC. Con ello se llegó a demostrar que es factible el uso de estos aceites vegetales peruanos como CBE novedosos, ya que se presenta una nueva alternativa a los CBE que son actualmente aceptados por la regulación europea en la elaboración de chocolates.

El desarrollo de este objetivo permitió publicar el artículo titulado "Evaluation of the Miscibility of Novel Cocoa Butter Equivalents by Raman Mapping and Multivariate Curve Resolution–Alternating

Least Squares" en la revista Foods (DOI: 10.3390/foods10123101) con índice H = 53 y ubicada en el cuartil 1 (Q1).

2.5. Capítulo V. Estudio de la cinética de cristalización, polimorfismo y punto de fusión de la manteca de cacao Criollo en presencia de aceites vegetales durante el proceso de temperado de chocolate.

Se utilizó los dos tipos de CBE en combinación con el régimen de temperado para evaluar la cinética de cristalización, polimorfismo, propiedades físicas y térmicas de dos tipos de chocolates oscuros [con aceite de sacha inchi (Ch-SIO) y con aceite de coco (Ch-CNO)]. Se estudió la cristalización isotérmica de los CBE y de los chocolates. Se pudo notar que el aceite de sacha inchi cristalizó a temperaturas inferiores a cero grados y al igual que el aceite de coco, sus propiedades térmicas se modificaron cuando fueron mezclados con la MC para formar su correspondiente CBE. El aceite de coco cristalizó más rápido que la MC, pero al mezclarse con ésta, su velocidad de cristalización y entalpía de fusión se redujeron. Los parámetros cinéticos de la cristalización isotérmica de los chocolates oscuros mostraron que la velocidad de cristalización de la MC se incrementa como consecuencia de los CBE y temperado, obteniendo una cristalización más rápida en el Ch-SIO (7,08 ± 0,15 min) (Tabla A7) que en el Ch-CNO (7,25 ± 0,18 min) (Tabla A8). Tanto el tipo de CBE como el régimen de temperado produjeron chocolates con altos porcentajes de forma β_2 [92.56 ± 1.49% en Ch-SIO (Tabla A9) y 90.3 ± 1.18% en Ch-CNO (Tabla A10)] que superan los valores establecidos en la bibliografía, la presencia de esta forma polimórfica en los chocolates fue corroborada con los bajos valores del índice de blancura. Así mismo, aunque estos factores también causaron cambios en las propiedades físicas (Tabla A11, A12, A13, A14) y térmicas de los chocolates, dichas propiedades se mantuvieron dentro de valores aceptables establecidos por (Beckett, 2009). Con esto se demuestra que es factible el uso de los aceites de coco y sacha inchi en la elaboración de chocolates oscuros.

El desarrollo de este objetivo permitió someter para publicación el artículo titulado "Effect of tempering and cocoa butter equivalents on the crystallization kinetics, polymorphism, and physical and thermal properties of dark chocolates"

en la revista LWT – Food Science and Technology con índice H = 147 y ubicada en el cuartil 1 (Q1).

3. Metodología

La Figura 1 muestra el proceso que se tuvo en cuenta para desarrollar los objetivos y actividades de manera secuencial. La tesis fue organizada de tal manera que cada objetivo específico nos lleve a la publicación de un artículo científico en revista Q1 o Q2.

Estudio del proceso de cristalización y polimorfismo de la manteca de cacao en la cadena de fabricación de chocolate oscuro a partir de cacao (*Theobroma cacao* L.) variedad Criollo

Caracterizar la cinética de cristalización, polimorfismo y punto de fusión de la manteca de cacao Criollo durante el proceso de fermentación.

Monitoreo del proceso de fermentación espontánea de cacao Criollo

Cinética de cristalización de la MC

Polimorfismo de la MC

Punto de fusión de la MC

Evaluar la miscibilidad de la manteca de cacao Criollo con aceites vegetales.

Elaboración de CBE mezclando manteca de cacao y aceites vegetales

Caracterización espectral Raman de los aceites puros y los CBE

Obtención de imágenes químicas Raman de los CBE

Evaluación cualitativa y cuantitativa de la miscibilidad de los CBE

Caracterizar la cinética de cristalización, polimorfismo y punto de fusión de la manteca de cacao Criollo en presencia de aceites vegetales durante el proceso de temperado de chocolate.

Cinética de cristalización y polimorfismo de los CBE

Efecto de CBE y régimen de temperado en elaboración de chocolate oscuro

Polimorfismo, propiedades térmicas y físicas de chocolate oscuro

Figura 1. Proceso seguido para conseguir los objetivos de la tesis.

4. Producción científica.

4.1. Artículos publicados.

- Formation of aromatic compounds precursors during fermentation of Criollo and Forastero cocoa, en la revista Heliyon (DOI: 10.1016/j.heliyon.2019.e01157) con índice H = 46 y ubicada en el cuartil 1 (Q1).

- Kinetics Crystallization and Polymorphism of Cocoa Butter Throughout the Spontaneous Fermentation Process, en la revista Foods (DOI: 10.3390/foods11121769) con índice H = 53 y ubicada en el cuartil 1 (Q1).

- Evaluation of the Miscibility of Novel Cocoa Butter Equivalents by Raman Mapping and Multivariate Curve Resolution–Alternating Least Squares, en la revista Foods (DOI: 10.3390/foods10123101) con índice H = 53 y ubicada en el cuartil 1 (Q1).

4.2. Artículo en proceso de publicación.

- Effect of tempering and cocoa butter equivalents on the crystallization kinetics, polymorphism, and physical and thermal properties of dark chocolates, en la revista LWT – Food Science and Technology con índice H = 147 y ubicada en el cuartil 1 (Q1).

4.3. Ponencia en congreso internacional.

- Participación como ponente en: 4th International Webinar on Chemistry and Pharmaceutical Chemistry, realizado el 11 y 12 de marzo del 2022, con el tema "Evaluation of the Miscibility of Novel Cocoa Butter Equivalents by Raman Mapping and Multivariate Curve Resolution–Alternating Least Squares"

CAPÍTULO I. REVISIÓN DEL TEMA DE FERMENTACIÓN DE CACAO CRIOLLO

Review Article

Formation of aromatic compounds precursors during fermentation of Criollo and Forastero cocoa

Efraín M. Castro-Alayo [a,c,*], Guillermo Idrogo-Vásquez [a], Raúl Siche [b],
Fiorella P. Cardenas-Toro [c]

[a] Institute of Research, Innovation and Development for the Agricultural and Agroindustrial Sector of the Amazonas
Region (IIDAA - Amazonas), Faculty of Engineering and Agricultural Sciences, Toribio Rodríguez de Mendoza
National University of Amazonas, Higos Urco Street 342-350-356, Chachapoyas, Amazonas, Peru

[b] Institute of Research and Development, National University of Trujillo, Av. Juan Pablo II s/n, University City,
Trujillo, Peru

[c] Section of Industrial Engineering, Department of Engineering, Pontifical Catholic University of Peru, Av.
Universitaria 1801, San Miguel, Lima 32, Peru

* Corresponding author.
E-mail addresses: efrain.castro@untrm.edu.pe, efrain.castro@pucp.edu.pe (E.M. Castro-Alayo).

Abstract

There are three main genetic varieties of cocoa (*Theobroma cacao* L) used in
chocolate making: Forastero, Trinitario and Criollo, which are distinguished by
their aroma, an attribute that determines their quality. Criollo cocoa is of the
highest quality and is used in the manufacture of fine chocolates because of its
fruity aroma. The aroma of Criollo cocoa is defined by volatile compounds such
as pyrazines and aldehydes, which are formed during roasting of the bean, from
aroma precursors (reducing sugars and free amino acids) that are generated
inside the bean via enzymatic reactions during fermentation; for this reason,
fermentation is the most important process in the value chain. This review
discusses the production of aroma precursors of Criollo and Forastero cocoa by
studying the kinetics of spontaneous fermentation and the role of starter cultures

Formation of aromatic compounds precursors during fermentation of Criollo and Forastero cocoa

Efraín M. Castro-Alayo[a,c,*], Guillermo Idrogo-Vásquez[a], Raúl Siche[b], Fiorella P. Cardenas-Toro[c]

[a] Institute of Research, Innovation and Development for the Agricultural and Agroindustrial Sector of the Amazonas Region (IIDAA - Amazonas), Faculty of Engineering and Agricultural Sciences, Toribio Rodríguez de Mendoza National University of Amazonas, Higos Urco Street 342-350-356, Chachapoyas, Amazonas, Peru

[b] Institute of Research and Development, National University of Trujillo, Av. Juan Pablo II s/n, University City, Trujillo, Peru

[c] Section of Industrial Engineering, Department of Engineering, Pontifical Catholic University of Peru, Av. Universitaria 1801, San Miguel, Lima 32, Peru

* Corresponding author.

E-mail addresses: efrain.castro@untrm.edu.pe, efrain.castro@pucp.edu.pe (E.M. Castro-Alayo).

1.1. Abstract

There are three main genetic varieties of cocoa (Theobroma cacao L) used in chocolate making: Forastero, Trinitario and Criollo, which are distinguished by their aroma, an attribute that determines their quality. Criollo cocoa is of the highest quality and is used in the manufacture of fine chocolates because of its fruity aroma. The aroma of Criollo cocoa is defined by volatile compounds such as pyrazines and aldehydes, which are formed during roasting of the bean, from aroma precursors (reducing sugars and free amino acids) that are generated inside the bean via enzymatic reactions during fermentation; for this reason, fermentation is the most important process in the value chain. This review discusses the production of aroma precursors of Criollo and Forastero cocoa by studying the kinetics of spontaneous fermentation and the role of starter cultures to produce aroma precursors. Fine aroma precursors produced in the pulp during the fermentation phase will migrate into the bean when it's permeability is improved and then retained during the drying phase. Diffusion of aroma precursors into the cocoa bean may be possible, this process is mathematically characterized by the coefficient of molecular diffusion D, which des Production of peruvian cocoa cribe the process of mass transfer via Fick's Second Law. The current state of knowledge is analyzed based on existing research and reports some gaps in the literature, suggesting future research that will be necessary for a better understanding of cocoa fermentation.

Keywords: Food technology, Food science

1.2. Introduction

Cocoa (*Theobroma cacao* L) and its most important products, such as chocolate, are known as luxury foods that provide an astringent taste and typical aroma (Pedan et al., 2017). The fruit of this tree is a pod that contains seeds, commonly known as cocoa beans (Kongor et al., 2016); when harvested, they are surrounded by a sweet, acidic, aromatic mucilage that is pleasant to the palate and is known as pulp; this material is difficult to extract by mechanical means. There are three commonly recognized genetic varieties: Forastero, Criollo, and Trinitario; a fourth variety that grows in Ecuador is called Nacional

(Afoakwa et al., 2011). Criollo is the finest variety of cocoa. Cocoa varieties classification is largely based on the aspect of the fruit, so the terms associated to Criollo are descriptive of the fruit characters (Ascrizzi et al., 2017), however it is the least studied. The production of cocoa is led by Forastero, and Criollo contributes a smaller amount to world production, approximately 5% (Afoakwa, 2010). In Latin American production, Peruvian cocoa is of interest for its quality; however, its production is insufficient for international demand. In Amazonas, Peru, dry fermented Criollo cocoa bean is produced for the Italian market, and this product has received the designation of the origin "Cacao Amazonas Peru" by the Peruvian state.

The most important attribute for which the cocoa bean is commercially accepted is its aroma, which also determines its quality. The aroma is formed by volatile compounds that are perceived by the smell receptors of the olfactory tissue of the nasal cavity (Belitz et al., 2009). The aroma of the genetic varieties mentioned above is used for commercial classification into divided into two types of cocoa: bulk/ordinary cocoa (Forastero) and cocoa with a fine aroma (Criollo and Trinitario) (Kongor et al., 2016; Chetschik et al., 2017). The volatile compounds of the cocoa aroma and chocolate are formed during the roasting of the bean, transforming the molecules known as aroma precursors, which are generated during fermentation by proteolysis of the proteins stored inside this bean (Janek et al., 2016). Adequate quantities and proportions of the formed precursors are essential for the optimal production of aromatic volatiles compounds (Afoakwa, 2010). In Criollo cocoa (Frauendorfer and Schieberle, 2008) revealed concentrations above the odor threshold for 22 compounds in the unroasted and 27 compounds in the roasted cocoa beans, respectively. It is also assumed that cocoa pulp has an impact on the development of aroma during fermentation, due to the possible migration of aroma compounds from the pulp to the bean tissue, and is considered a deposit for the fineness of cocoa (Chetschik et al., 2017).

To improve the quality of cocoa, the effects of the use of starter cultures composed of different types of microorganisms that can lead a controlled fermentation is investigated. Although experimental applications in clone cocoa fermentations of these cultures have given good results (Schwan, 1998; Sandhya et al., 2016), the process is still performed spontaneously, at least among small

17

producers (Vázquez-Ovando et al., 2016). There are no studies on the use of starter culture in fermentation of Criollo cocoa, all studies on the subject mentioned in this document refer to cocoa of other varieties. Therefore, this review to discuss about the production of cocoa aroma precursors during spontaneous and controlled fermentation. The role of the microorganisms in the production of aroma precursors, that influence in the final content of aromatics compounds, and its production kinetics in cocoa beans are analyzed. The current state of knowledge is analyzed based on existing research and reports about some gaps in knowledge, suggesting future research that will be necessary for a better understanding of Criollo cocoa fermentation.

1.3.   Main text

1.3.1.   Formation of the aromatic compounds in cocoa beans

1.3.1.1.   Volatile aromatic compounds in Criollo cocoa

The aroma and taste of chocolate depends on the origin and genotype of the cocoa bean (Menezes et al., 2016), which has been used by the International Cocoa Organization in numerous studies to conclude that, in general, cocoas from different origins have different aroma profiles, thus eliminating market competition among them (ICCO, 2017a). Volatile aromatic compounds are present in traces, mainly at levels of a few µg/kg or no more than a few mg/kg, with approximately 100 different pyrazines present in the predominant aroma fraction (Beckett, 2009).

Criollo cocoa is of high value and is a fine cocoa used to produce high-quality chocolates. The fine aromas include fruit notes (fresh and ripe), floral, herbal, wood, nuts and caramel notes; monoterpenes such as linalool are also part of the compounds responsible for the fine aroma in cocoa; therefore, fine cocoas contain higher amounts of linalool than bulk cocoa (Ziegleder, 1990). Frauendorfer and Schieberle (2008) analyzed unroasted and roasted Criollo cocoa, they concluded that various compounds contributing to the aroma of roasted cocoa beans, such as 3-methylbutanoic acid, ethyl 2-methylbutanoate and 2-phenylethanol, were already present in unroasted, fermented cocoa beans and were not increased during roasting. Table 1.3-1 shows the compounds of the

fine aroma identified in Criollo cocoa of different origins and processing stages (fresh, fermented and roasted bean) (Ascrizzi et al., 2017; Tran et al., 2015). In the Peruvian Criollo cocoa, linalool was not found as the main component, the presence of this component will depend on the geographical origin where the cocoa is cultivated; however, other components responsible for the aroma of floral and caramel were founded.

Table 1.3-1. Components of fine aroma identified in samples of Criollo cocoa of different origins.

Aromatic compound	Description	Provided by Amedei's factory (country not identified)*		Peru**
		Raw cocoa beans, fermented and dried, husked, %	Roasted cocoa beans with husk, %	Roasted cocoa beans, µg/g
2-Heptanol	Citrus, fresh, lemon grass-likee	0.7	0.2	
Phenylethyl alcohol	Flowery, spicy, honey-like, rose	1.6	0.8	
Ethyl octanoate	Fruity, floral, pineapple	0.5	0.3	
Ethyl phenylacetate	Fruit, sweet, honey-like	0.5	0.4	
Ethyl decanoate	Pear, grape, brandy	0	0.1	
Acetophenone	Sweet, almond, flowery, must-like	0.2	0	
cis-Linalool oxide (furanoid)	Sweet, nutty	0.2	0	
Linalool	Flowery	1.2	0.5	
trans-Linalool oxide (pyranoid)	Floral	0.2	0.1	
2-Phenylethylacetate	Fruity, sweet, flowery	2.5	1.5	0.73
1,3-Butanediol	Sweet, flowery, caramel			16.21
2,3-Butanediol	Sweet, flowery			5.12

*Ascrizzi et al., 2017, **Tran et al., 2015.

The basic aromas of cocoa beans include pleasant and balanced chocolate notes (ICCO, 2017b), and the aromas of cocoa and chocolate are attributed to 2,3,5,6-tetramethylpyrazine (TMP) and 2,3,5-trimethylpyrazine (TrMP), which form the so-called basic notes (Sukha et al., 2013). In addition to pyrazines, aldehydes also contribute to the chocolate aroma (Diab et al., 2014). Chocolate manufacturers separate cocoa beans into fines and bulk; fines are characterize their peculiar notes and are used to produce fine chocolates (Ascrizzi et al., 2017), while bulk beans are used to produce low-quality chocolates and products such as cocoa powder (Vargas Jentzsch et al., 2016). Table 1.3-2 shows a comparison between the roasted dry fermented beans of Criollo cocoa obtained from Tumbes (Peru), Grenada and Venezuela, and Forastero cocoa from Ghana (Africa); the named sensory description is

accepted by U. S flavor industry (FEMA, 2018). In fact, there is a clear quantitative difference between the volatile aroma compounds of fine cocoa and bulk cocoa (Tran et al., 2015), fines (Peru) have higher levels of pyrazine than bulk beans (Ghana) and a higher percentage of 1,3-butanediol, which gives notes of sweet, floral and caramel (Tran et al., 2015), to mention just one example. In Criollo cocoa beans from Venezuela, 1,3-butanediol was identified (Álvarez, 2016). 3-methylbutanal (malty) is a Strecker aldehyde (Frauendorfer and Schieberle, 2008) and it is crucial aroma compound contributing to the chocolate aroma intensity (Van Durme et al., 2016; Saputro et al., 2018). Excluding the basic aromas of cocoa, the majority of fine aroma features depend on the sensory quality of ripe pod: for Criollo beans, caramel and walnut notes are due to the very sweet nature of their pulp (Ascrizzi et al., 2017). The Criollo cacao from Granada has a greater amount of 3-methylbutanal than those from the other countries, also this cacao and the one from Venezuela contain linalool as one of its components; this corroborates the fact that the geographical origin influences the aromatic profile of Criollo cocoa; however, research is still scarce.

Table 1.3-2. Comparison of aromatic notes of fine and bulk cocoa in dry and roasted fermented bean.

Aroma notes	Identified component	Sensory description	Percentage contribution to aroma			
			Fine (Criollo - Peru)[2]	Fine (Criollo - Grenada)[3]	Fine (Criollo - Venezuela)[4]	Bulk (Forastero - Ghana)[2]
Fine notes	3–methylbutanal		0.73	8.08	0.5	0.41
	1,3–butanediol	Sweet, floral and caramel[2]	13.18	NI	I	11.11
	Linalool	Coriander, Floral, Lavender, Lemon, Rose[1]	NI	0.03	I	NI
Basic notes	2– phenylethylacetate	Frutal, sweet, floral[1]	0.73	0.22	I	0.27
	TrMP	Cocoa, Earth, Must, Potato, Roast[1]	4.4	0.22	I	3.65
	TMP	Cocoa, Coffee, Green, Mocha, Roast[1]	17.28	NI	0.5	5.49

1. FEMA, 2018; 2. Tran et al. (2015); 3. Frauendorfer and Schieberle (2008); 4. Álvarez (2016).

NI: not identified, I: identified, but no value.

1.3.1.2. Development of volatile aromatic compounds from aroma precursors

Typical aromatic compounds are developed during the roasting stage (Ascrizzi et al., 2017) from aroma precursors by the Maillard reaction (Giacometti et al., 2015). The fermentation of cocoa pulp is crucial for the generation of aroma precursors, and this process is performed by microorganisms such as yeast, lactic acid bacteria (LAB) and acetic acid bacteria (AAB) (John et al., 2016). Fresh beans with low precursor content will have limited commercial use, and fermentation will not be able to rectify this shortfall; therefore, an appropriate amount and ratio of aroma precursors are essential for the optimal production of volatile aromatic compounds in roasting (Afoakwa et al., 2008; Aprotosoaie et al., 2016). Tran et al. (2015) related the degree of fermentation of fermented cocoa beans from different origins with the presence of aroma precursors, establishing as well fermented when there is a high concentration of free amino acids and absence of sucrose (Table 1.3-3). In Criollo from Peru, a higher concentration of amino acids was found than in Vietnam and Ghana varieties, so it could be said that it has a better potential to generate aromatic compounds during roasting, provided that the fermentation has been carried out efficiently.

Table 1.3-3. Aroma precursors found in different varieties and origin of cocoa beans.

| | Clone/variety | | |
	Criollo	Trinitario × Forastero	Forastero
Hybrid name	Tumbes	TD10	PA7xIFC5
Origin	Peru	Vietnam	Ghana
Sucrose, mg/g	0	0	2.42 ± 0.18
Glucose, mg/g	0	0	0
Fructose, mg/g	4.61 ± 0.98	10.01 ± 0.13	7.18 ± 1.15
Leucine, mg/g	3.14 ± 0.01	2.75 ± 0.02	2.00 ± 0.07
Alanine, mg/g	2.27 ± 0.00	2.05 ± 0.01	1.38 ± 0.06
Phenylalanine, mg/g	2.45 ± 0.00	2.14 ± 0.03	1.58 ± 0.10
Tyrosine, mg/g	1.55 ± 0.01	1.33 ± 0.01	1.09 ± 0.05

Data extracted from Table 2 published by Tran et al. (2015).

The results of previous studies have shown that peptides and free hydrophobic amino acids, such as leucine, alanine, phenylalanine and tyrosine,

are precursors that contribute to the aroma formation of cocoa and chocolate (Voigt, 2009; Sukha et al., 2017) and develop during fermentation (Hashim et al., 1998) through the proteolysis of vicilin-class globulin (VCG) (Janek et al., 2016; Kumari et al., 2016), which is induced by acetic and lactic acids (Voigt et al., 2016) and cooperative action of the aspartic endoprotease and carboxypeptidase that are present in mature cocoa beans and those that are not germinated. Hydrophilic peptides and free hydrophobic amino acids contribute to the aroma by their reaction with fructose and glucose (Afoakwa, 2010) during roasting. In the pulp, sucrose is hydrolyzed to glucose and fructose by the invertase activity of the yeast, as well as in the bean by diffusion of acetic acid, lactic acid and ethanol, together with the production of heat (de Melo Pereira et al., 2013) (Figure 1.3-1). Approximately 25% of free amino acids and 70% of glucose and fructose are used (Beckett, 2009). Leucine and glucose produce aromatic notes described as "sweet chocolate" (Afoakwa, 2010). Recent work concludes that there is no clear quantitative correlation between the amounts of precursors and the aromatic compounds formed (Tran et al., 2015; Frauendorfer and Schieberle, 2008), while others claim that Criollo cocoa beans contain high levels of precursors that can produce high levels of pyrazines (Giacometti et al., 2015), however, pyrazines are not responsible for the fine aroma of Criollo cocoa. The compounds 3-methylbutanal and phenylacetaldehyde (honey, green, floral (Crafack et al., 2014)) correspond to the so-called aldehydes of Strecker degradation, which are the products derived from valine, leucine, isoleucine and phenylalanine. The compounds 3-methylbutanal, 2-methylbutanal and 2-methylpropanal provide a fruity aroma and contribute to the sugary taste that is characteristic of Criollo cocoa (Álvarez et al., 2012). In a previous analysis of dry fermented beans of Criollo cocoa produced by the Asociación de Productores Cafetaleros y Cacaoteros de Amazonas (APROCAM)-Peru, 28.08% of 3-methylbutanal and 9.17% of 2-methylbutanal were detected (data not yet published). In addition to the endogenous formation of the precursors, there is growing evidence of the exogenous influence of the pulp directly on the development of the aroma (Sukha et al., 2017). It is believed that aromatic compounds directly penetrate from the pulp into the bean tissue during fermentation and can be retained during the drying process (Eskes et al., 2012).
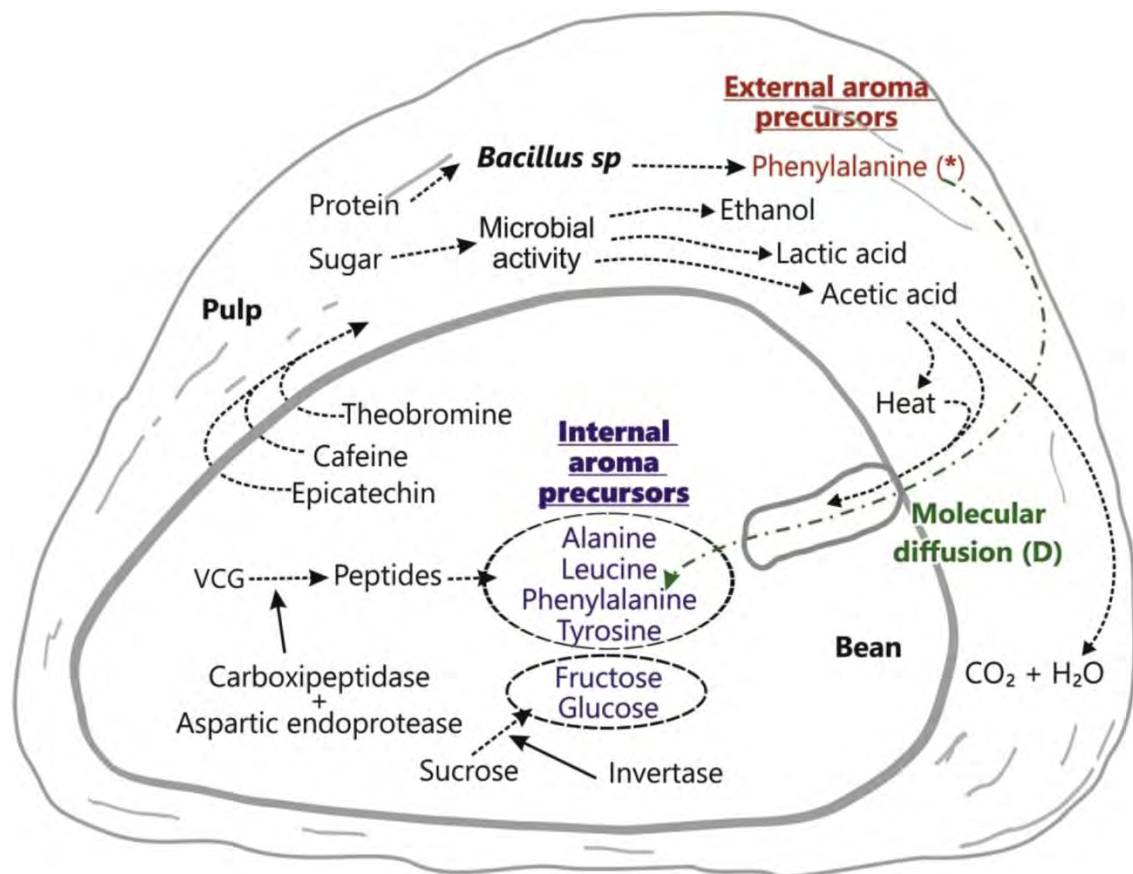
Figure 1.3-1. Aroma precursors produced during cocoa bean fermentation by microbial action and its molecular diffusion (adapted from Beckett, 2009). (*) In addition to the internal production of phenylalanine from the VCG, this amino acid can also be produced by Bacillus in the pulp of the bean, then called external precursor, and later enter the interior of the bean by molecular diffusion to be part of the internal precursors.

There are few studies on volatiles compounds of Criollo cocoa, (Rodriguez-Campos et al., 2011, 2012; Ramos et al., 2014) characterized the dynamics of volatile compounds during fermentation of cacao varieties, including the bulk Forastero and various cacao hybrids, but the fine-flavor cultivars Criollo were not assessed. The volatile aromatic compounds present in Criollo, Forastero, and Trinitario cocoa beans from the same origin have been characterized (Qin et al., 2016; Tran et al., 2015; Counet et al., 2004) but changes in aroma precursors occurring during fermentation Criollo cocoa were not reported.

1.3.2. Action of the microorganisms in the production of aroma precursors and aromatics compounds

In spontaneous fermentation of cocoa beans Forastero hybrid from Ivory Coast (Visintin et al., 2016), isolated 106 yeasts, 105 LAB and 82 AAB which were identified by means of rep-PCR grouping and sequencing of the rRNA genes. Oxygen is one of the factors that determines the microbial succession. Yeasts and LAB are the predominating microbial species at the initial phase of the fermentation process (Romanens et al., 2018). Jamili (2016); Ardhana (2003) states that the yeast at most the number and the type found in 24–36 hours after fermentation of cocoa because of their role in the process of degradation the various types of sugar that contained in the cocoa bean pulp. Visintin et al. (2017) found that in fermentation of two different cocoa hybrids (PS1319 and SJ02), the yeast *(Saccharomyces* cerevisiae and *Torulaspora delbrueckii*) metabolism results in ethanol production. In region called Agneby-Tiassa, species of Pichia *kudriazevii* and *Candida nitrativorans* was isolated; they are resistant to high temperatures (40 °C) and high ethanol concentrations (20%). Moreover, they exhibited pectin-hydrolysing enzymatic activities, suggesting its key role in the degradation of cocoa bean pulp during fermentation (Samagaci et al., 2016).

Spontaneous Malaysian cocoa bean box fermentations were carried out with high-quality raw material, resulting in successfully fermented dry cocoa beans and good chocolates produced thereof, it is likely that the prevailing species Hanseniaspora *opuntiae*, *S. cerevisiae*, *Lactobacillus fermentum* and *Acetobacter pasteurianus* were responsible for it (Papalexandratou et al., 2013). In cocoa beans fermentation performed in Abidjan (South East of Ivory Coast) (Koné et al., 2016), identified yeasts that produced a total of 33 aroma compounds, among all yeasts involved *P. kudriavzevii*, *S. cerevisiae*, *Galactomyces geotrichum* and *Wickerhamomyces anomalus* could be considered as the most important contributors to the formation of cocoa specific aromatic compounds. Yeasts produced ethanol from sugars, and LAB produced lactic acid, acetic acid, ethanol, and mannitol from sugars and/or citrate (Camu et al., 2007; Papalexandratou et al., 2013). The experiment conducted by (Magalhães da Veiga Moreira et al., 2016) in Porto Híbrido 9, Porto

Híbrido 15 and Porto Híbrido 16 cocoa beans at the Vale do Juliana farm in Igrapiúna, Bahia, Brazil, Hanseniaspora uvarum, *P. kluyveri*, *P. caribbica* and *S. cerevisiae* were the predominant yeasts in the three fermentations. *L. plantarum*, *A. pasteurianus*, Bacillus *cereus* and Lysinibacillus *fusiformis* were the common bacterial species isolated from the fermentations. Twenty-seven volatile compounds were identified during the cocoa fermentation of all hybrids (Koffi et al., 2018). investigated 743 yeast strains, two strains *S. cerevisiae* YB14 and *P. kudriavzevii* YP13 were able on one hand to resist to most parameters such as temperature, pH, ethanol, organics acid, and on the other hand they were able to produce specific enzymes like pectinase, β-glucosidase, protease necessary to have a good cocoa fermentation process, and finally to produce acetoin which is desirable for flavor development in the fermentation process. These two strains could therefore be used as starter cultures which may contribute to the control of cocoa fermentation in Ivory Coast. Other results shown that *P. kudriazevii* and *Candida nitrativorans* are key players in cocoa bean fermentation in the Agneby-Tiassa region and they are promising candidates for developing starter cocktails that could be used to improve the overall efficiency of cocoa fermentation in Ivory Coast (Samagaci et al., 2016). Furthermore some specific yeast isolates could be used as biological markers to predict the determining of chocolate sensorial characteristics and to indicate the geographical origin or processing story of cocoa bean batches (Koné et al., 2016). Actually, it was concluded that the growth of LAB and AAB may not be essential for the fermentation of cocoa beans (Ho et al., 2018).

The experiment conducted by (de Melo Pereira et al., 2013) at a cocoa farm located in the city of Itajuípe, Bahia State, Brazil, the dominant species of major physiological roles were *S. cerevisiae* and *Hanseniaspora sp*. in the yeast group; *L. fermentum* and *L. plantarum*in the LAB group; *A. tropicalis* belonging to the AAB group; and *Bacillus subtilis* in the Bacillaceae family. It demonstrated that at least three species of *Bacillus* are involved in cocoa fermentation, namely *B. subtilis*, *B. flexus* and *B. megaterium* (de Melo Pereira et al., 2013). Aerobic spore-forming bacteria, such as *Bacillus* strains, produce a variety of chemical compounds, including 2,3-butanediol, pyrazines, acetic acid and lactic acid, under fermentative conditions, which may contribute to the acidity and perhaps, at times, to off-flavors of fermented cocoa beans (Schwan, 1998).

Increased aeration, increased pH value (3.5–5.0) of cocoa pulp, and a rise in temperature to about 45 °C in the cocoa mass in the later stages of fermentation are associated with the development of bacteria of the genus *Bacillus* (Schwan and Wheals, 2004).

In Forastero and Trinitario cultivars at commercial fermentations in East Java, Indonesia was investigated. The later stages of fermentation were dominated by the presence of *Bacillus* species, mostly, *B. pumilus* and *B. licheniformis* (Ardhana, 2003; Nielsen et al., 2007). With regard to the fate of *Bacillus spp*. towards the end of the fermentation, this constitutes a microbial group that persists until the end (Lima et al., 2011). *Bacillus spp*. has also been classified as responsible for the production of TMP (de Melo Pereira et al., 2013) and 2,3-butanediol (sweet, floral (Crafack et al., 2014; Ardhana, 2003)) during cocoa fermentation; a temperature of 50–55 °C assists in this formation (Selamat et al., 1994).

The role of bacilli in cocoa fermentation is not well known (Nielsen et al., 2007). However (Ouattara et al., 2008) suggest that *Bacillus sp*. is liable to produce at least one enzyme during cocoa fermentation, so the degradation of the pulp during cocoa fermentation might not be only due to pectinolytic enzymes produced by yeasts but rather by a combined action of enzymes produced by both yeast and *Bacillus* strains. Ouattara et al. (2017) assumed that, during the latter stage of cocoa fermentation when simple sugars are depleted, production of pectate lyases (Pel) in *Bacillus* is stimulated by DegU gene to supply microbial cells with carbon source from polymeric pectic compounds. It is possible that *Bacillus spp*. play a bigger role in box fermentations than in heap fermentations, but more fermentations need to be investigated before firm conclusions can be drawn (Nielsen et al., 2007).

In other raw materials, the result showed that *Bacillus sp*. KR-8104 growth and the production of α-amylase on a wheat bran substrate could successfully (Hashemi et al., 2011). The production of L-phenylalanine (phenylalanine) is related to strains of *B. subtilis* (De Boer and Dijkhuizen, 1990). In brewery wastes, *B. subtilis* UO-01 was studied. Protease production delay seemed to be related to the consumption of non-protein and protein nitrogen, the maximum protease level (9.77 EU/mL) was obtained at pH 7.1 and 37.8 °C (Sánchez Blanco et al., 2016). In soya roasted cotyledons fermented for 18 h and 36 h at

35 °C, growth of *B. subtilis* led to the formation of volatile compounds: acetoin, 2,5-dimethylpyrazine (2,5-DMP) and TrMP (Owens et al., 1997). 2,5-DMP and TMP were produced using *B. subtilis* IFO 3013 grown on soybeans (Besson et al., 1997).

In a previous analysis of dry fermented beans of Criollo cocoa from APROCAM, considerable amounts of TMP, TrMP, 2,3-butanediol and acetoin (butter, creamy, green pepper (FEMA, 2018)) were founds (data not yet published). The presence of these compounds would lead us to think that in addition to the yeasts, LAB and AAB there may be certain *Bacillus* strains during the spontaneous fermentation of Criollo cocoa, however there is no information to corroborate this hypothesis, since the data so far found only they refer to other varieties or clones of cocoa. Likewise, in previous studies (not in cocoa) the production of phenylalanine by *B. subtillis* has been reported, which gives the possibility of finding this amino acid in spontaneous cocoa fermentation and we would be facing a process of production of "external aroma precursors" by microbial action on the outside of the cocoa bean (Fig. 1.3.1).

1.3.3.   Solid-state fermentation (SSF) of cocoa beans

1.3.3.1.   Spontaneous fermentation

Fresh cocoa beans are very astringent and do not develop the delicious and typical chocolate aromas alone (Papalexandratou and Nielsen, 2016) because they do not contain specific aroma precursors (Kadow et al., 2015); thus, the reason for the fermentation of cocoa is to reach biochemical reactions inside the bean that lead to the formation of aroma precursors, flavor and color, reduction of bitter and astringent tastes, and improvement of the physical appearance of cocoa (Apriyanto et al., 2017). Well-conducted fermentation is a prerequisite for the production of high-quality chocolates; if performed improperly, the production of specific aroma compounds will fail during the post-processing stages (Crafack et al., 2013). A 5-day fermentation period is common for the Forastero cultivar while shorter periods of about 2–3 days are required for Criollo and Nacional cultivars (Cevallos-Cevallos et al., 2018). In Peru, fermentation systems are used in wooden fermentation boxes, forming a batch process. These boxes act as bioreactors; the process begins at room temperature (27 °C) and

ends at approximately 50 °C in seven days, with the transfer of the beans from one box to another from the second day to incorporate air. Cocoa beans are fermented by small producers in a traditional and uncontrolled process known as spontaneous fermentation (Magalhães da Veiga Moreira et al., 2017). During fermentation, small amounts of free water are present, and this process is characterized as SSF (Nielsen et al., 2014).

Until the pods open, the beans are sterile microbiologically. Once the pod is opened, the beans are exposed to numerous sources of microorganisms, including the hands of farmers and utensils. The immediate effect is the initiation of microbiological attack on the pulp sugars by the yeasts, and this action is followed by the LAB and AAB (Afoakwa, 2010). This succession is directed by yeasts, which dominate the microbial population during the first hours, followed by the LAB, which decrease after 48 hours of fermentation, and finally the AAB increase in number (Ardhana, 2003). The fermentation of cocoa beans occurs in two phases. The first involves reactions that occur in the pulp, and the second involves several hydrolytic reactions that occur within the bean (Pereira et al., 2012). While the first phase is performed at 25–45 °C, the second phase is at 42–52 °C (Kadow et al., 2015). Changes in pH, temperature, sugar content and fermentation products or metabolites exert a selection pressure on existing natural biotypes, favoring the strains that are better adapted to this environment (Pereira et al., 2012). These metabolites kill the bean and trigger a series of biochemical reactions in their interior (Pereira et al., 2016), generating aroma precursors (Fernández Maura et al., 2016); the pulp is solubilized, giving rise to a liquid material (exudate) that drains through the holes of the fermenter boxes (Ardhana, 2003), and this material serves as a way of transport for the metabolites of fermentation.

The pulp is the base substrate for microorganisms during fermentation. It is important to define the best state of the pulp for a successful fermentation according to the best results of quality determining components (Voigt and Lieberei, 2014). In fine cocoas, the level of the basic aromatic components (basic notes) of cocoa (and chocolate) is usually low due to the short duration of the fermentation (2–4 days), compared to bulk cocoa (5–7 days) (Torres-Moreno et al., 2012). The findings of previous studies show that linalool is a constituent of the pulp that is transferred to the beans during fermentation (Voigt and

Lieberei, 2014). Linalool can be produced by *S. cerevisiae* from the catabolism of leucine (Carrau et al., 2005). It is possible that glycosidase enzymes (α-arabinosidase, β-galactosidase, α-mannosidase) play an important role in the release of this compounds (Voigt and Lieberei, 2014). For example, 1,020 ppb of linalool was found in dry fermented Criollo cocoa beans (Chetschik et al., 2017), or, in another study, 130 µg/kg (Frauendorfer and Schieberle, 2008).

The quality of beans is strongly dependent on the degree and time of acidification of the cotyledon during the fermentation process (Voigt and Lieberei, 2014). Cocoa fermentation at a pH of approximately 5 shows a cocoa with the highest potential for specific aromas (Janek et al., 2016). It is known that strong acidification of the cotyledon (pH < 5) during the fermentation produces a poor potential of aroma in the cocoa beans, because the activity of carboxypeptidase is optimal at approximately pH 5.5 and is reduced to pH < 5. At pH values >5.5, the aspartic endoprotease is inactivated (Voigt et al., 1994).

Spontaneous fermentation is an empirical procedure, which may not yield beans of consistent quality, which requires the chocolate industry to continuously modify its formulations (de Melo Pereira et al., 2013). Common problems involve acidity levels and incomplete fermentation, resulting in deficient or unpleasant aromas (Schwan, 1998). The studies carried out in a simulated medium of cocoa pulp and indicate that there could be competition among specific strains called *L. plantarum*, *L. fermentum* and *A. pasteurianus* during the spontaneous fermentation process, improving the aroma of the bean (Lefeber et al., 2010); however, there is no further information on how this has improved the fermentation process of the cocoa bean under field conditions (Ghosh, 2016), and thus producers still use spontaneous fermentation for their commercial cocoa. As a alternative (de Melo Pereira et al., 2013), described the first experimental validation of the stainless steel tank method for cocoa bean fermentation. They concluded that the use of stainless steel tanks may be of great interest for those who seek improved control over the cocoa fermentation process and/or to optimize cocoa fermentation through the use of starter cultures. In accord (Mota-Gutierrez et al., 2018), found that the microbial dynamics and associations between the bacteria, yeast and metabolites were found to depend on the type of fermentation. With the growth of niche markets for chocolate manufacturers, a better understanding of the factors that contribute to flavor

variations will have significant commercial implications (Afoakwa et al., 2008). As a consequence of the increasing implementation of traceability systems in the food industry, detailed information about how products are handled could be transferred to the producers and could be used to optimize the processes (Saltini et al., 2013).

Although it is true that cocoa fermentation has been widely studied, there are few works on spontaneous fermentation of Criollo cocoa, in the work made by (Cevallos-Cevallos et al., 2018), spontaneous fermentation was carried out in a greenhouse at ambient temperature (about 35 °C) for Forastero, Criollo and Nacional cultivars; fine-flavor cultivars were characterized by the presence of significant amounts of hydrocarbons such as valencene, aromadendrene, germacrene, 1,3 cyclohexadiene and octacosane while fermented beans of the Forastero bulk cocoa showed negligible levels of these volatiles. In Amazonas, the fermentation process is the same for both Criollo cocoa and CCN 51 clone (bulk cocoa); the same boxes are used and a product is obtained in 7 days, which leads to obtaining cocoa beans of different qualities. This is a problem that has not yet been solved due to the lack of research.

1.3.3.2. Fermentation controlled by starter culture

As far as we know, the use of starter cultures in Criollo cocoa fermentation has not been studied; therefore, the studies analyzed here generally correspond to cocoa clones. Studies of fermentation and chocolate using PS1319 hybrid cocoa and starter cultures can provide important results for improving the fermentation of cocoa and the quality of chocolate (Batista et al., 2016). The use of LAB starter cultures could lead to a controlled fermentation process and thus the possibility of controlling the aroma (Saltini et al., 2013). SSF was used to ferment Forastero cocoa with a starter culture; it was found that a 10% culture composed of *S. cerevisiae*, *L. plantarum* and *A. aceti* was adequate to produce chocolate with 7.5 out of 10 points on a hedonic scale for acceptability of the aroma of chocolates produced from cocoa beans fermented with starter culture (Sandhya et al., 2016). Other researchers have inoculated starter culture composed of *S. cerevisiae*, *L. plantarum* and *A. pasteurianus* in the fermentation of cocoa hybrids; the fermentation process was accelerated, and the chocolates

made with inoculated beans were bitter, sweet and cocoa-flavored, with considerable amounts of 3-methylbutanal, 2-phenylethylacetate (Magalhães da Veiga Moreira et al., 2017). In the roasted liquor of cocoa produced from fermentations of hybrids inoculated with *L. fermentum* L18, *A. pasteurianus* A149, *P. kluyveri* and Kluyveromyces marxianus, 1,3-butanediol was detected (Crafack et al., 2014). Thus, inoculation affects the profiles of volatile compounds and their relative concentrations, which influence the sensory characteristics of chocolate (Batista et al., 2016).

Results reported by (Pereira et al., 2017) indicated that inoculated fermentations with *P. kudriavzevii* LPB06 and *P. kudriavzevii* LPB07 generated cocoa beans with better color development and richer aroma composition, suggesting that cocoa-associated yeast diversity at strain level can be exploited for flavor modulation of cocoa beans. In fermentation inoculated with *S. cerevisiae* FNCC 3056, Lactococcus lactis FNC 0086 and *A. aceti* FNCC 0016, an increase of hydrophobic amino acids was obtained, demonstrating that the addition of inoculum can gradually degrade protein to produce more hydrophobic amino acids as aroma precursors (Apriyanto et al., 2017). LAB can also metabolize sugars and organic acids to produce various aldehydes, ketones and other volatile components that can impact the sensory quality of the bean (Ardhana, 2003). It is known that some compounds come from the metabolism of yeasts, such as phenylethylacetate (fruit, sweet, honey (Magalhães da Veiga Moreira et al., 2016)), 2-phenylethanol (honey, floral (Magalhães da Veiga Moreira et al., 2016)), 2-phenylacetic acid and acetoin (butter, cream (Batista et al., 2016; Visintin et al., 2017)). Table 1.3-4 shows that in the fermentation of cocoa hybrids controlled by a starter culture, it is possible to obtain aromatic compounds identified in Criollo cocoa (Crafack et al., 2014; Batista et al., 2016; Visintin et al., 2017; Magalhães da Veiga Moreira et al., 2017). It may not be necessary to use starter cultures to improve the aromatic quality of Criollo cacao, which is why this type of research has not been carried out with this variety, since its own genetics and origin would determine its fine aroma. However, we consider it important to study the process of fermentation of Criollo cocoa to have a standard process based on the amount of aroma precursors produced. Then, so that the Forastero cocoa fermentation reaches this standard, a type and concentration of the starter culture would be necessary. From the

isolation of the best strains found in the Criollo cocoa fermentation, this culture would be developed and used in Forastero cocoa fermentation.

Table 1.3-4. Fine aroma compounds produced by starter culture.

Starter culture	Sample	Raw material	Fine aroma components identified	Source
S. cerevisiae UFLA CA11 *P. kluivery* CCMA0237 *Hanseniaspora uvarum* CCMA0236	Chocolate and dry fermented beans	Hybrid PS1319, Brazil	2-Heptanol, 2-pentanol, Phenylethyl alcohol, 2-Methylbutanal, 2-Phenyl-2-butenal, Ethyl octanoate, Ethyl phenylacetate, 2-Heptanone, 2-Phenylethyl acetate, 2-pentanone, 2-nonanone, 2-undecanone, Acetophenone	Batista et al. (2016)
S. cerevisiae UFLA CCMA 0200 *L. plantarum* CCMA 0238 *Acetobacter pasteurianus* CCMA 0241	Chocolate	PH15 cocoa hybrid, Brazil	2-Heptanol, 2-pentanol, 2,3-Butanediol, Phenylethyl alcohol, 2-Phenyl-2-butenal, 2-Heptanone, Acetophenone, Linalool, trans-Linalool oxide (pyranoid), cis-Linalool oxide (furanoid), 2-nonanone	Magalhães da Veiga Moreira et al. (2017)
S. cerevisiae *Torulaspora delbrueckii*	Chocolate	Hybrids of cocoa: PS1319 and SJ02 de Brazil	2,3-Butanediol	Visintin et al. (2017)
P. kluyveri *Kluyveromyces marxianus*	Chocolate	Forastero from Ghana	2-pentanol, 1,3-Butanediol, 2,3-Butaandiol, 2-Methylbutanal, 2-Phenyl-2-butenal, Ethyl phenylacetate, Ethyl decanoate, Ethyl phenylacetate, 2-Heptanone, 2-nonanone, Linalool, trans-Linalool oxide (pyranoid), β-myrcene	Crafack et al. (2014)

1.3.4. SSF kinetics through mathematical modeling and its application in cocoa

A mathematical model serve as tools for engineers and scientists to develop an understanding of important systems and processes using mathematical equations (Ribas-García et al., 2011; Rasmuson, 2014), is an important instrument which allows understanding the behavior of food, predict results (Pinheiro et al., 2017), generalize the processes evaluating the optimal conditions that lead them (Kulov and Gordeev, 2014) and generate insurance control mechanisms for process quality (Balbinoti et al., 2018). A realistic kinetic model is required for the design, optimization and control of processes (Ccopa

Rivera et al., 2017). The SSF is driven by a complex interaction between various microorganisms and their metabolites. To control this process, and consequently the quality of the final product, a deep understanding of this interaction is necessary (Nielsen et al., 2014). Then, the optimal parameters to control the process can be determined through the development of kinetic models for the process (Liu et al., 2016). For example, progress has already been made in describing the process of SSF conducted by *S. cerevisiae* in the production of rice wine, for which a first-order kinetic model based on the analysis of the main metabolites of fermentation has been developed (Liu et al., 2015). In the case of cocoa, there have been some attempts to study the transition of the microbial population in heap fermentation, but there are no detailed studies of its kinetics (Ghosh, 2016). Recently (Moreno-Zambrano et al., 2018), has constructed a mathematical model using ordinary differential equations with two distinct types of state variables: (i) metabolite concentrations of glucose, fructose, ethanol, lactic acid and acetic acid and (ii) population sizes of yeast, LAB and AAB. However, it is worth mentioning that the spontaneous fermentation process will be specific for each batch of cocoa, therefore it will be necessary to develop a controlled fermentation that is a standard reference for the batches and thus be able to produce cocoa of the most uniform quality possible.

The study of SSF involves the determination of fermentation kinetics (e.g., biomass production, substrate consumption and production of metabolites). The data collection comprises the measurement of microbial growth quantified by standard methods of isolation and metabolic activity with high-performance liquid chromatography (HPLC) (Nielsen et al., 2014). Kinetic models use parameters that describe how quickly a microorganism can grow, such as the duration of the lag phase and generation time, and those models are used as the response variable for various conditions of pH, temperature, and water activity (Adams and Moss, 2008). Studies have demonstrated the utility of kinetic models that can predict cell growth and ethanol production from sugarcane fermentations (Ccopa Rivera et al., 2017). The influence of fermentation practices on the dynamics of the microbial population over 3 days in National cocoa (a type of fine cocoa) has been studied; analyzing the pulp and bean metabolites and sensory analysis of the chocolates produced from both fermentations (Papalexandratou et al., 2011); however, they did not develop a kinetic model that allows predicting the behavior

of the process. In SSF the water content of the solid substrate is usually maintained between 12 and 80% (Chen, 2013). The most important consideration for kinetics is the formation of biomass, either linear (equation 1.3-1), exponential (equation 1.3-2), logarithmic (equation 1.3-3) or two-phase formation (equation 1.3-4) (Ghosh, 2016). Where K is the linear growth rate, μ is the specific growth rate, x is the biomass at a time t, xm is the maximum biomass, ta is the time when the deceleration phase begins, k is the first order constant and L is a ratio between the growth rate in the deceleration phase and the specific growth rate during the exponential phase. It is still unknown to extent these calculations are valid in food processing SSF (Ghosh, 2016).

$$\frac{dx}{dt} = K \tag{1.3-1}$$

$$\frac{dx}{dt} = \mu x \tag{1.3-2}$$

$$\frac{dx}{dt} = \mu x \left[1 - \left(\frac{x}{x_m} \right) \right] \tag{1.3-3}$$

$$\frac{dx}{dt} = \left[\mu L e^{-k(t-t_0)} \right] x, t > t_0 \tag{1.3-4}$$

Previous studies suggest that the cotyledon of cocoa absorbs the aromatic components of the pulp during the fermentation process (Eskes et al., 2012). This cotyledon is considered a reservoir for fine notes (Chetschik et al., 2017); however, the exact mechanism by which this situation is reached and the role of the fermentation microflora in this process has not been investigated (Ali et al., 2013). The fine aroma precursors produced in the pulp during the fermentation phase will migrate into the bean when the permeability of the bean is improved and are then retained during the drying phase (Ascrizzi et al., 2017); then, the diffusion of aroma precursors into the Criollo and Forastero cocoa bean is possible; for example, during the process of fermentation of cocoa, the amino acid phenylalanine (external precursor) produced by bacillus in the pulp of cocoa can enter the bean by molecular diffusion and accumulate inside to join the amino acids (internal precursors) already produced during the internal reaction of the VCG, this way increase the amount of aroma precursors (Fig. I-1). The bean shell would be the barrier for this diffusion and its structure would determine the speed of this phenomenon and therefore the speed of the process to obtain an optimal

value. Theoretically, this process is characterized by the coefficient of molecular diffusion D. The experimental determination of this coefficient is indispensable to describe the process of mass transfer via Fick's Second Law (Koukouch et al., 2017) in a non-stationary state.

In other studies, it has been demonstrated that fermentations with added passion fruit pulp showed more pronounced aromas of interest, namely, fruit, acid and floral notes in cocoa beans (Ali et al., 2013). In the cucumber fermentation process, the exchange of malic acid, lactic acid, NaCl and sugar between the cucumber and its brine was monitored; an exponential equation that described the movement of the solutes during the fermentation was described, and the diffusion coefficient of the sugar was estimated between 1.80×10^{-9} and 9.18×10^{-9} m2/s, which was used to determine the optimal concentration of sugar within the cucumber at any time; to determine processing parameters in manufacturing, this process was modeled mathematically (Fasina et al., 2002). If this phenomenon occurs in the aforementioned food systems, it will also happen in the process of fermentation of Criollo and Forastero cocoa, where it will be necessary to characterize the phenomenon of transfer of aroma precursors to the interior of the bean to establish an optimal process time. In the case of Criollo de Amazonas cocoa, it is possible that the current fermentation time of 7 days is excessive and it would be risking the aromatic quality of the cocoa to obtain an acceptable percentage of fermentation. During the last decade, the analysis and the modeling of the kinetics of the convective drying of cocoa beans were the scope of several papers (Hii et al., 2008; Hii et al., 2009b; Hii et al., 2009a; Clement et al., 2009; MacManus Chinenye et al., 2010; Teh et al., 2016; Nwakuba et al., 2017; Olabinjo et al., 2017; Herman et al., 2018) leaving a side the study of the kinetic of formation and diffusion of aroma precursors through mathematical models that allow to improve processes, even more so in Criollo cacao there have been no advances.

1.4. Conclusions

The cocoa market has divided this product into fine aroma and bulk. Because bulk beans are more productive and resistant to diseases, studies are being carried out with the aim of improving their quality. The technology developed for this purpose is the use of starter cultures that help the fermentation

process making it more efficient, this culture will be mainly composed of yeasts, since they would be the most important microorganisms. However, this technology has not been widely adopted by cocoa farmers, at least in Peru the traditional process of spontaneous fermentation has been carried out for all varieties of cocoa, including Criollo and Forastero. To achieve the expected quality results, it is necessary to study the production of external aroma precursors by the microorganisms and the diffusion of these precursors towards the interior of the bean and how they come to be added to the internally generated precursors until reaching optimum concentrations. The study of this phenomenon of molecular diffusion must be carried out through mathematical modeling in order to predict these concentrations in a determined time. We consider it necessary to know in depth the process of fermentation of Criollo cocoa, the process of diffusion of external precursors and isolate the microorganisms founded in the process, from this, develop starter cultures that can be applied to the process of fermentation of cocoa in Forastero (bulk). Undoubtedly, the both origin and genetic factors will play an important role that should not be left aside.

Declarations

Author contribution statement. All authors listed have significantly contributed to the development and the writing of this article.

Competing interest statement. The authors declare no conflict of interest.

Additional information. No additional information is available for this paper.

1.5. References

Adams, M.R., Moss, M.O., 2008. Food Microbiology, third ed. RSC Publishing, Cambridge, UK, pp. 20-52.

Afoakwa, E.O., 2010. Chocolate Science and Technology. Wiley-Blackwell, Chichester, U.K.; Ames, Iowa, pp. 58-71.

Afoakwa, E.O., Paterson, A., Fowler, M., Ryan, A., 2008. Flavor formation and character in cocoa and chocolate: a critical review. Crit. Rev. Food Sci. Nutr. 48, 840-857.

Afoakwa, E.O., Quao, J., Budu, A.S., Takrama, J., Saalia, F.K., 2011. Effect of pulp preconditioning on acidification, proteolysis, sugars and free fatty acids concentration during fermentation of cocoa (Theobroma cacao) beans. Int. J. Food Sci. Nutr. 62, 755-764.

Ali, N.A., Baccus-Taylor, G.S.H., Sukha, D.A., Umaharan, P., 2013. The effect of cacao (*Theobroma cacao* L.) pulp on final flavour. In: III International Conference on Postharvest and Quality Management of Horticultural Products of Interest for Tropical Regions 1047, pp. 245-254.

Álvarez, C., Pérez, E., Boulanger, R., Lares, M., Ssemat, As, Davrieux, F., Emile, C., 2012. Identificaci_on de los compuestos arom_aticos en el cacao Criollo de Venezuela usando microextracci_on en fase s_olida y cromatografía de gases. Vitae 19, S370-S372. Disponible en: http://www.redalyc.org/articulo.oa?id=169823914116.

Álvarez, C., 2016. Identification of the volatile compounds in the roasting Venezuela criollo cocoa beans by gas chromatography-spectrometry mass. J. Nutr. Health Food Eng. 5 (4), 00178.

Apriyanto, M., Sutardi, S., Supriyanto, S., Harmayani, E., 2017. Amino acid analysis of cocoa fermented by high performance liquid chromatography (HPLC). Asian J. Dairy Food Res. 36, 156-160.

Aprotosoaie, A.C., Luca, S.V., Miron, A., 2016. Flavor chemistry of cocoa and cocoa products-An overview. Compr. Rev. Food Sci. Food Saf. 15, 73-91.

Ardhana, M., 2003. The microbial ecology of cocoa bean fermentations in Indonesia. Int. J. Food Microbiol. 86, 87-99.

Ascrizzi, R., Flamini, G., Tessieri, C., Pistelli, L., 2017. From the raw seed to chocolate: volatile profile of blanco de Criollo in different phases of the processing chain. Microchem. J. 133, 474-479.

Balbinoti, T.C.V., Jorge, L.M. de M., Jorge, R.M.M., 2018. Mathematical modeling of paddy (Oryza sativa) hydration in different thermal conditions assisted by Raman spectroscopy. J. Cereal. Sci. 79, 390-398.

Batista, N.N., Ramos, C.L., Dias, D.R., Pinheiro, A.C.M., Schwan, R.F., 2016. The impact of yeast starter cultures on the microbial communities and volatile compounds in cocoa fermentation and the resulting sensory attributes of chocolate. J. Food Sci. Technol. 53, 1101-1110.

Beckett, S.T. (Ed.), 2009. Industrial Chocolate Manufacture and Use, fourth ed. Wiley-Blackwell, Chichester, U.K.; Ames, Iowa, pp. 169-188.

Belitz, H.-D., Grosch, W., Schieberle, P., 2009. Food Chemistry, fourth ed. Springer Berlin Heidelberg, Berlin, Heidelberg, pp. 340-400.

Besson, I., Creuly, C., Gros, J.B., Larroche, C., 1997. Pyrazine production by Bacillus subtilis in solid-state fermentation on soybeans. Appl. Microbiol. Biotechnol. 47, 489-495.

Camu, N., De Winter, T., Verbrugghe, K., Cleenwerck, I., Vandamme, P., Takrama, J.S., Vancanneyt, M., De Vuyst, L., 2007. Dynamics and biodiversity of populations of lactic acid bacteria and acetic acid bacteria involved in spontaneous heap fermentation of cocoa beans in Ghana. Appl. Environ. Microbiol. 73, 1809-1824.

Carrau, F.M., Medina, K., Boido, E., Farina, L., Gaggero, C., Dellacassa, E., Versini, G., Henschke, P.A., 2005. De novo synthesis of monoterpenes by Saccharomyces cerevisiae wine yeasts. FEMS Microbiol. Lett. 243, 107-115.

Cevallos-Cevallos, J.M., Gysel, L., Maridueña-Zavala, M.G., Molina-Miranda, M.J., 2018. Time-related changes in volatile compounds during fermentation of bulk and fine-flavor cocoa (Theobroma cacao) beans. J. Food Qual. 2018, 1-14.

Ccopa Rivera, E., Yamakawa, C.K., Saad, M.B.W., Atala, D.I.P., Ambrosio, W.B., Bonomi, A., Nolasco Junior, J., Rossell, C.E.V., 2017. Effect of temperature on sugarcane ethanol fermentation: kinetic modeling and validation under very-highgravity fermentation conditions. Biochem. Eng. J. 119, 42-51.

Chen, H., 2013. Modern Solid State Fermentation: Theory and Practice. Springer Science & Business Media, pp. 23-74.

Chetschik, I., Kneubuhl, M., Chatelain, K., Schl€uter, A., Bernath, K., H€uhn, T., 2017. Investigations on the aroma of cocoa pulp (Theobroma cacao L.) and its influence on the odor of fermented cocoa beans. J. Agric. Food Chem. 66 (10), 2467-2472.

Clement, A.D., Emmanuel, A.N., Patrice, K., Benjamin, Y.K., 2009. Mathematical modelling of sun drying kinetics of thin layer cocoa (Theobroma cacao) beans. J. Appl. Sci. Res. 5, 1110-1116. https://www.researchgate.net/publication/228508629_Mathematical_Modelling_ of_Sun_Drying_Kinetics_of_Thin_Layer_Cocoa_Theobroma_Cacao_Beans.

Counet, C., Ouwerx, C., Rosoux, D., Collin, S., 2004. Relationship between procyanidins and flavor contents of cocoa liquors from different origins. J. Agric. Food Chem. 52, 6243-6249.

Crafack, M., Keul, H., Eskildsen, C.E., Petersen, M.A., Saerens, S., Blennow, A., Skovmand-Larsen, M., Swiegers, J.H., Petersen, G.B., Heimdal, H., Nielsen, D.S., 2014. Impact of starter cultures and fermentation techniques on the volatile aroma and sensory profile of chocolate. Food Res. Int. 63, 306-316.

Crafack, M., Mikkelsen, M.B., Saerens, S., Knudsen, M., Blennow, A., Lowor, S., Takrama, J., Swiegers, J.H., Petersen, G.B., Heimdal, H., Nielsen, D.S., 2013. Influencing cocoa flavour using Pichia kluyveri and Kluyveromyces marxianus in a defined mixed starter culture for cocoa fermentation. Int. J. Food Microbiol. 167, 103-116.

De Boer, L., Dijkhuizen, L., 1990. Microbial and enzymatic processes for Lphenylalanine production. Microb. Bioprod. 1-27.

de Melo Pereira, G.V., Magalhães, K.T., de Almeida, E.G., da Silva Coelho, I., Schwan, R.F., 2013. Spontaneous cocoa bean fermentation carried out in a novel-design stainless steel tank: influence on the dynamics of microbial populations and physicalechemical properties. Int. J. Food Microbiol. 161, 121-133.

Diab, J., Hertz-Schunemann, R., Streibel, T., Zimmermann, R., 2014. Online measurement of volatile organic compounds released during roasting of cocoa beans. Food Res. Int. 63, 344-352.

Eskes, A., Ahnert, D., Assemat, S., Seguine, E., 2012. Evidence for the Effect of the cocoa Bean Flavor Environment during Fermentation on the Final Flavor Profile of cocoa Liquor and Chocolate. INGENIC Newsletter. Available on: https://agritrop. cirad.fr/568108/1/document_568108.pdf (Accessed 30 October 2017).

Fasina, O., Fleming, H., Thompson, R., 2002. Mass transfer and solute diffusion in brined cucumbers. J. Food Sci. 67, 181-187.

FEMA, 2018. About FEMA j FEMA [WWW Document]. https://www.femaflavor. org/about (Accessed 27 September 2018).

Fernández Maura, Y., Balzarini, T., Clapé Borges, P., Evrard, P., De Vuyst, L., Daniel, H.-M., 2016. The environmental and intrinsic yeast diversity of Cuban cocoa bean heap fermentations. Int. J. Food Microbiol. 233, 34-43.

Frauendorfer, F., Schieberle, P., 2008. Changes in key aroma compounds of Criollo cocoa beans during roasting. J. Agric. Food Chem. 56, 10244-10251.

Ghosh, J.S., 2016. Solid state fermentation and food processing: a short review. J. Nutr. Food Sci. 06, 1-7.

Giacometti, J., Jolic, S.M., Josic, D., 2015. Cocoa processing and impact on composition. In: Preedy, V. (Ed.), Processing and Impact on Active Components in Food. Elsevier, pp. 605-612.

Hashemi, M., Mousavi, S.M., Razavi, S.H., Shojaosadati, S.A., 2011. Mathematical modeling of biomass and a-amylase production kinetics by Bacillus sp. in solidstate fermentation based on solid dry weight variation. Biochem. Eng. J. 53, 159-164.

Hashim, P., Selamat, J., Muhammad, S., Kharidah, S., Ali, A., 1998. Changes in free amino acid, peptide-N, sugar and pyrazine concentration during cocoa fermentation. J. Sci. Food Agric. 78, 535-542.

Herman, C., Spreutels, L., Turomzsa, N., Konagano, E.M., Haut, B., 2018. Convective drying of fermented Amazonian cocoa beans (Theobroma cacao var. Forasteiro). Experiments and mathematical modeling. Food Bioprod. Process. 108, 81-94.

Hii, C.L., Law, C.L., Cloke, M., 2009a. Modeling using a new thin layer drying model and product quality of cocoa. J. Food Eng. 90, 191-198.

Hii, C.L., Law, C.L., Cloke, M., 2008. Modelling of thin layer drying kinetics of cocoa beans during artificial and natural drying. J. Eng. Sci. Technol. 3, 1-10. https://www.revistavirtualpro.com/biblioteca/modelado-de-cinetica-de-secado-decapa-fina-de-granos-de-cacao-durante-secado-artificial-y-natural.

Hii, C.L., Law, C.L., Cloke, M., Suzannah, S., 2009b. Thin layer drying kinetics of cocoa and dried product quality. Biosyst. Eng. 102, 153-161.

Ho, V.T.T., Fleet, G.H., Zhao, J., 2018. Unravelling the contribution of lactic acid bacteria and acetic acid bacteria to cocoa fermentation using inoculated organisms. Int. J. Food Microbiol. 279, 43-56.

ICCO, 2017a. Study of the Chemical, Physical and Organoleptic Parameters to Establish the Difference between Fine and Bulk Cocoa [WWW Document]. URL. https://www.icco.org/about-cocoa/fine-or-flavour-cocoa/10-projects/144-study-the-chemical-physical-and-organoleptic-parameters-to-establish-the-difference-between-fine-and-bulk-cocoa.html (Accessed 17 May 2017).

ICCO, 2017b. Fine or Flavour Cocoa [WWW Document]. https://www.icco.org/about-cocoa/fine-or-flavour-cocoa.html (Accessed 17 May 2017).

Jamili, J., 2016. Diversity and the role of yeast in spontaneous cocoa bean fermentation from Southeast Sulawesi, Indonesia. Biodiversitas J. Biol. Divers. 17, 90-95.

Janek, K., Niewienda, A., Wöstemeyer, J., Voigt, J., 2016. The cleavage specificity of the aspartic protease of cocoa beans involved in the generation of the cocoaspecific aroma precursors. Food Chem. 211, 320-328.

John, W.A., Kumari, N., Böttcher, N.L., Koffi, K.J., Grimbs, S., Vrancken, G., D'Souza, R.N., Kuhnert, N., Ullrich, M.S., 2016. Aseptic artificial fermentation of cocoa beans can be fashioned to replicate the peptide profile of commercial cocoa bean fermentations. Food Res. Int. 89, 764-772.

Kadow, D., Niemenak, N., Rohn, S., Lieberei, R., 2015. Fermentation-like incubation of cocoa seeds (Theobroma cacao L.) e reconstruction and guidance of the fermentation process. LWT - Food Sci. Technol. 62, 357-361.

Koffi, O., Samagaci, L., Goualie, B., Niamke, S., 2018. Screening of potential yeast starters with high ethanol production for a small-scale cocoa fermentation in Ivory Coast. Food Environ. Saf. 17, 113-130. http://www.fia.usv.ro/fiajournal/index. php/FENS/article/view/572.

Koné, M.K., Guéhi, S.T., Durand, N., Ban-Koffi, L., Berthiot, L., Tachon, A.F., Brou, K., Boulanger, R., Montet, D., 2016. Contribution of predominant yeasts to the occurrence of aroma compounds during cocoa bean fermentation. Food Res. Int. 89, 910-917.

Kongor, J.E., Hinneh, M., de Walle, D.V., Afoakwa, E.O., Boeckx, P., Dewettinck, K., 2016. Factors influencing quality variation in cocoa (*Theobroma cacao*) bean flavour profile d a review. Food Res. Int. 82, 44-52.

Koukouch, A., Idlimam, A., Asbik, M., Sarh, B., Izrar, B., Bostyn, S., Bah, A., Ansari, O., Zegaoui, O., Amine, A., 2017. Experimental determination of the

effective moisture diffusivity and activation energy during convective solar drying of olive pomace waste. Renew. Energy 101, 565-574.

Kulov, N.N., Gordeev, L.S., 2014. Mathematical modeling in chemical engineering and biotechnology. Theor. Found. Chem. Eng. 48, 225-229.

Kumari, N., Kofi, K.J., Grimbs, S., D'Souza, R.N., Kuhnert, N., Vrancken, G., Ullrich, M.S., 2016. Biochemical fate of vicilin storage protein during fermentation and drying of cocoa beans. Food Res. Int. 90, 53-65.

Lefeber, T., Janssens, M., Camu, N., De Vuyst, L., 2010. Kinetic analysis of strains of lactic acid bacteria and acetic acid bacteria in cocoa pulp simulation media toward development of a starter culture for cocoa bean fermentation. Appl. Environ. Microbiol. 76, 7708-7716.

Lima, L.J.R., Almeida, M.H., Nout, M.J.R., Zwietering, M.H., 2011. Theobroma cacao L., "The Food of the Gods": quality determinants of commercial cocoa beans, with particular reference to the impact of fermentation. Crit. Rev. Food Sci. Nutr. 51, 731-761.

Liu, D., Zhang, H., Lin, C.-C., Xu, B., 2016. Optimization of rice wine fermentation process based on the simultaneous saccharification and fermentation kinetic model. Chin. J. Chem. Eng. 24, 1406-1412.

Liu, D., Zhang, H., Xu, B., Tan, J., 2015. Development of a kinetic model structure for simultaneous saccharification and fermentation in rice wine production: kinetic model structure for simultaneous saccharification and fermentation. J. Inst. Brew. 121, 589-596.

MacManus Chinenye, N., Ogunlowo, A., Olukunle, O., 2010. Cocoa bean (*Theobroma cacao* L.) drying kinetics. Chil. J. Agric. Res. 70, 633-639.

Magalhães da Veiga Moreira, I., de Figueiredo Vilela, L., da Cruz Pedroso Miguel, M., Santos, C., Lima, N., Freitas Schwan, R., 2017. Impact of a microbial cocktail used as a starter culture on cocoa fermentation and chocolate flavor. Molecules 22, 766.

Magalhães da Veiga Moreira, I., Gabriela da Cruz Pedrozo Miguel, M., Lacerda Ramos, C., Ferreira Duarte, W., Efraim, P., Freitas Schwan, R., 2016. Influence of cocoa hybrids on volatile compounds of fermented beans, microbial diversity during fermentation and sensory characteristics and acceptance of chocolates: cocoa hybrids influenced chocolate quality. J. Food Qual. 39, 839-849.

Menezes, A.G.T., Batista, N.N., Ramos, C.L., Silva, A.R. de A. e, Efraim, P., Pinheiro, A.C.M., Schwan, R.F., 2016. Investigation of chocolate produced from four different Brazilian varieties of cocoa (*Theobroma cacao* L.) inoculated with Saccharomyces cerevisiae. Food Res. Int. 81, 83-90.

Moreno-Zambrano, M., Grimbs, S., Ullrich, M.S., Hütt, M.T., 2018. A mathematical model of cocoa bean fermentation. R. Soc. Open Sci. 5, 180964.

Mota-Gutierrez, J., Botta, C., Ferrocino, I., Giordano, M., Bertolino, M., Dolci, P., Cannoni, M., Cocolin, L., 2018. Dynamics and biodiversity of bacterial and yeast communities during fermentation of cocoa beans. Appl. Environ. Microbiol. 84.

Nielsen, D.S., Arneborg, N., Jespersen, L., 2014. Mixed microbial fermentations and methodologies for their investigation. In: Schwan, R.F., Fleet, G. (Eds.), Cocoa and Coffee Fermentations. CRC Press/Taylor & Francis, pp. 1-42.

Nielsen, D.S., Teniola, O.D., Ban-Koffi, L., Owusu, M., Andersson, T.S., Holzapfel, W.H., 2007. The microbiology of Ghanaian cocoa fermentations analysed using culture-dependent and culture-independent methods. Int. J. Food Microbiol. 114, 168-186.

Nwakuba, N.R., Ejesu, P.K., Okafor, V.C., 2017. A mathematical model for predicting the drying rate of cocoa bean (Theobroma cacao L.) in a hot air dryer. Agric. Eng. Int. CIGR J 19 (3), 195-202. https://www.researchgate.net/publication/320336317_A_mathematical_model_for_predicting_the_drying_rate of_cocoa_bean_Theobroma_cacao_L_in_a_hot_air_dryer.

Olabinjo, O.O., Olajide, J.O., Olalusi, A.P., 2017. Mathematical modeling of sun and solar drying kinetics of fermented cocoa beans. Int. J. Environ. Agric. Biotechnol. 2, 2419-2426.

Ouattara, H.G., Koffi, B.L., Karou, G.T., Sangar_e, A., Niamke, S.L., Diopoh, J.K., 2008. Implication of Bacillus sp. in the production of pectinolytic enzymes during cocoa fermentation. World J. Microbiol. Biotechnol. 24, 1753-1760.

Ouattara, H.G., Reverchon, S., Niamke, S.L., Nasser, W., 2017. Regulation of the synthesis of pulp degrading enzymes in Bacillus isolated from cocoa fermentation. Food Microbiol. 63, 255-262.

Owens, J.D., Allagheny, N., Kipping, G., Ames, J.M., 1997. Formation of volatile compounds during Bacillus subtilis fermentation of soya beans. J. Sci. Food Agric. 74, 132-140.

Papalexandratou, Z., Falony, G., Romanens, E., Jimenez, J.C., Amores, F., Daniel, H.-M., De Vuyst, L., 2011. Species diversity, community dynamics, and metabolite kinetics of the microbiota associated with traditional Ecuadorian spontaneous cocoa bean fermentations. Appl. Environ. Microbiol. 77, 7698-7714.

Papalexandratou, Z., Lefeber, T., Bahrim, B., Lee, O.S., Daniel, H.-M., De Vuyst, L., 2013. Hanseniaspora opuntiae, Saccharomyces cerevisiae, Lactobacillus fermentum, and Acetobacter pasteurianus predominate during wellperformed Malaysian cocoa bean box fermentations, underlining the importance of these microbial species for a successful cocoa bean fermentation process. Food Microbiol. 35, 73-85.

Papalexandratou, Z., Nielsen, D.S., 2016. It's gettin' hot in here: breeding robust yeast starter cultures for cocoa fermentation. Trends Microbiol. 24, 166-168.

Pedan, V., Fischer, N., Bernath, K., H€uhn, T., Rohn, S., 2017. Determination of oligomeric proanthocyanidins and their antioxidant capacity from different chocolate manufacturing stages using the NP-HPLC-online-DPPH methodology. Food Chem. 214, 523-532.

Pereira, G.V.M., Alvarez, J.P., Neto, D.P. de C., Soccol, V.T., Tanobe, V.O.A., Rogez, H., G_oes-Neto, A., Soccol, C.R., 2017. Great intraspecies diversity of Pichia kudriavzevii in cocoa fermentation highlights the importance of yeast strain selection for flavor modulation of cocoa beans. LWT - Food Sci. Technol. 84, 290-297.

Pereira, G.V. d. M., Miguel, M.G. d. C.P., Ramos, C.L., Schwan, R.F., 2012. Microbiological and physicochemical characterization of small-scale cocoa fermentations and screening of yeast and bacterial strains to develop a defined starter culture. Appl. Environ. Microbiol. 78, 5395-5405.

Pereira, G.V. de M., Soccol, V.T., Soccol, C.R., 2016. Current state of research on cocoa and coffee fermentations. Curr. Opin. Food Sci. 7, 50-57.

Pinheiro, A.D.T., da Silva Pereira, A., Barros, E.M., Antonini, S.R.C., Cartaxo, S.J.M., Rocha, M.V.P., Goncalves, L.R.B., 2017. Mathematical modeling of the ethanol fermentation of cashew apple juice by a flocculent yeast: the effect of initial substrate concentration and temperature. Bioproc. Biosyst. Eng. 40, 1221-1235.

Qin, X.-W., Lai, J.-X., Tan, L.-H., Hao, C.-Y., Li, F.-P., He, S.-Z., Song, Y.-H., 2016. Characterization of volatile compounds in Criollo, Forastero, and Trinitario cocoa seeds (Theobroma cacao L.) in China. Int. J. Food Prop. 1-15.

Ramos, C.L., Dias, D.R., Miguel, M.G. da C.P., Schwan, R.F., 2014. Impact of different cocoa hybrids (Theobroma cacao L.) and S. cerevisiae UFLA CA11 inoculation on microbial communities and volatile compounds of cocoa fermentation. Food Res. Int. 64, 908-918.

Rasmuson, A., 2014. Mathematical Modeling in Chemical Engineering. Cambridge University Press, United Kingdom ; New York.

Ribas-García, M., Hurtado-Vargas, R., Garrido-Carralero, N., Domenech-López, F., Sabadí-Díaz, R., 2011. Metodología para la modelaci_on matem_atica de procesos. Caso de estudio, fermentaci_on alcoh_olica. ICIDCA Sobre Los Deriv. Ca~na Az_ucar 45.

Rodriguez-Campos, J., Escalona-Buendía, H.B., Contreras-Ramos, S.M., Orozco-Avila, I., Jaramillo-Flores, E., Lugo-Cervantes, E., 2012. Effect of fermentation time and drying temperature on volatile compounds in cocoa. Food Chem. 132, 277-288.

Rodriguez-Campos, J., Escalona-Buendía, H.B., Orozco-Avila, I., Lugo-Cervantes, E., Jaramillo-Flores, M.E., 2011. Dynamics of volatile and nonvolatile compounds in cocoa (Theobroma cacao L.) during fermentation and drying processes using principal components analysis. Food Res. Int. 44, 250-258.

Romanens, E., Näf, R., Lobmaier, T., Pedan, V., Leischtfeld, S.F., Meile, L., Schwenninger, S.M., 2018. A lab-scale model system for cocoa bean fermentation. Appl. Microbiol. Biotechnol. 102, 3349-3362.

Saltini, R., Akkerman, R., Frosch, S., 2013. Optimizing chocolate production through traceability: a review of the influence of farming practices on cocoa bean quality. Food Control 29, 167-187.

Samagaci, L., Ouattara, H., Niamk_e, S., Lemaire, M., 2016. Pichia kudrazevii and Candida nitrativorans are the most well-adapted and relevant yeast species fermenting cocoa in Agneby-Tiassa, a local Ivorian cocoa producing region. Food Res. Int. 89, 773-780.

Sandhya, M.V.S., Yallappa, B.S., Varadaraj, M.C., Puranaik, J., Rao, L.J., Janardhan, P., Murthy, P.S., 2016. Inoculum of the starter consortia and interactive metabolic process in enhancing quality of cocoa bean (Theobroma cacao) fermentation. LWT - Food Sci. Technol. 65, 731-738.

Sánchez Blanco, A., Palacios Durive, O., Batista P_erez, S., Díaz Montes, Z., Pérez Guerra, N., 2016. Simultaneous production of amylases and proteases by Bacillus subtilis in brewery wastes. Braz. J. Microbiol. 47, 665-674.

Saputro, A.D., Van de Walle, D., Hinneh, M., Van Durme, J., Dewettinck, K., 2018. Aroma profile and appearance of dark chocolate formulated with palm sugaresucrose blends. Eur. Food Res. Technol. 244, 1281-1292.

Schwan, R.F., 1998. Cocoa fermentations conducted with a defined microbial cocktail inoculum. Appl. Environ. Microbiol. 64, 1477-1483. https://www.ncbi.nlm.nih.gov/pmc/articles/PMC106173/.

Schwan, R.F., Wheals, A.E., 2004. The microbiology of cocoa fermentation and its role in chocolate quality. Crit. Rev. Food Sci. Nutr. 44, 205-221.

Selamat, J., Harun, S.M., others, 1994. Formation of methyl pyrazine during cocoa bean fermentation. Pertanika J. Trop. Agric. Sci. 17, 27-32. http://www.pertanika. upm.edu.my/Pertanika%20PAPERS.

Sukha, D.A., Bharath, S.M., Ali, N.A., Umaharan, P., 2013. An assessment of the quality attributes of the Imperial College Selections (ICS) cacao (Theobroma cacao L.) clones. In: III International Conference on Postharvest and Quality Management of Horticultural Products of Interest for Tropical Regions, pp. 237-243.

Sukha, D.A., Umaharan, P., Butler, D.R., 2017. The impact of pollen donor on flavor in cocoa. J. Am. Soc. Hortic. Sci. 142, 13-19.

Teh, Q.T.M., Tan, G.L.Y., Loo, S.M., Azhar, F.Z., Menon, A.S., Hii, C.L., 2016. The drying kinetics and polyphenol degradation of cocoa beans: cocoa drying and polyphenol degradation. J. Food Process. Eng. 39, 484-491.

Torres-Moreno, M., Tarrega, A., Costell, E., Blanch, C., 2012. Dark chocolate acceptability: influence of cocoa origin and processing conditions. J. Sci. Food Agric. 92, 404-411.

Tran, P.D., Van de Walle, D., De Clercq, N., De Winne, A., Kadow, D., Lieberei, R., Messens, K., Tran, D.N., Dewettinck, K., Van Durme, J., 2015. Assessing cocoa aroma quality by multiple analytical approaches. Food Res. Int. 77, 657-669.

Van Durme, J., Ingels, I., De Winne, A., 2016. Inline roasting hyphenated with gas chromatographyemass spectrometry as an innovative approach for assessment of cocoa fermentation quality and aroma formation potential. Food Chem. 205, 66-72.

Vargas Jentzsch, P., Ciobot_a, V., Salinas, W., Kampe, B., Aponte, P.M., Rösch, P., Popp, J., Ramos, L.A., 2016. Distinction of Ecuadorian varieties of fermented cocoa beans using Raman spectroscopy. Food Chem. 211, 274-280.

Vázquez-Ovando, A., Ovando-Medina, I., Adriano-Anaya, L., Betancur-Ancona, D., Salvador-Figueroa, M., 2016. Alcaloides y polifenoles del cacao, mecanismos

que regulan su biosíntesis y sus implicaciones en el sabor y aroma. Arch. Latinoam. Nutr. 66, 239-254. https://medes.com/publication/117717.

Visintin, S., Ramos, C.L., Batista, N.N., Dolci, P., Schwan, R.F., Cocolin, L., 2017. Impact of Saccharomyces cerevisiae and Torulaspora delbrueckii starter cultures on cocoa beans fermentation. Int. J. Food Microbiol. 257, 31-40.

Visintin, S., Alessandria, V., Valente, A., Dolci, P., Cocolin, L., 2016. Molecular identification and physiological characterization of yeasts, lactic acid bacteria and acetic acid bacteria isolated from heap and box cocoa bean fermentations in West Africa. Int. J. Food Microbiol. 216, 69-78.

Voigt, J., 2009. Origin of the chocolate-specific flavour notes: essential precursors are generated by proteolysis of a cocoa storage protein. Agro Food Ind. Hi-Tech 20 (6), 26-28. https://www.researchgate.net/publication/286122942_Origin_of_the_chocolates pecific_flavour_notes_Essential_precursors_are_generated_by_proteolysis_of_ a_cocoa_storage_protein.

Voigt, J., Biehl, B., Heinrichs, H., Kamaruddin, S., Marsoner, G.G., Hugi, A., 1994. In-vitro formation of cocoa-specific aroma precursors: aroma-related peptides generated from cocoa-seed protein by co-operation of an aspartic endoprotease and a carboxypeptidase. Food Chem. 49, 173-180.

Voigt, J., Janek, K., Textoris-Taube, K., Niewienda, A., Wöstemeyer, J., 2016. Partial purification and characterisation of the peptide precursors of the cocoa-specific aroma components. Food Chem. 192, 706-713.

Voigt, J., Lieberei, R., 2014. Biochemistry of cocoa fermentation. In: Cocoa and Coffee Fermentations. CRC Press/Taylor & Francis, pp. 193-206.

Ziegleder, G., 1990. Linalool contents as characteristic of some flavor grade cocoas. Z. Für Leb. -Forsch. A 191, 306-309. https://link.springer.com/article/10.1007/BF01202432.

CAPÍTULO II. ANÁLISIS BIBLIOMÉTRICO

2.1. Análisis bibliométrico

2.1.1. Ecuación de búsqueda

En la base de datos de Scopus se construyó la ecuación de búsqueda usando palabras clave por separado, de la siguiente manera: cocoa + butter + crystallization + chocolate. Posteriormente se redefinió la ecuación limitando la búsqueda a las áreas de interés relacionadas con el tema de los alimentos y se excluyó las áreas que no están relacionadas a los alimentos, obteniendo un total de 819 documentos publicados hasta la actualidad (año 2022). La ecuación de búsqueda quedó como se muestra en la siguiente tabla:

Tabla 2.1-1. Ecuación de búsqueda generada en Scopus.

cocoa AND butter AND crystallization AND chocolate AND (LIMIT-TO (SUBJAREA , "AGRI") OR LIMIT-TO (SUBJAREA , "CHEM") OR LIMIT-TO (SUBJAREA , "CENG") OR LIMIT-TO (SUBJAREA , "ENGI") OR LIMIT-TO (SUBJAREA , "BIOC") OR LIMIT-TO (SUBJAREA , "MATE")) AND (EXCLUDE (SUBJAREA , "PHYS") OR EXCLUDE (SUBJAREA , "IMMU") OR EXCLUDE (SUBJAREA , "MEDI") OR EXCLUDE (SUBJAREA , "SOCI")) AND (EXCLUDE (SUBJAREA , "NURS") OR EXCLUDE (SUBJAREA , "PHAR") OR EXCLUDE (SUBJAREA , "ENER") OR EXCLUDE (SUBJAREA , "ENVI")) AND (EXCLUDE (SUBJAREA , "BUSI") OR EXCLUDE (SUBJAREA , "COMP") OR EXCLUDE (SUBJAREA , "ARTS") OR EXCLUDE (SUBJAREA , "MATH")) AND (EXCLUDE (SUBJAREA , "MULT") OR EXCLUDE (SUBJAREA , "VETE"))

Usando la herramienta Bibliometrix de RStudio, se obtuvo los siguientes resultados:

2.1.2. Revistas científicas más relevantes para publicación de artículos científicos

De la Figura 2.1-1 podemos identificar las revistas más relevantes en base a la cantidad de artículos científicos publicados. La revista que tienen la mayor cantidad de publicaciones en este tema (100 artículos científicos) es JAOCS Journal of the American Oil Chemists´ Society de Alemania ubicada en el cuartil Q2 del área de ingeniería química, según Scimago (https://www.scimagojr.com/). Le sigue Food Research International del Reino Unido con 55 artículos

científicos, esta revista está ubicada en el cuartil Q1 del área de ciencia de los alimentos. Y la última revista considerada dentro de las más importantes es Food Chemistry del Reino Unido con 44 artículos publicados, ubicada en el cuartil Q1 del área de química analítica.
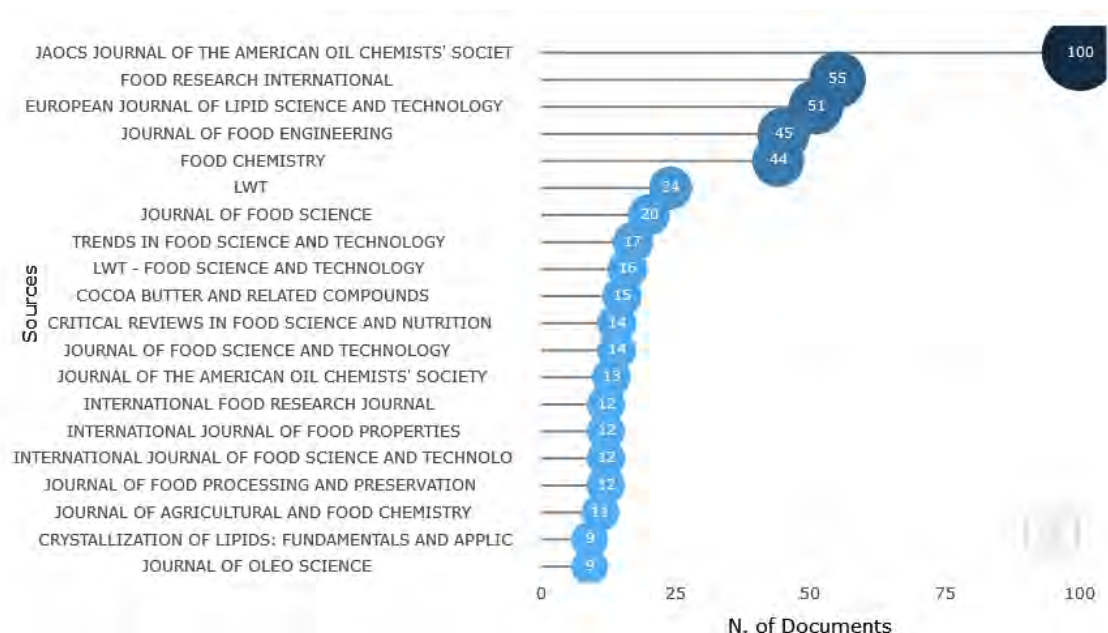
Figura 2.1-1. Revistas científicas más relevantes

2.1.3. Temas mayormente estudiados

La Figura 2.1-2 muestra las palabras más relevantes encontradas en los resúmenes de los artículos publicados. El tamaño de la palabra indica la frecuencia con la que ésta aparece en los resúmenes. Por lo que podemos entender que en los 819 documentos encontrados, la grasa es ampliamente estudiada, seguida por el chocolate, el cacao y el proceso de cristalización, pero cada uno por separado. Entonces, el resultado de la figura no significa que ya existan muchos estudios en el tema de la cristalización de la manteca de cacao en la elaboración de chocolate sino que hasta la actualidad, estos temas están siendo estudiados aisladamente. Por ejemplo, se ha encontrado estudios sobre cristalización de aceite de palma y otros equivalentes de manteca de cacao, pero no específicamente de la manteca de cacao como tal.

Figura 2.1-2. Nube de palabras

2.1.4. Justificación del tema de investigación.

El tipo de análisis factorial realizado con Bibliometrix fue Análisis Múltiple de Correspondencias (AMC) cuyas variables fueron los títulos de los trabajos publicados en Scopus. En ese sentido, la Figura 2.1-3 muestra la relación entre los diversos títulos (temas) encontrados y los clusters generados, a partir de los cuales se plantea la formación de áreas de investigación que pueden ser abordadas en la presente tesis. Notamos el arreglo de los temas en cinco grupos, dichos temas se relacionan para generar trabajos de investigación, y todos ellos pueden unirse para diseñar un trabajo más grande (tesis de doctorado) que es el objetivo de este análisis. Por un lado, podemos notar la conformación de un grupo relacionado al estudio de un sistema para asegurar la calidad de un alimento procesado como el chocolate, el segundo puede estar relacionado al comportamiento de la MC durante las fases de procesamiento de chocolate, un tercer grupo dedicado al estudio de las propiedades térmicas de los chocolates, un cuarto grupo para el estudio de los ácidos grasos de la MC y un quinto grupo para estudiar el polimorfismo y cristalización de la MC usando calorimetría diferencial de barrido. Es necesario resaltar que estos resultados no contemplan

53

la formación de un grupo dedicado a estudiar el polimorfismo y cinética de cristalización de la MC durante la fermentación del grano, que es parte de la propuesta de investigación de la presente tesis, por lo que consideramos que este es un tema aun no explorado y encajaría perfectamente en el proceso de investigación de la fabricación de chocolate oscuro. Siendo la fermentación una de las etapas más importantes en la fabricación de chocolate, los resultados muestran que existe vacío de conocimiento en el tema de investigación propuesto.

Figura 2.1-3. Identificación de vacíos de conocimiento

Para reforzar los resultados anteriores del análisis bibliométrico, se buscó información más específica relacionada al tema de tesis. Una manera de encontrar información más específica es usar comillas que junten palabras clave para considerarlas como un solo término. Para encontrar estudios que involucren solo a la manteca de cacao se tuvo que redefinir la ecuación a: **"cocoa butter" + crystallization + chocolate**, y considerando las debidas restricciones (o filtros) se encontró 113 documentos. La ecuación de búsqueda quedó de la siguiente manera:

Tabla 2.1-2. Ecuación de búsqueda redefinida.

TITLE-ABS-KEY ("cocoa butter" crystallization AND chocolate) AND (LIMIT-TO (SUBJAREA , "AGRI") OR LIMIT-TO (SUBJAREA , "CHEM") OR LIMIT-TO (SUBJAREA , "CENG") OR LIMIT-TO (SUBJAREA , "ENGI") OR LIMIT-TO (SUBJAREA , "BIOC") OR LIMIT-TO (SUBJAREA , "MATE")) AND (EXCLUDE (SUBJAREA , "PHYS") OR EXCLUDE (SUBJAREA , "IMMU") OR EXCLUDE (SUBJAREA , "SOCI") OR EXCLUDE (SUBJAREA , "BUSI")) AND (EXCLUDE (SUBJAREA , "ENER") OR EXCLUDE (SUBJAREA , "MATH") OR EXCLUDE (SUBJAREA , "NURS") OR EXCLUDE (SUBJAREA , "PHAR"))

2.1.5. Revistas científicas más relevantes para publicación de artículos científicos con ecuación redefinida

La Figura 2.1-4 nos muestra que nuevamente como en el caso anterior, la revista JAOCS Journal of the American Oil Chemists´ Society tiene una mayor cantidad de artículos publicados (20 artículos). Le sigue Journal of Food Engineering del Reino Unido con 10 artículos, esta revista está ubicada en el cuartil Q1 del área de ciencia de los alimentos. Cabe resaltar que al realizar una búsqueda más específica, el número de artículos por revista se reduce.
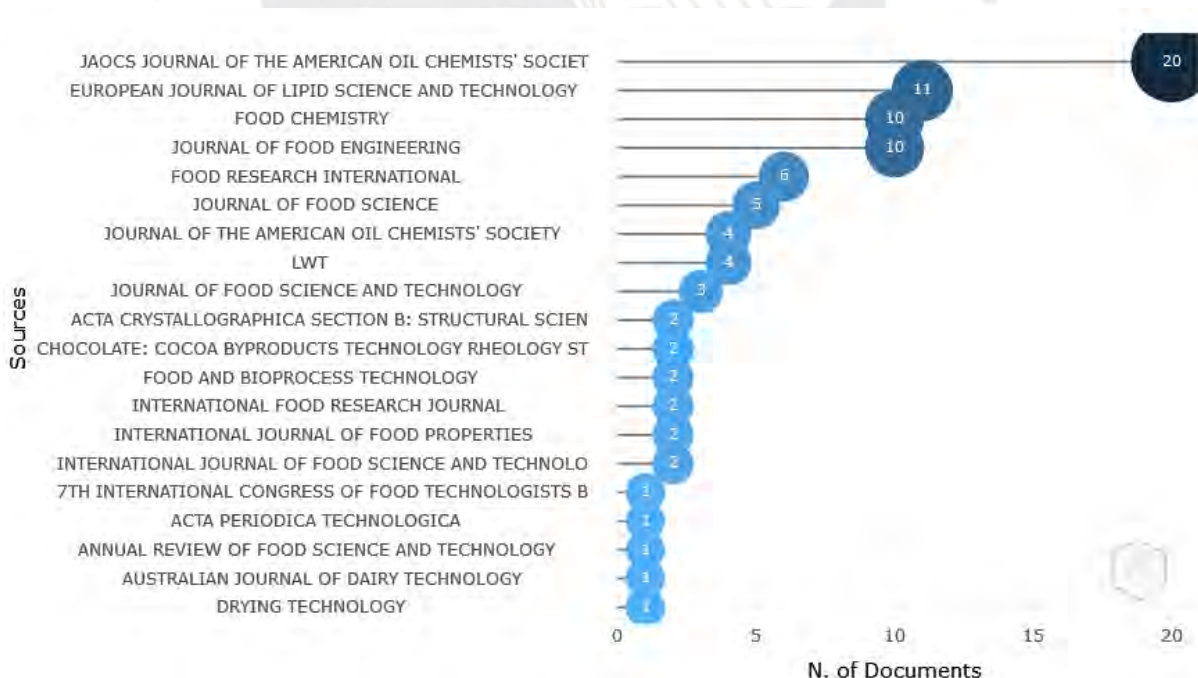
Figura 2.1-4. Revistas más relevantes para publicación de artículos científicos

2.1.6. Temas mayormente estudiados con ecuación redefinida

Considerando los 113 documentos, la Figura 2.1-5 nos muestra que los temas más estudiados son el chocolate y la manteca de cacao, existiendo pocos estudios relacionados a los fenómenos de cristalización y polimorfismo, y ninguno que relacione a éstos con el proceso de fermentación del cacao.

Figura 2.1-5. Temas estudiados

2.1.7. Justificación del tema de investigación con ecuación redefinida.

La Figura 2.1-6 muestra la conformación de 5 grupos de estudio que refuerzan la justificación del tema de investigación. Como en el caso anterior, se conforma un primer grupo que involucra el estudio del fenómeno de cristalización mediante calorimetría diferencial de barrido, un segundo grupo que podría investigar el comportamiento de la manteca de cacao durante la elaboración de chocolate y control de los parámetros de proceso, un tercer grupo que podría estudiar las propiedades físicas del chocolate y dos grupos adicionales que para nuestro análisis resultaron irrelevantes.

Figura 2.1-6. Justificación del tema de investigación

2.2. Conclusión.

Nuevamente, se demuestra que no se ha abordado el tema de la cristalización y polimorfismo de la manteca de cacao durante la fermentación. Así mismo, es necesario realizar el estudio de este fenómeno durante la cadena de fabricación de chocolate para conocer sus efectos en la calidad física de los chocolates oscuros. Por lo que se concluye que esta propuesta podría contribuir a aportar nueva información al proceso de fabricación de chocolate.

CAPÍTULO III. CINÉTICA DE CRISTALIZACIÓN, POLIMORFISMO Y PUNTO DE FUSIÓN DE LA MANTECA DE CACAO CRIOLLO DURANTE EL PROCESO DE FERMENTACIÓN

Kinetics Crystallization and Polymorphism of Cocoa Butter throughout the Spontaneous Fermentation Process

Efraín M. Castro-Alayo [1,2,3,*], Llisela Torrejón-Valqui [1], Marleni Medina-Mendoza [1], Ilse S. Cayo-Colca [4] and Fiorella P. Cárdenas-Toro [3]

[1] Instituto de Investigación, Innovación y Desarrollo para el Sector Agrario y Agroindustrial de la Región Amazonas (IIDAA), Facultad de Ingeniería y Ciencias Agrarias, Universidad Nacional Toribio Rodríguez de Mendoza de Amazonas, Calle Higos Urco 342-350-356, Chachapoyas 01001, Amazonas, Peru; llisela.torrejon@untrm.edu.pe (L.T.-V.); marleni.medina.epg@untrm.edu.pe (M.M.-M.)

[2] Programa de Doctorado en Ingeniería, Departamento de Ingeniería, Pontificia Universidad Católica del Perú, Av. Universitaria 1801, San Miguel, Lima 32, Peru

[3] Sección de Ingeniería Industrial, Departamento de Ingeniería, Pontificia Universidad Católica del Perú, Av. Universitaria 1801, San Miguel, Lima 32, Peru; fcardenas@pucp.pe

[4] Facultad de Ingeniería Zootecnista, Agronegocios y Biotecnología, Universidad Nacional Toribio Rodríguez de Mendoza de Amazonas, Calle Higos Urco 342-350-356, Chachapoyas 01001, Amazonas, Peru; icayo.fizab@untrm.edu.pe

* Correspondence: efrain.castro@untrm.edu.pe; Tel.: +51-986-376-463

Abstract: The spontaneous fermentation process of Criollo cocoa is studied for its importance in the development of chocolate aroma precursors. This research supports the importance of spontaneous fermentation, which was studied through the crystallization behavior and polymorphisms of cocoa butter (CB), the most abundant component of chocolate that is responsible for its quality physical properties. The k-means technique was used with the CB crystallization kinetics parameters to observe the division of the process during the first stage (day 0–3). The experimental crystallization time was 15.78 min and the second stage (day 4–7) was 17.88 min. The Avrami index (1.2–2.94) showed that the CB crystallizes in the form of a rod/needle/fiber or plate throughout the process. CB produced metastable crystals of polyforms β_1' and β_2'. Three days of fermentation are proposed to generate Criollo cocoa beans with acceptable CB crystallization times.

Keywords: criollo cocoa; cocoa butter; polymorphism; crystallization; differential calorimetry scanning; Avrami model; kinetics

1. Introduction

Cocoa butter (CB) is a natural fat extracted from cocoa beans [1]. CB has a crystalline structure that determines the final quality of chocolate [2,3]. CB has a crystal acylglycerols (TAGs) [4,5] that define its crystallization properties [6–8]. CB is mainly composed of 23.2–29.3% 1,3-di-stearoyl-2-oleoyl-glycerol (SOS), 34.2–38.6% 1-palmitoyl-2-oleoyl-3-stearoyl-glycerol (POS), and 13.5–17.1% 1,3-dipalmitoyl-2-oleoylglycerol (POP) [9,10]. These TAGs allow CB to crystallize in six polyforms, which are γ, α, β_2', β_1', β_2, and β_1, and are identified according to their melting temperatures (17.3, 23.3, 25.5, 27.5, 33.8, and 36.3 °C; respectively) [9,11–14] and stability. Although the contribution of POP is less than those of POS and SOS, its presence may influence the formation of metastable polymorphic forms in CB [15]. The polymorphism is related to the organoleptic and physical characteristics of the chocolate [16]. That means that CB crystals define the sensory characteristics of chocolate, such as flavor release, mouthfeel, and melting properties [3]. Characterizing these crystalline forms is crucial to meeting market needs, optimizing processes, or developing new products [17]. Therefore, CB crystallization is an important phenomenon that must be considered to obtain high-quality chocolates [18]. Obtaining the β_2 polyform

Kinetics Crystallization and Polymorphism of Cocoa Butter Throughout the Spontaneous Fermentation Process

Efraín M. Castro-Alayo[1,2,3]*, Llisela Torrejón-Valqui[1], Marleni Medina-Mendoza[1], Ilse S. Cayo-Colca[4], and Fiorella P. Cárdenas-Toro[3]

[1] Instituto de Investigación, Innovación y Desarrollo para el Sector Agrario y Agroindustrial de la Región Amazonas (IIDAA), Facultad de Ingeniería y Ciencias Agrarias, Universidad Nacional Toribio Rodríguez de Mendoza de Amazonas, Calle Higos Urco 342-350-356, 01001 Chachapoyas, Amazonas, Peru; llisela.torrejon@untrm.edu.pe (L.T.-V.); marleni.medina.epg@untrm.edu.pe (M.M.-M.)

[2] Programa de Doctorado en Ingeniería, Departamento de Ingeniería, Pontificia Universidad Católica del Perú, Av. Universitaria 1801, San Miguel 15088, Peru

[3] Sección de Ingeniería Industrial, Departamento de Ingeniería, Pontificia Universidad Católica del Perú, Av. Universitaria 1801, San Miguel 15088, Peru; fcardenas@pucp.pe

[4] Facultad de Ingeniería Zootecnista, Agronegocios y Biotecnología, Universidad Nacional Toribio Rodríguez de Mendoza de Amazonas, Calle Higos Urco 342-350-356, 01001 Chachapoyas, Amazonas, Peru; icayo.fizab@untrm.edu.pe

* Correspondence: efrain.castro@untrm.edu.pe; Tel.: +51-986376463

3.1. Abstract

The spontaneous fermentation process of Criollo cocoa is studied for its importance in the development of chocolate aroma precursors. This research supports the importance of spontaneous fermentation, which was studied through the crystallization behavior and polymorphisms of cocoa butter (CB), the most abundant component of chocolate that is responsible for its quality physical properties. The k-means technique was used with the CB crystallization kinetics parameters to observe the division of the process in two stages, during the first stage (day 0–3) the experimental crystallization time was 15.78 min and the second stage (day 4–7) was 17.88 min. The Avrami index (1.2–2.94) showed that the CB crystallizes in the form of a rod/needle/fiber or plate throughout the process. CB produced metastable crystals of polyforms β_1' and β_2'. Three days of fermentation are proposed to generate Criollo cocoa beans with acceptable CB crystallization times.

Keywords: Criollo cocoa; cocoa butter; polymorphism; crystallization; differential calorimetry scanning; Avrami model; kinetics

3.2. Introduction

Cocoa butter (CB) is a natural fat extracted from cocoa beans [1]. CB has a crystalline structure that determines the final quality of chocolate [2,3]. CB has a crystal acylglycerols (TAGs) [4,5] that define its crystallization properties [6–8]. CB is mainly composed of 23.2–29.3% 1,3-di-stearoyl-2-oleoyl-glycerol (SOS), 34.2–38.6% 1-palmitoyl-2-oleoyl-3-stearoyl-glycerol (POS), and 13.5–17.1% 1,3-dipalmitoyl-2-oleoylglycerol (POP) [9,10]. These TAGs allow CB to crystallize in six polyforms, which are γ, α, β_2'', β_1', β_2, and β_1, and are identified according to their melting temperatures (17.3, 23.3, 25.5, 27.5, 33.8, and 36.3 °C; respectively) [9,11–14] and stability. Although the contribution of POP is less than those of POS and SOS, its presence may influence the formation of metastable polymorphic forms in CB [15]. The polymorphism is related to the organoleptic and physical characteristics of the chocolate [16]. That means that CB crystals define the sensory characteristics of chocolate, such as flavor release, mouthfeel, and melting properties [3]. Characterizing these crystalline forms is crucial to

meeting market needs, optimizing processes, or developing new products [17]. Therefore, CB crystallization is an important phenomenon that must be considered to obtain high-quality chocolates [18]. Obtaining the β_2 polyform (form V) is very important for chocolate manufacturers [8,17,19–21] due to it giving the optimal characteristics of gloss, snap, texture, melting, sensation in the mouth, and bloom resistance [4,20,22].

In the chocolate manufacturing chain, the fermentation of cocoa beans is essential for the generation of aromatic compounds in chocolate [23–25] and other metabolites, such as amino acids, amines [26], and polyphenols [27], generated by biochemical reactions that are favored by temperature, pH, and time [28]. This process occurs spontaneously on farmers' farms, unlike other fermentation processes [29]. The fermentation methods used and the action of indigenous microorganisms result in a very heterogeneous process [29]. Therefore, controlling the process variables is necessary to obtain cocoa of better quality and homogeneity [28]. A widely studied fermentation process is acidification by acetic acid (the corresponding pH is a variable), whose action produces biochemical modifications related to chocolate flavor [30]. Although they could also be related to the crystallization behavior of CB during fermentation, there is not enough evidence for it [5,31]. Moreover, no studies have analyzed the crystallization of CB in its natural state during spontaneous fermentation (when CB is under the influence of other chemical components of the cocoa bean). We believe that the closest test to reality would be to study the crystallization of CB inside the cocoa bean without being influenced by any extraction method.

The most used method to describe the behavior of cocoa butter is the Avrami model, which describes the kinetics of crystallization and crystal growth [1,32,33]. Avrami's equation describes an initial period where crystallization occurs slowly and is followed by a rapid increase in the mass of the crystal formed. It is assumed that this process occurs under isothermal conditions, and crystal growth is by random nucleation and linear growth [34–36]. On the other hand, the analytical technique of X-ray diffraction (XRD) is the most used to study the polymorphism of fat crystals. However, access to XRD equipment is not easy in a research and development unit, so differential scanning calorimetry (DSC) [12] is an alternative. MacNaughtan et al. [37] demonstrated that the DSC

62

technique could provide reproducible kinetic data on the tristearin-tripalmitin crystallization and polymorphism. They also provided the identity of the polymorphs after the fusion of the crystallized material. Similarly, Simoes et al. [38] used DSC to study the polymorphic transition of CB from form $\beta_1^{'}$ to β_2, in the presence of emulsifiers and sugar.

Optimizing the fermentation process to obtain good quality cocoa beans involves studying the metabolites generated [39]. However, we also consider it necessary to describe the fermentation process based on the quantitative crystallization kinetics and CB polymorphism. Therefore, the objective of this work was to describe the kinetics of crystallization and polymorphism of CB throughout the spontaneous fermentation process.

3.3. Materials and Methods

3.3.1. Materials and Chemicals

Fresh Criollo cocoa beans and pure CB were provided by Cooperativa de Servicios Múltiples Aprocam (Bagua–Amazonas–Peru). The 1,3-dipalmitoyl-2-oleoylglycerol (POP) ≥ 99% standard was purchased from Sigma Aldrich.

3.3.2. Monitoring Fermentation

Considering the work carried out by Deus et al. [26], the spontaneous fermentation of Criollo cocoa was carried out in the Aprocam cocoa processing center. The cocoa pods were harvested and opened with a stainless-steel knife. The beans, surrounded by their pulp, were placed in polypropylene bags, taken to the processing center, and placed in 50 × 50 × 50 cm wooden boxes (40 kg capacity). The boxes were covered with jute bags to prevent the bean mass from losing heat. The bean mass was passed from one box to another to allow aeration. During each day of fermentation, the temperature and pH parameters were recorded. Cocoa bean samples (50 g) were extracted daily from the total mass, and we recorded the start time (Day 0) and end time of fermentation (day 7). The samples were packed in sterile polypropylene bags and stored in liquid nitrogen until they were taken to the UNTRM laboratory for physicochemical analysis in duplicate.

3.3.3. Physico-Chemical Parameters

3.3.3.1. Titratable Acidity and pH of the Cocoa Beans

The titratable acidity and pH were determined according to the AOAC 942.15 and 970.21 methods [40].

3.3.3.2. Moisture Content

According to Elbl et al. [41], with modifications, the moisture content of cocoa beans was determined using a halogen moisture analyzer (Mettler Toledo, Excellence plus HX204, Greifensee, Switzerland) based on the gravimetric principle. One gram of sample was weighed in an analyzer crucible and heated to 105 °C until a constant weight was obtained. The difference in weight (initial and final) calculated by the analyzer gave the moisture content.

3.3.3.3. Water Activity

According to [42], water activity was determined with a portable water activity analyzer (Rotronic AG, HygroPalm-HP23-AW-A, Bassersdorf, Switzerland), and the sample container was filled with cocoa beans up to 4/5 of its capacity. The A_w probe was placed immediately above the container. After 5 min, the AwQuick mode's A_w of the sample was recorded.

3.3.4. Crystallization and Melting Profiles of POP and CB Inside Cocoa Bean

According to Sonwai et al. [20] and Foubert et al. [43], with some modifications, the crystallization and melting profiles of POP and CB inside the cocoa beans were determined. A differential scanning calorimeter (DSC) (TA Instruments, Discovery DSC 2500, New Castle, DE, USA) was used. A 10–15 mg sample of cocoa bean was placed in an aluminum pan and hermetically sealed with the press. An empty pan was used as a reference. The sample was heated from room temperature to 60 °C and held for 15 min to ensure homogeneity and remove any crystal memory. The sample was cooled with a ramp of 5 °C/min to −20 °C and held for 15 min, and then heated at 5 °C/min to 60 °C. The Trios software determined the T_{onset}, T_{endset}, crystallization temperature T_c, melting temperature T_m, and enthalpy.

3.3.5. Isothermal Crystallization of Cocoa Butter Inside the Cocoa Bean

According to Toro-Vásquez et al. [44], Martini [31], and Ray et al. [11], from the T_c and T_m identified in 2.4, the experimental T_c was chosen, considering that the crystallization process occurs at low supercooling (0–4 °C below the T_m of the sample), so the T_c used were: 15, 16, 17, 18, and 19 °C. The samples were cocoa beans collected on each day of spontaneous fermentation. A sample of pure CB was established as a control. A 10–15 mg sample of cocoa bean was placed in an aluminum pan and hermetically sealed. For the isothermal crystallization analysis and to erase any crystal memory, the sample was heated to 60 °C for 20 min. The sample was cooled with a ramp of 3 °C min^{-1} until reaching the correspondent T_c. Then, it was kept for 90 min until the exotherm (peak) of crystallization was completed. Next, the sample was heated at 5 °C min−1 up to 60 °C to obtain the melting endotherm (peak) that served to identify the polymorphic forms of CB, which were found by comparing the T_m of the peaks with the literature. According to MacNaughtan et al. [37], reheating the sample does not influence its melting and crystallization behavior.

3.3.6. Kinetics Crystallization

The data from the isothermal crystallization were fitted to the Avrami equation (Equation (3.3-1)) [31,37,45] to calculate the crystallization kinetic parameters. The package Crystallization fit of Origin Pro Software created by Lorenzo et al. [46] was used.

$$1 - V_c(t) = \exp(-kt^n) \tag{3.3-1}$$

where V_c is the fraction of crystal formed at time t during crystallization, k is the crystallization rate constant, and n is the Avrami index related to the crystallization mechanism [33]. Equation (3.3-1) is expressed in logarithmic form as:

$$\ln\big[-\ln\big(1 - V_c(t)\big)\big] = \ln k + n \ln t \tag{3.3-2}$$

From the plot of $\ln\big[-\ln\big(1 - V_c(t)\big)\big]$ vs. $\ln t$, n was calculated as the slope of the graph. This is the so-called Avrami plot. k is a function of the crystallization

temperature and considers the crystal's nucleation and crystal growth rate [34]. n indicates the crystal growth mechanism [33]; that is, it indicates whether nucleation is instantaneous (when the nuclei appear all at once when the process begins) or sporadic (when the number of nuclei increases linearly with time) and whether nuclei grow as rods, disks, or spheres (Table 3.3-1). Fractional values of n indicate the simultaneous generation of two or more types of crystals or similar crystals from different types of nuclei [34].

Table 3.3-1. Values for the Avrami index, n, for different types of nucleation and growth.

n	Type of crystal growth and nucleation expected
3 + 1 = 4	Spherical crystals grow from sporadic nuclei
3 + 0 = 3	Spherical crystals grow from instantaneous nuclei
2 + 1 = 3	Crystals grow plate-like from sporadic nuclei
2 + 0 = 2	Crystals grow plate-like from instantaneous nuclei
1 + 1 = 2	Crystals grow as rod/needle/fiber from sporadic nuclei
1 + 0 = 1	Crystals grow as rod/needle/fiber from instantaneous nuclei.

In addition to k and n, $t_{1/2}$ describes the time taken to achieve half of the overall crystallization and is calculated using Equation (3.3-3):

$$t_{1/2} = \left(\frac{0.69315}{k}\right)^{1/n} \qquad (3.3\text{-}3)$$

Another important parameter is the crystallization induction time t_0. It is defined as the time required for the exotherm to begin to form [31] and calculated from the isothermal thermogram obtained by DSC. The t_0 is the time that elapses from the start of the isothermal process to the start of crystallization. This is the point of the thermogram where the sample's heat fluxes deviate significantly from the baseline [47].

3.3.7. Polymorphism

The method developed by Fernandes et al. [18] was used to study the CB polymorphism during spontaneous fermentation. The sample was heated at 5 °C min^{-1} for each T_c up to 60 °C until the crystals were melted (formed at the corresponding T_c). The polymorphic forms of CB were identified based on the T_m.

3.3.8. Statistical Analysis

Spontaneous fermentation samples were related to the CB crystallization behavior inside the cocoa bean, and unsupervised pattern recognition theory was used to form clusters using the k-means technique [48]. The isothermal crystallization kinetic parameters obtained by fitting the Avrami equation and the polymorphism results were analyzed by k-means cluster analysis using the RMarkdown software (Rstudio, version 2021.09.0+351, Boston, USA) to find CB crystallization patterns within cocoa beans throughout the fermentation. As cluster analysis is an exploratory method, no replicates of the measurements [48] were used to run the k-means.

3.4. Results

3.4.1. Monitoring Fermentation

According to Figure 3.4-1, the parameters of the spontaneous fermentation of the Criollo cocoa beans showed variations concerning the days of fermentation. Figure 3.4-1a shows that the temperature increased as the fermentation developed until day 4 (45.35 °C) and then decreased towards the end of the process (39.2 °C). Similar behavior can be verified in cocoa bean moisture. Figure 3.4-1b shows that the pH and titratable acidity showed the opposite behavior. While the pH decreased with the days of fermentation (from 6.83 to 4.55), the acidity increased (from 1.15 to 2.8 mEq NaOH 100 g^{-1}). Regarding the A_w, this parameter showed slight growth until the end of fermentation up to 0.95.
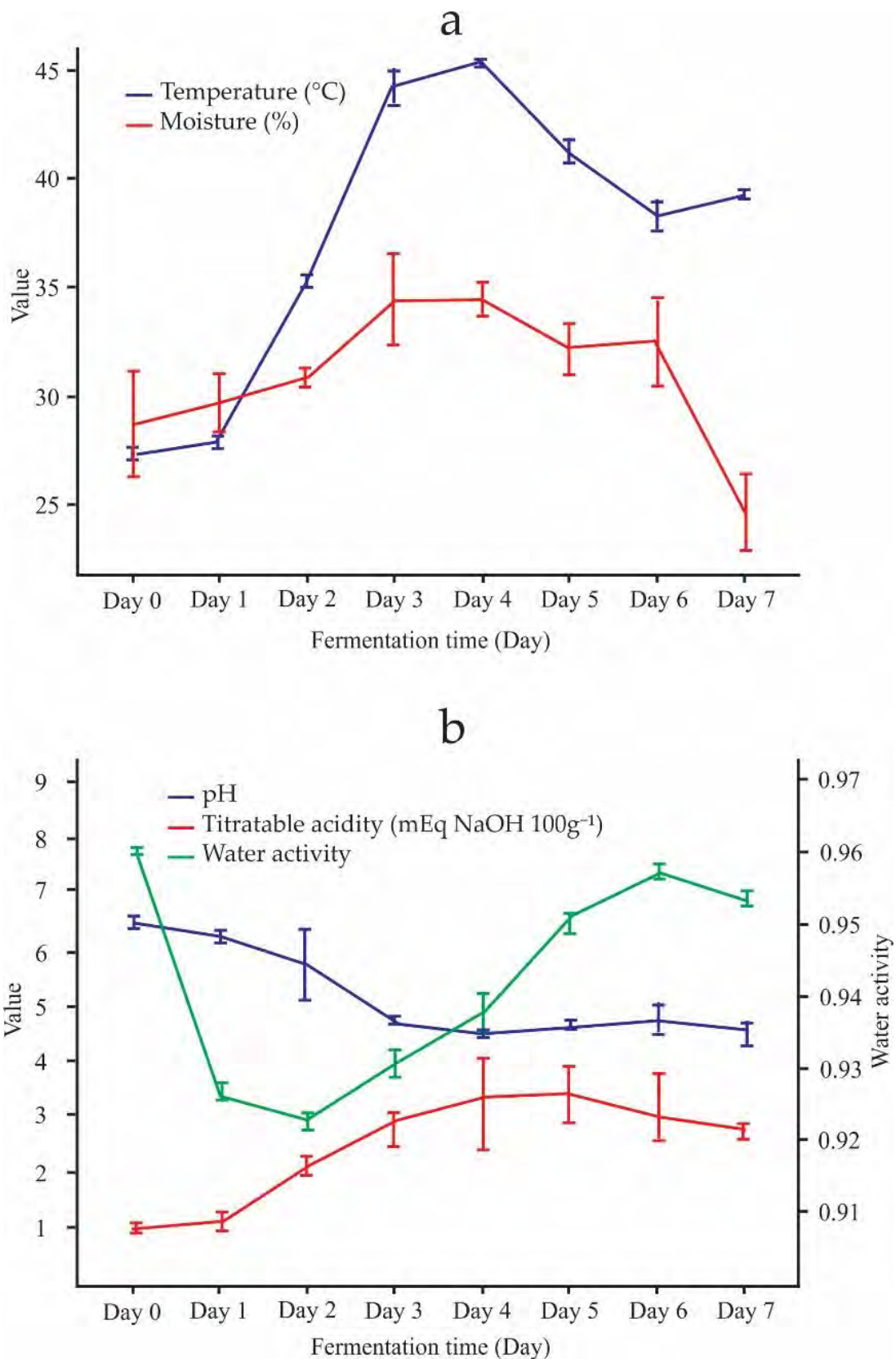
Figure 3.4-1. Evolution of spontaneous fermentation parameters of Criollo cocoa beans. (a) Evolution of temperature and moisture, (b) Evolution of pH, titratable acidity and water activity.

3.4.2. Crystallization and Melting Profiles

Table 3.4-1 shows CB's crystallization and melting profiles compared to one of its main triglycerides, 1,3-dipalmitoyl-2-oleoylglycerol (POP). The CB started to crystallize at 15.45 °C, and T_c was 12.93 °C. The POP began to crystallize at 12.07 °C, and T_c was 10.40 °C. Crystallization enthalpies were 48.42 J/g for CB and 54.91 J/g for POP. The CB fusion range was 15.05 °C (T_{onset}) to 26.04 °C (T_{endset}), and the peak was at 19.65 °C (T_m); this range was lower for POP (12.75–19.34 °C), and its fusion peak was 15.75 °C. T_c and T_m of CB were used to establish the experimental T_c for the kinetic crystallization, between 0 and 4 °C below T_m, thereby ensuring supercooling during isothermal kinetic crystallization. It can be seen that the melting enthalpy of CB (69.01 J/g) is lower than the melting enthalpy of POP (76.49 J/g).

Table 3.4-1. Crystallization and melting profiles of CB and POP standard polymorphism at 5 °C min^{-1}.

Sample	Crystallization				Melting				Polymorphic Form
	T_{onset} (°C)	T_c (°C)	T_{endset} (°C)	Enthalpy (J/g)	T_{onset} (°C)	T_m (°C)	T_{endset} (°C)	Enthalpy (J/g)	
CB	15.45	12.93	2.99	48.42	15.05	19.65	26.24	69.01	γ
POP	12.07	10.40	4.55	54.91	12.75	15.75	19.34	76.49	γ

3.4.3. Kinetics of Crystallization

Figure 3.4-2 shows the graphs resulting from fitting the CB isothermal crystallization experimental data at T_c = 15 °C to the Avrami equation using the Crystallization fit package of Origin Pro software (Version: 9.8, Origin Lab, Northampton, USA) 1 to 40% crystal conversion range was used, and the data fit of R^2 of 0.999 showed a good fit. The values of n and k were 2.53 and 2.87 × 10^{-3} min-n, respectively. The experimental half time, $t_{1/2}$, was 8.75 min. Figure 3.4-2a corresponds to the experimental data obtained by DSC. Figure 3.4-2b corresponds to the Avrami plot. Figure 3.4-2c shows the evolution of the untransformed fraction, $1 - V_c$, as a function of time. POP and CB data crystallization at 15 °C can be found in the supplementary material (Tablas A1, A2).
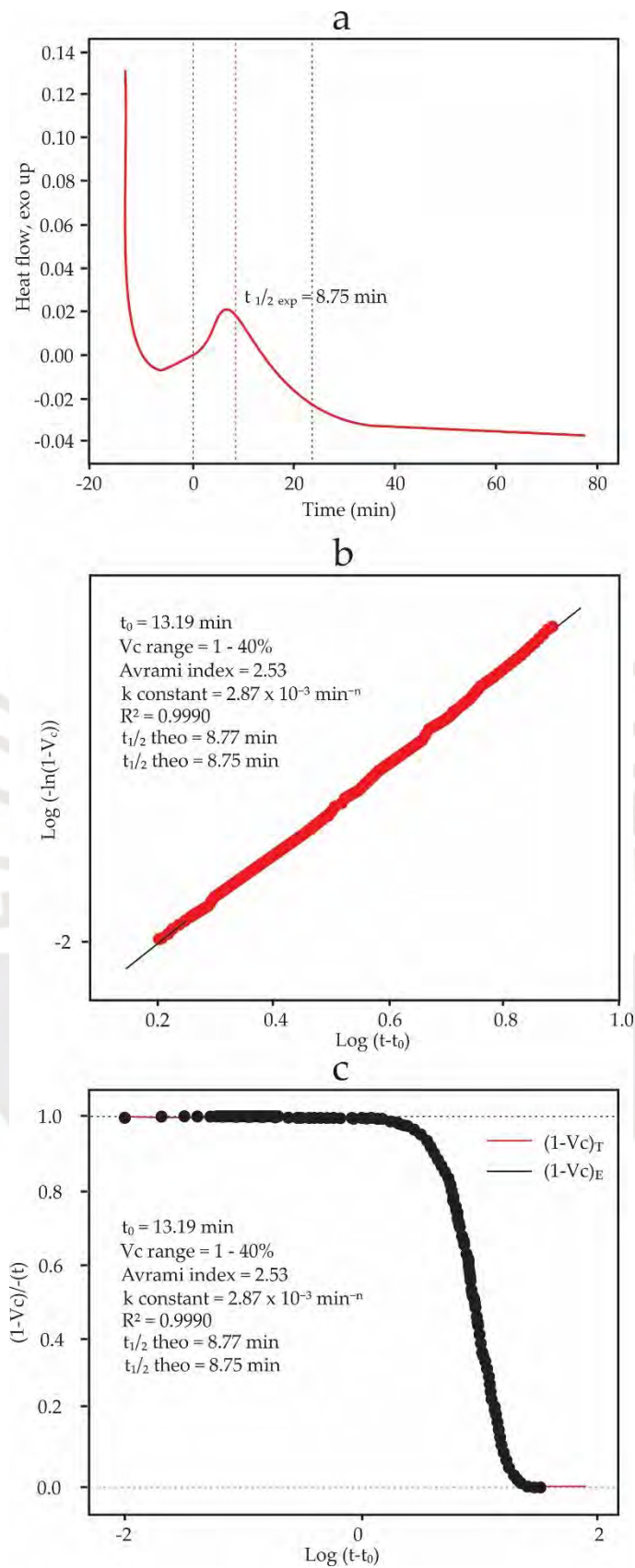
Figure 3.4-2. Results of fitting the CB isothermal crystallization data at 15 °C using the package Crystallization fit from Origin Pro. (a) Exothermal crystallization peak, (b) Avrami fitted range, (c) relative amorphous fraction.

70

The results in Table 3.4.2 describe the kinetics of the crystallization of CB and POP. The CB n value increases as T_c increases from 2.53 to 3.73. The opposite occurs with the value of k (from 2.87×10^{-3} to 8.54×10^{-5} min^{-n}). The $t_{1/2}$ increase means that the CB will need more time to crystallize at a higher crystallization temperature. The same crystallization behavior has the POP. All data have a good fit, determined by the high values of R^2.

Table 3.4-2. Crystallization kinetics of CB and POP standard at different T_c.

Crystallization Temperature (°C)	Sample	n	k (min^{-n})	t_0 (min)	$t_{1/2}$ theo (min)	$t_{1/2}$ exp (min)	R^2
15	CB	2.53	2.87×10^{-3}	13.19	8.77	8.75	0.9990
	POP	3.07	2.33×10^{-5}	5.89	28.54	28.57	0.9996
16	CB	2.91	5.97×10^{-4}	14.59	11.30	11.42	0.9993
	POP	2.94	1.94×10^{-5}	11.56	35.36	35.05	0.9920
17	CB	2.99	3.01×10^{-4}	16.20	13.28	13.29	0.9992
	POP	2.84	2.56×10^{-5}	14.33	36.18	36.70	0.9999
18	CB	3.42	9.70×10^{-5}	15.61	13.36	13.74	0.9997
	POP	2.35	6.04×10^{-5}	19.27	53.29	52.98	0.9998
19	CB	3.73	8.54×10^{-5}	17.85	15.90	16.35	0.9993
	POP	2.61	1.06×10^{-5}	35.27	70.13	72.17	0.9989

Table 3.4-3 shows the parameters of the Avrami equation at different T_c for the study of the kinetics of crystallization of CB inside the cocoa bean during spontaneous fermentation. All the data have a good fit due to the high value of R^2. For each T_c, it is shown that a lower k generates higher theoretical and experimental $t_{1/2}$. Therefore, slower crystallization happens when crystallization occurred at 17, 18, and 19 °C and from day 4 of spontaneous fermentation. The values of n range from 1.2 to 2.94, indicating that the crystals grow in rod/needle/fiber or plate-like types.

Table 3.4-3. Kinetics of crystallization parameters of CB inside cocoa beans during spontaneous fermentation.

Crystallization Temperature (°C)	Sample	n	k (min^{-n})	$t_{1/2}$ theo (min)	$t_{1/2}$ exp (min)	R^2
15	Non-fermented	2.13	1.11×10^{-2}	6.99	6.55	0.9992
	Day 0	2.09	8.68×10^{-3}	8.09	8.31	0.9984
	Day 1	2.66	1.04×10^{-3}	11.55	12.33	0.9993
	Day 2	2.58	1.53×10^{-3}	10.73	11.26	0.9994
	Day 3	1.76	2.44×10^{-2}	6.69	7.10	0.9918
	Day 4	2.51	1.75×10^{-3}	10.81	10.52	0.9995
	Day 5	2.76	8.06×10^{-4}	11.57	11.90	0.9998
	Day 6	2.04	3.02×10^{-3}	14.34	12.70	0.9999
	Day 7	2.34	3.32×10^{-3}	9.83	9.75	0.9994

	Non-fermented	1.51	2.56×10^{-2}	8.93	7.77	0.9921
	Day 0	1.78	1.59×10^{-2}	8.31	8.05	0.9973
	Day 1	2.13	2.38×10^{-3}	14.54	14.98	0.9991
	Day 2	2.49	1.65×10^{-3}	11.25	11.36	0.9998
16	Day 3	2.00	1.42×10^{-2}	6.96	6.93	0.9992
	Day 4	2.67	1.10×10^{-3}	11.14	10.80	0.9977
	Day 5	2.27	1.09×10^{-3}	17.24	16.43	0.9929
	Day 6	1.67	7.13×10^{-3}	15.43	14.27	0.9903
	Day 7	2.80	6.37×10^{-4}	11.14	12.60	0.9992
	Non-fermented	1.92	6.82×10^{-3}	11.14	10.58	0.9965
	Day 0	2.08	7.22×10^{-3}	8.97	9.17	0.9991
	Day 1	1.82	3.10×10^{-3}	15.64	12.35	0.9924
	Day 2	2.54	9.54×10^{-4}	13.41	13.30	0.9986
17	Day 3	2.43	2.93×10^{-3}	9.51	9.93	0.9998
	Day 4	2.94	5.68×10^{-4}	11.20	11.43	0.9999
	Day 5	2.47	1.77×10^{-3}	11.24	11.90	0.9985
	Day 6	2.45	9.05×10^{-4}	15.07	15.19	0.9990
	Day 7	2.35	1.49×10^{-3}	13.61	13.87	0.9999
	Non-fermented	2.10	3.61×10^{-3}	12.23	11.73	0.9952
	Day 0	1.79	6.78×10^{-3}	13.21	13.48	0.9936
	Day 1	1.73	8.77×10^{-3}	12.56	13.28	0.9984
	Day 2	2.94	2.51×10^{-4}	14.84	15.78	0.9994
18	Day 3	2.55	1.98×10^{-3}	9.91	10.14	0.9999
	Day 4	2.82	6.48×10^{-4}	11.89	12.33	0.9998
	Day 5	2.55	8.59×10^{-4}	13.74	14.24	0.9993
	Day 6	2.59	5.78×10^{-4}	15.40	15.43	0.9993
	Day 7	1.98	3.45×10^{-3}	14.63	13.94	0.9964
	Non-fermented	2.17	3.01×10^{-3}	12.29	12.28	0.9997
	Day 0	1.60	8.14×10^{-3}	16.01	14.08	0.9862
	Day 1	1.20	9.38×10^{-3}	12.02	12.24	0.9991
	Day 2	2.66	4.20×10^{-4}	16.12	17.18	0.9989
19	Day 3	2.09	2.75×10^{-3}	14.09	15.68	0.9985
	Day 4	2.94	1.72×10^{-4}	16.90	17.88	0.9981
	Day 5	2.29	1.66×10^{-3}	13.89	14.55	0.9995
	Day 6	2.57	4.73×10^{-4}	17.12	17.85	0.9996
	Day 7	2.68	3.88×10^{-4}	16.30	16.96	0.9986

Figure 3.4-3a shows the induction times, t_0, for CB inside cocoa beans during spontaneous fermentation. The relationship of the t_0 is direct; that is, as the T_c increases, the t_0 also increases. The highest t_0 corresponds to day 7 of fermentation, which means that the crystallization process started later on day seven than in the first days. Regarding the crystallization enthalpy, according to Figure 3.4-3b, this parameter shows a trend of increasing with T_c, generating the highest values at higher T_c. The opposite can be seen for the melting enthalpy (Figure 3.4-3c), which shows a decreasing trend with increasing T_c, presenting the lowest values on day 1 of fermentation.
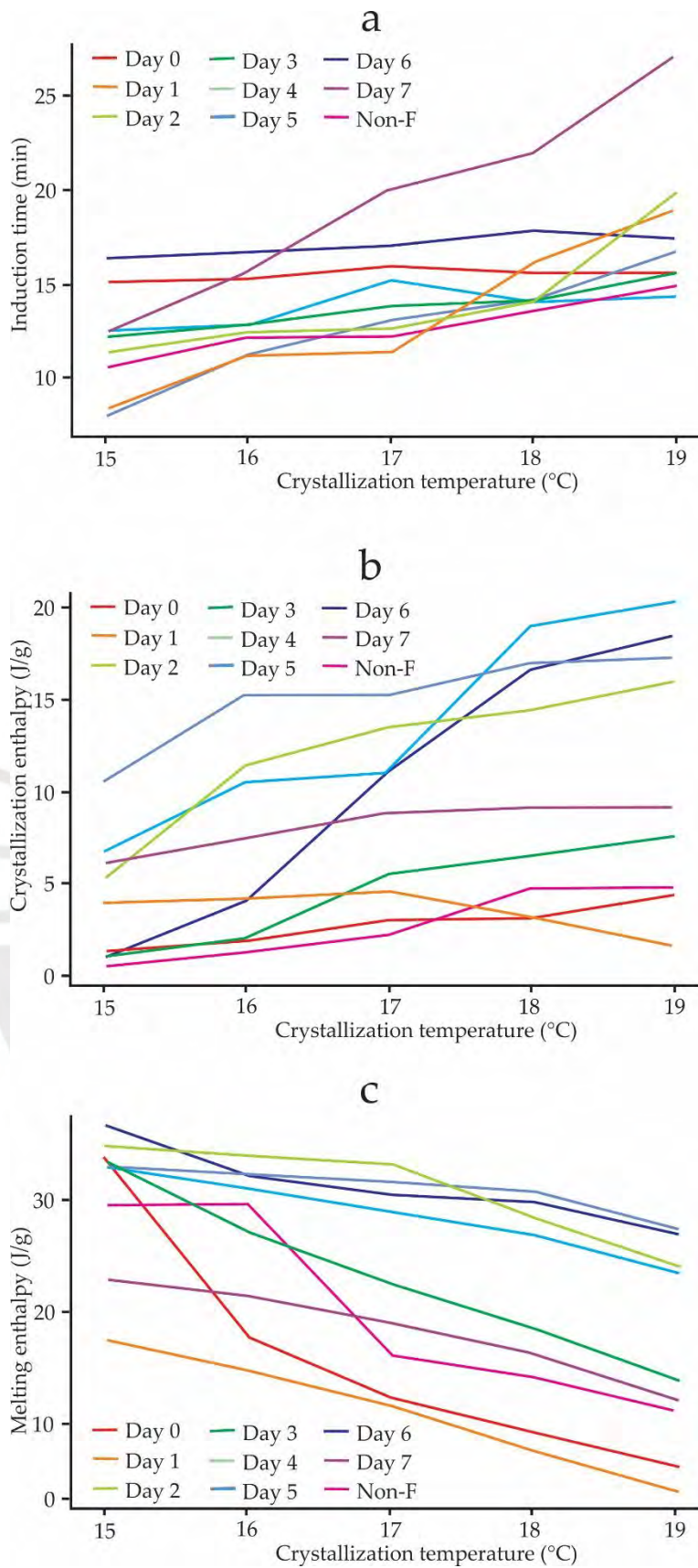
Figure 3.4-3. Induction times (a), crystallization enthalpy (b), and melting enthalpy (c) of the CB inside cocoa beans as a function of T_c during spontaneous fermentation.

Figure 3.4-4a shows the evolution of the induction time, crystallization, and melting enthalpies from the point of view of the spontaneous fermentation process. The crystallization induction times of non-fermented cocoa beans were lower than those of fermented ones in all T_c and increased each day of fermentation. The crystallization enthalpy reached its highest value on day 5 at 19 °C and had an increasing trend at each T_c. Non-fermented beans had the lowest values. Contrary to the enthalpy of crystallization, the melting enthalpy decreased with T_c, and had its highest values on day 6. The crystallization enthalpies were lower than the melting enthalpies during all days of fermentation.
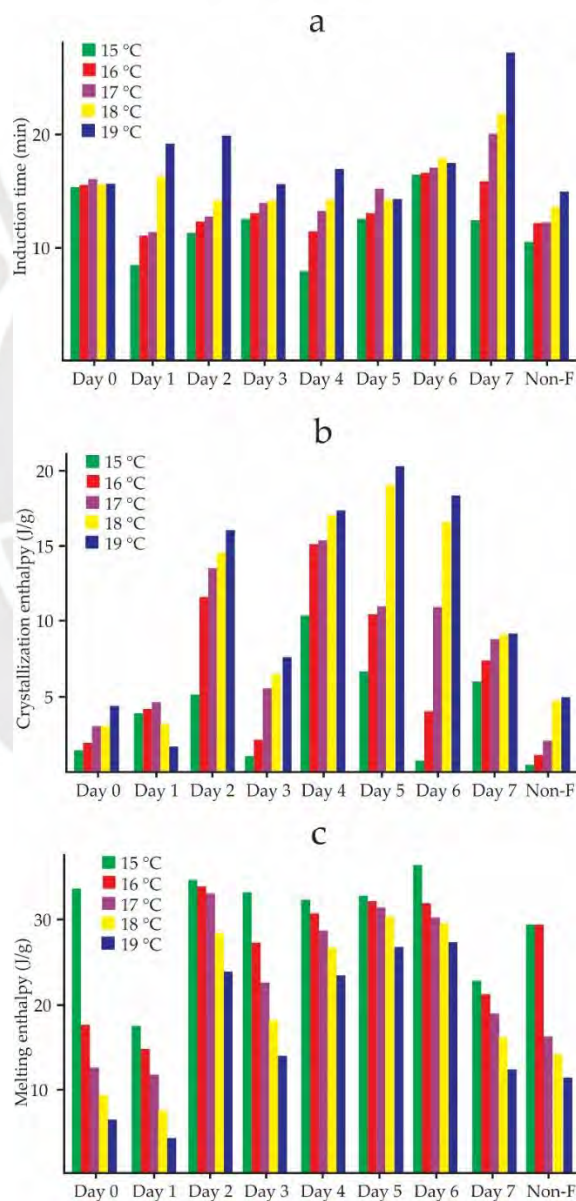
Figure 3.4-4. Induction times (a), crystallization enthalpy (b), and melting enthalpy (c) of the CB inside cocoa beans as a function of spontaneous fermentation days.

Figure 3.4-5 shows the results of the k-means analysis: the ratio between the between-cluster sum of squares and the total sum of squares is 31.1%. In Figure 3.4-5a, the samples with a fermentation day higher than 4 make up cluster 1, and the samples with less than four days of fermentation and the non-fermented samples make up cluster 2. In Figure 3.4-5b, each cluster shows the means of the kinetics of crystallization and polymorphic behavior parameters. Cluster 1 is formed by the samples with the highest n values and the lowest k values related to the highest values of $t_{1/2}$. These samples also have higher melting enthalpies and lower T_m values. The opposite occurs with cluster 2. These results mean that cluster 1 groups samples that crystallize more slowly with less stable polyforms and cluster 2 groups samples that crystallize faster with more stable polyforms. According to n, in cluster 1 are the samples whose crystals grew spherically and formed sporadic or instantaneous nuclei. Cluster 2 groups samples that crystallized as needles or fibers instantly or sporadically.
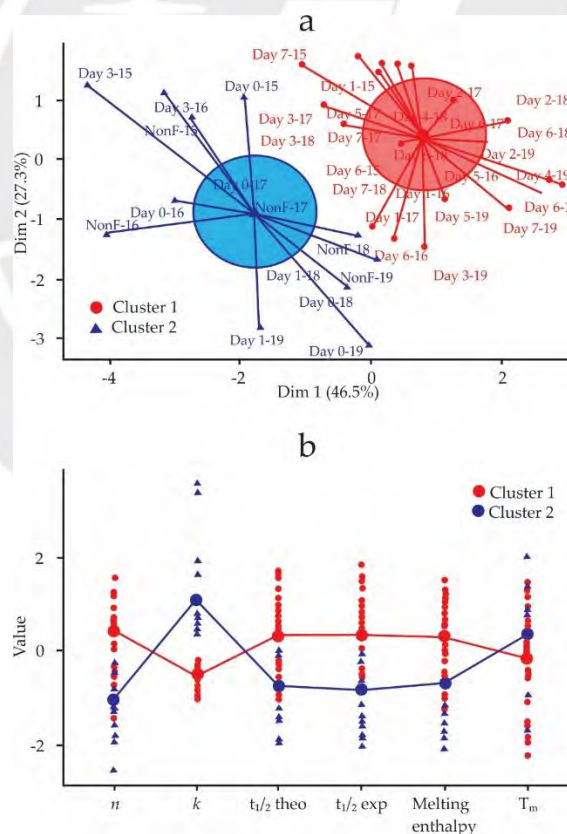
Figure 3.4-5. Clusters of kinetics parameters and polymorphic behavior of CB inside Criollo cocoa beans during spontaneous fermentation. (a) Division of the fermentation process into two stages (cluster), (b) Mean values of the crystallization kinetic parameters and polymorphism in each cluster.

Table 3.4-4 shows the polymorphic behavior of CB and POP crystals at different T_c. The T_m of all formed CB crystals increased directly with T_c, and the melting enthalpy decreased from 89.53 to 69.73 J/g. The melting range also increased. The T_c used in the experiment produced a single polyform β_1' in the CB. In the case of the POP, the T_m, enthalpy and the melting interval had the same trend as the CB but with higher values, and the polyforms generated were of type α and β_2''.

Table 3.4-4. Polymorphisms of CB and POP standard at different T_c.

Crystallization Temperature (°C)	Sample	Enthalpy (J/g)	T_{onset} (°C)	T_m (°C)	T_{endset}(°C)	Polymorphic Form
15	CB	89.53	19.82	25.80	28.59	β_1'
	POP	105.92	20.88	24.70	27.34	α
16	CB	87.16	20.48	26.27	28.80	β_1'
	POP	105.06	21.38	25.92	27.71	β_2'
17	CB	84.06	20.79	26.69	28.93	β_1'
	POP	104.67	23.18	26.66	28.29	β_2'
18	CB	75.80	21.42	27.01	29.04	β_1'
	POP	103.20	23.46	26.17	27.87	β_2'
19	CB	69.73	22.14	27.42	29.30	β_1'
	POP	80.23	24.25	26.56	28.09	β_2'

Table 3.4-5 shows the polymorphism of CB inside cocoa beans throughout fermentation. The CB polymorphic forms were identified according to the sample T_m after crystallization at a specific T_c. In all cases, the polymorphic forms identified were β_1' and β_2', which are thermally less stable. The melting ranges were between 19.06 and 30.35 °C. The melting enthalpies were higher when the crystallization was carried out at 15 °C than when it was carried out at 19 °C.

Table 3.4-5. Polymorphism of CB inside cocoa beans during spontaneous fermentation.

Crystallization Temperature (°C)	Sample	Enthalpy (J/g)	T_{onset} (°C)	T_m (°C)	T_{endset} (°C)	Polymorphic Form
15	Non-fermented	23.42	20.31	26.19	29.29	β_1'
	Day 0	33.81	20.66	26.32	30.22	β_1'
	Day 1	17.53	19.14	24.72	28.17	β_2'
	Day 2	34.89	20.26	25.73	28.76	β_1'
	Day 3	33.33	19.55	24.84	28.17	β_2'
	Day 4	32.55	19.62	25.42	29.04	β_1'
	Day 5	32.94	20.65	26.14	29.59	β_1'
	Day 6	36.58	20.81	26.96	30.01	β_1'
	Day 7	22.88	19.06	24.44	27.08	β_2'
16	Non-fermented	18.75	21.07	26.41	29.54	β_1'
	Day 0	17.69	22.38	26.48	28.81	β_1'
	Day 1	14.92	20.02	24.90	28.22	β_2'
	Day 2	33.92	20.78	25.79	28.67	β_1'
	Day 3	27.16	19.90	25.42	28.18	β_2'

	Day 4	30.88	20.14	25.69	29.07	β_1'
	Day 5	32.27	20.77	26.42	29.63	β_1'
	Day 6	31.99	21.90	27.10	30.35	β_1'
	Day 7	21.21	19.81	24.64	27.18	β_2'
	Non-fermented	16.19	21.40	26.69	29.86	β_1'
	Day 0	12.38	22.05	26.56	28.94	β_1'
	Day 1	11.61	20.83	25.28	28.28	β_2'
	Day 2	33.19	21.25	25.97	28.70	β_1'
17	Day 3	22.61	20.81	25.82	28.34	β_1'
	Day 4	28.87	20.89	26.03	29.34	β_1'
	Day 5	31.42	21.22	26.54	29.63	β_1'
	Day 6	30.35	21.17	25.78	28.49	β_1'
	Day 7	18.95	20.53	24.97	27.16	β_2'
	Non-fermented	14.17	22.20	27.15	30.06	β_1'
	Day 0	9.16	22.57	26.79	29.31	β_1'
	Day 1	7.53	21.66	25.77	28.37	β_1'
	Day 2	28.42	22.11	26.26	28.90	β_1'
18	Day 3	18.28	21.83	26.10	28.44	β_1'
	Day 4	26.78	21.73	26.38	29.63	β_1'
	Day 5	30.53	21.78	26.79	29.64	β_1'
	Day 6	29.60	21.85	26.20	28.62	β_1'
	Day 7	16.14	21.27	25.30	27.29	β_2'
	Non-fermented	11.21	23.19	27.63	30.30	β_1'
	Day 0	6.25	23.26	27.06	29.52	β_1'
	Day 1	4.01	22.42	26.42	28.65	β_1'
	Day 2	23.94	22.46	26.55	28.97	β_1'
19	Day 3	13.86	22.48	26.48	28.69	β_1'
	Day 4	23.45	22.12	26.83	29.66	β_1'
	Day 5	26.83	22.48	27.22	29.78	β_1'
	Day 6	27.27	22.35	26.62	28.82	β_1'
	Day 7	12.12	21.82	25.98	27.61	β_1'

3.5. Discussion

3.5.1. Monitoring Fermentation

There was a slight decrease in temperature throughout the spontaneous fermentation of Criollo cocoa beans, from 45.35 °C on day 4 to 39.20 °C at the end of fermentation (Figure 3.5-1a). It could have been caused by the existing climatic conditions in the cocoa processing center of Aprocam. This behavior of the fermentation process is normal, if we compare it with the results obtained by Deus et al. [26] and Chagas Junior et al. [49]. Chagas Junior et al. [49] observed similar behavior in cocoa fermentation carried out in 50 kg boxes, as the temperature reached 37 °C after 7 days of spontaneous fermentation. This behavior coincides with the results reported by Visintin et al. [50]. Moisture also had the same behavior as temperature, reaching values of 24.6% until the end of fermentation (Figure 3.5-1a). In the spontaneous fermentation carried out by

Deus et al. [26], decreasing of pH and increasing of the titratable acidity were observed, demonstrating that these behaviors are characteristic of a well-executed fermentation process [26,50–52]. Similar behavior was obtained during the spontaneous fermentation studied in this work. The A_w increased slightly throughout the fermentation (Figure 3.5-1b).

3.5.2. Crystallization and Melting Profiles of CB and POP

The CB crystallization profile showed that its crystallization begins at a T_{onset} of 15.45 °C and the peak is at T_c of 12.93 °C (Table 3.5-2); these results that agree with those reported by Bayés-García et al. [53] (T_{onset} = 16.6 °C and T_c = 13.5 °C) and Aumpai [54] (T_{onset} = 15.6 °C and T_c = 10.6 °C). Since CB is a mixture of TAGs, we must talk about melting range instead of melting temperature [55]. Bayés-García et al. [56] reported the melting behavior at 2 °C/min of bulk CB and unfermented cocoa beans, finding forms α and β_2' (T_{onset} and T_{endset} of ~17.5 and 28.6 °C, respectively), values close to those reported in Table 3.5-2. The difference in peak temperature is attributed to a different heating rate [57]. The POP crystallization results are according to Smith et al. [58]. The T_c and T_m of the POP are lower than those of the CB; however, their corresponding enthalpies are higher. The T_m of CB and POP indicate the presence of unstable polyforms of type γ. Based on what was established by Sasaki et al. [15] and Ghazani & Marangoni [8], this polymorphic behavior of CB would be influenced mainly by POP.

3.5.3. Kinetics Crystallization

Lorenzo et al. [46] suggested that the isothermal crystallization data with an R^2 of 0.999 should be considered well adjusted, considering a conversion range according to the analyzed material. Fernandes et al. [18] used a conversion range of 1 to 40% for the crystallization kinetics of chocolate. This same range was used in the present work, resulting in a good fit of the CB crystallization data that exceeded the value of 0.999, and the graphs that characterize the Avrami equation were obtained (Figure 3.5-2). Figure 3.5-2a shows CB crystallization's exothermic peak (exotherm); half of the crystallization was reached in 8.75 min. From this time, the secondary crystallization commenced. The initial descent in

Figure 3.5-2a corresponds to the thermal stabilization time of the DSC, and t_0 was calculated from the stabilization time until $t = 0$. The induction time is understood as the time necessary to initiate crystallization [46]. Figure 3.5-2b shows a linear fit of the experimental data, from which the slope and the intercept have been determined to obtain the parameters of the Avrami equation (Equation (3.5-1)). Considering a conversion range for V_c from 1 to 40% [18], an R^2 of 0.999 has been obtained, which shows a good data fit. Figure 3.5-2c compares the experimental and predicted values of the relative untransformed fraction as functions of time. The data show an excellent fit throughout the crystallization process, even beyond the primary crystallization.

The Avrami index n describes the forms in which crystal growth occurs (Table 3.5-1) [45,59]. According to Table 3.5-1, n can take values from 1 to 4. The CB's values of n increased from 2.53 at 15 °C to 3.73 at 19 °C. The crystal nuclei can grow from plate-like to spherical as T_c increases. POP's n values were reduced from 3.07 to 2.61 as the T_c increased, indicating that its crystal nuclei's growth behaves oppositely to that of CB.

On the other hand, decimal values of n indicate that both forms of crystal growth can co-occur, either sporadically or instantaneously. In the study carried out by Badu et al. [1], small values of n were obtained for Allanblackia seed oil and shea nut oil, which indicates their rapid nucleation and crystallization mechanism. The crystallization rate constant, k, of CB was higher than that of POP and increased with T_c; therefore, its crystallization is faster. This is demonstrated by the low $t_{1/2}$ values of the CB concerning the $t_{1/2}$ values of the POP.

Non-fermented cocoa beans show n values ranging from 2.13 at 15 °C to 2.17 at 19 °C (Table 3.5-4), and within them, CB crystals grow as rod/needle/fiber and plate. As fermentation began, the n values of the fermented cocoa beans changed every day from 1.20 to 2.94. However, they did not reach values similar to those of the CB (n = 3.73, spherical nuclei), indicating that the crystals grew the same as those of non-fermented beans. Crystallization kinetics experiments also showed that the parameters k, $t_{1/2}\ exp$, and $t_{1/2}\ theo$ changed throughout the fermentation process for all temperatures tested; i.e., the rate constant k was reduced, causing $t_{1/2}$ to increase, hence a slower CB crystallization process as

the fermentation progressed. This behavior is due to the chemical composition of the cocoa bean, which changes throughout fermentation by the generation of other components that influence the crystallization behavior of CB [11,60,61].

The induction time, t_0, is a function of the T_c [11,47,55]. Figure 3.5-3a shows an increasing trend of t_0 with T_c, being higher on day 7 at 19 °C (Figure 3.5-4a), which indicates that the crystallization of CB begins later in the last days of fermentation. This same trend was reported by Martini et al. [62] in the study carried out on anhydrous milk fat crystallization. Additionally, in this work, a decreasing trend of crystallization enthalpy concerning T_c was reported [62], contrary to what can be observed in Figure 3.5-3a, which shows an increasing trend, and whose highest values occur in the intermediate days of fermentation (Figure 3.5-4b). The unfermented cocoa beans had the lowest crystallization enthalpy values during all the days of fermentation. Figure 3.5-3c shows a decrease in the melting enthalpies of crystallized CB within the cocoa beans at different temperatures, and the lowest values occurred on day 1 of fermentation (Figure 3.5-4c). This happened because of the driving force (supercooling) decreases with increasing crystallization temperatures [63].

Deus et al. [26] used cluster analysis to divide the spontaneous fermentation of cocoa into two stages: the first grouped the first days of fermentation, characterized by high levels of pH and free amino acids; the second stage grouped the last days of fermentation, characterized by high temperatures, high total titratable acidity, and high levels of free bioactive amines. The unsupervised k-means classification method [64] applied to the CB crystallization kinetics parameters divided the fermentation into two stages (cluster) (Figure 3.5-5a). The first corresponds to day 0 to day 3 and the second from day 4 to day 7. These findings reinforce the statements of Castro-Alayo et al. [51] and Cevallos-Cevallos et al. [65], who mention that Criollo cocoa requires fermentation for 2 or 3 days. In this work, we established that a fermentation process that exceeds 4 days will produce cocoa beans in which the CB will crystallize more slowly later than in the first 3 days. In addition to that, such a fermentation will produce less stable polyforms of type β_1' and β_2'.

3.5.4. Polymorphism

It is crucial to study the polymorphic transitions of the CB because they influence the properties of chocolate [61]. The stability and melting temperatures (T_m) of the CB polyforms increase when they are transformed from γ to β_1. This irreversible transformation of phases depends on time and temperature, from the least stable to the most stable [18]. As mobility within the system increases due to a higher T_c, more stable polyforms are created without starting from the initial polyforms [55]. Crystals of form β_1' and β_2' are considered metastable [66]. In the case of CB, for all the T_c, only β_1' polyforms were formed (Table 3.5-5). The increase in T_c (15–19 °C) was insufficient to generate polymorphism from the less stable forms to the more stable ones. To achieve this, more considerable increases in T_c are necessary, according to what was reported by Fernandes et al. [18]. Similar behavior was noted in the POP for T_c values from 17 to 19 °C, where only the β_1' polyform was generated. However, at 15 °C, polyform α was generated due to its low melting point. The melting enthalpies of the crystallized polyforms of CB and POP decreased with T_c. For any T_c, the melting enthalpy of the POP is always greater than that corresponding to CB.

In the same way as the previous results, there was no evidence of any change in the CB polymorphism towards more stable polyforms as fermentation went on (Table 3.5-5). This means that, during fermentation and at any T_c, only metastable CB polyforms (β_1' and β_2') are formed within the cocoa beans. The melting enthalpies of these polymorphic crystals are lower than those corresponding to the enthalpies of pure CB throughout the entire fermentation process. The results of Tables 3.5-4 and 3.5-5 agree with what was established by Garbolino et al. [67], who state that the different results of the crystallization kinetics do not always produce changes in the polymorphism.

3.6. Conclusions

The present work allowed us to confirm the importance of the spontaneous fermentation process of Criollo cocoa analyzed from the point of view of the crystallization of cocoa butter. The parameters describing the kinetic crystallization of cocoa butter inside the Criollo cocoa bean show that only

metastable crystals corresponding to polyforms β_1' and β_2' can be formed during spontaneous fermentation. The growth of CB crystals occurs in the form of rod/needle/fiber and plate, just like non-fermented beans. The results allow the fermentation process to be divided into two stages: the first fermentation stage until day 3 and the second stage from day 4 to day 7. Low crystallization rates are obtained in this last stage, so the cocoa butter crystallizes more slowly. This happens due to the formation of other chemical components within the cocoa bean due to the fermentation process.

Supplementary: The following are available online at www.mdpi.com/xxx/s1, Tabla A1 and Tabla A2 shows the POP and CB isothermal crystallization data, respectively.

3.7. References

1. Badu: M.; Awudza, J.; Budd, P.M.; Yeates, S. Determination of Physical Properties and Crystallization Kinetics of Oil from Allanblackia Seeds and Shea Nuts Under Different Thermal Conditions. *Eur. J. Lipid Sci. Technol*. 2018, *120*, 1700156. https://doi.org/10.1002/ejlt.201700156.

2. Liu, W.; Yao, Y.; Li, C. Effect of Tempered Procedures on the Crystallization Behavior of Different Positions of Cocoa Butter Products. *Food Chem.* 2022, *370*, 131002. https://doi.org/10.1016/j.foodchem.2021.131002.

3. Yao, Y.; Liu, W.; Zhang, D.; Li, R.; Zhou, H.; Li, C.; Wang, S. Dynamic Changes in the Triacylglycerol Composition and Crystallization Behavior of Cocoa Butter. *LWT* 2020, *129*, 109490. https://doi.org/10.1016/j.lwt.2020.109490.

4. Ewens, H.; Metilli, L.; Simone, E. Analysis of the Effect of Recent Reformulation Strategies on the Crystallization Behaviour of Cocoa Butter and the Structural Properties of Chocolate. *Curr. Res. Food Sci.* 2021, *4*, 105–114. https://doi.org/10.1016/j.crfs.2021.02.009.

5. Servent, A.; Boulanger, R.; Davrieux, F.; Pinot, M.-N.; Tardan, E.; Forestier-Chiron, N.; Hue, C. Assessment of Cocoa (*Theobroma Cacao* L.) Butter Content and Composition throughout Fermentations. *Food Res. Int.* 2018, *107*, 675–682. https://doi.org/10.1016/j.foodres.2018.02.070.

6. Sirbu, D.; Grimbs, A.; Corno, M.; Ullrich, M.S.; Kuhnert, N. Variation of Triacylglycerol Profiles in Unfermented and Dried Fermented Cocoa Beans

of Different Origins. *Food Res. Int.* 2018, *111*, 361–370. https://doi.org/10.1016/j.foodres.2018.05.025.

7. Padar, S.; Jeelani, S.A.K.; Windhab, E.J. Crystallization Kinetics of Cocoa Fat Systems: Experiments and Modeling. *J. Am. Oil Chem. Soc.* 2008, *85*, 1115–1126. https://doi.org/10.1007/s11746-008-1312-0.

8. Ghazani, S.M.; Marangoni, A.G. The Ternary Solid State Phase Behavior of Triclinic POP, POS, and SOS and Its Relationship to CB and CBE Properties. *Cryst. Growth Des.* 2019, *19*, 704–713. https://doi.org/10.1021/acs.cgd.8b01273.

9. Norazlina, M.R.; Jahurul, M.H.A.; Hasmadi, M.; Sharifudin, M.S.; Patricia, M.; Lee, J.S.; Amir, H.M.S.; Noorakmar, A.W.; Riman, I. Effects of Fractionation Technique on Triacylglycerols, Melting and Crystallisation and the Polymorphic Behavior of Bambangan Kernel Fat as Cocoa Butter Improver. *LWT* 2020, *129*, 109558. https://doi.org/10.1016/j.lwt.2020.109558.

10. Jin, J.; Jin, Q.; Akoh, C.C.; Wang, X. StOSt-Rich Fats in the Manufacture of Heat-Stable Chocolates and Their Potential Impacts on Fat Bloom Behaviors. *Trends Food Sci. Technol.* 2021, *118*, 418–430. https://doi.org/10.1016/j.tifs.2021.10.005.

11. Ray, J.; MacNaughtan, W.; Chong, P.S.; Vieira, J.; Wolf, B. The Effect of Limonene on the Crystallization of Cocoa Butter. *J. Am. Oil Chem. Soc.* 2012, *89*, 437–445. https://doi.org/10.1007/s11746-011-1934-5.

12. Declerck, A.; Nelis, V.; Danthine, S.; Dewettinck, K.; Van der Meeren, P. *Characterisation* of Fat Crystal Polymorphism in Cocoa Butter by Time-Domain NMR and DSC Deconvolution. *Foods* 2021, *10*, 520. https://doi.org/10.3390/foods10030520.

13. Dahlenborg, H.; Millqvist-Fureby, A.; Bergenståhl, B. Effect of Shell *Microstructure* on Oil Migration and Fat Bloom Development in Model Pralines. *Food Struct.* 2015, *5*, 51–65. https://doi.org/10.1016/j.foostr.2015.06.002.

14. Talbot, G. Chocolate and Cocoa Butter-Structure and Composition. In *Cocoa Butter and Related Compounds*; Garti, N., Widlak, N.R., Eds.; AOCS Press: Urbana, IL, USA, 2012; pp. 1–34. ISBN 978-0-9830791-2-5.

15. Sasaki, M.; Ueno, S.; Sato, K. Polymorphism and Mixing Phase Behavior of Major Triacylglycerols of Cocoa Butter. In *Cocoa Butter and Related Compounds*; Garti, N., Widlak, N.R., Eds.; AOCS Press: Urbana, IL, USA, 2012; pp. 151–172.

16. Loisel, C.; Keller, G.; Lecq, G.; Bourgaux, C.; Ollivon, M. Phase Transitions and Polymorphism of Cocoa Butter. *J. Am. Oil Chem. Soc.* 1998, *75*, 425–439. https://doi.org/10.1007/s11746-998-0245-y.

17. Devos, N.; Reyman, D.; Sanchez-Cortés, S. Chocolate Composition and Its Crystallization Process: A Multidisciplinary Analysis. *Food Chem.* 2020, *342*, 128301. https://doi.org/10.1016/j.foodchem.2020.128301.

18. Fernandes, V.A.; Müller, A.J.; Sandoval, A.J. Thermal, Structural and *Rheological* Characteristics of Dark Chocolate with Different Compositions. *J. Food Eng.* 2013, *116*, 97–108. https://doi.org/10.1016/j.jfoodeng.2012.12.002.

19. Svanberg, L.; Ahrné, L.; Lorén, N.; Windhab, E. Effect of Sugar, Cocoa Particles and Lecithin on Cocoa Butter Crystallisation in Seeded and Non-*Seeded* Chocolate Model Systems. *J. Food Eng.* 2011, *104*, 70–80. https://doi.org/10.1016/j.jfoodeng.2010.09.023.

20. Sonwai, S.; Podchong, P.; Rousseau, D. Crystallization Kinetics of Cocoa Butter in the Presence of Sorbitan Esters. *Food Chem.* 2017, *214*, 497–506. https://doi.org/10.1016/j.foodchem.2016.07.092.

21. Pirouzian, H.R.; Konar, N.; Palabiyik, I.; Oba, S.; Toker, O.S. Pre-*Crystallization* Process in Chocolate: Mechanism, Importance and Novel Aspects. *Food Chem.* 2020, *321*, 126718. https://doi.org/10.1016/j.foodchem.2020.126718.

22. Chen, J.; Ghazani, S.M.; Stobbs, J.A.; Marangoni, A.G. Tempering of Cocoa Butter and Chocolate Using Minor Lipidic Components. *Nat. Commun.* 2021, *12*, 5018. https://doi.org/10.1038/s41467-021-25206-1.

23. Hernández, M.d.P.L.; Núñez, J.C.; Gómez, M.S.H.; Tovar, M.D.L. *Physicochemical* and Microbiological Dynamics of the Fermentation of the Ccn51 Cocoa Material in Three Maturity Stages. *Rev. Bras. Frutic.* 2019, *41*, 1-13 https://doi.org/10.1590/0100-29452019010.

24. Caligiani, A.; Marseglia, A.; Prandi, B.; Palla, G.; Sforza, S. Influence of Fermentation Level and Geographical Origin on Cocoa Bean Oligopeptide Pattern. *Food Chem.* 2016, *211*, 431–439. https://doi.org/10.1016/j.foodchem.2016.05.072.

25. Chagas Junior, G.C.A.; Ferreira, N.R.; Andrade, E.H.D.A.; do Nascimento, L.D.; Siqueira, F.C. de; Lopes, A.S. Profile of Volatile Compounds of On-Farm Fermented and Dried Cocoa Beans Inoculated with Saccharomyces Cerevisiae KY794742 and Pichia Kudriavzevii KY794725. *Molecules* 2021, *26*, 344. https://doi.org/10.3390/molecules26020344.

26. Deus, V.L.; Bispo, E.S.; Franca, A.S.; Gloria, M.B.A. Understanding Amino Acids and Bioactive Amines Changes during On-Farm Cocoa Fermentation. *J. Food Compos. Anal.* 2021, *97*, 103776. https://doi.org/10.1016/j.jfca.2020.103776.

27. Febrianto, N.A.; Zhu, F. Composition of Methylxanthines, Polyphenols, Key Odorant Volatiles and Minerals in 22 Cocoa Beans Obtained from Different Geographic Origins. *LWT* 2022, *153*, 112395. https://doi.org/10.1016/j.lwt.2021.112395.

28. Calvo, A.M.; *Botina*, B.L.; García, M.C.; Cardona, W.A.; Montenegro, A.C.; Criollo, J. Dynamics of Cocoa Fermentation and Its Effect on Quality. *Sci. Rep.* 2021, *11*, 16746. https://doi.org/10.1038/s41598-021-95703-2.

29. Moreno-*Zambrano*, M.; Ullrich, M.S.; Hütt, M.-T. Exploring Cocoa Bean Fermentation Mechanisms by Kinetic Modelling. *R. Soc. Open Sci*. 2022, *9*, 210274. https://doi.org/10.1098/rsos.210274.

30. Fang, Y.; Li, R.; Chu, Z.; Zhu, K.; Gu, F.; Zhang, Y. Chemical and Flavor Profile Changes of Cocoa Beans (*Theobroma Cacao* L.) during Primary Fermentation. *Food Sci. Nutr.* 2020, *8*, 4121–4133. https://doi.org/10.1002/fsn3.1701.

31. Martini, S. *Application* of DSC, Pulsed NMR, and Other Analytical Techniques to Study the Crystallization Kinetics of Lipids Models, Oil, Fats, and Their Blends in the Field of Food Technology. In *Differential Scanning Calorimetry. Applications in Fat and oil Technology*; CRC Press/Taylor & Francis: Boca Raton, FL, USA, 2015; pp. 163–195.

32. Jin, J.; Jin, Q.; Wang, X.; Akoh, C.C. Improving Heat and Fat Bloom Stabilities of "Dark Chocolates" by Addition of Mango Kernel Fat-Based Chocolate Fats. *J. Food Eng.* 2019, *246*, 33–41. https://doi.org/10.1016/j.jfoodeng.2018.10.027.

33. Hubbes, S.-S.; Danzl, W.; Foerst, P. Crystallization Kinetics of Palm Oil of Different Geographic Origins and Blends Thereof by the Application of the Avrami Model. *LWT* 2018, *93*, 189–196. https://doi.org/10.1016/j.lwt.2018.03.022.

34. Marangoni, A.G.; Wesdorp, L.H. Nucleation and Crystalline Growth Kinetics. In *Structure and Properties of Fat Crystal Networks*; CRC Press: Boca Raton, FL, USA, 2013; pp. 27–99.

35. *Sangwal*, K.; Sato, K. Nucleation and Crystallization Kinetics of Fats. In *Structure-Function Analysis of Edible Fats*; Elsevier: London, United Kingdom, 2018; pp. 21–72. ISBN 978-0-12-814041-3.

36. Davis, T.R.; Dimick, P.S. Isolation and Thermal Characterization of High-*Melting* Seed Crystals Formed during Cocoa Butter Solidification. *J. Am. Oil Chem. Soc.* 1989, *66*, 1488–1493. https://doi.org/10.1007/BF02661978.

37. *MacNaughtan*, W.; Farhat, I.A.; Himawan, C.; Starov, V.M.; Stapley, A.G.F. A Differential Scanning Calorimetry Study of the Crystallization Kinetics of Tristearin-Tripalmitin Mixtures. *J. Am. Oil Chem. Soc.* 2006, *83*, 15. https://doi.org/10.1007/s11746-006-1167-1.

38. Simoes, S.; Lelaj, E.; Rousseau, D. The Presence of Crystalline Sugar Limits the Influence of Emulsifiers on Cocoa Butter Crystallization. *Food Chem.* 2021, *346*, 128848. https://doi.org/10.1016/j.foodchem.2020.128848.

39. Santander, M.; Vaillant, F.; Sinuco, D.; Rodríguez, J.; Escobar, S. Enhancement of Fine Flavour Cocoa Attributes under a Controlled Postharvest Process. *Food Res. Int.* 2021, *143*, 110236. https://doi.org/10.1016/j.foodres.2021.110236.

40. AOAC Official Methods of Analysis. 1998. https://www.aoac.org/ (accessed on 05 May 2022).

41. Elbl, J.; Gajdziok, J.; Kolarczyk, J. 3D Printing of Multilayered Orodispersible Films with In-Process Drying. *Int. J. Pharm.* 2020, *575*, 118883. https://doi.org/10.1016/j.ijpharm.2019.118883.

42. Agoda-*Tandjawa*, G.; Dieudé-Fauvel, E.; Girault, R.; Baudez, J.-C. Using Water Activity Measurements to Evaluate Rheological Consistency and Structure Strength of Sludge. *Chem. Eng. J.* 2013, *228*, 799–805. https://doi.org/10.1016/j.cej.2013.05.012.

43. Foubert, I.; Vanrolleghem, P.A.; Thas, O.; Dewettinck, K. Influence of Chemical Composition on the Isothermal Cocoa Butter Crystallization. *J. Food Sci.* 2006, *69*, E478–E487. https://doi.org/10.1111/j.1365-2621.2004.tb09933.x.

44. Toro-Vazquez, J.F.; Rangel-Vargas, E.; Dibildox-Alvarado, E.; Charó-Alonso, M.A. Crystallization of Cocoa Butter with and without Polar Lipids Evaluated by Rheometry, Calorimetry and Polarized Light Microscopy. *Eur. J. Lipid Sci. Technol.* 2005, *107*, 641–655. https://doi.org/10.1002/ejlt.200501163.

45. Avrami, M. Kinetics of Phase Change. II Transformation-Time Relations for Random Distribution of Nuclei. *J. Chem. Phys.* 1940, *8*, 212–224. https://doi.org/10.1063/1.1750631.

46. Lorenzo, A.T.; Arnal, M.L.; Albuerne, J.; Müller, A.J. DSC Isothermal Polymer Crystallization Kinetics Measurements and the Use of the Avrami Equation to Fit the Data: Guidelines to Avoid Common Problems. *Polym. Test.* 2007, *26*, 222–231. https://doi.org/10.1016/j.polymertesting.2006.10.005.

47. Toro-Vazquez, J.F.; Briceño-Montelongo, M.; Dibildox-Alvarado, E.; Charó-Alonso, M.; Reyes-Hernández, J. Crystallization Kinetics of Palm Stearin in Blends with Sesame Seed Oil. *J. Am. Oil Chem. Soc.* 2000, *77*, 297–310. https://doi.org/10.1007/s11746-000-0049-x.

48. *Brereton*, R.G. *Applied Chemometrics for Scientist; First*; John Wiley and Sons: Chichester, UK, 2007.

49. Chagas Junior, G.C.A.; Ferreira, N.R.; Gloria, M.B.A.; Martins, L.H.d.S.; Lopes, A.S. Chemical Implications and Time Reduction of On-Farm Cocoa Fermentation by Saccharomyces Cerevisiae and Pichia Kudriavzevii. *Food Chem.* 2021, *338*, 127834. https://doi.org/10.1016/j.foodchem.2020.127834.

50. Visintin, S.; Ramos, C.L.; Batista, N.N.; Dolci, P.; Schwan, R.F.; Cocolin, L. Impact of Saccharomyces Cerevisiae and Torulaspora Delbrueckii Starter Cultures *on* Cocoa Beans Fermentation. *Int. J. Food Microbiol.* 2017, *257*, 31–40. https://doi.org/10.1016/j.ijfoodmicro.2017.06.004.

51. Castro-Alayo, E.M.; Idrogo-Vásquez, G.; Siche, R.; Cardenas-Toro, F.P. Formation of Aromatic Compounds Precursors during Fermentation of Criollo and Forastero Cocoa. *Heliyon* 2019, *5*, e01157. https://doi.org/10.1016/j.heliyon.2019.e01157.

52. Deus, V.L.; Bispo, E.S.; Franca, A.S.; Gloria, M.B.A. Influence of Cocoa Clones on the Quality and Functional Properties of Chocolate—Nitrogenous Compounds. *LWT* 2020, *134*, 110202. https://doi.org/10.1016/j.lwt.2020.110202.

53. Bayés-García, L.; Yoshikawa, S.; Aguilar-Jiménez, M.; Ishibashi, C.; Ueno, S.; Calvet, T. Heterogeneous Nucleation Effects of Talc Particles on

Polymorphic Crystallization of Cocoa Butter. *Cryst. Growth Des.* 2022, *22*, 213–227. https://doi.org/10.1021/acs.cgd.1c00859.

54. Aumpai, K.; Tan, C.P.; Huang, Q.; Sonwai, S. Production of Cocoa Butter Equivalent from Blending of Illipé Butter and Palm Mid-Fraction. *Food Chem.* 2022, *384*, 132535.

55. Marangoni, A.G.; McGauley, S.E. Relationship between Crystallization Behavior and Structure in Cocoa Butter. *Cryst. Growth Des.* 2003, *3*, 95–108. https://doi.org/10.1021/cg025580l.

56. Bayés-García, L.; Aguilar-Jiménez, M.; Calvet, T.; Koyano, T.; Sato, K. Crystallization and Melting Behavior of Cocoa Butter in Lipid Bodies of Fresh Cacao Beans. *Cryst. Growth Des.* 2019, *19*, 4127–4137. https://doi.org/10.1021/acs.cgd.9b00570.

57. Lu, C.; Zhang, B.; Zhang, H.; Guo, Y.; Dang, L.; Liu, Z.; Shu, Q.; Wang, Z. Solid–Liquid Phase Equilibrium and Phase Behaviors for Binary Mixtures Composed of Tripalmitoylglycerol (PPP), 1,3-Dipalmitoyl-2-Oleoyl-Glycerol (POP), and 1,2-Dioleoyl-3-Palmitoyl-Glycerol (POO). *Ind. Eng. Chem. Res.* 2019, *58*, 10044–10052. https://doi.org/10.1021/acs.iecr.9b01947.

58. Smith, K.W.; Cain, F.W.; Talbot, G. Kinetic Analysis of Nonisothermal Differential Scanning Calorimetry of 1,3-Dipalmitoyl-2-Oleoylglycerol. J. Agric. *Food Chem.* 2005, *53*, 3031–3040. https://doi.org/10.1021/jf048036o.

59. Avrami, M. Kinetics of Phase Change. I General Theory. *J. Chem. Phys.* 1939, *7*, 1103–1112. https://doi.org/10.1063/1.1750380.

60. Mello, N.A.; Cardoso, L.P.; Badan Ribeiro, A.P.; Bicas, J.L. The Effects of Limonene on the Crystallization of Palm Oil. *LWT* 2020, *133*, 110079. https://doi.org/10.1016/j.lwt.2020.110079.

61. Miyasaki, E.K.; dos Santos, C.A.; Vieira, L.R.; Ming, C.C.; Calligaris, G.A.; Cardoso, L.P.; Gonçalves, L.A.G. Acceleration of Polymorphic Transition of Cocoa Butter and Cocoa Butter Equivalent by Addition of D-limonene. *Eur.*

J. Lipid Sci. Technol. 2016, *118*, 716–723. https://doi.org/10.1002/ejlt.201400557.

62. Martini, S.; Carelli, A.A.; Lee, J. Effect of the Addition of Waxes on the Crystallization Behavior of Anhydrous Milk Fat. *J. Am. Oil Chem. Soc.* 2008, *85*, 1097–1104. https://doi.org/10.1007/s11746-008-1310-2.

63. Rashi*d*, N.A. Crystallisation Kinetics of Palm Stearin, Palm Kernel Olein and Their Blends. *Food Sci. Technol.* 2012, *46*, 571–573.

64. Gomez, N.A.; Sanchez, K.; Arguello, H. Non-Destructive Method for Classification of Cocoa Beans from Spectral Information. In Proceedings of the 2019 XXII Symposium on Image, Signal Processing and Artificial Vision (STSIVA), Bucaramanga, Colombia, 24–26 April 2019; pp. 1–5.

65. Cevallos-Cevallos, J.M.; Gysel, L.; Maridueña-Zavala, M.G.; Molina-Miranda, M.J. Time-Related Changes in Volatile Compounds during Fermentation of Bulk and Fine-Flavor Cocoa (*Theobroma Cacao*) Beans. *J. Food Qual.* 2018, *2018*, 1758381. https://doi.org/10.1155/2018/1758381.

66. Talbot, G. Chocolate Temper. In *Industrial Chocolate, Manufacture and Use*; Blackwell Publishing: Oxford, UK, 2009; pp. 261–275, ISBN 978-1-4051-3949-6.

67. Garbolino, C.; Bartoccini, M.; Flöter, E. The Influence of Emulsifiers on the Crystallisation Behaviour of a Palm Oil-based Blend. *Eur. J. Lipid Sci. Technol*. 2005, *107*, 616–626. https://doi.org/10.1002/ejlt.200501186.

CAPÍTULO IV. MISCIBILIDAD DE LA MANTECA DE CACAO CRIOLLO CON ACEITES VEGETALES

Evaluation of the Miscibility of Novel Cocoa Butter Equivalents by Raman Mapping and Multivariate Curve Resolution–Alternating Least Squares

Efraín M. Castro-Alayo [1,2,3,*], Llisela Torrejón-Valqui [1], Ilse S. Cayo-Colca [4] and Fiorella P. Cárdenas-Toro [2,3]

1 Facultad de Ingeniería y Ciencias Agrarias, Instituto de Investigación, Innovación y Desarrollo para el Sector Agrario y Agroindustrial de la Región Amazonas (IIDAA), Universidad Nacional Toribio Rodríguez de Mendoza de Amazonas, Calle Higos Urco 342-350-356, Chachapoyas 01001, Peru; llisela.torrejon@untrm.edu.pe

2 Sección de Ingeniería Industrial, Departamento de Ingeniería, Pontificia Universidad Católica del Perú, Av. Universitaria 1801, San Miguel 15088, Peru; fcardenas@pucp.pe

3 Programa de Doctorado en Ingeniería, Departamento de Ingeniería, Pontificia Universidad Católica del Perú, Av. Universitaria 1801, San Miguel 15088, Peru

4 Facultad de Ingeniería Zootecnista, Agronegocios y Biotecnología, Universidad Nacional Toribio Rodríguez de Mendoza de Amazonas, Calle Higos Urco 342-350-356, Chachapoyas 01001, Peru; icayo.fizab@untrm.edu.pe

* Correspondence: efrain.castro@untrm.edu.pe; Tel.: +51-98-637-6463

Abstract: Cocoa butter (CB) is an ingredient traditionally used in the manufacturing of chocolates, but its availability is decreasing due to its scarcity and high cost. For this reason, other vegetable oils, known as cocoa butter equivalents (CBE), are used to replace CB partially or wholly. In the present work, two Peruvian vegetable oils, coconut oil (CNO) and sacha inchi oil (SIO), are proposed as novel CBEs. Confocal Raman microscopy (CRM) was used for the chemical differentiation and polymorphism of these oils with CB based on their Raman spectra. To analyze their miscibility, two types of blends were prepared: CB with CNO, and CB with SIO. Both were prepared at 5 different concentrations (5%, 15%, 25%, 35%, and 45%). Raman mapping was used to obtain the chemical maps of the blends and analyze their miscibility through distribution maps, histograms and relative standard deviation (RSD). These values were obtained with multivariate curve resolution–alternating least squares. The results show that both vegetable oils are miscible with CB at high concentrations: 45% for CNO and 35% for SIO. At low concentrations, their miscibility decreases. This shows that it is possible to consider these vegetable oils as novel CBEs in the manufacturing of chocolates.

Keywords: cocoa butter; coconut oil; sacha inchi oil; confocal raman microscopy; raman mapping; multivariate curve resolution–alternating least squares; chocolate

1. Introduction

In the manufacture of chocolates, one of the main ingredients is cocoa butter (CB), which is the main contributor to the high fat content of chocolate. In total, 30 to 40% of the weight of chocolate is fat [1]. CB remains as a solid at 20 °C (with hard texture and snap) and melts rapidly at 33 °C, leading to the release of flavor and soft mouth-feel texture [2,3]. Cost and technical limitations have increased CB demand, although it is the main lipid phase in chocolate manufacturing. In addition, it is also used in combination with other vegetable oils, such as hydrogenated or partially hydrogenated soybean oil and palm oil [2–4]. Therefore, researchers have been searching for cheaper alternatives with similar characteristics to CB [2]. These alternatives should improve the physical properties and bloom resistance and reduce the health risks of the final product [3]. CB can be substituted with vegetable fats by blending to produce chocolate or replace CB either partially or wholly [2]. These are the so-called cocoa butter equivalents (CBE), which

Evaluation of the Miscibility of Novel Cocoa Butter Equivalents by Raman Mapping and Multivariate Curve Resolution–Alternating Least Squares

Efraín M. Castro-Alayo[1,2,3], Llisela Torrejón-Valqui[1], Ilse S. Cayo-Colca[4], Fiorella P. Cárdenas-Toro[2,3]

[1] Instituto de Investigación, Innovación y Desarrollo para el Sector Agrario y Agroindustrial de la Región Amazonas (IIDAA), Facultad de Ingeniería y Ciencias Agrarias, Universidad Nacional Toribio Rodríguez de Mendoza de Amazonas, Calle Higos Urco, Chachapoyas 342-350-356, Amazonas, Perú; llisela.torrejon@untrm.edu.pe

[2] Sección de Ingeniería Industrial, Departamento de Ingeniería, Pontificia Universidad Católica del Perú, Av. Universitaria 1801, San Miguel, Lima 32, Perú; fcardenas@pucp.pe

[3] Departamento de Ingeniería, Programa de Doctorado en Ingeniería, Pontificia Universidad Católica del Perú, Av. Universitaria 1801, San Miguel, Lima 32, Perú

[4] Facultad de Ingeniería Zootecnista, Agronegocios y Biotecnología, Universidad Nacional Toribio Rodríguez de Mendoza de Amazonas, Calle Higos Urco, Chachapoyas 342-350-356, Amazonas, Perú; icayo.fizab@untrm.edu.pe

4.1. Abstract

Cocoa butter (CB) is an ingredient traditionally used in the manufacturing of chocolates, but its availability is decreasing due to its scarcity and high cost. For this reason, other vegetable oils, known as cocoa butter equivalents (CBE), are used to replace CB partially or wholly. In the present work, two Peruvian vegetable oils, coconut oil (CNO) and sacha inchi oil (SIO), are proposed as novel CBEs. Confocal Raman microscopy (CRM) was used for the chemical differentiation and polymorphism of these oils with CB based on their Raman spectra. To analyze their miscibility, two types of blends were prepared: CB with CNO, and CB with SIO. Both were prepared at 5 different concentrations (5%, 15%, 25%, 35%, and 45%). Raman mapping was used to obtain the chemical maps of the blends and analyze their miscibility through distribution maps, histograms and relative standard deviation (RSD). These values were obtained with multivariate curve resolution–alternating least squares. The results show that both vegetable oils are miscible with CB at high concentrations: 45% for CNO and 35% for SIO. At low concentrations, their miscibility decreases. This shows that it is possible to consider these vegetable oils as novel CBEs in the manufacturing of chocolates.

Keywords: cocoa butter; coconut oil; sacha inchi oil; confocal Raman microscopy; Raman mapping; multivariate curve resolution–alternating least squares; chocolate

4.2. Introduction

In the manufacture of chocolates, one of the main ingredients is cocoa butter (CB), which is the main contributor to the high fat content of chocolate. In total, 30 to 40% of the weight of chocolate is fat [1]. CB remains as a solid at 20 °C (with hard texture and snap) and melts rapidly at 33 °C, leading to the release of flavor and soft mouth-feel texture [2,3]. Cost and technical limitations have increased CB demand, although it is the main lipid phase in chocolate manufacturing. In addition, it is also used in combination with other vegetable oils, such as hydrogenated or partially hydrogenated soybean oil and palm oil [2–4]. Therefore, researchers have been searching for cheaper alternatives with similar

characteristics to CB [2]. These alternatives should improve the physical properties and bloom resistance and reduce the health risks of the final product [3]. CB can be substituted with vegetable fats by blending to produce chocolate or replace CB either partially or wholly [2]. These are the so-called cocoa butter equivalents (CBE), which should be compatible with CB without presenting any eutectic behavior [5]. According to Norazlina et al. [2], CBEs are nonlauric fats that are obtained from the fractionation, interesterification and blending of fats and oils. CBEs have physicochemical, thermal and sensory attributes similar and compatible with those of CB, so they can be miscible in any proportion without changing the characteristics of CB (that is, they are fully compatible with CB properties) [2,6–8]. CBEs also possess TAGs similar to those in CB but are produced from low-cost vegetable oils [9]. Some countries allow the use of noncocoa vegetable fats or oils at a defined maximum level to improve the properties of chocolate [10]. The current legislation of the European Union allows the incorporation of up to 5% of CBE in the total weight of the chocolate [11], while the United States legislation does not specify this value [12–14]. European regulation only allows six vegetable oils to be used as CBE, specifically illipe, palm oil, sal, shea, kokum gurgi and mango kernel [11,13].

In the Peruvian amazon, sacha inchi (*Plukenetia huayabambana* L.) is cultivated. This plant is known as the Inca peanut and is an important source of phenolic compounds and high antioxidant capacity [15,16]. Sacha inchi oil (SIO) is emerging as a functional food due to its rich composition of polyunsaturated fatty acids, tocopherol and sterols. These compounds have shown multiple human health benefits [17]. Coconut oil (CNO) is used in food manufacturing. It is a saturated fat rich in small and medium chain fatty acids, comparable to animal fat [18]. The scientific and nonspecialized literature promotes the consumption of CNO based on the assumption that it is beneficial for health because it is low in cholesterol, reduces the risk of cardiovascular diseases, encourages weight loss, and improves cognitive functions, among others [19]. In Peru, these natural vegetable oils are produced, and could be good candidates to be considered novel CBEs.

During food manufacturing, some ingredients, even when they may be macroscopically miscible, can show microscopic heterogeneities that would cause instability and phase separation during storage [20]. This is a problem in

the manufacture of pharmaceutical tablets, but is also a problem in the manufacture of chocolates. To ensure the quality of the final product, analytical techniques are used to create chemical maps [21] and determinate their miscibility. Some researchers are developing methodologies based on Raman mapping (or Raman imaging) for the evaluation of miscibility between ingredients [20,22–24]. Raman spectroscopy can offer widespread food safety assessments in a nondestructive, easy to operate, sensitive, and rapid manner [25]. Raman mapping assimilates two important technologies, imaging and Raman spectroscopy, to simultaneously provide an image of, and spectral information regarding, food products [26]. The purpose of Raman mapping is to visualize the distribution of components by chemical properties in a sample [25] and to study heterogeneous materials, since it provides submicron spatial resolution with high sensitivity [27].

In Raman mapping, each pixel in the image corresponds to a Raman spectrum, which is compared to an established Raman database to determine the specific analytes or spectral background measurements in this location [25]. The spectral information obtained is complex, so multivariate analysis is necessary to unravel complex spectral data from Raman mapping data [21]. Multivariate curve resolution–alternating least squares (MCR–ALS) is a self-modeling curve resolution method that offers the possibility of extracting physically meaningful spectra associated with pure components from the mixed Raman spectra of real biological samples with the benefit of not requiring prior information about the nature of the sample [28]. Using MCR–ALS, Mitsutake et al. [22] found that CB and CNO present intermediate miscibility at concentrations of 75% and 25%, respectively, when used in the manufacture of pharmaceutical tablets.

Raman mapping is expected to be a useful tool for the food industry to assess the quality and safety of food [26]; however, there is scarce information on this topic. The present work focuses on two important approaches for the food industry: the search for natural sources of Peruvian origin for use in the chocolate industry as novel CBEs, and the use of a new non-destructive analysis technique to evaluate the miscibility of these natural sources with CB as a first step for the development of new CBEs. Thus, the objective of this work was to study the

miscibility of CNO, SIO, and CB using confocal Raman microscopy and MCR–ALS to propose novel CBEs for the chocolate industry.

4.3. Materials and Methods

4.3.1. Materials

The vegetable oils used were pure CNO and SIO, which were purchased from a local market in Chachapoyas, Peru. CB was provided by the Cooperativa de Servicios Múltiples Aprocam (Bagua, Amazonas, Peru).

4.3.2. Sample Preparation

Following Mitsutake et al. [22], the samples were prepared by heating them to 10 °C above the CB melting point; the materials were added while stirring until a visually homogeneous blend was obtained. Two batches were prepared: the first was composed of CB and CNO (CB-CNO), and the second was composed of CB and SIO (CB-SIO). Each batch contained 5 concentrations of vegetable oils, ranging from 5% to 45% (Table 4.3-1), and 3 replicates of each concentration were produced. The samples were placed in a chocolate mold and cooled to 4 °C for easy removal of the tablets. A piece of $1 \times 1\ cm^2$ was removed from each tablet for Raman mapping.

Table 4.3-1. Composition of the samples.

Sample	Cocoa Butter (%)	Coconut Oil (%)	Sacha Inchi Oil (%)
CB55-CNO45	55	45	---
CB65-CNO35	65	35	---
CB75-CNO25	75	25	---
CB85-CNO15	85	15	---
CB95-CNO05	95	05	---
CB55-SIO45	55	---	45
CB65-SIO35	65	---	35
CB75-SIO25	75	---	25
CB85-SIO15	85	---	15
CB95-SIO05	95	---	05

4.3.3. Raman Mapping

Following the process of Mitsutake et al. [22] with some modifications, the samples were mapped using a Raman confocal microscope system (Horiba Scientific, XploRA plus, Montpellier, France). Chemical maps were obtained by a 532 nm laser as an excitation light with a 50% filter. The experimental conditions were as follows: 100 nm slit width, pinhole 100 µm, x50/0.90 NA Vis-LWD air objective, and 1 s acquisition time with 2 accumulations. The Raman signal was obtained using a 600 lines/mm grating centered between 800 and 3100 cm^{-1}. The acquired spectra were corrected in a range from 1000 to 1800 cm^{-1}, smoothed, and baseline corrected using LabSpec 6 Suite software. Each sample generated a cube of data with dimensions of 25 × 25 × 761, where 25 was the number of pixels at the x and y axes and 761 was the number of spectral variables.

4.3.4. Data Analysis of Chemical Maps

According to Vajna et al. [29], before chemometric evaluation, all spectra were baseline corrected (this was done by using the same baseline points for all maps and component spectra). Then, the spectral range from 1000 to 1800 cm^{-1} was used for the corresponding evaluation. Raman chemical map data were analyzed by using Solo+MIA software (Eigenvector, Research, Inc. Wenatchee, WA, USA). The raw 3-dimensional data were unfolded into a 2-dimensional matrix. The estimation of pure component spectra from the Raman chemical maps was carried out by MCR-ALS. This technique is based on the following bilinear model (Equation (1)):

$$X = CS^T + E \qquad (1)$$

where X ($p * \lambda$) is the matrix containing the mapping spectra, S^T ($k * \lambda$) is the set of pure component spectra, and C ($p * k$) contains the vectors of spectral concentrations (each row in C contains the concentrations of the k ingredients). The matrix E represents the residual noise. MCR–ALS generated both the concentration matrix C (scores) and recovered spectrum matrix S^T (loadings)

from the dataset X in an iterative manner, using an initial estimation for either C or S^T and appropriate constraints.

Preprocessing and Constraints

The preprocessing technique was normalized (1-norm, area = 1). The normalization of concentration profiles or resolved spectra or use of reference concentration values within the optimization helps to suppress the rotational ambiguity [30]. The applied constraints were non-negativity, which forces the profiles to be formed by positive values and can be implemented replacing negative values by zeros [30], and equality, which makes the concentration profile and/or spectra of a component equal to a certain known predefined shape [30]. Pure CB, CNO, and SIO spectra were used as equality constraints.

4.3.5. Miscibility

To determinate the miscibility of the vegetable oils proposed as novel CBEs with CB, the homogeneity of the samples was quantitatively and qualitatively determined. The relative standard deviation (RSD) is a commonly used tool in the pharmaceutical industry to estimate the homogeneity of a component within a blend [31] and describe the distribution of the components quantitatively. The RSD was calculated from the ratio of the standard deviation (σ) and the mean (μ) of each measured image score. Using RMarkdown software, the RSD of the scores within a chemical image was calculated. A lower RSD of the chemical image corresponded to a more homogeneous distribution of the respective ingredient [29, 32, 33] and, therefore, its miscibility. Qualitatively, the homogeneity of the samples was analyzed using histograms. According to Gendrin et al. [33], a histogram showing a symmetric distribution with a narrow base and sharp peak is representative of a low-contrast image and therefore of a homogeneous sample. Conversely, an asymmetric histogram with a wide base and flatter peak or several modes is representative of a more contrasted image, i.e., a heterogeneous sample.

4.4. Results

4.4.1. Characterization of the Spectra of Cocoa Butter and Vegetable Oils

Figure 4.4-1 shows the characteristics of the Raman spectra of the pure components (CB, CNO, and SIO) in the full range (1000–3100 cm^{-1}) at room temperature (20 °C). In the CB spectra, the C–H stretching region shows peaks at 2885.7 and 2886.1 cm^{-1} which are assigned to alkyl-chain methylene symmetric (v_s) and antisymmetric (v_{as}) stretching. A peak at 2936.5 cm^{-1} associated with the terminal methyl $v_s(CH_3)$ stretch was observed. In the C=O stretching region, we can see 2 peaks at 1745.4 and 1733.8 cm^{-1}, which are representative of forms III and IV at room temperature (Figure 4.4-1). The full width at half maximum (FWHM) of the peak at 1745.4 cm^{-1} was 17.38 cm^{-1}. In the C=C stretching region [$v_s(C=C)$] of the olefinic band, we can see a peak at 1662.7 cm^{-1} (Table 4.4-2), representing the solid state of CB form IV at room temperature. This peak is of greater intensity in SIO due to its liquid state and is also related to the proportion of oleic acid. A total of 2 peaks at 1445.9 and 1462.9 cm^{-1} in the CH_2 and CH_3 deformation regions can also be seen. In the CH_2 twisting region, we can also see a peak at 1301.3 cm^{-1}, which is related to the degree of coupling of the alkyl chains in the lipids. The CB spectra also reveal 3 characteristic peaks of the CB polyforms, located in the C–C stretching range (1030–1183 cm^{-1}). The peak at 1102.21 cm^{-1} indicates the existence of CB in its solid state at room temperature. This peak is not present in CNO and SIO. The pure spectra of CB, CNO, and SIO look similar (Figure 4.4-2); however, we can find some differences in some peaks. CNO has a peak at 1662.7 cm^{-1} whose intensity is lower. SIO has high intensity peaks at 1276.7 cm^{-1} and 3020.2 cm^{-1} that the others do not have. These peaks are assigned to plane =CH deformation in an unconjugated *cis* C=C and asymmetric C=H stretch group. From Figure 4.4-2, we can see that the peak at 1745.3 cm^{-1} in CB is shown at 1747.93 cm^{-1} in CNO and at 1746.8 in SIO, and the peak at 1733.84 cm^{-1} in CB is shown at 1734.83 cm^{-1} in SIO. We found differences between the area ratios of the peaks at 1733.84 and 1745.43 cm^{-1}, which can be used as differentiation patterns between CB, CNO, and SIO.
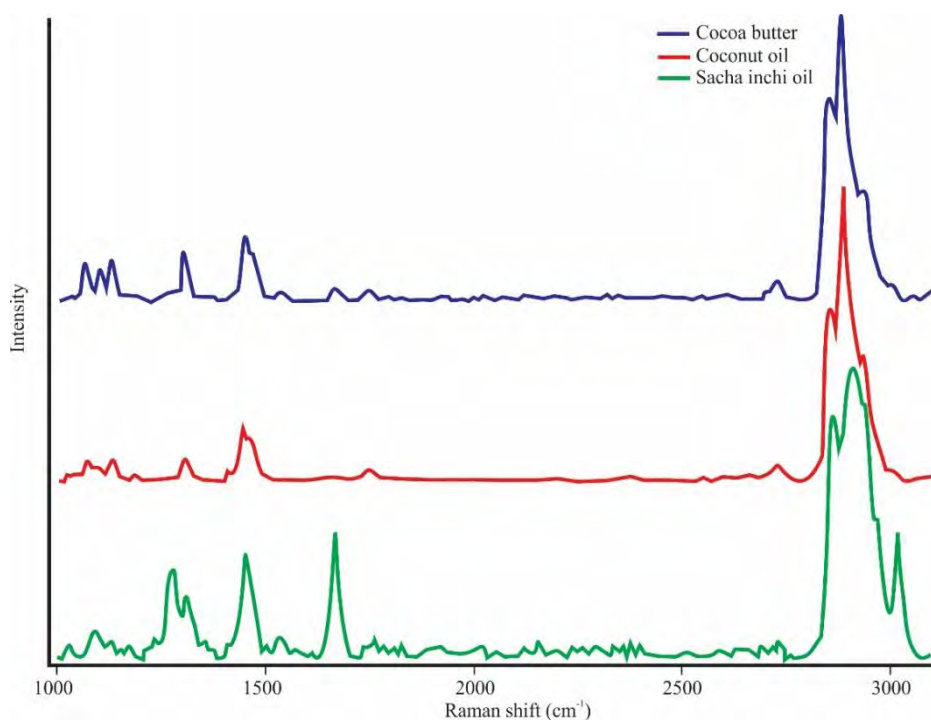
Figure 4.4-1. Raman spectra of the pure CB and vegetable oils in the full range (1000–3100 cm^{-1}) at room temperature (20 °C).

Table 4.4-1. Raman peaks for CB and vegetable oils.

Assignments[1]	Cocoa Butter (cm^{-1})	Coconut Oil (cm^{-1})	Sacha Inchi Oil (cm^{-1})
v_{as}(C–C)T	1066.2	1069.3	Nd
v(C–C)G	1102.9	1092.4	Nd
v_s(C–C)T	1132.3	1132.3	1125.7
τ(CH$_2$)	Nd	1268.8	Nd
τ(CH$_2$)	Nd	Nd	1276.7
τ(CH$_2$)	1301.3	1303.4	1308.8
δ(CH$_2$)	1445.9	1445.1	1449.9
δ_a(CH$_3$)	1462.9	Nd	Nd
v_s(C=C)	1662.3	1662.2	1662.7
v(C=O)	1733.8	Nd	1734.8
v(C=O)	1745.4	1747.9	1746.8
v(CH$_3$–CH$_2$)	2728.7	2730.8	2733.9
v_s(CH$_2$)	2855.7	2856.7	2863.4
v_{as}(CH$_2$)	2886.1	2886.1	2907.6
v_s(CH$_3$)	2936.5	2932.3	Nd
(=CH)$_2$	Nd	Nd	3020.2

[1]Assignments according to Bresson et al. (Bresson et al., 2011), and Jiménez-Sanchidrián et al. (Jiménez-Sanchidrián & Ruiz, 2016).
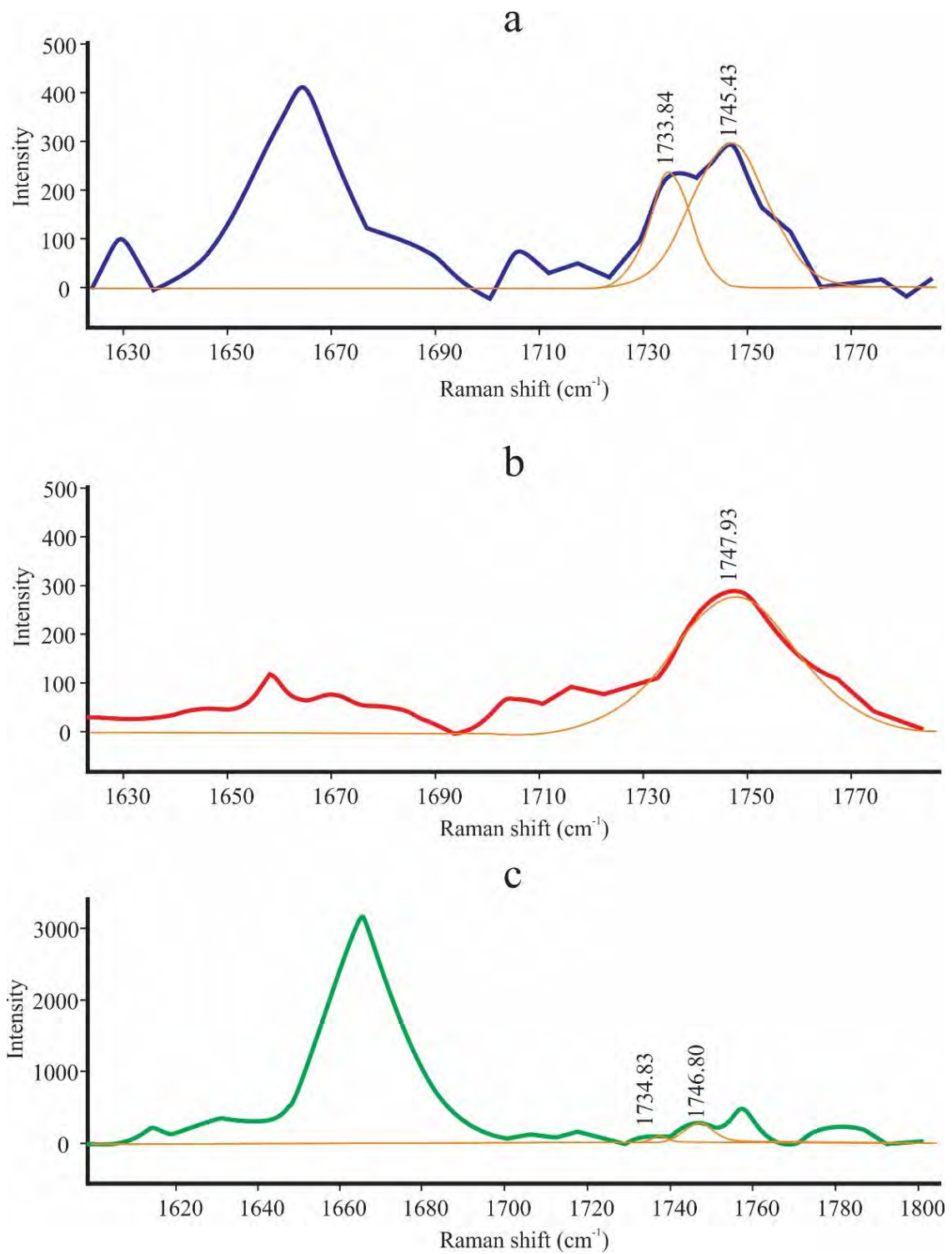
Figure 4.4-2. Carbonyl stretching region (1700-1780 cm^{-1}) of CB and vegetable oils: (a) CB; (b) CNO; and (c) SIO.

Table 4.4-2 shows the area ratios and FWHM of CB, CNO, and SIO in the mode of vibrations v(C=O). The lower FWHM values indicate a better arrangement of the crystals and their solid state; therefore, at room temperature, the crystals of CB (17.38 cm^{-1}) would have a better arrangement than those of CNO (27.52 cm^{-1}), demonstrating its solid state.

Table 4.4-2. FWHM and area ratios of the components of the Gaussian function of Raman spectra of CB, CNO, and SIO at room temperature (T = 20 °C).

Component	1733.84 cm^{-1}		1745.43 cm^{-1}		Area Ratio
	Area	FWHM	Area	FWHM	A1733.84/A1745.43
Sacha inchi oil	288.19	3.99	2751.58	9.04	0.11
Coconut oil	Nd	Nd	8112.33	27.52	Nd
Cocoa butter	2448.96	9.85	5366.85	17.38	0.46

4.4.2. Miscibility of Cocoa Butter and Vegetable Oils

Figure 4.4-3 shows the spectral range used for the miscibility analysis between CB, CNO, and SIO. The Raman spectra of the pure components are similar due to the similarity in their chemical composition. However, there are important differences that are considered for the analysis by MCR–ALS. These differences are mainly found in the C–C stretching region (1000–1200 cm^{-1}), the C=C stretching [vs(C=C)], and the carbonyl C=O stretching region (1700–1800 cm^{-1}). The peak located at 1662.77 cm^{-1} has a greater intensity in the SIO than in CB and CNO, and is characteristic of its liquid state.
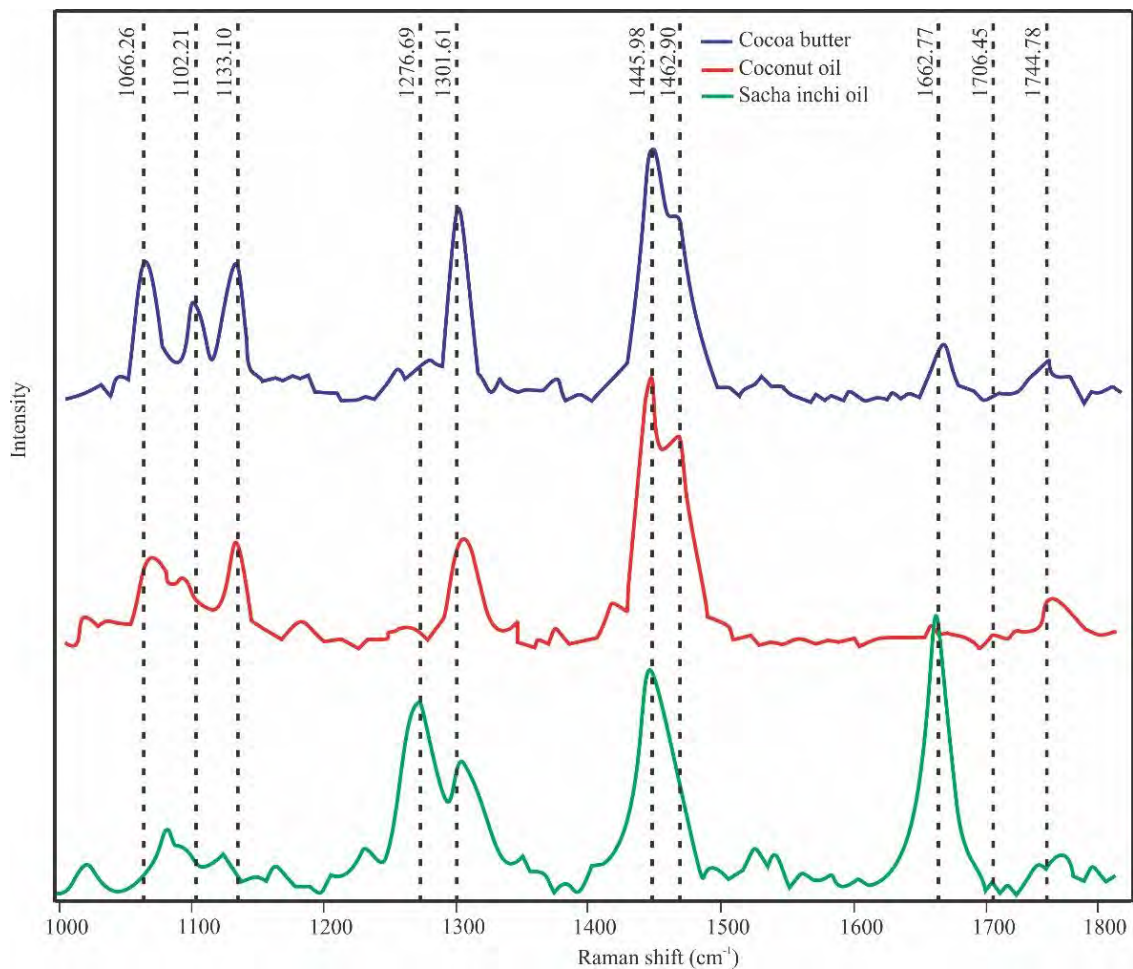
Figure 4.4-3. Raman spectral range used for analysis of the miscibility of CB and vegetable oils by MCR-ALS.

Figure 4.4-4 shows the effect of the 1-norm preprocessing technique on the raw data from samples CB75–CNO25 (Figure 4.4-4a) and CB75–SIO25 (Figure 4.4-4c) obtained by Solo + MIA (original data in Supplementary Material, Tabla A6). This method was able to correct the noise and scattering contributions in the raw data (Figure 4.4-4b,d) before fitting the data to the MCR–ALS model.
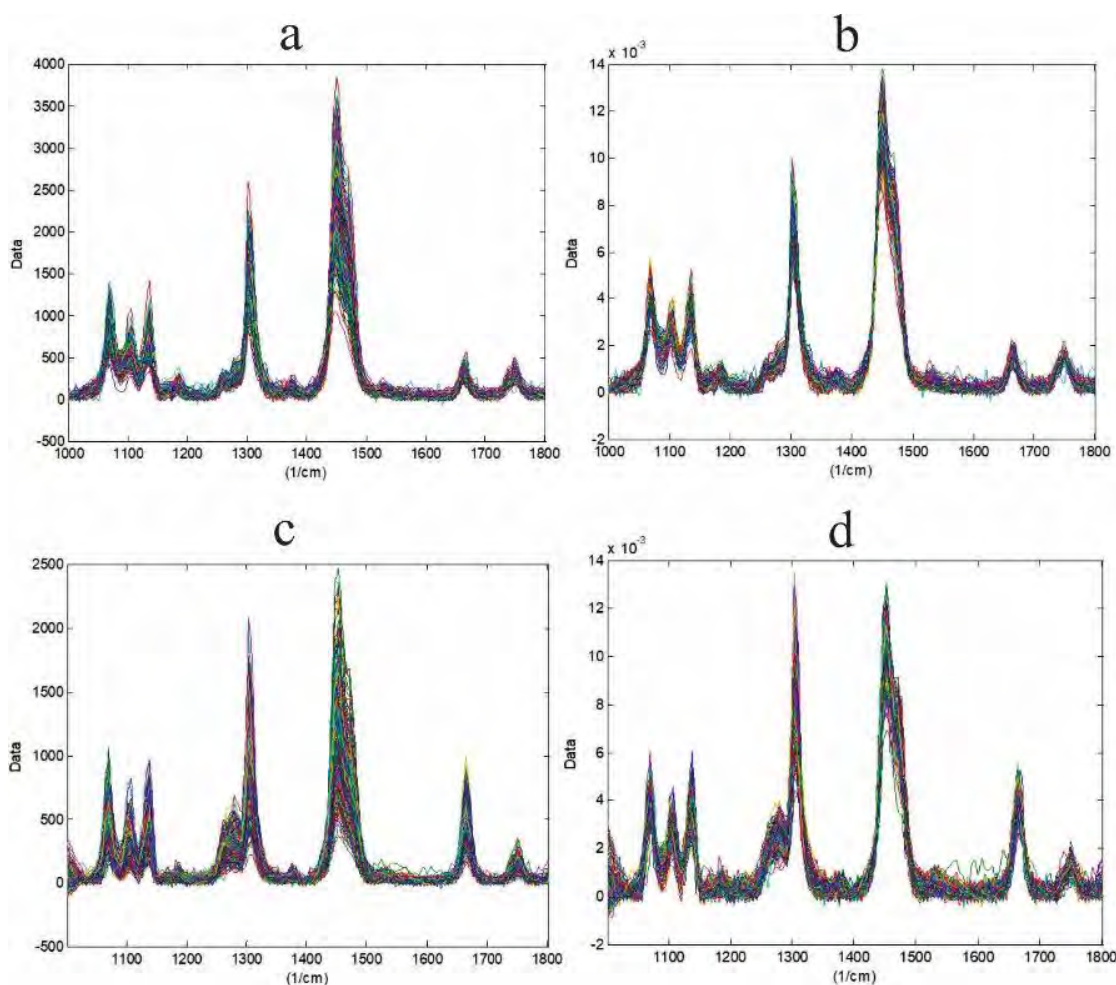
Figure 4.4-4. Raw data (a,c) and preprocessed data (b,d) from CB samples mixed with 25% CNO (a,b) and 25% SIO (c, d).

Table 4.4-3 shows the MCR–ALS quality parameters and correlation coefficients between the original spectra and the spectra recovered (S^T) by MCR–ALS. The quality parameter related to the fit of the model was the percentage of explained variance, whose values were between 94.59 and 98.46%, acceptable for our work. The use of the spectra of the pure compounds as equality constraints produced correlation coefficients between 0.9999 and 0.9993. With these values, it can be verified that component 1 was related to CB and component 2 was related to vegetable oils (CNO or SIO) according to the analyzed samples.

Table 4.4-3. MCR–ALS quality results and correlation coefficients between recovered spectra by the model and real spectra.

Sample	Numbers of Factor	Explained Variance (%)	MCR-ALS Component	Cocoa Butter	Vegetable Oil
CB55-CNO45	2	96.74	Comp 1	0.9999	0.9396
			Comp 2	0.9384	0.9999
CB65-CNO35	2	96.60	Comp 1	0.9997	0.9546
			Comp 2	0.9397	0.9996
CB75-CNO25	2	98.14	Comp 1	0.9998	0.9378
			Comp 2	0.9401	0.9999
CB85-CNO15	2	98.46	Comp 1	0.9996	0.9377
			Comp 2	0.9408	0.9999
CB95-CNO05	2	92.76	Comp 1	0.9999	0.9386
			Comp 2	0.9404	0.9998
CB55-SIO45	2	94.59	Comp 1	0.9998	0.5944
			Comp 2	0.6117	0.9993
CB65-SIO35	2	97.46	Comp 1	0.9999	0.5976
			Comp 2	0.6099	0.9995
CB75-SIO25	2	97.99	Comp 1	0.9998	0.9995
			Comp 2	0.6121	0.5976
CB85-SIO15	2	98.01	Comp 1	0.9999	0.5924
			Comp 2	0.6147	0.9993
CB95-SIO05	2	97.39	Comp 1	0.9997	0.5914
			Comp 2	0.6140	0.9995

Figure 4.4-5 shows a comparison between the spectrum recovered (S^T) by the MCR–ALS model and the original spectrum of the pure components. The restrictions used allowed for almost identical spectra with a good correlation. We can note that the spectrum of component 1 recovered by MCR–ALS is identical to the real spectra of CB (Figure 4.4-5a) and component 2 is identical to the real spectra of CNO (Figure 4.4-5b).
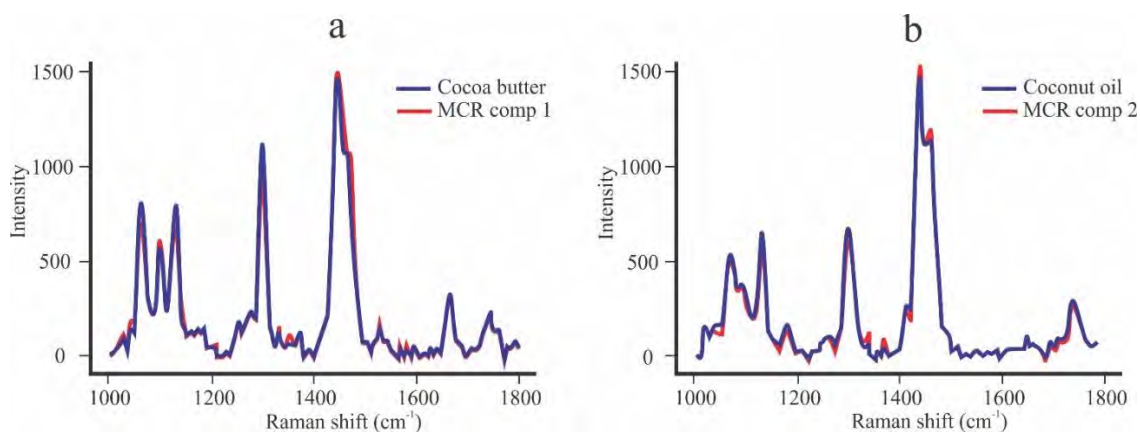
Figure 4.4-5. Comparison between the real spectra of the pure component and its respective spectrum recovered by MCR-ALS: (a) real and recovered spectra of CB; (b) real and recovered spectra of CNO.

Figure 4.4-6 shows the distribution maps and their corresponding histograms. These maps are constructed by the MCR–ALS model from the concentration matrix C and show the distribution of the compounds in the blend. The reddest areas correspond to higher concentrations and the greenest areas correspond to the lowest concentrations. We can note that, in general, the histograms corresponding to the distribution maps are peak-shaped and symmetric, which indicates that both the CNO (Figure 4.4-6a–e) and the SIO (Figure 4.4-6f–j) form a homogeneous blend with the CB. However, there are differences in the shapes between each histogram caused by the different concentrations of vegetable oil used in each sample.
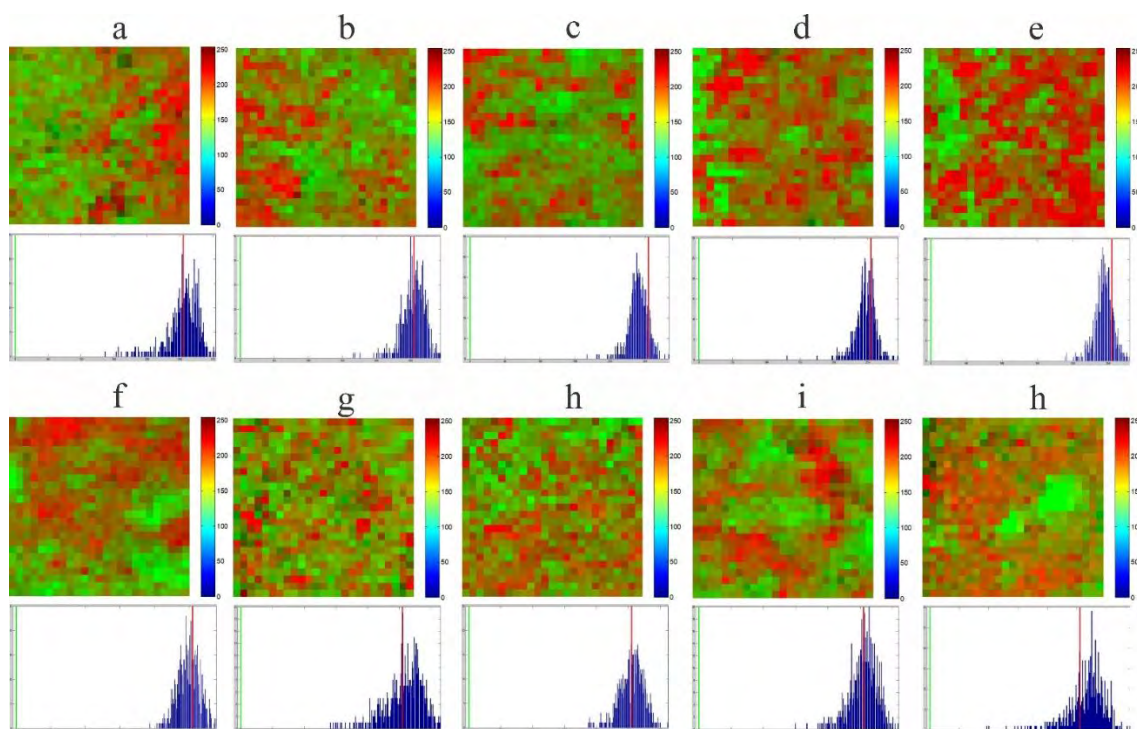
Figure 4.4-6. Distribution maps of the samples and their different concentrations: (a) CB55-CNO45; (b) CB65-CNO35; (c) CB75-CNO25; (d) CB85-CNO15; (e) CB95-CNO05; (f) CB55-SIO45; (g) CB65-SIO35; (h) CB75-SIO25; (i) CB85-SIO15; (j) CB95-SIO05.

Table 4.4-4 shows the quantitative analysis performed on the samples. The lowest RSD value of each component indicates its most homogeneous distribution in the sample. The RSD results show that CNO is more homogeneously distributed in the CB when its concentration is 45%, while its distribution is less homogeneous at 15% or 5%. The distribution of SIO in the sample is more homogeneous at 35% and less homogeneous at 15% or 5%. With these results, we can affirm that the CNO is more miscible with CB than SIO and that the miscibility of both oils improves by increasing their concentrations in the sample.

Table 4.4-4. Miscibility of vegetable oils with cocoa butter at different concentrations determined by their RSD.

Sample	Cocoa Butter RSD 1	Vegetable Oil RSD 1
CB55-CNO45	0.12 ± 0.01 ab	0.09 ± 0.02 b
CB65-CNO35	0.17 ± 0.03 ab	0.21 ± 0.09 ab
CB75-CNO25	0.23 ± 0.06 a	0.29 ± 0.09 ab
CB85-CNO15	0.21 ± 0.12 a	0.47 ± 0.13 a

CB95-CNO05	0.18 ± 0.04 ab	0.44 ± 0.23 a
CB55-SIO45	0.12 ± 0.02 ab	0.25 ± 0.03 ab
CB65-SIO35	0.10 ± 0.01 ab	0.15 ± 0.04 b
CB75-SIO25	0.10 ± 0.04 ab	0.18 ± 0.04 ab
CB85-SIO15	0.07 ± 0.01 b	0.24 ± 0.03 ab
CB95-SIO05	0.07 ± 0.02 b	0.19 ± 0.03 ab

[1]Different letters in the same column represent significant differences ($p \leq 0.05$).

4.5. Discussion

4.5.1. Characterization of the Spectra of Cocoa Butter and Vegetable Oils

According to Carmona et al. [36], the spectra were examined separately in the wavenumber region from 1000 to 3100 cm^{-1} to find differences between them. Then, although the spectra for edible vegetable oils were similar (Figure 4.4-1), it could be seen that they exhibit some differences which are small but enable their discrimination [35]. Wang et al. [37] reported a peak at 3016 cm^{-1} in the Chinese-specific peony seed oil spectrum. This peak is located in the region =C–H stretching vibration of the methyl linoleate group (cis, cis diene) of RCH=CHR, and it is used in the evaluation of oils with different unsaturation degrees. The SIO spectrum has a peak at 3020.2 cm^{-1} (Figure 4.4-1, Table 4.4-2) that is not present in CB and CNO. This peak demonstrates the degree of unsaturation of the SIO. In the characterization of the Raman spectra of CB at 22 °C carried out by Bresson et al. [34], 2 peaks were reported at 1744 and 1732 cm^{-1}, which are representative of forms III and IV. In the present work, these peaks were identified at 1745.4 and 1733.8 cm^{-1} (Figure 4.4-2, Table 4.4-2) and show that the existing conformational differences depend on the CB polymorphism. Bresson et al. [38] observed 3 components between 1750 and 1725 cm^{-1}, 1730, 1735, and 1744 cm^{-1}, which were attributed to the peak at 1735 cm^{-1} in CB or the peak at 1736 cm^{-1} in CBE for form V or VI. This peak was not observed in the CB, CNO, and SIO spectra (Figure 4.4-2, Table 4.4-3), so we can deduce that the V form was not present in the CB; therefore, the previous statement is corroborated.

In the olefinic band in the C=C stretching range (1200–1800 cm^{-1}), Bresson et al. [34] attributed the liquid form of CB to the intensity of the peak located at ~1661 cm^{-1}, as well as to the functional group present in oleic acid. That is, the higher intensity of this peak characterizes the liquid state of CB, and

the lower intensity characterizes the solid state (form IV). This coincides with what is observed in Figure 4.4-2a,c, in which this peak is located at 1662.7 cm^{-1} in CB, CNO, and SIO. There is a noticeable difference in the intensity of this peak, since it is higher in the SIO, which determines its liquid state at room temperature and its proportion of oleic acid. Likewise, this peak was observed at 1658 cm^{-1} by De Géa Neves et al. [18] in the Raman spectrum of CNO and was used as a differentiating pattern between CNO and other vegetable oils. The peak at 1445 cm^{-1} is related to the C–H deformation vibration, and the peak at 1658 cm^{-1} is assigned to cis C=C bonds, both of which provide the degree of unsaturation value [35,37]. Therefore, these peaks can be useful to determine the degree of unsaturation of CB, CNO, and SIO.

In the CB spectra, the stretching C-C region (1030–1183 cm^{-1}) allows its different polyforms to be identified. According to Bresson et al. [34], the existence of three peaks (1066.26, 1102.21, and 1133.10 cm^{-1}) (Figure 4.4-3) at room temperature allows us to recognize that it is the IV or V form and the solid state of CB. The physical state of these ingredients must also be taken into account; that is, at room temperature, the semisolid CNO only presented a peak at 1133.10 cm^{-1}, and the liquid SIO did not present any peak in this region. This characteristic of the SIO spectrum agrees with the spectra of peony seed oil, soybean oil, and extra virgin olive oil reported by Wang et al. [37]. Bresson et al. [34] affirms that the peak at 1100 cm^{-1} is representative of the solid state of CB and is not shown in the liquid state. This statement agrees with our results, since these peaks are not seen in CNO and SIO, which are not solid at room temperature.

To find differentiation patterns between CB and CBE, Bresson et al. [38] identified peaks at 1744, 1735, and 1730 cm^{-1} and found notable differences between the area ratios of these peaks. The results in Table 4.4-3 indicate that only two peaks were identified at 1733.84 and 1745.43 cm^{-1}, which correspond to the peaks mentioned above. The area ratios of CB and SIO are very different, making their differentiation possible. It was not possible to calculate the area ratio for the CNO because the peak at 1733.84 cm^{-1} was not found. FWHM is also an indicator of polymorphism in the sense that a decrease in this value indicates the transition of CB from a liquid to a solid due to the better arrangement of the crystals [34]. This statement agrees with the results of Table 4.4-3, since the semisolid state of CNO will produce a higher FWHM than CB, which is solid at

room temperature. The same behavior does not occur with SIO, since this vegetable oil is completely liquid at room temperature.

4.5.2. Miscibility of Cocoa Butter and Vegetable Oils

Following Mitsutake et al. [22], to start the analysis by MCR–ALS, the Raman range from 1000 to 1800 cm^{-1} was chosen, because it contains those peaks that allow differences to be found between the three materials studied. Therefore, Figure 4.4-3 shows the range of analysis and the main peaks that differentiate CB from CNO and SIO. The most striking difference is the high intensity of the peak of the SIO spectrum located at 1662.77 cm, which is related to its liquid state at room temperature. On the other hand, De Géa Neves et al. [18] reported the existence of peaks at 1264 and 1658 cm^{-1} in the CNO spectrum that differentiated it from other vegetable oils. In the present work, these peaks were shown at 1268.8 and 1662.2 cm^{-1}, and their intensity was very low with respect to CB and SIO. According to Castro et al. [39], to remove noise signals and optimize the results of the MCR–ALS model, the data were preprocessed using the Savitzky–Golay filter from LabSpec 6 and the 1-norm normalization method from Solo + MIA. Figure 4.4-4b,d shows the preprocessed data showing low scattering contributions, with which they were corrected, obtaining acceptable results according to Zhang et al. [39,40].

The analysis of mixtures has been a constant concern in any scientific domain [41]. MCR–ALS solves this problem by providing a chemically (scientifically) significant additive bi-linear model of pure contributions from an original data matrix [30]. This bilinear model could produce several solutions, known as rotational ambiguity, which is the primary source of uncertainty. Thus, selecting the appropriate constraints is essential to obtain optimal solutions [30,41,42]. Once the optimization process has been finished, the MCR–ALS results are the set of concentration profiles, spectra and quality parameters (explained variance) related to the model [30]. Therefore, nonnegativity and equality restrictions were applied to our data. With these considerations, the explained variance of the MCR–ALS model for all samples was between 94.59 and 98.46% (Table 4.4-4), which means that this model is capable of representing the original data with high precision. Mitsusake et al. [22] reported explained variance percentages between 98.9 and 99.6% in MCR–ALS when it was applied

to blends formulated using natural excipients, and Zhang et al. [40] reported values between 99.43 and 99.56% in the analysis of the constituents of commercial chocolate samples. The authors conclude that their results are well adjusted, and therefore, the MCR–ALS model is capable of constructing chemical maps of the samples. Although these values are higher than the results found in our work, we can say that our data fit the MCR–ALS model in such percentages.

Zhang et al. [40] worked with white chocolates, making a comparison between the spectrum of the pure components such as sucrose, lactose, butter and whey. The correlation coefficients between the pure spectra and those recovered by MCR–ALS with data preprocessing were between 0.6701 and 0.9910, which were considered satisfactory. The equality constraint fixes the recovered spectra or concentrations to specific known values [43]. This is the reason why the values of the correlation coefficient between the recovered spectra and the pure compounds are high (Table 4.4-4). Additionally, Figure 4.4-5 shows that there is no rotational ambiguity, because the recovered spectra (S^T) are identical to the original spectra. The same results were obtained for the other samples. Based on these results, we can affirm that the first spectrum recovered by MCR–ALS (component 1) corresponds to CB, while the second spectrum (component 2) corresponds to vegetable oil, according to the sample analyzed.

The mathematical analysis of each image allows for the extraction of parameters that are helpful in the interpretation of the images and in understanding of the blending process studied [31]. The data provided by Raman mapping contain spectral and spatial information; then, MCR–ALS can be used to visualize the concentration distribution maps of the different components present in a sample based on their individual spectral signals [44]. However, the quality of the Raman mapping is limited by the spectra of the individual compounds and their concentration, so the analysis becomes complex if the spectra of the components have common peaks [21], as is the case with CB, CNO and SIO (Figure 4.4-3). This was another reason why we decided to use the spectra of the pure compounds as equality constraints. It is important to mention that the values in matrix C are related to the concentrations, but they are not the real concentrations of the components of the blends, so the mean value should not be compared with the real concentration of each component [22]. Figure 4.4-6 shows the distribution maps of CB, CNO, and SIO in all the samples

analyzed constructed from the matrix of concentrations C obtained by MCR–ALS. Figure 4.4-6a shows a better distribution of CB and CNO at concentrations of 55 and 45%, respectively. Similarly, Figure 4.4-6g shows a better distribution of CB and SIO at concentrations of 65 and 35%, respectively. Both figures show better distribution than the others. Similar results were obtained by Scoutaris et al. [21] when analyzing mixtures of paracetamol (PMOL) and compritol 888 (C-888).

We consider that the miscibility of two components can be determined by their distribution in a chemical map, and homogeneous distribution is an indicator of good miscibility. The homogeneity of the samples is also analyzed using the histograms of the distribution map. According to Gendrin et al. [45], a histogram that exhibits a symmetric distribution with a narrow base and a sharp peak is representative of an image with a low contrast, and therefore a homogeneous sample. The histograms corresponding to each distribution map show a symmetric shape in all cases (Figure 4.4-6), with differences according to the actual concentration of each sample. Lyon et al. [46] prepared tablets composed of furosemide and excipients at five different degrees of mixing, reporting that the most homogeneous distribution was obtained in those samples whose histograms were symmetric.

The homogeneity of the samples can be quantitatively analyzed using the RSD. According to Scoutaris et al. [21], RSD has been used to compare the homogeneity of a sample; a low RSD value is interpreted as signifying higher homogeneity. Mitsusake et al. [22] showed that the standard deviation of histograms (STD) is used to evaluate the miscibility for the preformulation stage of pharmaceutical tablets. Therefore, we consider that both parameters are comparable. Lyon et al. [46] used the RSD of the histograms generated by the image scores to determine the homogeneity of the distribution of furosemide in tablets, observing a progressive increase in RSD as the degree of homogeneity decreased. Mitsutake et al. [22] observed an intermediate miscibility (STD = 6.9) between CB and CNO at real concentrations of 75 and 25%, respectively. Similar results were obtained in the present study (Table 4.4-4), in which it is shown that blends containing 45% CNO and 35% SIO have the lowest RSD; therefore, they form a more homogeneous blend with CB and are more miscible at those concentrations. In the elaboration of CBEs, the candidate vegetable oil must have an SOS triglyceride concentration similar to that of CB. To achieve this, it

undergoes a fractionation process [8]. In the case of CNO and SIO, they were used in their natural state, showing good miscibility with CB; therefore, they would be good candidates to be used as CBE.

Food products are complex mixtures of heterogeneous nature; obtaining chemical and spatial information from them is crucial for food safety and quality control [47]. For this, food detection technologies play a fundamental role [25]; therefore, it is urgent to develop rapid methods of nondestructive analysis to control the quality and safety of food and thus control its circulation in the market [47]. Chemical Raman imaging (CRI), in combination with chemometrics, can provide spectral information and spatial distributions of specific chemicals, analyzing them non-destructively [42,47–50]. However, in the food field, only a few investigations on the application of CRI have been reported [50]. CRM allows the application of Raman mapping with MCR-ALS to obtain the chemical characteristics of CB, CNO, and SIO through their Raman spectral fingerprint (Figure 4.4-1) and to identify the miscibility of these three components (Figure 4.4-6, Table 4.4-4), which demonstrates the usefulness of this methodology in initiating the development of new products in the chocolate industry. Some authors have also used this methodology, such as Liu et al. [51], who used chemical Raman mapping to study the compatibility between hydroxypropyl methylcellulose (HPMC) and gelatin. It was found that HPMC was easily adapted to form continuous and intermediate phases from the molecular interactions between both components. Mitsutake et al. [52] studied the miscibility and structural changes (polymorphism) in mixtures of natural and synthetic beeswax (BW) with copaiba oil using Raman mapping and MCR-ALS. Structural changes were found in the synthetic BWs, and the miscibility between both BWs with copaiba oil was not significantly different. It was also observed that the differences between the freshly prepared mixtures and those with three months of storage were more significant when the amount of oil was increased. On the other hand, Rodríguez et al. [12] studied the compatibility of shea butter and CB mixtures using the isosolid diagram but did not use Raman mapping.

Lauric acid and partially hydrogenated fats are not recommended in the chocolate industry because they can increase LDL cholesterol levels [53]. Norazlina et al. [2] reported the following CBE candidates: mean fraction of palm oil, mango seed fat, shea stearin, kokum fat, illipe butter, high oleic and stearic

sunflower oil, palm stearin, and bambangan kernel fat. However, this author does not report CNO and SIO. The results of the present work show CNO and SIO as possible candidates for novel CBE, as they demonstrate some advantages, such as their high degree of unsaturation, which makes them healthy fats, as well as their excellent molecular compatibility with CB demonstrated by their miscibility. However, it is necessary to carry out some additional studies, such as the investigation of their thermal and rheological properties at different concentrations of solid and liquid lipids and the investigation of their behaviors over time.

4.6. Conclusions

In the present work, the usefulness of the confocal Raman microscopy (CRM) technique to identify the chemical properties of cocoa butter, coconut oil and sacha inchi oil is demonstrated. These latter vegetable oils are proposed as candidates to be cocoa butter equivalents in the manufacture of chocolates. The main differences are in the physical state and the degree of unsaturation, which are differentiated by the intensity of the peaks in the Raman spectra. Likewise, the usefulness of the chemometric technique known as multivariate curve resolution–alternating least squares to analyze the miscibility of these vegetable oils with cocoa butter is demonstrated. We conclude that coconut oil is more miscible with cocoa butter at a 45% concentration, and sacha inchi oil is more miscible at a 35% concentration. Between the two vegetable oils, coconut oil is more miscible than sacha inchi oil. We consider that this work is the first step in finding novel CBEs for developing new chocolates. Further work is necessary to evaluate their thermal, rheological, and sensorial properties.

acquisition, I.S.C.-C. All authors have read and agreed to the published version of the manuscript.

Institutional Review Board Statement: Not applicable.

Institutional Consent Statement: Not applicable.

Data Availability Statement: The data presented in this study are available in Supplementary materials.

Conflicts of Interest: The authors declare no conflict of interest.

4.7. References

1. Ewens, H.; Metilli, L.; Simone, E. Analysis of the effect of recent reformulation strategies on the crystallization behaviour of cocoa butter and the structural properties of chocolate. Curr. Res. Food Sci. 2021, 4, 105–114. https://doi.org/10.1016/j.crfs.2021.02.009.

2. Norazlina, M.; Jahurul, M.; Hasmadi, M.; Mansoor, A.; Norliza, J.; Patricia, M.; George, M.R.; Noorakmar, A.; Lee, J.; Fan, H. Trends in blending vegetable fats and oils for cocoa butter alternative application: A review. Trends Food Sci. Technol. 2021, 116, 102–114. https://doi.org/10.1016/j.tifs.2021.07.016.

3. Watanabe, S.; Yoshikawa, S.; Sato, K. Formation and properties of dark chocolate prepared using fat mixtures of cocoa butter and

symmetric/asymmetric stearic-oleic mixed-acid triacylglycerols: Impact of molecular compound crystals. Food Chem. 2021, 339, 127808. https://doi.org/10.1016/j.foodchem.2020.127808.

4. Toro-Vazquez, J.F.; Charó-Alonso, M.A.; Morales-Rueda, J.A.; Pérez-Martínez, J.D. Molecular Interactions of Triacylglycerides in Blends of Cocoa Butter with trans-free Vegetable Oils. In Cocoa Butter and Related Compounds; AOCS Press: Urbana, IL, USA, 2012; pp. 393–416.

5. Bootello, M.A.; Hartel, R.W.; Garcés, R.; Martínez-Force, E.; Salas, J.J. Evaluation of high oleic-high stearic sunflower hard stearins for cocoa butter equivalent formulation. Food Chem. 2012, 134, 1409–1417. https://doi.org/10.1016/j.foodchem.2012.03.040.

6. Bahari, A.; Akoh, C.C. Texture, rheology and fat bloom study of 'chocolates' made from cocoa butter equivalent synthesized from illipe butter and palm mid-fraction. LWT—Food Sci. Technol. 2018, 97, 349–354. https://doi.org/10.1016/j.lwt.2018.07.013.

7. Jahurul, M.; Zaidul, I.; Norulaini, N.; Sahena, F.; Jinap, S.; Azmir, J.; Sharif, K.; Omar, A.M. Cocoa butter fats and possibilities of substitution in food products concerning cocoa varieties, alternative sources, extraction methods, composition, and characteristics. J. Food Eng. 2013, 117, 467–476. https://doi.org/10.1016/j.jfoodeng.2012.09.024.

8. Segman, O.; Wiesman, Z.; Yarmolinsky, L. Methods Ant Technologies Related to Shea Butter Chemophysical Properties and to the Delivery of Bioactives in Chocolate and Related Products. In Cocoa Butter and Related Compounds; AOCS Press: Urbana, IL, USA, 2012; pp. 417–441.

9. Kang, K.K.; Jeon, H.; Kim, I.-H.; Kim, B.H. Cocoa butter equivalents prepared by blending fractionated palm stearin and shea stearin. Food Sci. Biotechnol. 2013, 22, 347–352. https://doi.org/10.1007/s10068-013-0087-8.

10. Talbot, G. Chocolate and Cocoa Butter—Structure and Composition. In Cocoa Butter and Related Compounds; AOCS Press: Urbana, IL, USA, 2012; pp. 1–34, ISBN 978-0-9830791-2-5.

11. Beckett, T.S. Industrial Chocolate Manufacture and Use, 4th ed; Wiley-Blackwell.: Chichester, UK, 2009; ISBN 978-1-4051-3949-6.

12. Rodriguez-Negrette, A.C.; Huck-Iriart, C.; Herrera, M.L. Physical Chemical Properties of Shea/Cocoa Butter Blends and their Potential for Chocolate Manufacture. J. Am. Oil Chem. Soc. 2019, 96, 239–248. https://doi.org/10.1002/aocs.12189.

13. EUR-Lex Directive 2000/36/EC of the European Parliament and of the Council of 23 June 2000 Relating to Cocoa and Chocolate Products Intended for Human Consumption. Available online: https://eur-lex.europa.eu/eli/dir/2000/36/2013-11-18 (accessed on 2 December 2021).

14. CFR Code of Federal Regulations. Title 21-Part 163: Cacao Products. Available online: https://www.ecfr.gov/current/title-21/chapter-I/subchapter-B/part-163 (accessed on 2 December 2021).

15. Medina-Mendoza, M.; Rodriguez-Pérez, R.J.; Rojas-Ocampo, E.; Torrejón-Valqui, L.; Fernández-Jeri, A.B.; Idrogo-Vásquez, G.; Cayo-Colca, I.S.; Castro-Alayo, E.M. Rheological, bioactive properties and sensory preferences of dark chocolates with partial incorporation of Sacha Inchi (Plukenetia volubilis L.) oil. Heliyon 2021, 7, e06154. https://doi.org/10.1016/j.heliyon.2021.e06154.

16. Chirinos, R.; Zuloeta, G.; Pedreschi, R.; Mignolet, E.; Larondelle, Y.; Campos, D. Sacha inchi (Plukenetia volubilis): A seed source of polyunsaturated fatty acids, tocopherols, phytosterols, phenolic compounds and antioxidant capacity. Food Chem. 2013, 141, 1732–1739. https://doi.org/10.1016/j.foodchem.2013.04.078.

17. Ramos-Escudero, F.; Morales, M.T.; Escudero, M.R.; Muñoz, A.M.; Chavez, K.C.; Asuero, A.G. Assessment of phenolic and volatile compounds of commercial Sacha inchi oils and sensory evaluation. Food Res. Int. 2021, 140, 110022. https://doi.org/10.1016/j.foodres.2020.110022.

18. Neves, M.D.G.; Poppi, R.J. Monitoring of Adulteration and Purity in Coconut Oil Using Raman Spectroscopy and Multivariate Curve Resolution. Food

Anal. Methods 2017, 11, 1897–1905. https://doi.org/10.1007/s12161-017-1093-x.
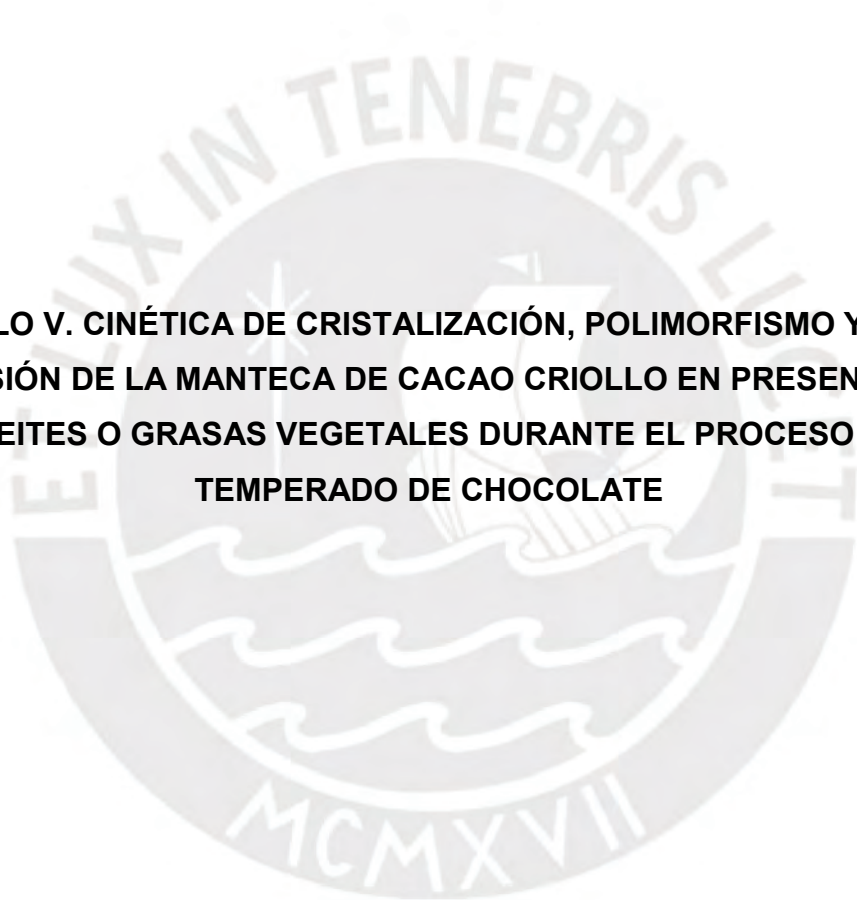
19. Jayawardena, R.; Swarnamali, H.; Ranasinghe, P.; Misra, A. Health effects of coconut oil: Summary of evidence from systematic reviews and meta-analysis of interventional studies. Diabetes Metab. Syndr. Clin. Res. Rev. 2021, 15, 549–555. https://doi.org/10.1016/j.dsx.2021.02.032.

20. da Silva, G.H.R.; Ribeiro, L.N.; Mitsutake, H.; Guilherme, V.A.; DE Castro, S.; Poppi, R.; Breitkreitz, M.C.; de Paula, E. Optimised NLC: A nanotechnological approach to improve the anaesthetic effect of bupivacaine. Int. J. Pharm. 2017, 529, 253–263. https://doi.org/10.1016/j.ijpharm.2017.06.066.

21. Scoutaris, N.; Vithani, K.; Slipper, I.; Chowdhry, B.; Douroumis, D. SEM/EDX and confocal Raman microscopy as complementary tools for the characterization of pharmaceutical tablets. Int. J. Pharm. 2014, 470, 88–98. https://doi.org/10.1016/j.ijpharm.2014.05.007.

22. Mitsutake, H.; Ribeiro, L.N.; da Silva, G.H.R.; Castro, S.R.; de Paula, E.; Poppi, R.; Breitkreitz, M.C. Evaluation of miscibility and polymorphism of synthetic and natural lipids for nanostructured lipid carrier (NLC) formulations by Raman mapping and multivariate curve resolution (MCR). Eur. J. Pharm. Sci. 2019, 135, 51–59. https://doi.org/10.1016/j.ejps.2019.05.002.

23. Mitsutake, H.; DE Castro, S.; de Paula, E.; Poppi, R.; Rutledge, D.N.; Breitkreitz, M.C. Comparison of different chemometric methods to extract chemical and physical information from Raman images of homogeneous and heterogeneous semi-solid pharmaceutical formulations. Int. J. Pharm. 2018, 552, 119–129. https://doi.org/10.1016/j.ijpharm.2018.09.058.

24. Breitkreitz, M.C.; Sabin, G.P.; Polla, G.; Poppi, R. Characterization of semi-solid Self-Emulsifying Drug Delivery Systems (SEDDS) of atorvastatin calcium by Raman image spectroscopy and chemometrics. J. Pharm. Biomed. Anal. 2013, 73, 3–12. https://doi.org/10.1016/j.jpba.2012.03.054.

25. Petersen, M.; Yu, Z.; Lu, X. Application of Raman Spectroscopic Methods in Food Safety: A Review. Biosensors 2021, 11, 187. https://doi.org/10.3390/bios11060187.

26. Yaseen, T.; Sun, D.-W.; Cheng, J.-H. Raman imaging for food quality and safety evaluation: Fundamentals and applications. Trends Food Sci. Technol. 2017, 62, 177–189. https://doi.org/10.1016/j.tifs.2017.01.012.

27. Liu, X.; Zhang, N.; Yu, L.; Zhou, S.; Shanks, R.; Zheng, J. Imaging the phase of starch–gelatin blends by confocal Raman microscopy. Food Hydrocoll. 2016, 60, 7–10. https://doi.org/10.1016/j.foodhyd.2016.03.005.

28. Neves, A.C.d.O.; Zougagh, M.; Ríos, Á.; Tauler, R.; Wakamatsu, K.; Galván, I. Pheomelanin Subunit Non-Destructive Quantification by Raman Spectroscopy and Multivariate Curve Resolution-Alternating Least Squares (MCR-ALS). Chemom. Intell. Lab. Syst. 2021, 217, 104406. https://doi.org/10.1016/j.chemolab.2021.104406.

29. Vajna, B.; Pataki, H.; Nagy, Z.; Farkas, I.; Marosi, G. Characterization of melt extruded and conventional Isoptin formulations using Raman chemical imaging and chemometrics. Int. J. Pharm. 2011, 419, 107–113. https://doi.org/10.1016/j.ijpharm.2011.07.023.

30. de Juan, A.; Jaumot, J.; Tauler, R. Multivariate Curve Resolution (MCR). Solving the mixture analysis problem. Anal. Methods 2014, 6, 4964–4976. https://doi.org/10.1039/c4ay00571f.

31. Osorio, J.G.; Stuessy, G.; Kemeny, G.J.; Muzzio, F.J. Characterization of pharmaceutical powder blends using in situ near-infrared chemical imaging. Chem. Eng. Sci. 2014, 108, 244–257. https://doi.org/10.1016/j.ces.2013.12.027.

32. Amigo, J.M. Practical issues of hyperspectral imaging analysis of solid dosage forms. Anal. Bioanal. Chem. 2010, 398, 93–109. https://doi.org/10.1007/s00216-010-3828-z.

33. Gendrin, C.; Roggo, Y.; Collet, C. Pharmaceutical applications of vibrational chemical imaging and chemometrics: A review. J. Pharm. Biomed. Anal. 2008, 48, 533–553. https://doi.org/10.1016/j.jpba.2008.08.014.

34. Bresson, S.; Rousseau, D.; Ghosh, S.; El Marssi, M.; Faivre, V. Raman spectroscopy of the polymorphic forms and liquid state of cocoa butter. Eur. J. Lipid Sci. Technol. 2011, 113, 992–1004. https://doi.org/10.1002/ejlt.201100088.

35. Jiménez-Sanchidrián, C.; Ruiz, J.R. Use of Raman spectroscopy for analyzing edible vegetable oils. Appl. Spectrosc. Rev. 2016, 51, 417–430. https://doi.org/10.1080/05704928.2016.1141292.

36. Carmona, M.Á.; Lafont, F.; Jiménez-Sanchidrián, C.; Ruiz, J.R. Raman spectroscopy study of edible oils and determination of the oxidative stability at frying temperatures: Raman Spectroscopy Study of Edible Oils. Eur. J. Lipid Sci. Technol. 2014, 116, 1451–1456. https://doi.org/10.1002/ejlt.201400127.

37. Wang, H.; Xin, Y.; Ma, H.; Fang, P.; Li, C.; Wan, X.; He, Z.; Jia, J.; Ling, Z. Rapid detection of Chinese-specific peony seed oil by using confocal Raman spectroscopy and chemometrics. Food Chem. 2021, 362, 130041. https://doi.org/10.1016/j.foodchem.2021.130041.

38. Bresson, S.; Lecuelle, A.; Bougrioua, F.; El Hadri, M.; Baeten, V.; Courty, M.; Pilard, S.; Rigaud, S.; Faivre, V. Comparative structural and vibrational investigations between cocoa butter (CB) and cocoa butter equivalent (CBE) by ESI/MALDI-HRMS, XRD, DSC, MIR and Raman spectroscopy. Food Chem. 2021, 363, 130319. https://doi.org/10.1016/j.foodchem.2021.130319.

39. Castro, R.C.; Ribeiro, D.S.; Santos, J.L.; Páscoa, R.N. Comparison of near infrared spectroscopy and Raman spectroscopy for the identification and quantification through MCR-ALS and PLS of peanut oil adulterants. Talanta 2021, 230, 122373. https://doi.org/10.1016/j.talanta.2021.122373.

40. Zhang, X.; de Juan, A.; Tauler, R. Multivariate Curve Resolution Applied to Hyperspectral Imaging Analysis of Chocolate Samples. Appl. Spectrosc. 2015, 69, 993–1003. https://doi.org/10.1366/14-07819.

41. de Juan, A.; Tauler, R. Multivariate Curve Resolution: 50 years addressing the mixture analysis problem—A review. Anal. Chim. Acta 2021, 1145, 59–78. https://doi.org/10.1016/j.aca.2020.10.051.

42. Gupta, S.; Román-Ospino, A.D.; Baranwal, Y.; Hausner, D.; Ramachandran, R.; Muzzio, F.J. Performance assessment of linear iterative optimization technology (IOT) for Raman chemical mapping of pharmaceutical tablets. J. Pharm. Biomed. Anal. 2021, 205, 114305. https://doi.org/10.1016/j.jpba.2021.114305.

43. MCR Constraints—Eigenvector Research Documentation Wiki. Available online: https://www.wiki.eigenvector.com/index.php?title=MCR_Constraints (accessed on 30 October 2021).

44. Firmani, P.; Hugelier, S.; Marini, F.; Ruckebusch, C. MCR-ALS of hyperspectral images with spatio-spectral fuzzy clustering constraint. Chemom. Intell. Lab. Syst. 2018, 179, 85–91. https://doi.org/10.1016/j.chemolab.2018.06.007.

45. Gendrin, C. Monitoring galenical process development by near infrared chemical imaging: One case study. Eur. J. Pharm. Biopharm. 2008, 68, 828–837. https://doi.org/10.1016/j.ejpb.2007.08.008.

46. Lyon, R.C.; Lester, D.S.; Lewis, E.N.; Lee, E.; Yu, L.X.; Jefferson, E.H.; Hussain, A.S. Near-infrared spectral imaging for quality assurance of pharmaceutical products: Analysis of tablets to assess powder blend homogeneity. AAPS PharmSciTech 2002, 3, E17.

47. Wang, K.; Li, Z.; Li, J.; Lin, H. Raman spectroscopic techniques for nondestructive analysis of agri-foods: A state-of-the-art review. Trends Food Sci. Technol. 2021, 118, 490–504. https://doi.org/10.1016/j.tifs.2021.10.010.

48. Metilli, L.; Francis, M.; Povey, M.; Lazidis, A.; Marty-Terrade, S.; Ray, J.; Simone, E. Latest advances in imaging techniques for characterizing soft, multiphasic food materials. Adv. Colloid Interface Sci. 2020, 279, 102154. https://doi.org/10.1016/j.cis.2020.102154.

49. Gómez-Mascaraque, L.G.; Tran, C.; O'Callaghan, T.; Hogan, S.A. Use of confocal Raman imaging to understand the microstructure of anhydrous milk fat-based oleogels. Food Struct. 2021, 30, 100228. https://doi.org/10.1016/j.foostr.2021.100228.

50. Long, Y.; Huang, W.; Wang, Q.; Fan, S.; Tian, X. Integration of textural and spectral features of Raman hyperspectral imaging for quantitative determination of a single maize kernel mildew coupled with chemometrics. Food Chem. 2021, 372, 131246. https://doi.org/10.1016/j.foodchem.2021.131246.

51. Liu, X.; Ji, Z.; Peng, W.; Chen, M.; Yu, L.; Zhu, F. Chemical mapping analysis of compatibility in gelatin and hydroxypropyl methylcellulose blend films. Food Hydrocoll. 2020, 104, 105734. https://doi.org/10.1016/j.foodhyd.2020.105734.

52. Mitsutake, H.; da Silva, G.; Ribeiro, L.; de Paula, E.; Poppi, R.; Rutledge, D.; Breitkreitz, M. Raman Imaging and Chemometrics Evaluation of Natural and Synthetic Beeswaxes as Matrices for Nanostructured Lipid Carriers Development. Braz. J. Anal. Chem. 2021, 8. https://doi.org/10.30744/brjac.2179-3425.ar-13-2021.

53. Huang, Z.; Guo, Z.; Xie, D.; Cao, Z.; Chen, L.; Wang, H.; Jiang, L.; Shen, Q. Rhizomucor miehei lipase-catalysed synthesis of cocoa butter equivalent from palm mid-fraction and stearic acid: Characteristics and feasibility as cocoa butter alternative. Food Chem. 2021, 343, 128407. https://doi.org/10.1016/j.foodchem.2020.128407.

CAPÍTULO V. CINÉTICA DE CRISTALIZACIÓN, POLIMORFISMO Y PUNTO DE FUSIÓN DE LA MANTECA DE CACAO CRIOLLO EN PRESENCIA DE ACEITES O GRASAS VEGETALES DURANTE EL PROCESO DE TEMPERADO DE CHOCOLATE

Effect of tempering and cocoa butter equivalents on the crystallization kinetics, polymorphism, and physical and thermal properties of dark chocolates

Efraín M. Castro-Alayo[1,2,3*], César R. Balcázar-Zumaeta[1], Llisela Torrejón-Valqui[1], Marleni Medina-Mendoza[1], Ilse S. Cayo-Colca[4], Fiorella P. Cárdenas-Toro[3]

[1] Instituto de Investigación, Innovación y Desarrollo para el Sector Agrario y Agroindustrial de la Región Amazonas (IIDAA), Facultad de Ingeniería y Ciencias Agrarias, Universidad Nacional Toribio Rodríguez de Mendoza de Amazonas, Calle Higos Urco 342-350-356, Chachapoyas, Amazonas, Perú. Efrain.castro@untrm.edu.pe

[2] Programa de Doctorado en Ingeniería, Departamento de Ingeniería, Pontificia Universidad Católica del Perú, Av. Universitaria 1801, San Miguel, Lima 32, Perú; efrain.castro@pucp.edu.pe

[3] Sección de Ingeniería Industrial, Departamento de Ingeniería, Pontificia Universidad Católica del Perú, Av. Universitaria 1801, San Miguel, Lima 32, Perú; fcardenas@pucp.pe

[4] Facultad de Ingeniería Zootecnista, Agronegocios y Biotecnología, Universidad Nacional Toribio Rodríguez de Mendoza de Amazonas, Calle Higos Urco 342-350-356, Chachapoyas, Amazonas, Perú.

* Correspondence: efrain.castro@untrm.edu.pe; Tel.: +51-986376463

Submitted article.

5.1. Abstract

Different vegetable oils are being studied to be used as cocoa butter equivalent (CBE) in manufacturing chocolates. These CBEs can be combined with tempering to obtain chocolates with appropriate properties. In this work, the effect of two CBEs obtained by binary blends of coconut oil and sacha inchi oil with cocoa butter (CB/CNO and CB/SIO, respectively) and two tempering regimens (low and high) on the crystallization kinetics polymorphism and physical and thermal properties of dark chocolates were studied. Differential scanning calorimetry was used to obtain the isothermal crystallization data of two chocolates (Ch-CNO and Ch-SIO), which were fitted to the Avrami equation to obtain the kinetic parameters. Both factors generated form β_2 in percentages of 92.56 ± 1.49 for Ch-SIO and 90.3 ± 1.18 for Ch-CNO; whiteness index low values corroborated this fact. The chocolates' texture, rheology, and thermal properties were within acceptable limits. Both CBEs accelerated the CB crystallization process inside the chocolates, obtaining faster crystallization in Ch-SIO (7.08 ± 0.15 min) than in Ch-CNO (7.25 ± 0.18 min). The results demonstrate that using CNO and SIO in producing dark chocolates is feasible.

Keywords: Criollo cocoa beans, dark chocolate, kinetics crystallization, polymorphism, Avrami equation.

5.2. Introduction

Chocolate is made up of solid particles dispersed in a matrix of crystallized fat composed mainly of cocoa butter (CB) (Ewens et al., 2021), whose crystalline structure determines the quality of chocolate (Liu et al., 2022). During crystallization, the triacylglycerols (TAGs) molecules contained in the CB are arranged, resulting in crystals of six different forms (polymorphism) (Talbot, 2009), and depending on the production process conditions (Norazlina et al., 2020). The forms in which CB crystallizes are γ, α, β_2', β_1', β_2, and β_1, ordered according to their increased stability and melting temperatures (17.3, 23.3, 25.5, 27.5, 33.8, and 36.3 °C, respectively) (Declerck et al., 2021; Ray et al., 2012). In the manufacture of chocolate, the form β_2 (form V) is required because it gives chocolate its sensorial characteristics such as flavor release (Yao et al., 2020),

127

texture, glossiness, melting, and mouth feeling (J. Chen et al., 2021; Padar et al., 2008). Therefore, it is essential to carry out further studies on the CB crystallization involved in producing high-quality chocolates (Fernandes et al., 2013; Hubbes et al., 2018).

Crystallization is the CB transition from liquid to solid (Campos & Marangoni, 2012) due to the effect of temperature; it begins with nucleation (pre-crystallization) during the tempering stage and ends with TAGs increasing while melting during storage (Padar et al., 2008; Sonwai et al., 2017). In chocolate manufacturing, the tempering stage leads to CB crystallization (J. Chen et al., 2021), allowing the chocolate mass to be thermally treated to produce a small fraction of fat crystals of suitable type and size, highly stable and homogeneously dispersed (Windhab, 2009). The goal of tempering is to develop sufficient crystal seeds to allow the CB to crystallize into more stable polymorphic forms (Talbot, 2009). Most studies on CB crystallization have focused on optimizing the tempering parameters to ensure that 60-80% of these form β_2 crystals are obtained (Sonwai et al., 2017; Pirouzian et al., 2020). To optimize this transition, the CB in chocolate must crystallize as quickly as possible to the form β_2 (Devos et al., 2020). Thus, knowing the CB crystallization speed is critical for producing good chocolate (Pirouzian et al., 2020). This speed can be determined with the Avrami equation in the study of the CB crystallization kinetics (Jin et al., 2019).

In order to develop new recipes that improve chocolate quality, diverse reformulation strategies have been studied (Ewens et al., 2021), such as using vegetable fats and oils to include or replace the CB (Ewens et al., 2021; Watanabe et al., 2020). These ingredients are known as cocoa butter equivalents (CBE), which must be compatible with the CB (Castro-Alayo et al., 2021; Bootello et al., 2012). Furthermore, the European Union Directive 2000/36/EC allows using vegetable fats and oils as CBE (illipe, palm, sal, shea, kokum gurgi, and mango kernel). When vegetable oils are mixed with CB, the molecular compatibility between the CB TAGs is modified, affecting their crystallization kinetics and polymorphism. As a consequence, the physical properties of the crystallized system are different from those observed in pure CB (Ewens et al., 2021). Aumpai et al. (2022) produced CBE by mixing illipe butter with palm mid-fraction proportions of 75/25 and reported a crystallization and melting profile comparable to CB. Additionally, 5% of this blend was incorporated into chocolates

128

showing a similar hardness to chocolate made with only CB. In a research carried out by Castro-Alayo et al. (2021), the use of novel CBEs derived from Peruvian vegetable oils blends such as sacha inchi (SIO) and coconut (CNO) mixed with CB in proportions of 65/35 and 55/45, respectively, was proposed. These CBEs showed miscibility and homogeneity and were demonstrated to be suitable for use in chocolate production.

In this research, the CBEs proposed by Castro *et al*. (2021) were incorporated into dark chocolates. Then chocolates were analyzed according to the tempering regimen and CBEs percentage to determine their effect on the crystallization kinetics, polymorphism, physical and thermal properties.

5.3. Materials and Methods

5.3.1. Materials.

Dried fermented Criollo cocoa beans and CB was provided by the Cooperativa de Servicios Múltiples Aprocam (Bagua–Amazonas–Peru). SIO and CNO were bought from local market.

5.3.2. Preparation of CBEs.

According to Castro-Alayo et al. (2021), two CBEs composed of 65/35 CB/SIO blends and 55/45 CB/CNO were prepared. The CB was melted at 50 °C in a magnetic stirrer with a hot plate, and each vegetable oil was added separately. The resulting blend was stirred until an entirely homogeneous sample was gotten. The blend was refrigerated and placed in chocolate molds to obtain the CBEs. After 15 min, the CBEs were removed from the mold and stored until analysis.

5.3.3. Crystallization and melting temperatures of vegetable oils and CBEs.

To obtain the crystallization and melting temperatures (T_c and T_m, respectively) of the CB, SIO, CNO, and CBEs, the procedure of Sonwai et al. (2017) and Chaleepa et al. (2010) was used with some modifications. The crystallization and melting profiles of the samples were determined with a differential scanning calorimeter (DSC) (TA Instruments, Discovery DSC 2500, New Castle, USA). A sample of approximately 5 mg was placed in a Tzero low-

mass aluminum pan and hermetically sealed with a sample press. An empty pan served as a reference and was used to obtain the baseline settings. Samples were heated from room temperature to 60 °C and held for 10 min to ensure homogeneity and remove any crystal memory. Then, the samples were cooled (10 °C/min to -35 °C) and held for 10 min, followed by heating from 10 °C/min to 60 °C. The Trios software determined the crystallization onset/peak temperatures and enthalpy.

5.3.4. Chocolate preparation.

According to Medina-Mendoza *et al.* (2021), Criollo cocoa beans were selected according to their size to obtain uniform beans, then were roasted at 120 °C for 2 hours and processed in a bean grinder to obtain the cocoa nibs. Subsequently, the nibs were ground to obtain the cocoa liquor. The conching stage was done in a stone wheel refiner for 20 hours; at this stage, the cocoa liquor (75%), sugar (20%), and the CBEs were added in different proportions (1, 3, and 5%) according to the experimental design. In this stage, two types of chocolate were produced according to the CBE used: dark chocolate with CB/CNO (Ch-CNO) and dark chocolate with CB/SIO (Ch-SIO). Considering that minor temperature variations (0.5–1 °C) in tempering can change the properties of chocolate (Windhab, 2009), the dark chocolate mass was tempered with high (50°C, 30.4°C, or 33.8°C) and low (50°C, 29.4°C or 32.8°C) regimes during 20 minutes. After tempering, the mass was placed in chocolate molds and frozen to facilitate unmolding. Afterward, the dark chocolates were packed and placed in refrigeration until analysis.

5.3.5. Isothermal crystallization of the CBEs and dark chocolates.

Isothermal crystallization was carried out considering the method used by Fernandes *et al.* (2013). The results of T_c and T_m obtained in 2.2.1 were taken to choose the appropriate Tc. In addition, the crystallization was carried out at a low supercooling (0°C - 4 °C below the T_m of the sample) (Martini, 2015); from this, the chosen T_c were 17, 18, and 19 °C. Next, samples of 5-10 mg were placed in a Tzero low-mass aluminum pan and hermetically sealed; an empty pan was used as a reference. Samples were heated to 50 °C and held at this temperature

for 3 min to erase thermal history. Then, they were cooled at a 60 °C/min rate until the corresponding T_c and kept at this temperature for 90 min for isothermal crystallization (exotherm). Subsequently, the samples were heated at 20 °C/min up to 50 °C (endotherm), showing the crystals melting temperature and enthalpy at the corresponding T_c. The melting temperature obtained in the endothermic reaction served to identify the form generated during the crystallization compared to that from the literature (MacNaughtan et al., 2006).

5.3.6. Crystallization kinetics.

The Origin Pro Software Crystallization Fit created by Lorenzo et al. (2007) was used to calculate the crystallization kinetic parameters. Previously, the data obtained from the isothermal crystallization were fitted to the Avrami equation (Eq. 5.5-1) (Martini, 2015; MacNaughtan et al., 2006; Avrami, 1940).

$$1 - V_c(t) = \exp(-kt^n) \qquad\qquad (5.5\text{-}1)$$

V_c is the fraction of crystal formed at time t during crystallization, k is the crystallization rate constant, and n is the Avrami index related to the crystallization mechanism (Hubbes et al., 2018). Equation 5.5-1 can be expressed in a logarithmic form as:

$$\ln\left[-\ln\left(1 - V_c(t)\right)\right] = \ln k + n \ln t \qquad\qquad (5.5\text{-}2)$$

From the $\ln\left[-\ln\left(1 - V_c(t)\right)\right]$ plot vs. $\ln t$, n was obtained from the slope of the graph.

The $t_{1/2}$ described the time taken to achieve half of the overall crystallization and was calculated using Eq. 5.5-3:

$$t_{1/2} = \left(\frac{0.69315}{k}\right)^{1/n} \qquad\qquad (5.5\text{-}3)$$

Another critical parameter is the crystallization induction time (t_0), defined as the time necessary for the crystallization peak to occur (Martini, 2015). The isothermal thermogram obtained by DSC was used for the t_0 calculation, where t_0 is the time that passes from the isothermal process to the crystallization start

(point of the thermogram at which the heat flux of the sample deviates significantly from the baseline) (Toro-Vazquez et al., 2000).

5.3.7. Polymorphism.

According to Calva-Estrada et al. (2020), with some modifications, the sample was loaded into a Tzero low-mass aluminum pan and heated at a rate of 20°C/min from 20°C to 50°C; an empty pan was taken as a reference. A fast heating rate prevented the transition from a low to a higher stability forms (Nightingale et al., 2011). Melting properties included the onset temperature (T_{onset}), peak temperature (T_m), end temperature (T_{endset}), and melting enthalpy, calculated by the Trios Software. According to Declerck et al. (2021), the deconvolution of the melting peak was done assuming that the endothermic heat flow result is a function of the temperature through multiple Gaussian contributions. Then, the form β_2 specific percentage was calculated by deconvolution of the endotherm peak using Equation 5.5-4 and the Origin Pro software. In Equation 5.5-4, ΔH_{total} is the total accumulated enthalpy of each individual form.

$$\% \, form \, = \frac{\Delta H_{form,i}}{\Delta H_{total}} * 100 \qquad (5.5\text{-}4)$$

5.3.8. Physical properties.

5.3.8.1. Color.

The color of the chocolates was measured according to Mahato et al. (2022). A colorimeter (Konica Minolta, Chroma meter CR-400, Osaka, Japan) was used for the measurement of the parameters L* (lightness between 0, black and 100, white), a* (from + value, red to – value, green) and b* (from + value, yellow to – value, blue) and their identification in the three-dimensional visible color space. The whiteness index (WI) was calculated using Equation 5.5-5 (Nightingale et al., 2011).

$$WI = 100 - [(100 - L)^2 + a^2 + b^2]^{0.5} \qquad (5.5\text{-}5)$$

With the values L*, a* and b*, the Hue angle (h_{ab}^*) and the Chroma value (C_{ab}^*) were calculated using the following equations:

$$h_{ab}^* = arctan \frac{b^*}{a^*}$$
(5.5-6)

$$C_{ab}^* = \sqrt{a^{*2} + b^{*2}}$$
(5.5-7)

5.3.8.2. Texture.

The dark chocolates' hardness and fracturability properties were determined with a texture analyzer (Brookfield, CT3 Texture Analyzer, United States) according to Gregersen *et al.* (2015) and Limbardo *et al.* (2017), with some modifications. A needle probe was used to prick the chocolates to a depth of 3 mm at a speed of 0.5 mm/s and two prick cycles. Each sample's dark chocolate bar dimension was 115 × 50 × 7 mm, and measurements were made in triplicate at room temperature.

5.3.8.3. Rheology

According to Medina-Mendoza *et al.* (2021), the dark chocolate Casson plastic viscosity and Casson yield stress were determined with the IOCCC method using a rheometer (Anton Paar, Model MCR 92, Austria) equipped with a concentric cylinder. Samples were first melted at 50 °C for 60 min, put into a cup, and preconditioned at 40 °C for 60 s. The measurements were analyzed with the equipment Rheo-Compass Software based on Casson Model.

5.3.9. Experimental design

A 3 × 2 factorial completely randomized design was achieved in order to evaluate the effect of the CBE concentration at three levels (1, 3, and 5%) and the tempering regime at two levels (high and low) on the crystallization kinetics, polymorphism, and physical and thermal properties of dark chocolates. Two ways analysis of variance (ANOVA) and Tukey's multiple comparisons test were performed to determine the effect of the factors and their interactions at a significance level of 95%. The experiments were performed in triplicate, and the data was analyzed using Rmakdown from RStudio Software.

5.4.   Results and discussion.

5.4.1. Crystallization and melting properties of CB, vegetable oils, and CBEs.

Table 5.4-1 shows the crystallization and melting temperatures of CB, vegetable oils, and CBEs. CB has a crystallization and a melting peak at 12.04 ± 0.14 °C and 19.56 ± 0.24 °C; respectively, values close to those reported by Bresson *et al.* (2021). Figure 5.4-1b shows two crystallization peaks in the CNO exotherm at 4.23 ± 0.44 °C and -5.28 ± 0.64 °C (Table 5.4-1). These values coincide with those reported by Ng et al. (2021). The highest CNO melting peak was at 23.59 ± 0.22 °C (Figure 5.4-1b), possibly due to the content of long-chain fatty acids (Ng *et al*., 2021). As reported by Teles dos Santos *et al.* (2016), a melting peak was found in CB, CNO, and CB/CNO (Figure 5.4-1a,b, and d, respectively), indicating that almost all TAGs melt in a narrow temperature range (0.72 ± 0.13 - 27.22 ± 0.15 °C). SIO exhibits crystallization peaks at -7.16 ± 0.23 °C and melting peaks at -4.60 ± 0.29 °C, similar to the reported by Y. Chen et al. (2022), who found similar behavior in olive oil-based diacylglycerol stearin (O-DAGS). It can also be noted that CBEs show different thermal behavior than pure vegetable oils (Figures 5.4-1d, e), as stated by Y. Chen et al. (2022), this is possibly due to the formation of unstable crystals that can decrease crystallization and melting temperatures. The fusion and crystallization enthalpy are other thermal parameters that show significant differences between oils and CBEs. Table 5.4-1 shows that CNO has the highest values of crystallization enthalpy (92.21 ± 0.90 J/g) and fusion (107.98 ± 0.86 J/g) but are reduced when mixed with CB. The differences between the thermal properties of CB, vegetable oils, and CBEs are mainly due to their different molecular entities (Martini et al., 2015; Jahurul et al., 2019).

Table 5.4-1. Crystallization and melting properties of CB, vegetable oils (SIO, CNO) and the CBEs.

Sample	Crystallization*					Melting*			
	T_{onset} (°C)	T_{c1} (°C)	T_{endset} (°C)	T_{c2} (°C)	Enthalpy (J/g)	T_{onset} (°C)	T_m (°C)	T_{endset} (°C)	Enthalpy (J/g)
CB	16.32 ± 0.15a	12.04 ± 0.14a	1.72 ± 0.45a		48.43 ± 0.74d	14.67 ± 0.06a	19.56 ± 0.24b	27.22 ± 0.15a	78.98 ± 0.06b
CNO	6.85 ± 1.09d	4.23 ± 0.44c	-13.97 ± 0.79b	-5.28 ± 0.64	92.21 ± 0.90a	14.28 ± 0.66a	23.59 ± 0.22a	26.35 ± 0.97a	107.98 ± 0.86a
SIO	-4.08 ± 0.28e	-7.16 ± 0.23e	-21.85 ± 0.13d		18.49 ± 0.45e	-31.05 ± 2.04d	-4.60 ± 0.29d	2.62 ± 0.59c	29.02 ± 1.08d
CB/CNO	10.31 ± 0.75c	-0.31 ± 0.12d	-17.34 ± 0.35c		79.03 ± 1.09b	0.72 ± 0.13b	16.92 ± 0.14c	23.58 ± 0.63b	79.17 ± 1.95b
CB/SIO	13.22 ± 0.24b	7.86 ± 0.03b	-17.92 ± 0.13c		59.09 ± 0.60c	-20.93 ± 0.48c	16.90 ± 0.19c	24.67 ± 0.27b	58.35 ± 1.14c

* Indicates mean values ± standard deviation. Values in the same column with different letters demonstrate significant differences between them.
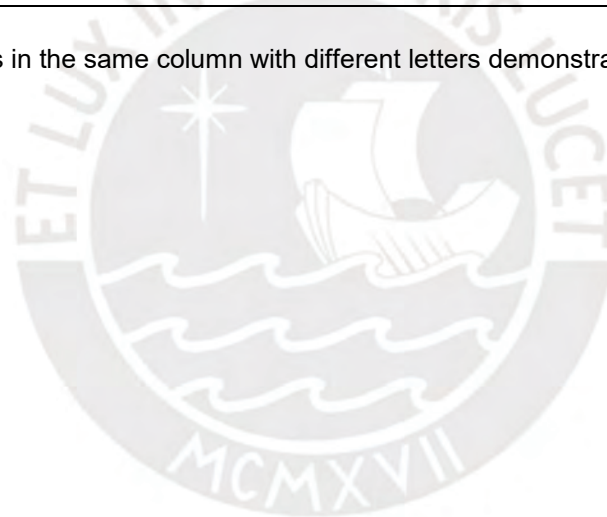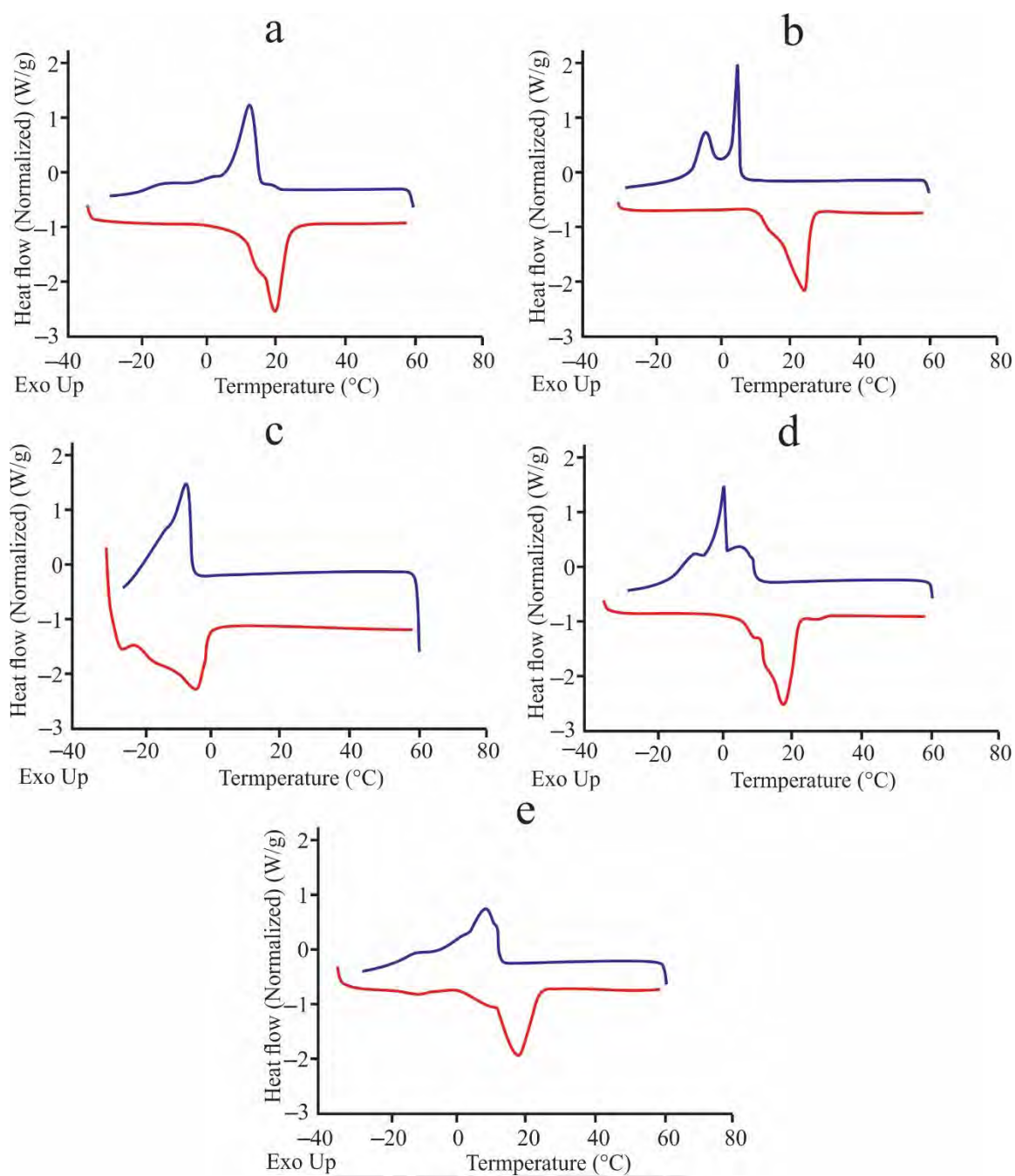
Figure 5.4-1. Crystallization (exothermic peak, blue) and melting (endothermic peak, red) profiles obtained by DSC for (a) CB, (b) CNO, (c) SIO, (d) CB/CNO, and (e) CB/SIO.

5.4.2. Isothermal crystallization kinetics of CB, vegetable oils, and CBEs.

Table 5.4-2 shows the parameters of the isothermal crystallization kinetics of CB, vegetable oils, and CBEs. The SIO did not present crystallization peaks at the studied temperatures (Figure 5.4-2a), so it was not possible to calculate its crystallization parameters. Figure 5.4-2b shows the original DSC isothermal crystallization data for CB and the baseline for calculating the kinetic parameters. The data good fit is corroborated by Figure 5.4-2c, even exceeding primary crystallization ($1 - V_c$ = 50%), and Figure 5.4-2d (R^2 = 0.9997). Table 5.4-2 shows that the n value for all the samples varies from 1.92 to 2.98, which means that the crystal nuclei grew plate-like during the isothermal crystallization, varying between sporadic growth ($n \sim 3$) and rapid growth ($n \sim 2$) (Marangoni & Wesdorp, 2013). These results agree with the data reported by Rashid (2012) for palm stearin and palm kernel olein blends. Likewise, the highest crystallization rate (k = 3.38×10^{-2} min^{-n} at 14 °C) corresponded to CNO, and the lowest rate (k = 2.58×10^{-4} min^{-n} at 16 °C) corresponded to CB/CNO (Table 5.4-2), corroborated by the $t_{1/2}\ exp$ low and high value (3.25 min and 21.90 min; respectively) of both samples. This means that the addition of CNO to the CB delays the nucleation of the blend (CB/CNO), results contrary to those obtained by Joshi et al. (2020). At 14 °C, the crystallization induction time (t_0) is shorter in CNO (2.63 min) than in CB (12.97 min); when both are mixed to produce CBE. The t_0 of the blend CB/CNO is improved (11.75 min), showing that CNO accelerates CB crystallization; this behavior is convenient for easier production of more stable crystal nuclei in the system (Saberi et al., 2011).

Table 5.4-2. Kinetic parameters of isothermal crystallization of CB, vegetable oils, and CBEs.

Crystallization temperature (°C)	Sample	n	k (min^{-n})	$t_{1/2}\ theo$ (min)	$t_{1/2}\ exp$ (min)	t_0 (min)	R^2
14	CB	2.11	6.86×10^{-3}	8.91	8.46	12.97	0.9988
	CNO	2.57	3.38×10^{-2}	3.23	3.25	2.63	0.9999
	SIO	NC	NC	NC	NC	NC	NC
	CB/CNO	1.92	2.71×10^{-3}	17.99	20.10	11.75	0.9886
	CB/SIO	2.52	1.39×10^{-3}	11.69	11.82	11.34	0.9998
15	CB	2.50	3.43×10^{-3}	8.34	8.43	14.99	0.9997
	CNO	2.70	3.37×10^{-2}	3.06	3.17	3.03	0.9997
	SIO	NC	NC	NC	NC	NC	NC

	CB/CNO	2.04	1.48×10^{-3}	20.23	24.31	12.15	0.9803
	CB/SIO	2.79	4.87×10^{-4}	13.47	13.23	15.79	0.9978
	CB	2.69	1.07×10^{-3}	11.09	11.18	15.20	0.9997
	CNO	2.27	3.08×10^{-2}	3.94	3.83	3.03	0.9997
16	SIO	NC	NC	NC	NC	NC	NC
	CB/CNO	2.72	2.58×10^{-4}	18.25	21.90	13.17	0.9958
	CB/SIO	2.98	2.32×10^{-4}	14.61	14.66	21.67	0.9988

NC. Not calculated.

Values were calculated for one replica.
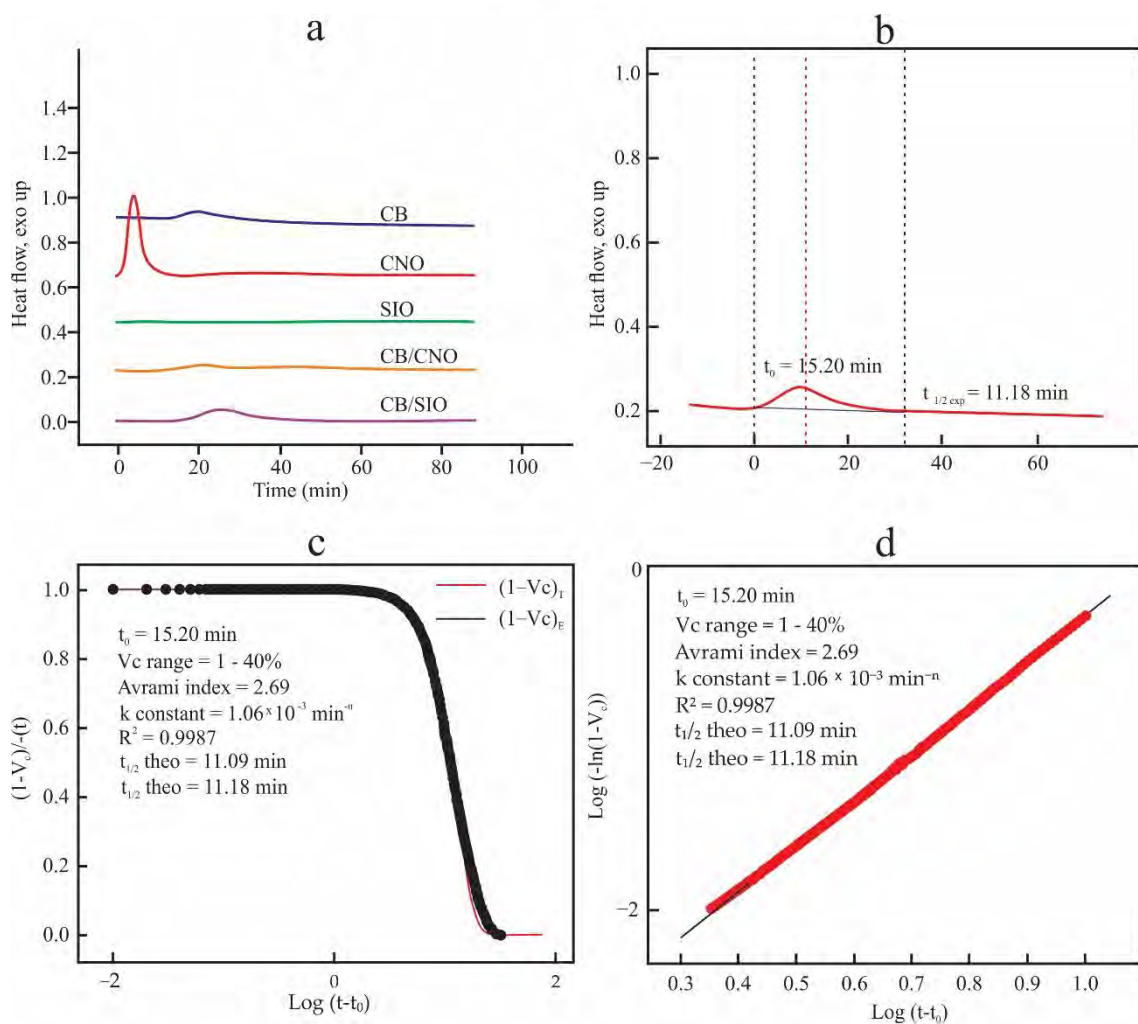
Figure 5.4-2. Fit of the isothermal crystallization data to the Avrami equation. (a) Isothermal crystallization peaks at 16 °C, (b) Original CB data, (c) Relative amorphous fraction of CB, (d) Avrami plot of CB.

5.4.3. Polymorphism, thermal and physical properties of dark chocolates.

Figure 5.4-3 shows the melting peaks deconvolution of dark chocolates made with CBEs at different tempering regimes. The results for Ch-CNO chocolate show T_m between 32.00 ± 0.99 °C and 32.70 ± 0.79 °C (Table 5.4-3), which corresponds to the melting temperature of the form β_2 (Calva-Estrada et al., 2020). For T_m, the studied factors and their interaction did not show a significant effect (p=0.745). However, the high melting ranges (26.01 ± 0.84 °C - 35.01 ± 0.59 °C) allowed the generation of polymorph β_1' (IV) in a low percentage (data not shown) and a higher percentage of form β_2 (84.99 ± 1.11 % - 90.3 ± 1.18 %). In this case, both factors and their interaction showed significant effects (p<0.05), reaching the highest percentage of form β_2 with high tempering and 5% CB/CNO. Likewise, the factors and their interaction had significant effects (p<0.05) on the Ch-CNO chocolates melting enthalpy (48.69 ± 0.36 J/g - 51.25 ± 0.13 J/g), whose values were within those reported by Calva-Estrada et al. (2020). The Casson plastic viscosity values are between 1.19 ± 0.02 Pa.s and 1.41 ± 0.02 Pa.s, values lower than those obtained by Bahari & Akoh (2018) when used CBE (enzymatically synthesized from illipe butter and mid palm fraction) in dark chocolates; however, the Casson yield stress values were higher (10.71 ± 0.08 - 21.44 ± 0.18). The hardness and fracturability are reduced as the CNO percentage increases in both tempering regimes, similar to those reported by Limbardo et al. (2017).
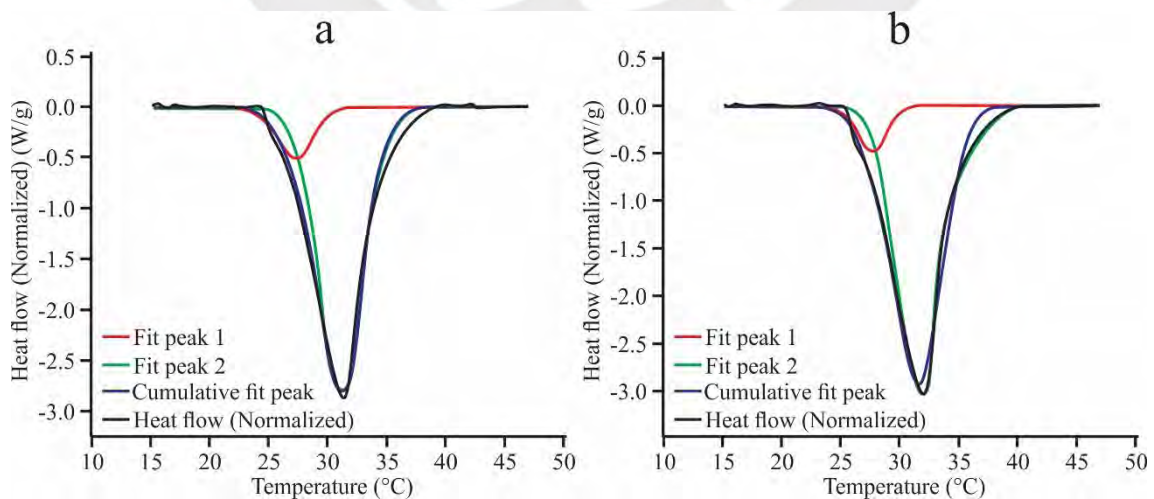
Figure 5.4-3. Peak deconvolution. (a) Dark chocolate with CB/CNO, (b) Dark chocolate with CB/SIO.

Table 5.4-3. Polymorphism, thermal and physical properties of dark chocolates made with different CBE concentrations and tempering regimes.

Tempering	CBE Concentration (%)	T_{onset} (°C)	T_m (°C)	T_{endset} (°C)	Enthalpy (J/g)	Form β_2 (%)	Casson plastic viscosity (Pa.s)	Casson yield stress (Pa)	Hardeness (N)	Fracturability (N)	L	Hue	Chroma	WI
Ch-CNO														
High	1	26.51 ± 0.54	32.52 ± 0.97	34.78 ± 1.09	49.48 ± 0.29	89.38 ± 0.72	1.39 ± 0.03	21.44 ± 0.18	12.89 ± 0.65	12.22 ± 0.54	29.30 ± 0.41	0.26 ± 0.05	11.07 ± 0.18	28.44 ± 0.42
	3	26.48 ± 0.69	32.31 ± 1.04	34.36 ± 0.97	48.69 ± 0.36	85.99 ± 0.28	1.41 ± 0.02	20.54 ± 0.22	12.37 ± 0.59	12.24 ± 0.48	29.18 ± 0.03	1.28 ± 0.03	10.89 ± 0.09	28.35 ± 0.03
	5	26.65 ± 0.70	32.70 ± 0.79	35.01 ± 0.59	50.56 ± 0.20	90.3 ± 1.18	1.25 ± 0.02	11.42 ± 0.57	11.28 ± 0.32	11.28 ± 0.32	29.38 ± 0.15	4.71 ± 0.49	10.25 ± 0.01	28.64 ± 0.15
Low	1	26.01 ± 0.84	32.00 ± 0.99	33.99 ± 0.98	50.37 ± 0.34	84.99 ± 1.11	1.28 ± 0.04	20.63 ± 0.37	13.28 ± 0.13	13.05 ± 0.34	29.50 ± 0.23	1.61 ± 0.27	10.71 ± 0.02	28.69 ± 0.23
	3	26.29 ± 0.45	32.56 ± 0.63	34.67 ± 0.41	50.68 ± 0.19	88.98 ± 0.64	1.40 ± 0.00	20.09 ± 0.63	13.48 ± 0.18	11.63 ± 0.98	29.49 ± 0.51	3.36 ± 2.39	10.43 ± 0.26	28.73 ± 0.54
	5	26.13 ± 0.84	32.19 ± 1.31	34.37 ± 1.15	51.25 ± 0.13	87.4 ± 0.58	1.19 ± 0.02	10.71 ± 0.08	10.99 ± 0.21	10.86 ± 0.19	29.35 ± 0.21	3.93 ± 0.20	10.48 ± 0.09	28.58 ± 0.22
Ch-SIO														
High	1	26.97 ± 0.32	32.61 ± 0.55	34.71 ± 0.56	48.90 ± 0.49	91.92 ± 0.86	1.30 ± 0.02	20.26 ± 0.17	14.28 ± 0.42	10.94 ± 0.96	28.39 ± 0.32	2.51 ± 0.26	10.41 ± 0.05	27.64 ± 0.31
	3	27.65 ± 0.68	33.26 ± 0.67	35.44 ± 0.63	55.84 ± 0.44	92.56 ± 1.49	1.28 ± 0.03	8.49 ± 0.31	13.24 ± 0.19	13.24 ± 0.19	28.35 ± 0.21	1.93 ± 0.34	10.78 ± 0.08	27.55 ± 0.22
	5	26.90 ± 0.10	32.80 ± 0.28	34.79 ± 0.23	50.19 ± 0.10	90.53 ± 1.08	1.26 ± 0.05	17.77 ± 0.92	12.66 ± 0.63	10.82 ± 0.53	28.48 ± 0.05	2.16 ± 0.63	10.74 ± 0.20	27.67 ± 0.06
Low	1	26.77 ± 0.31	32.83 ± 0.60	34.85 ± 0.49	50.40 ± 0.40	91.92 ± 0.33	1.28 ± 0.02	20.17 ± 0.31	13.46 ± 0.18	12.82 ± 0.46	29.40 ± 0.26	2.10 ± 0.40	10.17 ± 0.02	28.67 ± 0.25
	3	27.04 ± 0.35	32.84 ± 0.44	34.85 ± 0.38	55.46 ± 0.06	92.27 ± 1.02	1.28 ± 0.01	8.44 ± 0.04	10.79 ± 0.27	10.79 ± 0.27	29.32 ± 0.20	0.37 ± 0.19	10.16 ± 0.02	28.59 ± 0.20
	5	26.92 ± 0.23	32.82 ± 0.30	35.10 ± 0.30	51.54 ± 0.29	91.26 ± 0.76	1.26 ± 0.05	17.40 ± 0.41	13.28 ± 0.32	9.43 ± 1.61	29.13 ± 0.42	2.48 ± 0.40	10.38 ± 0.05	28.37 ± 0.41

Values are expressed as mean ± standard deviation for three replicates.

The Ch-CNO chocolates' luminosity and WI did not show significant differences; these results could also be indicators of form β_2 generation during tempering. This statement is demonstrated by the low WI values obtained by Ch-CNO chocolates (28.35 ± 0.03 - 28.73 ± 0.54) since WI values greater than 40 are indicators of fat bloom (Jin et al., 2019; Puchol-Miquel et al., 2020). Color control is better understood if, in addition to L*, the Hue angle and Chroma values are measured (Wrolstad & Smith, 2017), then the color coordinates confirm that the Ch-CNO chocolate becomes darker as the CB/CNO concentration increase and tends to make it less reddish.

In the case of Ch-SIO chocolate, no significant differences were found in T_{onset}, T_{endset}, and T_m values. The T_m values were between 32.00 ± 0.99 °C and 32.70 ± 0.79 °C. Similar to Ch-CNO, the melting enthalpy values were between 48.69 ± 0.36 J/g and 51.25 ± 0.13 J/g. The highest percentage of form β_2 was obtained with a high tempering regimen and 3% CB/SIO. Both factors did not significantly affect the Casson plastic viscosity, but they did have a significant effect on the Casson yield stress, whose value decreased while CB/SIO concentration increased, the same as the chocolate hardness and fracturability.

The results show that both types of chocolate have properties with acceptable values, so we can affirm that using these new CBE in producing dark chocolates is feasible. Regarding luminosity, Ch-SIO chocolates were darker when working with a high tempering regime and less prone to fat bloom (low WI values). The Hue angle and Chroma value were low and fell in the same region as the Ch-CNO chocolates. Although both chocolates were tempered for 20 minutes, the tempering regimen and CBE showed a significant effect on the polymorphism, and thermal and physical properties of both types of chocolate (Ch-CNO and Ch-SIO), having Ch-SIO more than 90% of form β_2. Ewens *et al.* (2021) affirm that a CBE candidate should not affect the functionality of the chocolate CB, and Windhab (2009) affirms that a good tempering should allow the generation of a more stable form (β_2). These statements support our results since the physical properties of the chocolates were within the values established by Becket (2009).

5.4.4. Isothermal crystallization kinetics of dark chocolates.

Table 5.4-4 shows the results obtained for the isothermal crystallization of the Ch-CNO and Ch-SIO chocolates. Like MacNaughtan et al. (2006), it has been shown that the DSC technique can produce information to identify the crystallized material melting temperatures and its corresponding form at 17, 18, and 19 °C (Figure 5.4-4). The CBEs tempering regime type and their interactions had no significant effect on T_{onset}, T_m, and T_{endset} (p > 0.05) at the crystallization temperatures studied, results that agree with Afoakwa *et al.* (2008) when they stated that neither the particle size, the fat content, nor the addition of lecithin influence the parameters as mentioned above. Also, we can consider a melting range between 20.04 ± 0.87 °C and 30.69 ± 0.12 °C in which form β'_2 (20–27 °C) (Beckett, 2009), β'_1 (26–28 °C) and β_2 (29–34 °C) (Calva-Estrada et al., 2020) were obtained in both types of chocolate, showing preponderance of form β'_1 (Figure 5.4-4). The studied factors had significant effects on the chocolate melting enthalpy and the kinetic parameters, showing that at a high crystallization temperature, tempering regime, and CBE concentration, less energy is required to melt it (Table 5.4-4).

Table 5.4-4. Kinetic parameters of isothermal crystallization of dark chocolates with different CBE concentrations and tempering regimes.

Crystallization temperature (°C)	Tempering	CBE Concentration (%)	T_{onset} (°C)	T_m (°C)	T_{endset} (°C)	Enthalpy (J/g)	n	k (min^{-n})	$t_{1/2}$ theo (min)	$t_{1/2}$ exp (min)	t_0 (min)
Ch-CNO											
17	High	1	21.37 ± 0.34	28.05 ± 0.45	30.42 ± 0.17	48.32 ± 0.23	2.43 ± 0.01	$2.25\times10^{-3} \pm 0.18\times10^{-3}$	10.54 ± 0.48	10.08 ± 0.37	10.74 ± 0.40
		3	20.64 ± 0.13	27.70 ± 0.55	29.71 ± 0.52	43.80 ± 0.16	2.62 ± 0.04	$1.72\times10^{-3} \pm 0.08\times10^{-3}$	9.81 ± 0.22	9.74 ± 0.17	10.13 ± 0.00
		5	20.05 ± 1.35	27.84 ± 0.44	29.81 ± 0.47	46.56 ± 0.32	2.57 ± 0.02	$2.05\times10^{-3} \pm 0.10\times10^{-3}$	9.63 ± 0.14	9.49 ± 0.08	10.67 ± 0.30
	Low	1	20.89 ± 0.15	27.87 ± 0.56	29.95 ± 0.61	47.44 ± 0.21	2.33 ± 0.02	$6.68\times10^{-3} \pm 0.29\times10^{-3}$	7.31 ± 0.25	7.25 ± 0.18	13.37 ± 0.19
		3	20.77 ± 0.24	27.91 ± 0.65	30.01 ± 0.54	45.28 ± 0.06	2.50 ± 0.05	$3.40\times10^{-3} \pm 0.63\times10^{-3}$	8.41 ± 0.22	8.33 ± 0.25	11.41 ± 0.23
		5	20.57 ± 0.13	27.69 ± 0.56	30.06 ± 0.28	48.50 ± 0.40	2.24 ± 0.06	$5.73\times10^{-3} \pm 0.43\times10^{-3}$	8.52 ± 0.24	8.18 ± 0.11	11.96 ± 0.00
18	High	1	21.63 ± 0.35	28.33 ± 0.42	30.62 ± 0.13	46.12 ± 0.27	2.53 ± 0.13	$1.68e\times10^{-3} \pm 0.41\times10^{-3}$	10.97 ± 0.37	10.57 ± 0.16	8.72 ± 0.00
		3	20.15 ± 0.83	27.94 ± 0.56	29.99 ± 0.50	43.45 ± 0.36	2.88 ± 0.04	$0.83\times10^{-3} \pm 0.03\times10^{-3}$	10.33 ± 0.31	10.31 ± 0.22	8.65 ± 0.13
		5	20.19 ± 1.02	28.03 ± 0.39	29.96 ± 0.40	43.59 ± 0.25	3.12 ± 0.06	$0.41\times10^{-3} \pm 0.06\times10^{-3}$	10.87 ± 0.26	10.86 ± 0.24	8.85 ± 0.23
	Low	1	21.42 ± 0.19	28.18 ± 0.56	30.18 ± 0.59	44.63 ± 0.29	2.45 ± 0.04	$2.63\times10^{-3} \pm 0.27\times10^{-3}$	9.68 ± 0.27	9.52 ± 0.18	10.06 ± 0.31
		3	20.78 ± 0.90	28.14 ± 0.60	30.22 ± 0.52	42.32 ± 0.18	2.57 ± 0.15	$1.41\times10^{-3} \pm 0.29\times10^{-3}$	11.18 ± 0.87	10.90 ± 0.66	8.84 ± 0.41
		5	20.04 ± 0.87	27.92 ± 0.57	30.01 ± 0.53	45.50 ± 0.37	2.72 ± 0.04	$0.95\times10^{-3} \pm 0.04\times10^{-3}$	11.42 ± 0.54	11.20 ± 0.73	9.18 ± 0.23
19	High	1	20.33 ± 0.12	28.53 ± 0.44	30.69 ± 0.12	42.71 ± 0.08	2.56 ± 0.03	$1.38\times10^{-3} \pm 0.39\times10^{-3}$	11.39 ± 0.96	11.43 ± 0.84	15.78 ± 0.64
		3	20.19 ± 0.15	28.15 ± 0.53	30.12 ± 0.46	41.59 ± 0.14	2.53 ± 0.02	$1.71\times10^{-3} \pm 0.21\times10^{-3}$	10.68 ± 0.31	10.77 ± 0.26	13.04 ± 0.46
		5	20.30 ± 0.15	28.24 ± 0.41	30.13 ± 0.37	40.27 ± 0.06	2.81 ± 0.03	$0.55\times10^{-3} \pm 0.05\times10^{-3}$	12.66 ± 0.41	12.76 ± 0.28	12.49 ± 0.30
	Low	1	20.36 ± 0.32	28.40 ± 0.58	30.38 ± 0.57	41.71 ± 0.28	2.59 ± 0.02	$1.43\times10^{-3} \pm 0.16\times10^{-3}$	10.83 ± 0.38	10.74 ± 0.29	11.88 ± 0.23
		3	20.42 ± 0.21	28.37 ± 0.61	30.35 ± 0.52	40.39 ± 0.20	2.64 ± 0.03	$1.12\times10^{-3} \pm 0.16\times10^{-3}$	11.44 ± 0.99	11.39 ± 1.02	12.23 ± 0.46
		5	20.28 ± 0.06	28.13 ± 0.56	30.15 ± 0.54	41.31 ± 0.34	2.60 ± 0.08	$1.36\times10^{-3} \pm 0.09\times10^{-3}$	10.95 ± 0.64	11.00 ± 0.45	13.98 ± 0.34
Ch-SIO											
17	High	1	20.66 ± 0.26	27.75 ± 0.46	29.83 ± 0.43	48.27 ± 0.21	2.32 ± 0.09	$6.57\times10^{-3} \pm 0.39\times10^{-3}$	7.47 ± 0.45	7.39 ± 0.33	13.50 ± 0.23
		3	20.72 ± 0.12	27.86 ± 0.58	30.05 ± 0.61	50.25 ± 0.14	2.41 ± 0.04	$4.49\times10^{-3} \pm 0.17\times10^{-3}$	8.03 ± 0.19	7.91 ± 0.13	13.30 ± 0.11

		5	20.45 ± 0.09	27.84 ± 0.12	29.90 ± 0.13	47.49 ± 0.15	2.08 ± 0.08	$11.2 \times 10^{-3} \pm 1.96 \times 10^{-3}$	7.27 ± 0.14	7.08 ± 0.15	13.50 ± 0.12
		1	20.66 ± 0.07	28.04 ± 0.51	30.23 ± 0.56	49.53 ± 0.01	2.27 ± 0.06	$6.46 \times 10^{-3} \pm 0.24 \times 10^{-3}$	7.83 ± 0.33	7.70 ± 0.24	13.40 ± 0.11
	Low	3	20.93 ± 0.06	28.02 ± 0.00	29.98 ± 0.41	52.57 ± 0.32	2.51 ± 0.12	$2.69 \times 10^{-3} \pm 0.31 \times 10^{-3}$	9.16 ± 0.80	8.98 ± 0.58	12.50 ± 0.46
		5	20.48 ± 0.05	27.75 ± 0.33	29.92 ± 0.34	40.68 ± 0.53	2.43 ± 0.06	$2.77 \times 10^{-3} \pm 0.04 \times 10^{-3}$	9.78 ± 0.54	9.50 ± 0.46	10.80 ± 0.20
		1	21.32 ± 0.31	28.22 ± 0.21	30.09 ± 0.44	47.66 ± 0.21	2.44 ± 0.02	$2.58 \times 10^{-3} \pm 0.28 \times 10^{-3}$	9.90 ± 0.62	9.87 ± 0.57	10.50 ± 0.23
	High	3	21.25 ± 0.15	28.15 ± 0.56	30.27 ± 0.62	49.60 ± 0.21	2.56 ± 0.11	$1.80 \times 10^{-3} \pm 0.19 \times 10^{-3}$	10.30 ± 1.14	10.10 ± 0.90	10.30 ± 0.69
		5	20.64 ± 0.79	28.12 ± 0.12	30.10 ± 0.13	44.80 ± 0.11	2.53 ± 0.01	$2.48 \times 10^{-3} \pm 0.15 \times 10^{-3}$	9.29 ± 0.17	9.18 ± 0.14	10.00 ± 0.10
18		1	21.35 ± 0.11	28.33 ± 0.48	30.45 ± 0.50	47.62 ± 0.16	2.74 ± 0.04	$1.17 \times 10^{-3} \pm 0.09 \times 10^{-3}$	10.20 ± 0.10	10.30 ± 0.04	10.20 ± 0.11
	Low	3	21.52 ± 0.11	28.11 ± 0.35	30.19 ± 0.38	48.63 ± 0.31	2.60 ± 0.08	$1.43 \times 10^{-3} \pm 0.20 \times 10^{-3}$	10.20 ± 0.10	10.60 ± 0.24	10.20 ± 0.11
		5	20.09 ± 0.98	28.02 ± 0.34	30.05 ± 0.31	40.60 ± 0.30	2.52 ± 0.05	$1.82 \times 10^{-3} \pm 0.09 \times 10^{-3}$	10.60 ± 0.36	10.30 ± 0.31	9.06 ± 0.11
		1	20.84 ± 0.67	28.39 ± 0.32	30.26 ± 0.37	44.76 ± 0.08	3.09 ± 0.09	$0.18 \times 10^{-3} \pm 0.03 \times 10^{-3}$	14.40 ± 1.03	14.30 ± 0.71	8.99 ± 0.65
	High	3	20.23 ± 0.27	28.36 ± 0.56	30.40 ± 0.64	46.52 ± 0.16	2.78 ± 0.05	$0.57 \times 10^{-3} \pm 0.06 \times 10^{-3}$	12.90 ± 0.84	12.80 ± 0.59	10.90 ± 0.61
		5	20.33 ± 0.29	28.34 ± 0.11	30.27 ± 0.17	42.25 ± 0.08	3.02 ± 0.12	$0.19 \times 10^{-3} \pm 0.02 \times 10^{-3}$	15.20 ± 1.05	15.00 ± 0.61	9.06 ± 0.77
19		1	20.83 ± 0.74	28.59 ± 0.48	30.64 ± 0.49	44.46 ± 0.28	2.92 ± 0.11	$0.41 \times 10^{-3} \pm 0.03 \times 10^{-3}$	12.80 ± 1.21	12.90 ± 1.01	10.50 ± 0.65
	Low	3	20.51 ± 0.11	28.32 ± 0.35	30.40 ± 0.36	45.55 ± 0.24	3.24 ± 0.07	$0.14 \times 10^{-3} \pm 0.05 \times 10^{-3}$	13.80 ± 0.24	14.00 ± 0.25	9.87 ± 0.30
		5	20.22 ± 0.13	28.21 ± 0.32	30.17 ± 0.33	40.62 ± 0.28	2.93 ± 0.08	$0.27 \times 10^{-3} \pm 0.04 \times 10^{-3}$	14.60 ± 0.52	14.40 ± 0.35	9.74 ± 0.20

Values are expressed as mean ± standard deviation for three replicates.
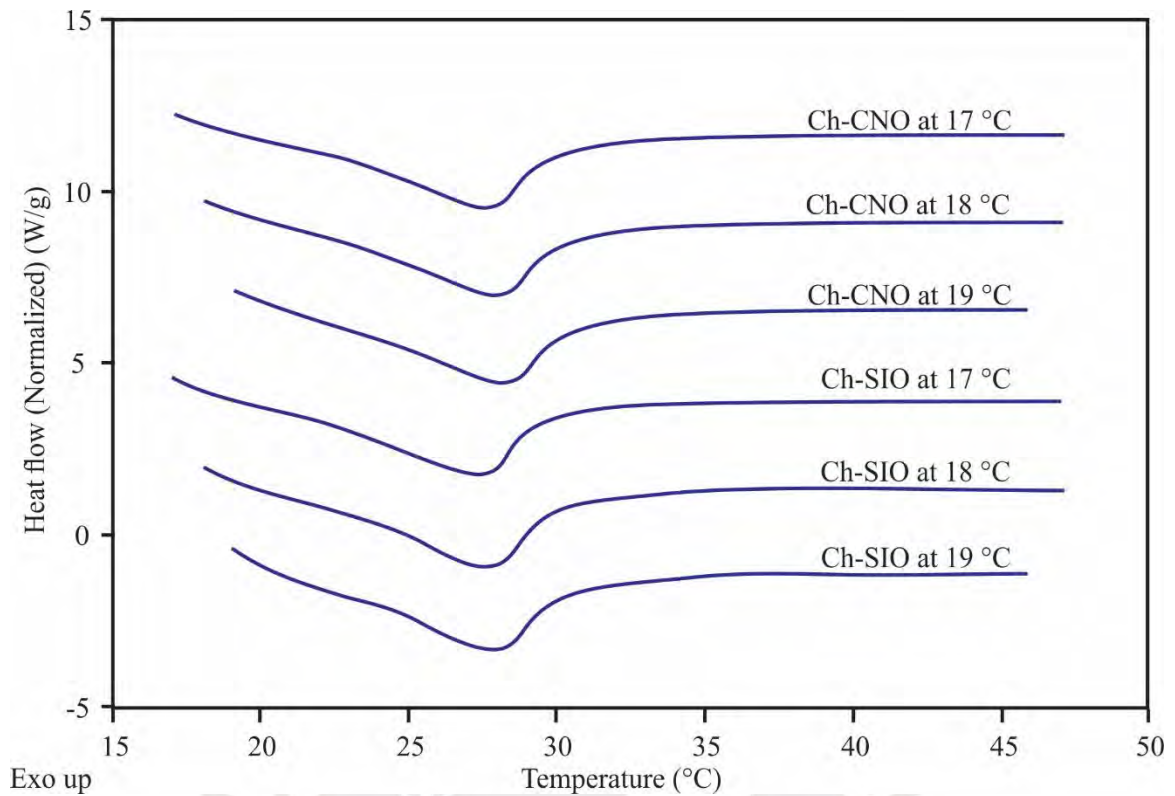
Figure 5.4-4. Melting ranges of dark chocolates and their polymorphic forms. The samples correspond to a high tempering regime and 1% CBE.

The isothermal crystallization data obtained by DSC for Ch-CNO and Ch-SIO were fitted to the Avrami equation, getting a correlation coefficient R^2 close to 1. This fit allowed finding the crystallization kinetic parameters contained in Table 5.4-4. The Avrami parameters characterize the crystallization process and are a function of the crystallization temperatures (Marangoni & Wesdorp, 2013) and the chocolate formulation (Fernandes et al., 2013). The values of n indicate the crystal growth mechanism; according to Marangoni & Wesdorp (2013), the values of n greater than 2 (Table 5.4-4) obtained in both chocolates indicate that the combination of tempering and CBE cause the crystal nuclei to grow like-plate sporadically and instantly. In the case of Ch-SIO crystallized at 19 °C, spherical nuclei with sporadic growth were observed. The parameters of n and k are related to the half-time crystallization (Equation 5.4-3), so their values will determine the chocolates' crystallization speed. Table 5.4-4 shows that the factors studied also had effects on the half-time crystallization of both chocolates, obtaining a faster crystallization in the Ch-CNO chocolates processed with low tempering and low concentration of CB/CNO ($t_{1/2} \, exp$ = 7.25 ± 0.18 min), as well

145

as Ch-SIO chocolates processed with low tempering and low concentration of CB/SIO ($t_{1/2} \; exp$ = 7.08 ± 0.15 min). Using crystallization temperatures between 23 °C and 24 °C in chocolates made with different formulations, Fernandes *et al.* (2013) obtained n values between 3 and 4 (instantaneous and sporadic spherical growth); moreover, the fastest crystallization occurred between 20 and 30 min, demonstrating that the chocolate formulation influenced these results. In addition to the formulation and crystallization temperatures, the tempering and type of CBE also influence the chocolates' crystallization behavior. Avrami's equation gives a non-crystallized fraction ($1 - V_c$) equal to 1 when the crystallization time is zero, so any value below 1 indicates that crystallization has started (Lorenzo et al., 2007). The time to start the chocolate crystallization is the induction time, t_0. Chocolate that crystallized at 19 °C with high tempering and 1% CB/CNO obtained the longest induction time (15.78 ± 0.64 min), while chocolate that crystallized at 18 °C with high tempering and 3% CB/CNO had the shortest one (8.65 ± 0.13 min). According to these results, using vegetable oils as CBEs and tempering can reduce the induction time of chocolate crystallization. However, it is necessary to be careful with the type and amount of CBE used in the production of chocolates since it will have effects on the crystallization behavior of the final product, such as the acceleration of the crystallization process (Ewens et al., 2021; Mello et al., 2020; Ghazani & Marangoni, 2018).

5.5. Conclusions

Sacha inchi oil crystallizes at temperatures below zero, and like coconut oil, its properties change when mixed with cocoa butter. Coconut oil crystallizes faster than cocoa butter; however, when mixed with cocoa butter to be used as CBE, its crystallization rate and fusion enthalpy are reduced. Using these vegetable oils as CBE for the production of dark chocolates is feasible because the proportions studied combined with the tempering regimen modified its physical, thermal, and crystallization kinetic properties; furthermore, the levels remained within acceptable values. Likewise, coconut oil allowed the production of dark chocolates with percentages of form β_2 greater than 80%, while the chocolates with sacha inchi oil exceeded 90%. The CBEs also accelerate the chocolate crystallization process, being faster in the chocolates with sacha inchi

oil and processed with high tempering and CBE concentration than in the chocolates with coconut oil. All the chocolates had the same nucleation pattern that responds to the generation of plate-shaped nuclei with sporadic and instantaneous crystal growth.

5.6.   References

Afoakwa, E. O., Paterson, A., Fowler, M., & Vieira, J. (2008). Characterization of melting properties in dark chocolates from varying particle size distribution and

composition using differential scanning calorimetry. *Food Research International*, 41(7), 751–757. https://doi.org/10.1016/j.foodres.2008.05.009

Aumpai, K., Tan, Ch. P., Huang, Q., & Sonwai, S. (2022). Production of cocoa butter equivalent from blending of illipé butter and palm mid-fraction. *Food Chemistry*, 8.

Avrami, M. (1940). Kinetics of Phase Change. II Transformation-Time Relations for Random Distribution of Nuclei. *The Journal of Chemical Physics*, 8(2), 212–224. https://doi.org/10.1063/1.1750631

Bahari, A., & Akoh, C. C. (2018). Texture, rheology and fat bloom study of 'chocolates' made from cocoa butter equivalent synthesized from illipe butter and palm mid-fraction. *LWT - Food Science and Technology*, 97, 349–354. https://doi.org/10.1016/j.lwt.2018.07.013

Beckett, S. T. (Ed.). (2009). Industrial chocolate manufacture and use (4th ed). Wiley-Blackwell.

Bootello, M. A., Hartel, R. W., Garcés, R., Martínez-Force, E., & Salas, J. J. (2012). Evaluation of high oleic-high stearic sunflower hard stearins for cocoa butter equivalent formulation. *Food Chemistry*, 134(3), 1409–1417. https://doi.org/10.1016/j.foodchem.2012.03.040

Bresson, S., Lecuelle, A., Bougrioua, F., El Hadri, M., Baeten, V., Courty, M., Pilard, S., Rigaud, S., & Faivre, V. (2021). Comparative structural and vibrational investigations between cocoa butter (CB) and cocoa butter equivalent (CBE) by ESI/MALDI-HRMS, XRD, DSC, MIR and Raman spectroscopy. *Food Chemistry*, 363, 130319. https://doi.org/10.1016/j.foodchem.2021.130319

Calva-Estrada, S. J., Utrilla-Vázquez, M., Vallejo-Cardona, A., Roblero-Pérez, D. B., & Lugo-Cervantes, E. (2020). Thermal properties and volatile compounds profile of commercial dark-chocolates from different genotypes of cocoa beans (Theobroma cacao L.) from Latin America. *Food Research International*, 136, 109594. https://doi.org/10.1016/j.foodres.2020.109594

Campos, R., & Marangoni, A. (2012). Molecular Composition Dynamics and Structure of Cocoa Butter. In *Cocoa butter and related compounds* (p. 546). AOCS Press.

Castro-Alayo, E. M., Torrejón-Valqui, L., Cayo-Colca, I. S., & Cárdenas-Toro, F. P. (2021). Evaluation of the Miscibility of Novel Cocoa Butter Equivalents by Raman Mapping and Multivariate Curve Resolution–Alternating Least Squares. *Foods*, 10(12), 3101. https://doi.org/10.3390/foods10123101

Chaleepa, K., Szepes, A., & Ulrich, J. (2010). Dry fractionation of coconut oil by melt crystallization. *Chemical Engineering Research and Design*, 88(9), 1217–1222. https://doi.org/10.1016/j.cherd.2010.01.026

Chen, J., Ghazani, S. M., Stobbs, J. A., & Marangoni, A. G. (2021). Tempering of cocoa butter and chocolate using minor lipidic components. *Nature Communications*, 12(1), 5018. https://doi.org/10.1038/s41467-021-25206-1

Chen, Y., Wang, W., Zhang, W., Tan, C.-P., Lan, D., & Wang, Y. (2022). Characteristics and feasibility of olive oil-based diacylglycerol plastic fat for use in compound chocolate. *Food Chemistry*, 391, 133254. https://doi.org/10.1016/j.foodchem.2022.133254

Declerck, A., Nelis, V., Danthine, S., Dewettinck, K., & Van der Meeren, P. (2021). Characterisation of Fat Crystal Polymorphism in Cocoa Butter by Time-Domain NMR and DSC Deconvolution. *Foods*, 10(3), 520. https://doi.org/10.3390/foods10030520

Devos, N., Reyman, D., & Sanchez-Cortés, S. (2020). Chocolate composition and its crystallization process: A multidisciplinary analysis. *Food Chemistry*, 128301. https://doi.org/10.1016/j.foodchem.2020.128301

Ewens, H., Metilli, L., & Simone, E. (2021). Analysis of the effect of recent reformulation strategies on the crystallization behaviour of cocoa butter and the structural properties of chocolate. *Current Research in Food Science*, 4, 105–114. https://doi.org/10.1016/j.crfs.2021.02.009

Fernandes, V. A., Müller, A. J., & Sandoval, A. J. (2013). Thermal, structural and rheological characteristics of dark chocolate with different compositions. *Journal of Food Engineering*, 116(1), 97–108. https://doi.org/10.1016/j.jfoodeng.2012.12.002

Ghazani, S. M., & Marangoni, A. G. (2018). Facile lipase-catalyzed synthesis of a chocolate fat mimetic. *Scientific Reports*, 8(1), 15271. https://doi.org/10.1038/s41598-018-33600-x

Gregersen, S. B., Miller, R. L., Hammershøj, M., Andersen, M. D., & Wiking, L. (2015). Texture and microstructure of cocoa butter replacers: Influence of composition and cooling rate. *Food Structure*, 4, 2–15. https://doi.org/10.1016/j.foostr.2015.03.001

Hubbes, S.-S., Danzl, W., & Foerst, P. (2018). Crystallization kinetics of palm oil of different geographic origins and blends thereof by the application of the Avrami model. *LWT-Food Science and Technology*, 93, 189–196. https://doi.org/10.1016/j.lwt.2018.03.022

Jahurul, M. H. A., Ping, L. L., Sharifudin, M. S., Hasmadi, M., Mansoor, A. H., Lee, J. S., Noorakmar, B. W., Amir, H. M. S., Jinap, S., Mohd Omar, A. K., & Zaidul, I. S. M. (2019). Thermal properties, triglycerides and crystal morphology of bambangan (Mangifera pajang) kernel fat and palm stearin blends as cocoa butter alternatives. *LWT- Food Science and Technology*, 107, 64–71. https://doi.org/10.1016/j.lwt.2019.02.053

Jin, J., Jin, Q., Wang, X., & Akoh, C. C. (2019). Improving heat and fat bloom stabilities of "dark chocolates" by addition of mango kernel fat-based chocolate fats. *Journal of Food Engineering*, 246, 33–41. https://doi.org/10.1016/j.jfoodeng.2018.10.027

Joshi, R., Lohumi, S., Joshi, R., Kim, M. S., Qin, J., Baek, I., & Cho, B.-K. (2020). Raman spectral analysis for non-invasive detection of external and internal parameters of fake eggs. *Sensors and Actuators B-Chemical*, 303. https://doi.org/10.1016/j.snb.2019.127243

Limbardo, R. P., Santoso, H., & Witono, J. R. (2017, November). The effect of coconut oil and palm oil as substituted oils to cocoa butter on chocolate bar texture and melting point. Article in International Seminar on Fundamental and Application of Chemical Engineering 2016, East Java, Indonesia.

Liu, W., Yao, Y., & Li, C. (2022). Effect of tempered procedures on the crystallization behavior of different positions of cocoa butter products. *Food Chemistry*, 370, 131002. https://doi.org/10.1016/j.foodchem.2021.131002

Lorenzo, A. T., Arnal, M. L., Albuerne, J., & Müller, A. J. (2007). DSC isothermal polymer crystallization kinetics measurements and the use of the Avrami equation to fit the data: Guidelines to avoid common problems. *Polymer Testing*, 26(2), 222–231. https://doi.org/10.1016/j.polymertesting.2006.10.005

MacNaughtan, W., Farhat, I. A., Himawan, C., Starov, V. M., & Stapley, A. G. F. (2006). A differential scanning calorimetry study of the crystallization kinetics of tristearin-tripalmitin mixtures. *Journal of the American Oil Chemists' Society*, 83(1), 1–9. https://doi.org/10.1007/s11746-006-1167-1

Mahato, D. K., Jadhav, S. R., Mukurumbira, A. R., Keast, R., Liem, D. G., Shah, R., & Gamlath, S. (2022). Physicochemical properties and microbial safety of reduced-sugar chocolate-flavored milk. *Journal of Food Processing and Preservation*, 46(e16409), 1–12. https://doi.org/10.1111/jfpp.16409

Marangoni, A. G., & Wesdorp, L. H. (2013). Nucleation and crystalline growth kinetics. In *structure and properties of fat crystal networks* (Second, pp. 27–99). CRC Press.

Martini, S. (2015). Application of DSC, pulsed NMR, and other analytical techniques to study the crystallization kinetics of lipids models, oil, fats, and their blends in the field of food technology. In *Differential scanning calorimetry. Applications in fat and oil technology* (First, pp. 163–195). CRC Press/Taylor & Francis.

Martini, S., Tan, C. Y., & Jana, S. (2015). Physical Characterization of Wax/Oil Crystalline Networks: Wax/oil crystalline networks…. *Journal of Food Science*, 80(5), C989–C997. https://doi.org/10.1111/1750-3841.12853

Medina-Mendoza, M., Rodriguez-Pérez, R. J., Rojas-Ocampo, E., Torrejón-Valqui, L., Fernández-Jeri, A. B., Idrogo-Vásquez, G., Cayo-Colca, I. S., & Castro-Alayo, E. M. (2021). Rheological, bioactive properties and sensory preferences of dark chocolates with partial incorporation of Sacha Inchi (Plukenetia volubilis L.) oil. *Heliyon*, 7(2), e06154. https://doi.org/10.1016/j.heliyon.2021.e06154

Mello, N. A., Cardoso, L. P., Badan Ribeiro, A. P., & Bicas, J. L. (2020). The effects of limonene on the crystallization of palm oil. *LWT-Food Science and Technology*, 133, 110079. https://doi.org/10.1016/j.lwt.2020.110079

Ng, S. P., Khor, Y. P., Lim, H. K., Lai, O. M., Wang, Y., Wang, Y., Nehdi, I. A., & Tan, C. P. (2021). In-depth characterization of palm-based diacylglycerol-virgin coconut oil blends with enhanced techno-functional properties. *LWT-Food Science and Technology*, 145, 111327. https://doi.org/10.1016/j.lwt.2021.111327

Nightingale, L. M., Lee, S.-Y., & Engeseth, N. J. (2011). Impact of Storage on Dark Chocolate: Texture and Polymorphic Changes. *Journal of Food Science*, 76(1), C142–C153. https://doi.org/10.1111/j.1750-3841.2010.01970.x

Norazlina, M. R., Jahurul, M. H. A., Hasmadi, M., Sharifudin, M. S., Patricia, M., Lee, J. S., Amir, H. M. S., Noorakmar, A. W., & Riman, I. (2020). Effects of fractionation technique on triacylglycerols, melting and crystallisation and the polymorphic behavior of bambangan kernel fat as cocoa butter improver. *LWT-Food Science and Technology*, 129, 109558. https://doi.org/10.1016/j.lwt.2020.109558

Padar, S., Jeelani, S. A. K., & Windhab, E. J. (2008). Crystallization Kinetics of Cocoa Fat Systems: Experiments and Modeling. *Journal of the American Oil Chemists' Society*, 85(12), 1115–1126. https://doi.org/10.1007/s11746-008-1312-0

Pirouzian, H. R., Konar, N., Palabiyik, I., Oba, S., & Toker, O. S. (2020). Pre-crystallization process in chocolate: Mechanism, importance and novel aspects. *Food Chemistry*, 321, 126718. https://doi.org/10.1016/j.foodchem.2020.126718

Puchol-Miquel, M., Palomares, C., Barat, J. M., & Perez-Esteve, É. (2020). Formulation and physicochemical and sensory characterisation of chocolate made from reconstituted cocoa liquor and high cocoa content. *LWT-Food Science and Technology*, 110492. https://doi.org/10.1016/j.lwt.2020.110492

Rashid, N. A. (2012). Crystallisation kinetics of palm stearin, palm kernel olein and their blends. *LWT-Food Science and Technology*, 46, 571-573.

Ray, J., MacNaughtan, W., Chong, P. S., Vieira, J., & Wolf, B. (2012). The Effect of Limonene on the Crystallization of Cocoa Butter. *Journal of the American Oil Chemists' Society*, 89(3), 437–445. https://doi.org/10.1007/s11746-011-1934-5

Saberi, A. H., Lai, O.-M., & Toro-Vázquez, J. F. (2011). Crystallization kinetics of palm oil in blends with palm-based diacylglycerol. *Food Research International*, 44(1), 425–435. https://doi.org/10.1016/j.foodres.2010.09.029

Sonwai, S., Podchong, P., & Rousseau, D. (2017). Crystallization kinetics of cocoa butter in the presence of sorbitan esters. *Food Chemistry*, 214, 497–506. https://doi.org/10.1016/j.foodchem.2016.07.092

Talbot, G. (2009). Chocolate temper. In *Industrial chocolate, manufacture and use* (Fourth edition, pp. 261–275). Blackwell Publishing.

Teles dos Santos, M., Viana, I. S., Ract, J. N. R., & Le Roux, G. A. C. (2016). Thermal properties of palm stearin, canola oil and fully hydrogenated soybean oil blends: Coupling experiments and modeling. *Journal of Food Engineering*, 185, 17–25. https://doi.org/10.1016/j.jfoodeng.2016.03.029

Toro-Vazquez, J. F., Briceño-Montelongo, M., Dibildox-Alvarado, E., Charó-Alonso, M., & Reyes-Hernández, J. (2000). Crystallization kinetics of palm stearin in blends with sesame seed oil. *Journal of the American Oil Chemists' Society*, 77(3), 297–310. https://doi.org/10.1007/s11746-000-0049-x

Watanabe, S., Yoshikawa, S., & Sato, K. (2020). Formation and Properties of Dark Chocolate Prepared Using Fat Mixtures of Cocoa Butter and symmetric/asymmetric stearic-oleic mixed-acid triacylglycerols: Impact of

Molecular Compound Crystals. *Food Chemistry*, 127808. https://doi.org/10.1016/j.foodchem.2020.127808

Windhab, E. J. (2009). Tempering. In *Industrial Chocolate. Manufacture and Use* (Fourth Edition, p. 276). Blackwell Publishing. York, UK.

Wrolstad, R. E., & Smith, D. E. (2017). Color Analysis. In *Food Analysis* (Fifth edition, p. 644). Springer.

Yao, Y., Liu, W., Zhang, D., Li, R., Zhou, H., Li, C., & Wang, S. (2020). Dynamic changes in the triacylglycerol composition and crystallization behavior of cocoa butter. *LWT-Food Science and Technology*, 129, 109490. https://doi.org/10.1016/j.lwt.2020.109490

CONCLUSIONES

Las conclusiones que se presentan a continuación corresponden a los aportes generados durante la realización de los experimentos que llevaron al cumplimiento de los objetivos de la presente tesis.

Durante la fermentación espontánea de cacao Criollo estudiada en el presente trabajo, la cual fue realizada en siete días, se pudo notar que la velocidad de cristalización de la manteca de cacao en el interior del grano fue más rápida durante los primeros tres días. Por lo que, en términos de cristalización de la manteca de cacao, sería suficiente realizar un proceso de fermentación en tres días. Así mismo, los estudios cinéticos y polimorfismo demostraron que durante la fermentación espontánea de cacao Criollo, la manteca de cacao estuvo presente en forma de cristales metaestables β_1' y β_2', el crecimiento de estos cristales fue como agujas, fibras, varillas o plato, que se fueron formando esporádica o instantáneamente.

Se demostró la utilidad de la Microscopía Confocal Raman para determinar de manera cualitativa a traves de histogramas de imágenes químicas, y cuantitativa a traves de la desviación estándar relativa, que existe alta miscibilidad de los aceites de coco y sacha inchi con la manteca de cacao, a concentraciones de 45% y 35%, respectivamente. Dicha miscibilidad debe ser una propiedad de los aceites vegetales necesaria para elaborar nuevos equivalentes de manteca de cacao con la finalidad de utilizarlos en la fabricación de chocolate. La técnica también permitió establecer que la principal diferencia entre estos aceites está en el grado de insaturación, evidenciado por la alta intensidad del pico a 1662,7 cm^{-1} en el espectro Raman del aceite de sacha inchi. Además, la técnica fue capáz de identificar el estado polimórfico β_2' y β_1' de la manteca de cacao, evidenciado por los picos a 1745,4 cm^{-1} y 1733,8 cm^{-1} en el espectro Raman de la manteca de cacao.

Las propiedades térmicas y cristalización de los aceites de coco y sacha inchi cambiaron al ser mezclados con manteca de cacao para elaborar CBEs, en consecuencia, la entalpía de fusión y la tasa de cristalización se redujeron. Estos aceites utilizados como CBE y los regímenes de temperado produjeron chocolates oscuros con porcentajes de forma β_2 que superaron los valores teóricos aceptados para la fabricación de chocolates; también aceleraron la

cristalización de la manteca de cacao en los chocolates, produciendo cristales como plato que aparecieron esporádica e instantáneamente. Así también, los nuevos CBEs modificaron las propiedades físicas y térmicas de los chocolates dentro de valores aceptables. Estos resultados demuestran que es factible usar estos aceites peruanos en la elaboración de chocolates oscuros, existiendo la posibilidad de agregarse a la lista de aceites vegetales permitidos por la legislación europea.

RECOMENDACIONES

Desde el punto de vista de la mejora de procesos, el presente trabajo demuestra que considerando la cristalización de la manteca de cacao como factor decisivo, será posible reducir el tiempo de fermentación espontánea del cacao Criollo de siete a tres días, lo cual permitirá tener mayor disponibilidad de tiempo en el módulo de fermentación para procesar la producción de manera más rápida y cumplir a tiempo con los pedidos de los clientes. Así también, es factible el uso de aceite de coco y aceite de sacha inchi para crear nuevos equivalentes de manteca de cacao, e incorporarlos como ingredientes en la fabricación de chocolates oscuros, ya que permitirán acelerar la cristalización de los chocolates y por tanto reducir el consumo energético en el temperado. Usando estos aceites se puede obtener chocolates oscuros con altos porcentajes de forma β_2 y características aceptables. Se crea también, la posibilidad de incorporar un nuevo procedimiento en la fabricación de chocolates oscuros, que consiste en la verificación de la miscibilidad y homogeneidad de los ingredientes con la manteca de cacao antes de ser incorporados al proceso de fabricación, lo cual permitirá conocer si los ingredientes son idóneos para ser utilizados.

REFERENCIAS

Afoakwa, E. O., Paterson, A., Fowler, M., & Ryan, A. (2008). Flavor Formation and Character in Cocoa and Chocolate: A Critical Review. *Critical Reviews in Food Science and Nutrition*, *48*(9), 840-857. https://doi.org/10.1080/10408390701719272

Afoakwa, E. O., Paterson, A., Fowler, M., & Vieira, J. (2009). Influence of tempering and fat crystallization behaviours on microstructural and melting properties in dark chocolate systems. *Food Research International*, *42*(1), 200-209. https://doi.org/10.1016/j.foodres.2008.10.007

Afoakwa, E. O., Quao, J., Budu, A. S., Takrama, J., & Saalia, F. K. (2011). Effect of pulp preconditioning on acidification, proteolysis, sugars and free fatty acids concentration during fermentation of cocoa (*Theobroma cacao*) beans. *International Journal of Food Sciences and Nutrition*, *62*(7), 755-764. https://doi.org/10.3109/09637486.2011.581224

Aprotosoaie, A. C., Luca, S. V., & Miron, A. (2016). Flavor Chemistry of Cocoa and Cocoa Products-An Overview: Flavor chemistry of cocoa …. *Comprehensive Reviews in Food Science and Food Safety*, *15*(1), 73-91. https://doi.org/10.1111/1541-4337.12180

Ascrizzi, R., Flamini, G., Tessieri, C., & Pistelli, L. (2017). From the raw seed to chocolate: Volatile profile of Blanco de Criollo in different phases of the processing chain. *Microchemical Journal*, *133*, 474-479. https://doi.org/10.1016/j.microc.2017.04.024

Assi-Clair, B. J., Koné, M. K., Kouamé, K., Lahon, M. C., Berthiot, L., Durand, N., Lebrun, M., Julien-Ortiz, A., Maraval, I., Boulanger, R., & Guéhi, T. S. (2019). Effect of aroma potential of Saccharomyces cerevisiae fermentation on the volatile profile of raw cocoa and sensory attributes of chocolate produced thereof. *European Food Research and Technology*. https://doi.org/10.1007/s00217-018-3181-6

Bayés-García, L., Aguilar-Jiménez, M., Calvet, T., Koyano, T., & Sato, K. (2019). Crystallization and Melting Behavior of Cocoa Butter in Lipid Bodies of Fresh

Cacao Beans. *Crystal Growth & Design*, *19*(7), 4127-4137. https://doi.org/10.1021/acs.cgd.9b00570

Beckett, S. T. (Ed.). (2009). *Industrial chocolate manufacture and use* (4th ed). Wiley-Blackwell.

Biswas, N., Cheow, Y. L., Tan, C. P., & Siow, L. F. (2017). Physical, rheological and sensorial properties, and bloom formation of dark chocolate made with cocoa butter substitute (CBS). *LWT - Food Science and Technology*, *82*, 420-428. https://doi.org/10.1016/j.lwt.2017.04.039

Bresson, S., Rousseau, D., Ghosh, S., Marssi, M. E., & Faivre, V. (2011). Raman spectroscopy of the polymorphic forms and liquid state of cocoa butter. *European Journal of Lipid Science and Technology*, *113*(8), 992-1004. https://doi.org/10.1002/ejlt.201100088

Caligiani, A., Marseglia, A., Prandi, B., Palla, G., & Sforza, S. (2016). Influence of fermentation level and geographical origin on cocoa bean oligopeptide pattern. *Food Chemistry*, *211*, 431-439. https://doi.org/10.1016/j.foodchem.2016.05.072

Campos, R., & Marangoni, A. (2012). Molecular Composition Dynamics and Structure of Cocoa Butter. En *Cocoa butter and related compounds* (p. 546). AOCS Press.

Castro-Alayo, E. M., Idrogo-Vásquez, G., Siche, R., & Cardenas-Toro, F. P. (2019). Formation of aromatic compounds precursors during fermentation of Criollo and Forastero cocoa. *Heliyon*, *5*(1), e01157. https://doi.org/10.1016/j.heliyon.2019.e01157

Chagas Junior, G. C. A., Ferreira, N. R., & Lopes, A. S. (2021). The microbiota diversity identified during the cocoa fermentation and the benefits of the starter cultures use: An overview. *International Journal of Food Science & Technology*, *56*(2), 544-552. https://doi.org/10.1111/ijfs.14740

Chen, H., Zhou, P., Song, C., Jin, G., & Wei, L. (2022). An approach to manufacturing heat-stable and bloom-resistant chocolate by the combination of

oleogel and sweeteners. *Journal of Food Engineering*, *330*, 111064. https://doi.org/10.1016/j.jfoodeng.2022.111064

Chen, J., Ghazani, S. M., Stobbs, J. A., & Marangoni, A. G. (2021). Tempering of cocoa butter and chocolate using minor lipidic components. *Nature Communications*, *12*(1), 5018. https://doi.org/10.1038/s41467-021-25206-1

Chen, Y., Wang, W., Zhang, W., Tan, C.-P., Lan, D., & Wang, Y. (2022). Characteristics and feasibility of olive oil-based diacylglycerol plastic fat for use in compound chocolate. *Food Chemistry*, *391*, 133254. https://doi.org/10.1016/j.foodchem.2022.133254

Dahlenborg, H., Millqvist-Fureby, A., & Bergenståhl, B. (2015). Effect of shell microstructure on oil migration and fat bloom development in model pralines. *Food Structure*, *5*, 51-65. https://doi.org/10.1016/j.foostr.2015.06.002

Davis, T. R., & Dimick, P. S. (1989). Lipid composition of high-melting seed crystals formed during cocoa butter solidification. *Journal of the American Oil Chemists' Society*, *66*(10), 1494-1498. https://doi.org/10.1007/BF02661979

Declerck, A., Nelis, V., Danthine, S., Dewettinck, K., & Van der Meeren, P. (2021). Characterisation of Fat Crystal Polymorphism in Cocoa Butter by Time-Domain NMR and DSC Deconvolution. *Foods*, *10*(3), 520. https://doi.org/10.3390/foods10030520

Devos, N., Reyman, D., & Sanchez-Cortés, S. (2020). Chocolate composition and its crystallization process: A multidisciplinary analysis. *Food Chemistry*, 128301. https://doi.org/10.1016/j.foodchem.2020.128301

Ewens, H., Metilli, L., & Simone, E. (2021). Analysis of the effect of recent reformulation strategies on the crystallization behaviour of cocoa butter and the structural properties of chocolate. *Current Research in Food Science*, *4*, 105-114. https://doi.org/10.1016/j.crfs.2021.02.009

Fernandes, V. A., Müller, A. J., & Sandoval, A. J. (2013). Thermal, structural and rheological characteristics of dark chocolate with different compositions. *Journal*

of Food Engineering, *116*(1), 97-108. https://doi.org/10.1016/j.jfoodeng.2012.12.002

Hernández, M. del P. L., Núñez, J. C., Gómez, M. S. H., & Tovar, M. D. L. (2019). Physicochemical and microbiological dynamics of the fermentation of the ccn51 cocoa material in three maturity stages. *Revista Brasileira de Fruticultura*, *41*(3). https://doi.org/10.1590/0100-29452019010

ICCO. (2017). *Fine or Flavour Cocoa*. https://www.icco.org/about-cocoa/fine-or-flavour-cocoa.html

Jiménez-Sanchidrián, C., & Ruiz, J. R. (2016). Use of Raman spectroscopy for analyzing edible vegetable oils. *Applied Spectroscopy Reviews*, *51*(5), 417-430. https://doi.org/10.1080/05704928.2016.1141292

Jin, J., Jin, Q., Wang, X., & Akoh, C. C. (2019). Improving heat and fat bloom stabilities of "dark chocolates" by addition of mango kernel fat-based chocolate fats. *Journal of Food Engineering*, *246*, 33-41. https://doi.org/10.1016/j.jfoodeng.2018.10.027

Lechter, A. (2012). Effect of Minor Components on Cocoa Butter Polymorphism and Kinetics of Crystallization. En *Cocoa Butter and Related Compounds* (pp. 213-232). AOCS Press.

Liendo, R., Padilla, F. C., & Quintana, A. (1997). Characterization of cocoa butter extracted from Criollo cultivars of Theobroma cacao L. *Food Research International*, *30*(9), 727-731. https://doi.org/10.1016/S0963-9969(98)00025-8

Liu, W., Yao, Y., & Li, C. (2022). Effect of tempered procedures on the crystallization behavior of different positions of cocoa butter products. *Food Chemistry*, *370*, 131002. https://doi.org/10.1016/j.foodchem.2021.131002

Loisel, C., Lecq, G., Keller, G., & Ollivon, M. (1998). Dynamic Crystallization of Dark Chocolate as Affected by Temperature and Lipid Additives. *Journal of Food Science*, *63*(1), 73-79. https://doi.org/10.1111/j.1365-2621.1998.tb15679.x

Marty-Terrade, S., & Marangoni, A. G. (2012). Impact of cocoa butter origin on crystal behavior. En *Cocoa butter and related compounds* (pp. 245-274). AOCS Press.

Michel, S., Baraka, L. F., Ibañez, A. J., & Mansurova, M. (2021). Mass Spectrometry-Based Flavor Monitoring of Peruvian Chocolate Fabrication Process. *Metabolites, 11*(2), 71. https://doi.org/10.3390/metabo11020071

Norazlina, M. R., Jahurul, M. H. A., Hasmadi, M., Sharifudin, M. S., Patricia, M., Lee, J. S., Amir, H. M. S., Noorakmar, A. W., & Riman, I. (2020). Effects of fractionation technique on triacylglycerols, melting and crystallisation and the polymorphic behavior of bambangan kernel fat as cocoa butter improver. *LWT, 129*, 109558. https://doi.org/10.1016/j.lwt.2020.109558

OEC. (2022). *Chocolate y demás preparaciones alimenticias que contengan cacao | OEC*. OEC - The Observatory of Economic Complexity. https://oec.world/es/profile/hs/chocolate

Ostrowska-Ligęza, E., Dolatowska-Żebrowska, K., Wirkowska-Wojdyła, M., Bryś, J., & Górska, A. (2021). Comparison of Thermal Characteristics and Fatty Acids Composition in Raw and Roasted Cocoa Beans from Peru (Criollo) and Ecuador (Forastero). *Applied Sciences, 11*(6), 2698. https://doi.org/10.3390/app11062698

Pirouzian, H. R., Konar, N., Palabiyik, I., Oba, S., & Toker, O. S. (2020). Pre-crystallization process in chocolate: Mechanism, importance and novel aspects. *Food Chemistry, 321*, 126718. https://doi.org/10.1016/j.foodchem.2020.126718

Prosapio, V., & Norton, I. T. (2019). Development of fat-reduced chocolate by using water-in-cocoa butter emulsions. *Journal of Food Engineering, 261*, 165-170. https://doi.org/10.1016/j.jfoodeng.2019.06.018

Santander Muñoz, M., Rodríguez Cortina, J., Vaillant, F. E., & Escobar Parra, S. (2020). An overview of the physical and biochemical transformation of cocoa seeds to beans and to chocolate: Flavor formation. *Critical Reviews in Food Science and Nutrition, 60*(10), 1593-1613. https://doi.org/10.1080/10408398.2019.1581726

Santos, D. S., Rezende, R. P., Santos, T. F. dos, Marques, E. de L. S., Ferreira, A. C. R., Silva, A. B. de C. e, Romano, C. C., Santos, D. W. da C., Dias, J. C. T., & Tavares Bisneto, J. D. (2020). Fermentation in fine cocoa type Scavina: Change in standard quality as the effect of use of starters yeast in fermentation. *Food Chemistry*, *328*, 127110. https://doi.org/10.1016/j.foodchem.2020.127110

Sasaki, M., Ueno, S., & Sato, K. (2012). Polymorphism and mixing phase behavior of major triacylglycerols of cocoa butter. En *Cocoa butter and related compounds (Edited by Garti N and Widlak N. R.)* ((Edited by Garti N and Widlak N. R.), pp. 151-172). AOCS Press.

Servent, A., Boulanger, R., Davrieux, F., Pinot, M.-N., Tardan, E., Forestier-Chiron, N., & Hue, C. (2018). Assessment of cocoa (Theobroma cacao L.) butter content and composition throughout fermentations. *Food Research International*, *107*, 675-682. https://doi.org/10.1016/j.foodres.2018.02.070

Sirbu, D., Grimbs, A., Corno, M., Ullrich, M. S., & Kuhnert, N. (2018). Variation of triacylglycerol profiles in unfermented and dried fermented cocoa beans of different origins. *Food Research International*, *111*, 361-370. https://doi.org/10.1016/j.foodres.2018.05.025

Smith, K. W., Zand, I., & Talbot, G. (2008). Effect of Antibloom Fat Migration from a Nut Oil Filling on the Polymorphic Transformation of Cocoa Butter. *Journal of Agricultural and Food Chemistry*, *56*(5), 1602-1605. https://doi.org/10.1021/jf072151s

Sonwai, S., Podchong, P., & Rousseau, D. (2017). Crystallization kinetics of cocoa butter in the presence of sorbitan esters. *Food Chemistry, 214*, 497-506. https://doi.org/10.1016/j.foodchem.2016.07.092

Svanberg, L., Ahrné, L., Lorén, N., & Windhab, E. (2011). Effect of pre-crystallization process and solid particle addition on microstructure in chocolate model systems. *Food Research International*, *44*(5), 1339-1350. https://doi.org/10.1016/j.foodres.2011.01.018

Teixeira, G. L., Ghazani, S. M., Corazza, M. L., Marangoni, A. G., & Ribani, R. H. (2018). Assessment of subcritical propane, supercritical CO_2 and Soxhlet

extraction of oil from sapucaia (Lecythis pisonis) nuts. *The Journal of Supercritical Fluids*, *133*, 122-132. https://doi.org/10.1016/j.supflu.2017.10.003

TGSC. (2021). *TGSC Information System*. The Good Scents Company Information System Providing Information for the Flavor, Fragrance, Food and Cosmetic Industries. http://www.thegoodscentscompany.com/search2.html

Toro-Vázquez, J. F., Charó-Alonso, M. A., Morales-Rueda, J. A., & Pérez-Martínez, D. (2012). Molecular interactions of triacylglycerides in blends of cocoa butter with trans-free vegetable oils. En *Cocoa butter and related compounds* (pp. 393-416). AOCS Press.

Watanabe, S., Yoshikawa, S., & Sato, K. (2020). Formation and Properties of Dark Chocolate Prepared Using Fat Mixtures of Cocoa Butter and symmetric/asymmetric stearic-oleic mixed-acid triacylglycerols: Impact of Molecular Compound Crystals. *Food Chemistry*, 127808. https://doi.org/10.1016/j.foodchem.2020.127808

Yao, Y., Liu, W., Zhang, D., Li, R., Zhou, H., Li, C., & Wang, S. (2020). Dynamic changes in the triacylglycerol composition and crystallization behavior of cocoa butter. *LWT*, *129*, 109490. https://doi.org/10.1016/j.lwt.2020.109490

ANEXOS

Anexo 1. Datos correspondientes al Capítulo III

Tabla A1. Data original de cinética de cristalización isotérmica a 15 °C de la MC, obtenida por DSC.

Time (min)	Heat Flow (Normalized) (W/g)	Time (min)	Heat Flow (Normalized) (W/g)	Time (min)	Heat Flow (Normalized) (W/g)	Time (min)	Heat Flow (Normalized) (W/g)
35	0.197	57.52	0.084	80.05	0.035	102.57	0.03
35.18	0.159	57.7	0.084	80.23	0.035	102.75	0.03
35.36	0.11	57.88	0.083	80.4	0.035	102.93	0.03
35.54	0.097	58.06	0.082	80.59	0.035	103.11	0.03
35.72	0.091	58.24	0.081	80.76	0.035	103.29	0.03
35.9	0.087	58.42	0.081	80.95	0.035	103.47	0.03
36.08	0.084	58.6	0.08	81.13	0.035	103.65	0.03
36.26	0.081	58.79	0.079	81.31	0.035	103.83	0.03
36.44	0.079	58.96	0.078	81.49	0.035	104.01	0.03
36.62	0.076	59.14	0.078	81.67	0.034	104.19	0.03
36.8	0.074	59.33	0.077	81.85	0.034	104.37	0.03
36.98	0.072	59.51	0.076	82.03	0.034	104.55	0.03
37.16	0.071	59.69	0.076	82.21	0.034	104.73	0.03
37.34	0.069	59.86	0.075	82.39	0.034	104.91	0.03
37.52	0.068	60.04	0.074	82.57	0.034	105.09	0.03
37.7	0.066	60.23	0.074	82.75	0.034	105.27	0.03
37.88	0.065	60.41	0.073	82.93	0.034	105.45	0.03
38.06	0.064	60.59	0.072	83.11	0.034	105.63	0.03
38.24	0.064	60.77	0.072	83.29	0.034	105.81	0.03
38.43	0.063	60.95	0.071	83.47	0.034	105.99	0.03
38.61	0.062	61.13	0.07	83.65	0.034	106.17	0.03
38.79	0.061	61.31	0.07	83.83	0.034	106.35	0.03
38.96	0.061	61.49	0.069	84.01	0.034	106.53	0.03
39.14	0.06	61.67	0.069	84.19	0.034	106.71	0.03
39.33	0.06	61.85	0.068	84.37	0.033	106.89	0.03
39.51	0.06	62.03	0.067	84.55	0.033	107.07	0.03
39.69	0.059	62.21	0.067	84.73	0.033	107.25	0.03
39.86	0.059	62.39	0.066	84.91	0.033	107.43	0.03
40.04	0.059	62.57	0.065	85.09	0.033	107.61	0.03
40.23	0.058	62.75	0.065	85.27	0.033	107.79	0.03
40.41	0.058	62.93	0.064	85.45	0.033	107.97	0.03
40.59	0.058	63.11	0.064	85.63	0.033	108.15	0.03
40.77	0.058	63.29	0.063	85.81	0.033	108.33	0.03
40.95	0.058	63.47	0.063	85.99	0.033	108.51	0.03
41.13	0.057	63.65	0.062	86.17	0.033	108.69	0.03
41.31	0.057	63.83	0.062	86.35	0.033	108.87	0.03
41.49	0.057	64.01	0.061	86.53	0.033	109.05	0.03

41.67	0.057	64.19	0.061	86.71	0.033	109.23	0.03
41.85	0.057	64.37	0.06	86.89	0.033	109.41	0.03
42.03	0.057	64.55	0.06	87.07	0.033	109.59	0.03
42.21	0.057	64.73	0.059	87.25	0.033	109.78	0.03
42.39	0.057	64.91	0.059	87.43	0.032	109.95	0.03
42.57	0.057	65.09	0.058	87.61	0.032	110.14	0.03
42.75	0.057	65.27	0.058	87.79	0.032	110.31	0.03
42.93	0.057	65.45	0.057	87.97	0.032	110.5	0.03
43.11	0.057	65.63	0.057	88.15	0.032	110.68	0.03
43.29	0.057	65.81	0.056	88.33	0.032	110.85	0.03
43.47	0.057	65.99	0.056	88.51	0.032	111.04	0.03
43.65	0.058	66.17	0.055	88.69	0.032	111.21	0.03
43.83	0.058	66.35	0.055	88.87	0.032	111.4	0.03
44.01	0.058	66.53	0.054	89.05	0.032	111.58	0.03
44.19	0.058	66.71	0.054	89.23	0.032	111.76	0.03
44.37	0.058	66.89	0.054	89.41	0.032	111.94	0.03
44.55	0.059	67.07	0.053	89.6	0.032	112.12	0.03
44.73	0.059	67.25	0.053	89.78	0.032	112.3	0.03
44.91	0.059	67.43	0.052	89.95	0.032	112.48	0.03
45.09	0.06	67.61	0.052	90.14	0.032	112.66	0.03
45.27	0.06	67.79	0.051	90.31	0.032	112.84	0.03
45.45	0.06	67.97	0.051	90.5	0.032	113.02	0.03
45.63	0.061	68.15	0.051	90.68	0.032	113.2	0.03
45.81	0.061	68.33	0.05	90.85	0.032	113.38	0.03
45.99	0.061	68.51	0.05	91.04	0.032	113.56	0.03
46.17	0.061	68.69	0.049	91.22	0.032	113.74	0.03
46.35	0.062	68.87	0.049	91.4	0.032	113.92	0.03
46.53	0.062	69.05	0.048	91.58	0.032	114.1	0.03
46.71	0.062	69.24	0.048	91.76	0.032	114.28	0.03
46.89	0.063	69.41	0.048	91.94	0.032	114.46	0.03
47.07	0.063	69.6	0.047	92.12	0.032	114.64	0.03
47.25	0.063	69.78	0.047	92.3	0.032	114.82	0.029
47.43	0.064	69.95	0.047	92.48	0.031	115	0.029
47.61	0.064	70.14	0.046	92.66	0.032	115.18	0.029
47.79	0.064	70.31	0.046	92.84	0.032	115.36	0.029
47.97	0.065	70.5	0.045	93.02	0.032	115.54	0.029
48.15	0.065	70.68	0.045	93.2	0.031	115.72	0.029
48.33	0.065	70.86	0.045	93.38	0.031	115.9	0.03
48.51	0.065	71.04	0.044	93.56	0.031	116.08	0.03
48.69	0.066	71.22	0.044	93.74	0.031	116.26	0.03
48.88	0.066	71.4	0.044	93.92	0.031	116.44	0.03
49.06	0.066	71.58	0.044	94.1	0.031	116.62	0.03
49.24	0.067	71.76	0.043	94.28	0.031	116.8	0.03
49.41	0.067	71.94	0.043	94.46	0.031	116.98	0.03
49.59	0.067	72.12	0.043	94.64	0.031	117.16	0.03
49.78	0.068	72.3	0.042	94.82	0.031	117.34	0.03

49.96	0.068	72.48	0.042	95	0.031	117.52	0.03
50.14	0.068	72.66	0.042	95.18	0.031	117.7	0.029
50.32	0.069	72.84	0.042	95.36	0.031	117.88	0.03
50.5	0.069	73.02	0.041	95.54	0.031	118.06	0.03
50.68	0.07	73.2	0.041	95.72	0.031	118.24	0.03
50.86	0.071	73.38	0.041	95.9	0.031	118.42	0.029
51.04	0.071	73.56	0.041	96.08	0.031	118.6	0.029
51.22	0.072	73.74	0.04	96.26	0.031	118.78	0.029
51.4	0.073	73.92	0.04	96.44	0.031	118.96	0.03
51.58	0.073	74.1	0.04	96.62	0.031	119.14	0.03
51.76	0.074	74.28	0.04	96.8	0.031	119.32	0.029
51.94	0.075	74.46	0.039	96.98	0.031	119.5	0.03
52.12	0.076	74.64	0.039	97.16	0.031	119.68	0.029
52.3	0.076	74.82	0.039	97.34	0.031	119.86	0.029
52.48	0.078	75	0.039	97.52	0.031	120.05	0.029
52.66	0.079	75.18	0.039	97.7	0.031	120.23	0.029
52.84	0.079	75.36	0.039	97.88	0.031	120.4	0.029
53.02	0.08	75.54	0.038	98.06	0.031	120.59	0.03
53.2	0.081	75.72	0.038	98.24	0.031	120.76	0.029
53.38	0.082	75.9	0.038	98.42	0.031	120.95	0.029
53.56	0.083	76.08	0.038	98.6	0.031	121.13	0.029
53.74	0.083	76.26	0.038	98.78	0.031	121.3	0.029
53.92	0.084	76.44	0.038	98.96	0.031	121.49	0.029
54.1	0.085	76.62	0.037	99.14	0.031	121.67	0.029
54.28	0.086	76.8	0.037	99.32	0.031	121.85	0.03
54.46	0.086	76.98	0.037	99.5	0.031	122.03	0.03
54.64	0.086	77.16	0.037	99.69	0.031	122.21	0.03
54.82	0.087	77.34	0.037	99.86	0.031	122.39	0.03
55	0.087	77.52	0.037	100.05	0.03	122.57	0.03
55.18	0.088	77.7	0.037	100.23	0.03	122.75	0.029
55.36	0.088	77.88	0.036	100.4	0.03	122.93	0.029
55.54	0.088	78.06	0.036	100.59	0.031	123.11	0.029
55.72	0.088	78.24	0.036	100.76	0.031	123.29	0.029
55.9	0.088	78.42	0.036	100.95	0.031	123.47	0.029
56.08	0.087	78.6	0.036	101.13	0.031	123.65	0.029
56.26	0.087	78.78	0.036	101.31	0.03	123.83	0.029
56.44	0.087	78.96	0.036	101.49	0.03	124.01	0.029
56.62	0.087	79.14	0.036	101.67	0.03	124.19	0.029
56.8	0.086	79.33	0.036	101.85	0.03	124.37	0.029
56.98	0.086	79.5	0.036	102.03	0.03	124.55	0.029
57.16	0.085	79.69	0.035	102.21	0.03	124.73	0.029
57.34	0.085	79.86	0.035	102.39	0.03	124.91	0.029

Tabla A2. Data original de cinética de cristalización isotérmica a 15 °C de POP, obtenida por DSC.

Time (min)	Heat Flow (Normalized) (W/g)	Time (min)	Heat Flow (Normalized) (W/g)	Time (min)	Heat Flow (Normalized) (W/g)	Time (min)	Heat Flow (Normalized) (W/g)
35	0.089	57.54	0.058	80.09	0.035	102.64	0.01
35.18	0.069	57.73	0.059	80.27	0.034	102.81	0.01
35.36	0.02	57.91	0.06	80.45	0.034	103	0.01
35.54	0.015	58.09	0.061	80.63	0.033	103.18	0.01
35.72	0.012	58.27	0.061	80.81	0.033	103.36	0.009
35.9	0.01	58.45	0.062	80.99	0.033	103.54	0.01
36.08	0.01	58.63	0.063	81.17	0.032	103.72	0.01
36.26	0.009	58.81	0.064	81.35	0.032	103.9	0.01
36.44	0.009	58.99	0.064	81.53	0.031	104.08	0.009
36.62	0.008	59.17	0.065	81.71	0.031	104.26	0.009
36.81	0.008	59.35	0.066	81.89	0.03	104.44	0.009
36.99	0.008	59.53	0.066	82.07	0.03	104.62	0.009
37.16	0.008	59.71	0.067	82.25	0.029	104.8	0.009
37.34	0.008	59.89	0.068	82.44	0.029	104.98	0.009
37.53	0.008	60.07	0.068	82.61	0.029	105.16	0.009
37.71	0.008	60.25	0.069	82.8	0.028	105.34	0.009
37.89	0.008	60.43	0.069	82.98	0.028	105.52	0.009
38.07	0.008	60.61	0.07	83.16	0.027	105.7	0.009
38.25	0.008	60.79	0.07	83.34	0.027	105.88	0.009
38.43	0.008	60.97	0.071	83.52	0.026	106.06	0.009
38.61	0.008	61.15	0.071	83.7	0.026	106.24	0.009
38.79	0.008	61.33	0.072	83.88	0.026	106.42	0.009
38.97	0.008	61.51	0.072	84.06	0.025	106.6	0.009
39.15	0.008	61.69	0.073	84.24	0.025	106.78	0.009
39.33	0.008	61.87	0.073	84.42	0.025	106.96	0.009
39.51	0.008	62.06	0.073	84.6	0.024	107.14	0.009
39.69	0.008	62.24	0.074	84.78	0.024	107.32	0.009
39.87	0.008	62.41	0.074	84.96	0.024	107.5	0.009
40.05	0.008	62.59	0.074	85.14	0.023	107.69	0.009
40.23	0.008	62.78	0.074	85.32	0.023	107.86	0.009
40.41	0.008	62.96	0.075	85.5	0.023	108.05	0.009
40.59	0.008	63.14	0.075	85.68	0.022	108.23	0.009
40.77	0.009	63.32	0.075	85.86	0.022	108.41	0.009
40.95	0.009	63.5	0.075	86.04	0.022	108.59	0.009
41.13	0.008	63.68	0.075	86.22	0.021	108.77	0.009
41.31	0.008	63.86	0.075	86.4	0.021	108.95	0.009
41.49	0.009	64.04	0.075	86.58	0.021	109.13	0.009
41.67	0.009	64.22	0.075	86.76	0.021	109.31	0.009
41.86	0.009	64.4	0.075	86.94	0.02	109.49	0.009
42.04	0.009	64.58	0.075	87.12	0.02	109.67	0.009
42.21	0.009	64.76	0.075	87.3	0.02	109.85	0.009

42.39	0.009	64.94	0.075	87.49	0.019	110.03	0.009
42.58	0.009	65.12	0.075	87.66	0.019	110.21	0.009
42.76	0.009	65.3	0.075	87.85	0.019	110.39	0.009
42.94	0.009	65.48	0.075	88.03	0.019	110.57	0.009
43.12	0.009	65.66	0.075	88.21	0.018	110.75	0.009
43.3	0.009	65.84	0.075	88.39	0.018	110.93	0.009
43.48	0.009	66.02	0.075	88.57	0.018	111.11	0.009
43.66	0.009	66.2	0.075	88.75	0.018	111.29	0.009
43.84	0.009	66.38	0.074	88.93	0.018	111.47	0.009
44.02	0.01	66.56	0.074	89.11	0.017	111.65	0.009
44.2	0.01	66.74	0.074	89.29	0.017	111.83	0.009
44.38	0.01	66.92	0.074	89.47	0.017	112.01	0.009
44.56	0.01	67.11	0.073	89.65	0.017	112.19	0.009
44.74	0.01	67.29	0.073	89.83	0.016	112.37	0.009
44.92	0.01	67.46	0.073	90.01	0.016	112.55	0.009
45.1	0.01	67.64	0.073	90.19	0.016	112.74	0.009
45.28	0.011	67.83	0.072	90.37	0.016	112.91	0.009
45.46	0.011	68.01	0.072	90.55	0.016	113.1	0.009
45.64	0.011	68.19	0.071	90.73	0.016	113.28	0.009
45.82	0.011	68.37	0.071	90.91	0.016	113.46	0.009
46	0.011	68.55	0.071	91.09	0.015	113.64	0.009
46.18	0.012	68.73	0.07	91.27	0.015	113.82	0.009
46.36	0.012	68.91	0.07	91.45	0.015	114	0.009
46.54	0.012	69.09	0.069	91.63	0.015	114.18	0.009
46.72	0.012	69.27	0.069	91.81	0.015	114.36	0.009
46.91	0.013	69.45	0.069	91.99	0.015	114.54	0.009
47.09	0.013	69.63	0.068	92.17	0.014	114.72	0.009
47.26	0.013	69.81	0.068	92.35	0.014	114.9	0.009
47.44	0.014	69.99	0.067	92.54	0.014	115.08	0.009
47.63	0.014	70.17	0.067	92.71	0.014	115.26	0.009
47.81	0.015	70.35	0.066	92.9	0.014	115.44	0.009
47.99	0.015	70.53	0.066	93.08	0.014	115.62	0.009
48.17	0.015	70.71	0.065	93.26	0.013	115.8	0.009
48.35	0.016	70.89	0.065	93.44	0.013	115.98	0.009
48.53	0.016	71.07	0.064	93.62	0.013	116.16	0.009
48.71	0.017	71.25	0.064	93.8	0.013	116.34	0.009
48.89	0.017	71.43	0.063	93.98	0.013	116.52	0.009
49.07	0.018	71.61	0.062	94.16	0.013	116.7	0.009
49.25	0.019	71.79	0.062	94.34	0.013	116.88	0.008
49.43	0.019	71.97	0.061	94.52	0.013	117.06	0.009
49.61	0.02	72.15	0.061	94.7	0.013	117.24	0.009
49.79	0.021	72.34	0.06	94.88	0.012	117.42	0.009
49.97	0.021	72.51	0.06	95.06	0.012	117.6	0.009
50.15	0.022	72.7	0.059	95.24	0.012	117.79	0.009
50.33	0.022	72.88	0.059	95.42	0.012	117.96	0.009
50.51	0.023	73.06	0.058	95.6	0.012	118.15	0.009

50.69	0.024	73.24	0.057	95.78	0.012	118.33	0.009
50.87	0.025	73.42	0.057	95.96	0.012	118.51	0.009
51.05	0.026	73.6	0.056	96.14	0.012	118.69	0.009
51.23	0.026	73.78	0.056	96.32	0.012	118.87	0.009
51.41	0.027	73.96	0.055	96.5	0.012	119.05	0.008
51.59	0.028	74.14	0.054	96.68	0.011	119.23	0.009
51.77	0.029	74.32	0.054	96.86	0.011	119.41	0.009
51.96	0.03	74.5	0.053	97.04	0.011	119.59	0.009
52.14	0.031	74.68	0.052	97.22	0.011	119.77	0.008
52.31	0.031	74.86	0.052	97.4	0.011	119.95	0.008
52.49	0.032	75.04	0.051	97.59	0.011	120.13	0.008
52.68	0.033	75.22	0.051	97.76	0.011	120.31	0.008
52.86	0.034	75.4	0.05	97.95	0.011	120.49	0.008
53.04	0.035	75.58	0.05	98.13	0.011	120.67	0.008
53.22	0.036	75.76	0.049	98.31	0.011	120.85	0.008
53.4	0.037	75.94	0.048	98.49	0.011	121.03	0.008
53.58	0.038	76.12	0.048	98.67	0.011	121.21	0.008
53.76	0.039	76.3	0.047	98.85	0.011	121.39	0.008
53.94	0.04	76.48	0.046	99.03	0.011	121.57	0.009
54.12	0.041	76.66	0.046	99.21	0.01	121.75	0.008
54.3	0.042	76.84	0.045	99.39	0.01	121.93	0.008
54.48	0.043	77.02	0.045	99.57	0.01	122.11	0.009
54.66	0.044	77.2	0.044	99.75	0.01	122.29	0.008
54.84	0.045	77.39	0.043	99.93	0.01	122.47	0.009
55.02	0.045	77.56	0.043	100.11	0.01	122.65	0.008
55.2	0.046	77.75	0.042	100.29	0.01	122.84	0.009
55.38	0.047	77.93	0.042	100.47	0.01	123.01	0.009
55.56	0.048	78.11	0.041	100.65	0.01	123.2	0.009
55.74	0.049	78.29	0.04	100.83	0.01	123.38	0.009
55.92	0.05	78.47	0.04	101.01	0.01	123.56	0.008
56.1	0.051	78.65	0.039	101.19	0.01	123.74	0.008
56.28	0.052	78.83	0.039	101.37	0.01	123.92	0.008
56.46	0.053	79.01	0.038	101.55	0.01	124.1	0.008
56.64	0.054	79.19	0.038	101.73	0.01	124.28	0.008
56.82	0.055	79.37	0.037	101.91	0.01	124.46	0.008
57.01	0.055	79.55	0.037	102.09	0.01	124.64	0.008
57.19	0.056	79.73	0.036	102.27	0.01	124.82	0.008
57.36	0.057	79.91	0.036	102.45	0.01	125	0.008

Tabla A3. Data original de cinética de cristalización isotérmica de MC en el interior del grano de cacao Criollo a los siete días de fermentación.

Temperatura de cristalización = 15 °C

Time (min)	Heat Flow (Normalized) (W/g)	Time (min)	Heat Flow (Normalized) (W/g)	Time (min)	Heat Flow (Normalized) (W/g)	Time (min)	Heat Flow (Normalized) (W/g)
35	0.145	57.55	0.02	80.09	0.009	102.64	0.008
35.18	0.084	57.73	0.02	80.27	0.009	102.82	0.008
35.36	0.033	57.91	0.02	80.45	0.009	103	0.008
35.54	0.024	58.09	0.02	80.63	0.009	103.18	0.008
35.72	0.021	58.27	0.02	80.81	0.009	103.36	0.008
35.91	0.019	58.45	0.019	80.99	0.009	103.54	0.008
36.09	0.018	58.63	0.019	81.17	0.009	103.72	0.008
36.26	0.017	58.81	0.019	81.35	0.009	103.9	0.008
36.44	0.016	58.99	0.019	81.54	0.009	104.08	0.008
36.63	0.016	59.17	0.019	81.71	0.009	104.26	0.008
36.81	0.016	59.35	0.019	81.9	0.009	104.44	0.008
36.99	0.016	59.53	0.019	82.08	0.009	104.62	0.008
37.17	0.015	59.71	0.019	82.26	0.009	104.8	0.008
37.35	0.015	59.89	0.018	82.44	0.009	104.98	0.008
37.53	0.015	60.07	0.018	82.62	0.009	105.16	0.008
37.71	0.015	60.25	0.018	82.8	0.009	105.34	0.008
37.89	0.015	60.43	0.018	82.98	0.009	105.52	0.008
38.07	0.015	60.61	0.018	83.16	0.009	105.7	0.008
38.25	0.014	60.79	0.018	83.34	0.009	105.88	0.008
38.43	0.014	60.97	0.017	83.52	0.009	106.06	0.008
38.61	0.014	61.16	0.017	83.7	0.009	106.24	0.008
38.79	0.014	61.34	0.017	83.88	0.009	106.42	0.008
38.97	0.014	61.51	0.017	84.06	0.009	106.6	0.008
39.15	0.014	61.69	0.017	84.24	0.009	106.79	0.008
39.33	0.013	61.88	0.017	84.42	0.009	106.96	0.008
39.51	0.013	62.06	0.017	84.6	0.009	107.15	0.008
39.69	0.013	62.24	0.016	84.78	0.009	107.33	0.008
39.87	0.013	62.42	0.016	84.96	0.009	107.51	0.008
40.05	0.013	62.6	0.016	85.14	0.009	107.69	0.008
40.23	0.013	62.78	0.016	85.32	0.009	107.87	0.008
40.41	0.013	62.96	0.016	85.5	0.009	108.05	0.008
40.59	0.013	63.14	0.016	85.68	0.009	108.23	0.008
40.77	0.013	63.32	0.016	85.86	0.009	108.41	0.008
40.96	0.013	63.5	0.016	86.04	0.009	108.59	0.008
41.14	0.013	63.68	0.015	86.22	0.009	108.77	0.008
41.31	0.013	63.86	0.015	86.4	0.009	108.95	0.008
41.49	0.012	64.04	0.015	86.59	0.009	109.13	0.008
41.68	0.012	64.22	0.015	86.76	0.009	109.31	0.008
41.86	0.012	64.4	0.015	86.95	0.009	109.49	0.008

42.04	0.012	64.58	0.015	87.13	0.009	109.67	0.008
42.22	0.012	64.76	0.015	87.31	0.009	109.85	0.008
42.4	0.012	64.94	0.015	87.49	0.009	110.03	0.008
42.58	0.012	65.12	0.015	87.67	0.008	110.21	0.008
42.76	0.012	65.3	0.015	87.85	0.008	110.39	0.008
42.94	0.012	65.48	0.014	88.03	0.008	110.57	0.008
43.12	0.012	65.66	0.014	88.21	0.008	110.75	0.008
43.3	0.012	65.84	0.014	88.39	0.008	110.93	0.008
43.48	0.012	66.02	0.014	88.57	0.008	111.11	0.008
43.66	0.012	66.21	0.014	88.75	0.009	111.29	0.008
43.84	0.012	66.39	0.014	88.93	0.008	111.47	0.008
44.02	0.012	66.56	0.014	89.11	0.008	111.65	0.008
44.2	0.012	66.74	0.014	89.29	0.009	111.84	0.008
44.38	0.012	66.93	0.014	89.47	0.008	112.01	0.008
44.56	0.012	67.11	0.013	89.65	0.008	112.2	0.008
44.74	0.012	67.29	0.013	89.83	0.008	112.38	0.008
44.92	0.012	67.47	0.013	90.01	0.008	112.56	0.008
45.1	0.012	67.65	0.013	90.19	0.008	112.74	0.008
45.28	0.013	67.83	0.013	90.37	0.008	112.92	0.008
45.46	0.013	68.01	0.013	90.55	0.009	113.1	0.008
45.64	0.013	68.19	0.013	90.73	0.008	113.28	0.008
45.82	0.013	68.37	0.013	90.91	0.008	113.46	0.008
46.01	0.013	68.55	0.013	91.09	0.008	113.64	0.008
46.19	0.013	68.73	0.013	91.27	0.008	113.82	0.008
46.36	0.013	68.91	0.013	91.45	0.008	114	0.008
46.54	0.013	69.09	0.012	91.64	0.008	114.18	0.008
46.73	0.013	69.27	0.012	91.81	0.008	114.36	0.008
46.91	0.013	69.45	0.012	92	0.008	114.54	0.008
47.09	0.013	69.63	0.012	92.18	0.008	114.72	0.008
47.27	0.013	69.81	0.012	92.36	0.008	114.9	0.008
47.45	0.013	69.99	0.012	92.54	0.008	115.08	0.008
47.63	0.014	70.17	0.012	92.72	0.008	115.26	0.008
47.81	0.014	70.35	0.012	92.9	0.008	115.44	0.008
47.99	0.014	70.53	0.012	93.08	0.008	115.62	0.008
48.17	0.014	70.71	0.012	93.26	0.008	115.8	0.008
48.35	0.014	70.89	0.012	93.44	0.008	115.98	0.008
48.53	0.014	71.07	0.012	93.62	0.008	116.16	0.008
48.71	0.014	71.25	0.012	93.8	0.008	116.34	0.008
48.89	0.015	71.44	0.012	93.98	0.008	116.52	0.008
49.07	0.015	71.61	0.012	94.16	0.008	116.7	0.008
49.25	0.015	71.8	0.012	94.34	0.008	116.89	0.008
49.43	0.015	71.98	0.011	94.52	0.008	117.06	0.008
49.61	0.015	72.16	0.011	94.7	0.008	117.25	0.008
49.79	0.015	72.34	0.011	94.88	0.008	117.43	0.008
49.97	0.016	72.52	0.011	95.06	0.008	117.61	0.008
50.15	0.016	72.7	0.011	95.24	0.008	117.79	0.008

50.33	0.016	72.88	0.011	95.42	0.008	117.97	0.008
50.51	0.016	73.06	0.011	95.6	0.008	118.15	0.008
50.69	0.017	73.24	0.011	95.78	0.008	118.33	0.008
50.87	0.017	73.42	0.011	95.96	0.008	118.51	0.008
51.06	0.017	73.6	0.011	96.14	0.008	118.69	0.008
51.24	0.017	73.78	0.011	96.32	0.008	118.87	0.008
51.41	0.017	73.96	0.011	96.5	0.008	119.05	0.008
51.59	0.018	74.14	0.011	96.69	0.008	119.23	0.008
51.78	0.018	74.32	0.011	96.86	0.008	119.41	0.008
51.96	0.018	74.5	0.011	97.05	0.008	119.59	0.008
52.14	0.018	74.68	0.011	97.23	0.008	119.77	0.008
52.32	0.019	74.86	0.011	97.41	0.008	119.95	0.008
52.5	0.019	75.04	0.01	97.59	0.008	120.13	0.008
52.68	0.019	75.22	0.01	97.77	0.008	120.31	0.008
52.86	0.019	75.4	0.01	97.95	0.008	120.49	0.008
53.04	0.019	75.58	0.01	98.13	0.008	120.67	0.008
53.22	0.02	75.76	0.01	98.31	0.008	120.85	0.008
53.4	0.02	75.94	0.01	98.49	0.008	121.03	0.008
53.58	0.02	76.12	0.01	98.67	0.008	121.21	0.008
53.76	0.02	76.3	0.01	98.85	0.008	121.39	0.008
53.94	0.02	76.49	0.01	99.03	0.008	121.57	0.008
54.12	0.02	76.66	0.01	99.21	0.008	121.75	0.008
54.3	0.02	76.85	0.01	99.39	0.008	121.94	0.008
54.48	0.021	77.03	0.01	99.57	0.008	122.11	0.008
54.66	0.021	77.21	0.01	99.75	0.008	122.3	0.008
54.84	0.021	77.39	0.01	99.93	0.008	122.48	0.009
55.02	0.021	77.57	0.01	100.11	0.008	122.66	0.009
55.2	0.021	77.75	0.01	100.29	0.008	122.84	0.008
55.38	0.021	77.93	0.01	100.47	0.008	123.02	0.008
55.56	0.021	78.11	0.01	100.65	0.008	123.2	0.008
55.74	0.021	78.29	0.01	100.83	0.008	123.38	0.008
55.92	0.021	78.47	0.01	101.01	0.008	123.56	0.008
56.11	0.021	78.65	0.01	101.19	0.008	123.74	0.008
56.29	0.021	78.83	0.01	101.37	0.008	123.92	0.008
56.46	0.021	79.01	0.01	101.55	0.008	124.1	0.008
56.64	0.021	79.19	0.01	101.74	0.008	124.28	0.008
56.83	0.021	79.37	0.01	101.91	0.008	124.46	0.008
57.01	0.021	79.55	0.01	102.1	0.008	124.64	0.008
57.19	0.02	79.73	0.01	102.28	0.008	124.82	0.009
57.37	0.02	79.91	0.009	102.46	0.008	125	0.008

Tabla A4. Parámetros cinéticos y térmicos de la manteca de cacao en el interior del grano durante fermentación espontánea.

Sample	Avrami_index	Rate_constant	t_theo	t_exp	Melt_Enthalpy	Melting_Peak
Unf_15	2.13	1.11E-02	6.99	6.55	23.42	26.19
Day0_15	2.09	8.68E-03	8.09	8.31	33.81	26.32
Day1_15	2.66	1.04E-03	11.55	12.33	17.53	24.72
Day2_15	2.58	1.53E-03	10.73	11.26	34.89	25.73
Day3_15	1.76	2.44E-02	6.69	7.1	33.33	24.84
Day4_15	2.51	1.75E-03	10.81	10.52	32.55	25.42
Day5_15	2.76	8.06E-04	11.57	11.9	32.94	26.14
Day6_15	2.04	3.02E-03	14.34	12.7	36.58	26.96
Day7_15	2.34	3.32E-03	9.83	9.75	22.88	24.44
Unf_16	1.51	2.56E-02	8.93	7.77	18.75	26.41
Day0_16	1.78	1.59E-02	8.31	8.05	17.69	26.48
Day1_16	2.13	2.38E-03	14.54	14.98	14.92	24.9
Day2_16	2.49	1.65E-03	11.25	11.36	33.92	25.79
Day3_16	2	1.42E-02	6.96	6.93	27.16	25.42
Day4_16	2.67	1.10E-03	11.14	10.8	30.88	25.69
Day5_16	2.27	1.09E-03	17.24	16.43	32.27	26.42
Day6_16	1.67	7.13E-03	15.43	14.27	31.99	27.1
Day7_16	2.8	6.37E-04	11.14	12.6	21.21	24.64
Unf_17	1.92	6.82E-03	11.14	10.58	16.19	26.69
Day0_17	2.08	7.22E-03	8.97	9.17	12.38	26.56
Day1_17	1.82	3.10E-03	15.64	12.35	11.61	25.28
Day2_17	2.54	9.54E-04	13.41	13.3	33.19	25.97
Day3_17	2.43	2.93E-03	9.51	9.93	22.61	25.82
Day4_17	2.94	5.68E-04	11.2	11.43	28.87	26.03
Day5_17	2.47	1.77E-03	11.24	11.9	31.42	26.54
Day6_17	2.45	9.05E-04	15.07	15.19	30.35	25.78
Day7_17	2.35	1.49E-03	13.61	13.87	18.95	24.97
Unf_18	2.1	3.61E-03	12.23	11.73	14.17	27.15
Day0_18	1.79	6.78E-03	13.21	13.48	9.16	26.79
Day1_18	1.73	8.77E-03	12.56	13.28	7.53	25.77
Day2_18	2.94	2.51E-04	14.84	15.78	28.42	26.26
Day3_18	2.55	1.98E-03	9.91	10.14	18.28	26.1
Day4_18	2.82	6.48E-04	11.89	12.33	26.78	26.38
Day5_18	2.55	8.59E-04	13.74	14.24	30.53	26.79
Day6_18	2.59	5.78E-04	15.4	15.43	29.6	26.2
Day7_18	1.98	3.45E-03	14.63	13.94	16.14	25.3
Unf_19	2.17	3.01E-03	12.29	12.28	11.21	27.63
Day0_19	1.6	8.14E-03	16.01	14.08	6.25	27.06
Day1_19	1.2	9.38E-03	12.02	12.24	4.01	26.42
Day2_18	2.66	4.20E-04	16.12	17.18	23.94	26.55
Day3_19	2.09	2.75E-03	14.09	15.68	13.86	26.48

Day4_19	2.94	1.72E-04	16.9	17.88	23.45	26.83
Day5_19	2.29	1.66E-03	13.89	14.55	26.83	27.22
Day6_19	2.57	4.73E-04	17.12	17.85	27.27	26.62
Day7_19	2.68	3.88E-04	16.3	16.96	12.12	25.98

Tabla A5. Códigos de RMarkdown para la identificación de clusters mediante la técnica k-means

```r setup, include=FALSE
knitr::opts_chunk$set(echo = TRUE)
options(repos = list(CRAN="http://cran.rstudio.com/"))
```

```r
library(tidyverse)
library(cluster)
library(factoextra)
install.packages("NbClust")
library(NbClust)
```

```r
data<-read.table("Cluster.txt",header = TRUE)
data
```

```r
rownames(data) <- data$Sample
data
```

```r
attach(data)
data1<-select(data,-Sample)
data1
```

```r
df_kinetic<-data1
df_kinetic
```

```r
df_kinetic<-scale(df_kinetic)
head(df_kinetic)
```

```r
m.distancia_kinetic<-get_dist(df_kinetic,method = "euclidean")
fviz_dist(m.distancia_kinetic,gradient =
list(low="blue",mid="white",high="red"))
```

```r
fviz_nbclust(df_kinetic,kmeans,method = "wss")
```

```r
fviz_nbclust(df_kinetic,kmeans,method = "silhouette")
```

```r
fviz_nbclust(df_kinetic,kmeans,method = "gap_stat")
```

````{r}
resnumclust_kinetic<-NbClust(df_kinetic,distance = "euclidean",min.nc =
2,max.nc = 10,method = "kmeans",index = "alllong")
fviz_nbclust(resnumclust_kinetic)
````

````{r}
k2<-kmeans(df_kinetic,centers = 2,nstart = 25)
k2
str(k2)
````

````{r}
fviz_cluster(k2,data = df_kinetic)
````

````{r}
fviz_cluster(k2,data = df_kinetic,ellipse.type = "euclid",repel =
TRUE,star.plot=TRUE)
````

````{r}
fviz_cluster(k2,data = df_kinetic,ellipse.type = "norm")
````

````{r}
res2<-hcut(df_kinetic,k=2,stand = TRUE)
fviz_dend(res2,rect = TRUE,cex = 0.5,k_colors = c("red","#2E9FDF"))
````

````{r}
res4<-hcut(df_kinetic,k=4,stand = TRUE)
fviz_dend(res4,rect = TRUE,cex = 0.5,k_colors =
c("red","#2E9FDF","green","black"))
````

````{r}
data1 %>%
 mutate(Cluster=k2$cluster) %>%
 group_by(Cluster) %>%
 summarise_all("mean")
````

````{r}
data1<-scale(df_kinetic)
df_kinetic<-as.data.frame(df_kinetic)
df_kinetic$clus<-as.factor(k2$cluster)
df_kinetic
````

````{r}
df_kinetic$clus<-factor(df_kinetic$clus)
````

````{r}
data_long<-
gather(df_kinetic,cinetica,valor,Avrami_index:Melting_Peak,factor_key = TRUE)
data_long
````

```{r}
ggplot(data_long,aes(as.factor(x=cinetica),y=valor,group=clus,colour=clus))+s
tat_summary(fun=mean,geom="pointrange",size=1)+stat_summary(geom =
"line")+geom_point(aes(shape=clus))
```

Anexo 2. Datos correspondientes al Capítulo IV
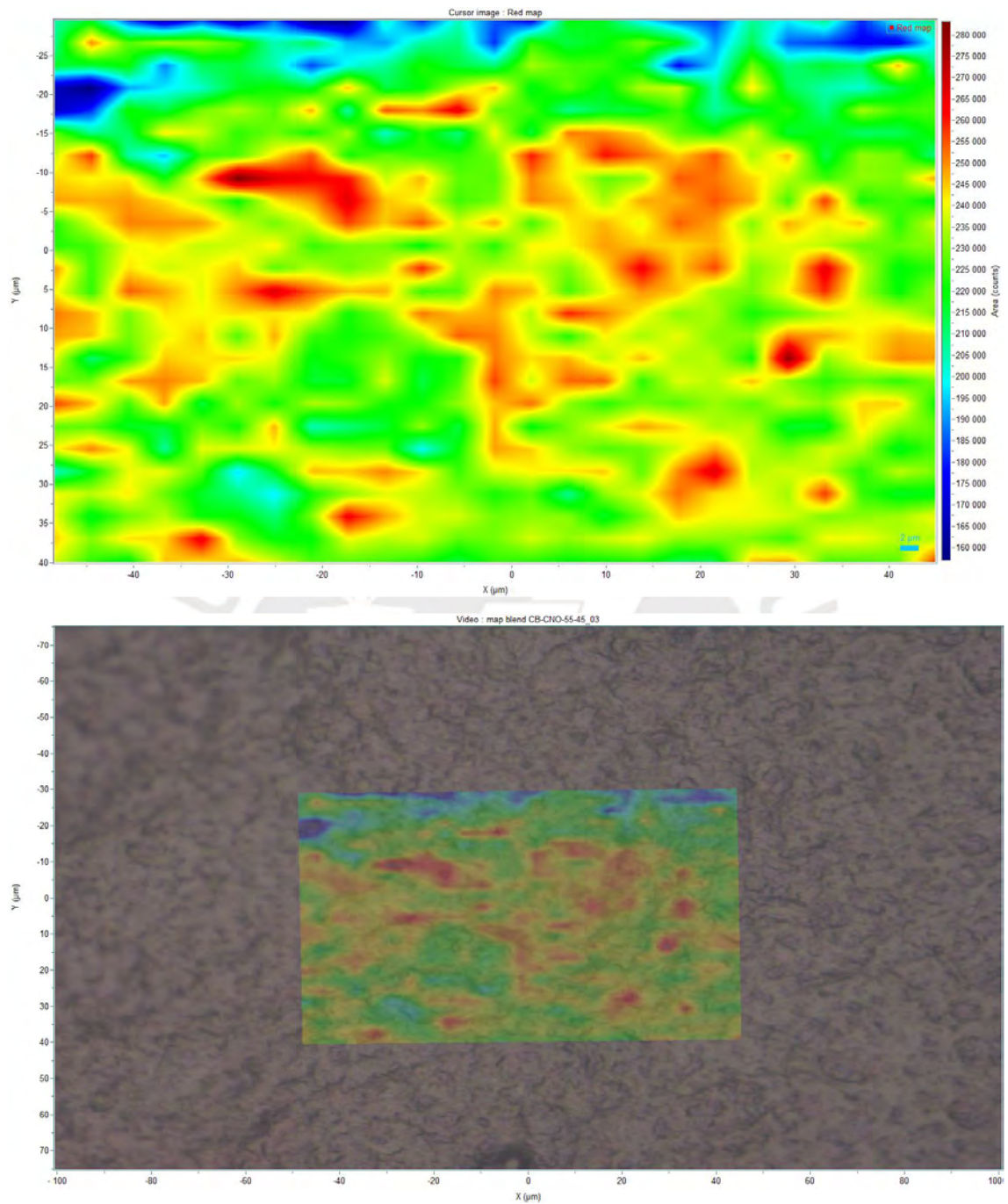
Figura A1. Imágenes químicas de las mezclas CB55-CNO45 obtenidas por MCR
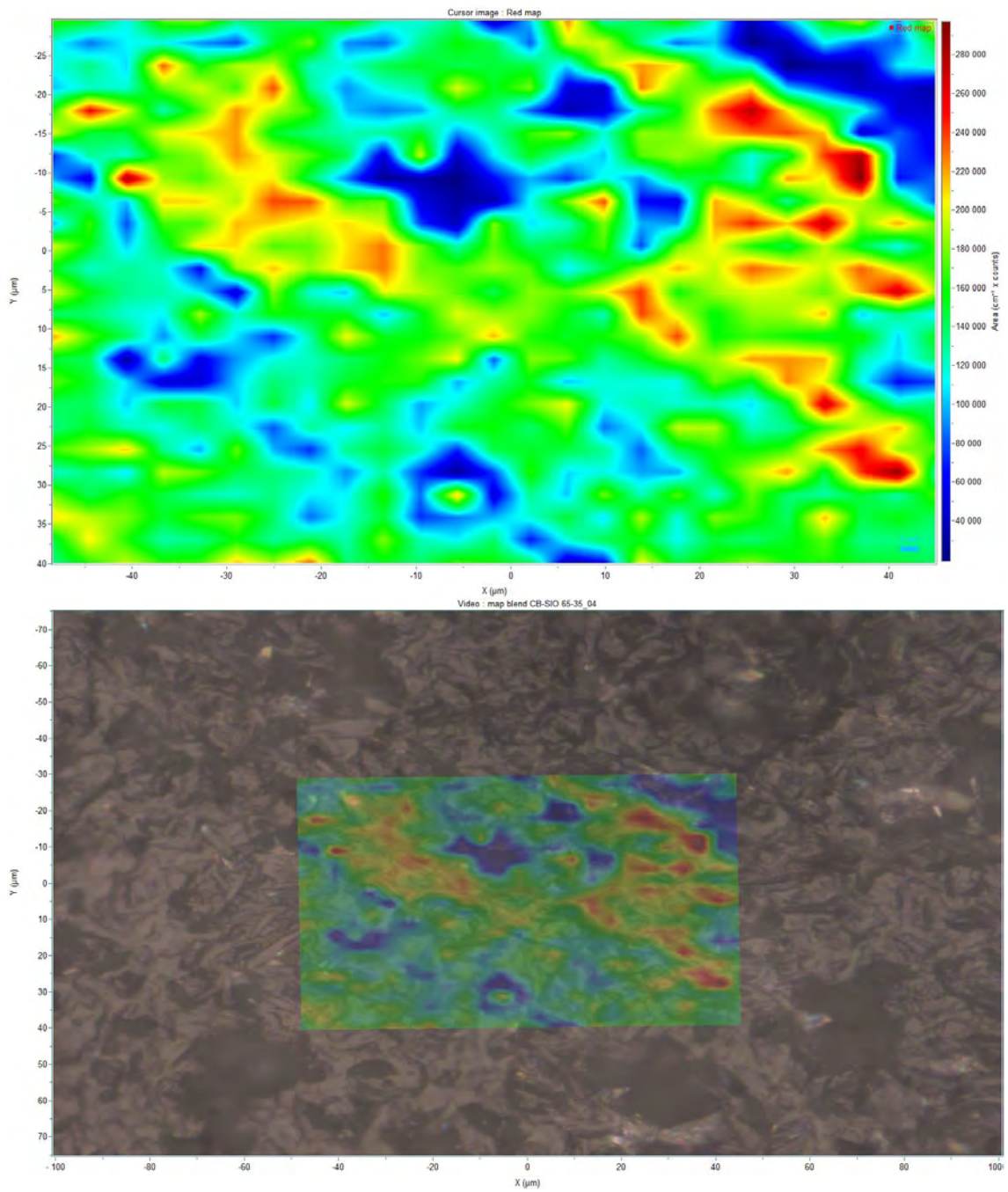
Figura A2. Imágenes químicas de las mezclas CB65-SIO35 obtenidas por MCR.

Tabla A6

Corresponde a los datos de las imágenes químicas de las mezclas CB75–CNO25 y CB75–SIO25, y los espectros puros de CB, CNO y SIO obtenidos por MCR. Los datos están disponibles en:

https://www.mdpi.com/article/10.3390/foods10123101/s1

Anexo 3. Datos correspondientes al Capítulo V

Tabla A7. Datos originales de cinética de cristalización isotérmica a 19 °C de Ch-SIO a temperado alto y 5% de CB/SIO.

Time (min)	Heat Flow (Normalized) (W/g)	Time (min)	Heat Flow (Normalized) (W/g)	Time (min)	Heat Flow (Normalized) (W/g)	Time (min)	Heat Flow (Normalized) (W/g)
195.61	0.779	218.16	0.073	240.7	0.041	263.25	0.039
195.79	0.78	218.34	0.073	240.88	0.041	263.43	0.039
195.97	0.752	218.52	0.073	241.06	0.041	263.61	0.039
196.15	0.718	218.7	0.073	241.24	0.041	263.79	0.039
196.33	0.683	218.88	0.072	241.42	0.041	263.97	0.039
196.52	0.651	219.06	0.072	241.6	0.041	264.15	0.039
196.7	0.617	219.24	0.072	241.78	0.041	264.33	0.039
196.88	0.148	219.42	0.071	241.97	0.041	264.51	0.039
197.05	0.041	219.6	0.071	242.15	0.041	264.69	0.039
197.23	0.029	219.78	0.071	242.33	0.041	264.87	0.039
197.42	0.029	219.96	0.071	242.5	0.041	265.05	0.039
197.6	0.031	220.14	0.07	242.68	0.041	265.23	0.039
197.78	0.033	220.32	0.07	242.87	0.041	265.41	0.039
197.96	0.035	220.5	0.069	243.05	0.041	265.59	0.039
198.14	0.037	220.68	0.069	243.23	0.041	265.77	0.039
198.32	0.038	220.86	0.069	243.41	0.041	265.95	0.039
198.5	0.039	221.04	0.069	243.59	0.041	266.13	0.039
198.68	0.039	221.22	0.069	243.77	0.041	266.31	0.039
198.86	0.039	221.4	0.069	243.95	0.041	266.49	0.039
199.04	0.039	221.58	0.068	244.13	0.041	266.67	0.039
199.22	0.04	221.77	0.068	244.31	0.041	266.85	0.039
199.4	0.04	221.95	0.068	244.49	0.041	267.03	0.039
199.58	0.04	222.13	0.068	244.67	0.041	267.22	0.039
199.76	0.04	222.3	0.068	244.85	0.041	267.4	0.039
199.94	0.039	222.48	0.067	245.03	0.041	267.58	0.039
200.12	0.039	222.67	0.067	245.21	0.04	267.75	0.039
200.3	0.039	222.85	0.067	245.39	0.04	267.93	0.039
200.48	0.039	223.03	0.066	245.57	0.04	268.12	0.039
200.66	0.039	223.21	0.066	245.75	0.04	268.3	0.039
200.84	0.039	223.39	0.066	245.93	0.04	268.48	0.039
201.02	0.039	223.57	0.066	246.11	0.04	268.66	0.039
201.2	0.039	223.75	0.065	246.29	0.04	268.84	0.039
201.38	0.039	223.93	0.065	246.47	0.04	269.02	0.039
201.57	0.039	224.11	0.065	246.65	0.04	269.2	0.039
201.75	0.039	224.29	0.064	246.83	0.04	269.38	0.039
201.93	0.039	224.47	0.064	247.02	0.04	269.56	0.039
202.1	0.039	224.65	0.064	247.2	0.04	269.74	0.039
202.28	0.039	224.83	0.063	247.38	0.04	269.92	0.039
202.47	0.039	225.01	0.063	247.55	0.04	270.1	0.039

202.65	0.039	225.19	0.063	247.73	0.04	270.28	0.039
202.83	0.04	225.37	0.062	247.92	0.04	270.46	0.039
203.01	0.04	225.55	0.061	248.1	0.04	270.64	0.039
203.19	0.04	225.73	0.061	248.28	0.04	270.82	0.039
203.37	0.04	225.91	0.06	248.46	0.04	271	0.039
203.55	0.04	226.09	0.06	248.64	0.04	271.18	0.039
203.73	0.04	226.27	0.059	248.82	0.04	271.36	0.039
203.91	0.04	226.45	0.059	249	0.04	271.54	0.039
204.09	0.04	226.63	0.058	249.18	0.04	271.72	0.039
204.27	0.04	226.82	0.058	249.36	0.04	271.9	0.039
204.45	0.04	227	0.057	249.54	0.04	272.08	0.039
204.63	0.04	227.18	0.057	249.72	0.04	272.27	0.039
204.81	0.04	227.35	0.056	249.9	0.04	272.45	0.039
204.99	0.04	227.53	0.056	250.08	0.04	272.63	0.039
205.17	0.04	227.72	0.055	250.26	0.04	272.8	0.039
205.35	0.041	227.9	0.055	250.44	0.04	272.98	0.039
205.53	0.041	228.08	0.055	250.62	0.04	273.17	0.039
205.71	0.041	228.26	0.054	250.8	0.04	273.35	0.039
205.89	0.041	228.44	0.054	250.98	0.04	273.53	0.039
206.07	0.041	228.62	0.053	251.16	0.04	273.71	0.039
206.25	0.041	228.8	0.053	251.34	0.04	273.89	0.039
206.43	0.041	228.98	0.052	251.52	0.04	274.07	0.039
206.62	0.042	229.16	0.052	251.7	0.04	274.25	0.039
206.8	0.042	229.34	0.052	251.88	0.04	274.43	0.039
206.98	0.042	229.52	0.051	252.07	0.04	274.61	0.039
207.15	0.042	229.7	0.051	252.25	0.04	274.79	0.039
207.33	0.042	229.88	0.051	252.43	0.04	274.97	0.039
207.52	0.042	230.06	0.05	252.6	0.04	275.15	0.039
207.7	0.043	230.24	0.05	252.78	0.04	275.33	0.039
207.88	0.043	230.42	0.05	252.97	0.04	275.51	0.039
208.06	0.043	230.6	0.049	253.15	0.039	275.69	0.039
208.24	0.043	230.78	0.049	253.33	0.039	275.87	0.039
208.42	0.044	230.96	0.049	253.51	0.04	276.05	0.039
208.6	0.044	231.14	0.049	253.69	0.04	276.23	0.039
208.78	0.044	231.32	0.048	253.87	0.039	276.41	0.039
208.96	0.044	231.5	0.048	254.05	0.039	276.59	0.039
209.14	0.045	231.68	0.048	254.23	0.039	276.77	0.039
209.32	0.045	231.87	0.047	254.41	0.039	276.95	0.039
209.5	0.045	232.05	0.047	254.59	0.039	277.13	0.039
209.68	0.046	232.23	0.047	254.77	0.039	277.32	0.039
209.86	0.046	232.4	0.047	254.95	0.039	277.49	0.039
210.04	0.047	232.58	0.046	255.13	0.039	277.68	0.039
210.22	0.047	232.77	0.046	255.31	0.039	277.86	0.039
210.4	0.048	232.95	0.046	255.49	0.039	278.03	0.039
210.58	0.048	233.13	0.046	255.67	0.039	278.22	0.039
210.76	0.049	233.31	0.046	255.85	0.039	278.4	0.039

210.94	0.05	233.49	0.045	256.03	0.039	278.58	0.039
211.12	0.05	233.67	0.045	256.21	0.039	278.76	0.039
211.3	0.051	233.85	0.045	256.39	0.039	278.94	0.039
211.48	0.052	234.03	0.045	256.57	0.039	279.12	0.039
211.67	0.052	234.21	0.045	256.75	0.039	279.3	0.039
211.85	0.053	234.39	0.045	256.93	0.039	279.48	0.039
212.03	0.054	234.57	0.044	257.12	0.039	279.66	0.039
212.2	0.055	234.75	0.044	257.3	0.039	279.84	0.039
212.38	0.056	234.93	0.044	257.48	0.039	280.02	0.039
212.57	0.056	235.11	0.044	257.65	0.039	280.2	0.039
212.75	0.057	235.29	0.044	257.83	0.039	280.38	0.039
212.93	0.058	235.47	0.044	258.02	0.039	280.56	0.039
213.11	0.059	235.65	0.044	258.2	0.039	280.74	0.039
213.29	0.06	235.83	0.044	258.38	0.039	280.92	0.039
213.47	0.061	236.01	0.043	258.56	0.039	281.1	0.039
213.65	0.062	236.19	0.043	258.74	0.039	281.28	0.039
213.83	0.063	236.37	0.043	258.92	0.039	281.46	0.039
214.01	0.064	236.55	0.043	259.1	0.039	281.64	0.039
214.19	0.065	236.73	0.043	259.28	0.039	281.82	0.039
214.37	0.065	236.92	0.043	259.46	0.039	282	0.039
214.55	0.066	237.1	0.043	259.64	0.039	282.18	0.039
214.73	0.067	237.28	0.043	259.82	0.039	282.37	0.039
214.91	0.068	237.45	0.043	260	0.039	282.54	0.039
215.09	0.069	237.63	0.043	260.18	0.039	282.73	0.039
215.27	0.069	237.82	0.043	260.36	0.039	282.91	0.039
215.45	0.07	238	0.043	260.54	0.039	283.08	0.039
215.63	0.071	238.18	0.042	260.72	0.039	283.27	0.039
215.81	0.071	238.36	0.042	260.9	0.039	283.45	0.039
215.99	0.072	238.54	0.042	261.08	0.039	283.63	0.039
216.17	0.072	238.72	0.042	261.26	0.039	283.81	0.039
216.35	0.072	238.9	0.042	261.44	0.039	283.99	0.039
216.53	0.073	239.08	0.042	261.62	0.039	284.17	0.039
216.72	0.073	239.26	0.042	261.8	0.039	284.35	0.039
216.9	0.073	239.44	0.042	261.98	0.039	284.53	0.039
217.08	0.074	239.62	0.042	262.17	0.039	284.71	0.039
217.25	0.074	239.8	0.042	262.35	0.039	284.89	0.039
217.43	0.074	239.98	0.042	262.53	0.039	285.07	0.039
217.62	0.074	240.16	0.042	262.7	0.039	285.25	0.039
217.8	0.074	240.34	0.041	262.88	0.039	285.43	0.039
217.98	0.074	240.52	0.042	263.07	0.039	285.61	0.039

Tabla A8. Datos originales de cinética de cristalización isotérmica a 19 °C de Ch-CNO a temperado bajo y 1% de CB/CNO.

Time (min)	Heat Flow (Normalized) (W/g)	Time (min)	Heat Flow (Normalized) (W/g)	Time (min)	Heat Flow (Normalized) (W/g)	Time (min)	Heat Flow (Normalized) (W/g)
195.61	0.662	218.15	0.067	240.7	0.036	263.24	0.034
195.79	0.668	218.33	0.066	240.88	0.036	263.42	0.034
195.97	0.647	218.52	0.066	241.06	0.036	263.6	0.034
196.15	0.617	218.7	0.066	241.24	0.036	263.78	0.034
196.33	0.586	218.88	0.065	241.42	0.036	263.97	0.034
196.51	0.559	219.05	0.065	241.6	0.036	264.15	0.034
196.69	0.591	219.24	0.064	241.78	0.036	264.33	0.034
196.87	0.153	219.42	0.064	241.96	0.036	264.5	0.034
197.05	0.041	219.6	0.063	242.14	0.036	264.69	0.033
197.23	0.027	219.78	0.063	242.32	0.036	264.87	0.034
197.41	0.026	219.96	0.063	242.5	0.035	265.05	0.034
197.59	0.027	220.14	0.062	242.68	0.035	265.23	0.034
197.77	0.029	220.32	0.062	242.86	0.035	265.41	0.034
197.95	0.03	220.5	0.061	243.04	0.035	265.59	0.034
198.13	0.032	220.68	0.061	243.22	0.035	265.77	0.034
198.32	0.033	220.86	0.061	243.4	0.035	265.95	0.033
198.5	0.034	221.04	0.06	243.58	0.035	266.13	0.033
198.68	0.034	221.22	0.06	243.77	0.035	266.31	0.034
198.85	0.034	221.4	0.06	243.95	0.035	266.49	0.034
199.04	0.034	221.58	0.06	244.13	0.035	266.67	0.034
199.22	0.034	221.76	0.06	244.3	0.035	266.85	0.034
199.4	0.034	221.94	0.059	244.49	0.035	267.03	0.034
199.58	0.034	222.12	0.059	244.67	0.035	267.21	0.034
199.76	0.034	222.3	0.059	244.85	0.035	267.39	0.034
199.94	0.034	222.48	0.059	245.03	0.035	267.57	0.033
200.12	0.034	222.66	0.058	245.21	0.035	267.75	0.033
200.3	0.034	222.84	0.058	245.39	0.035	267.93	0.034
200.48	0.034	223.02	0.058	245.57	0.035	268.11	0.034
200.66	0.034	223.2	0.057	245.75	0.035	268.29	0.034
200.84	0.034	223.38	0.057	245.93	0.035	268.47	0.034
201.02	0.034	223.57	0.057	246.11	0.035	268.65	0.034
201.2	0.034	223.75	0.056	246.29	0.035	268.83	0.034
201.38	0.034	223.93	0.056	246.47	0.035	269.02	0.033
201.56	0.034	224.1	0.056	246.65	0.035	269.2	0.033
201.74	0.034	224.29	0.056	246.83	0.035	269.38	0.033
201.92	0.034	224.47	0.055	247.01	0.035	269.55	0.033
202.1	0.034	224.65	0.055	247.19	0.035	269.74	0.033
202.28	0.034	224.83	0.055	247.37	0.034	269.92	0.033
202.46	0.034	225.01	0.054	247.55	0.035	270.1	0.033
202.64	0.034	225.19	0.054	247.73	0.035	270.28	0.033
202.82	0.034	225.37	0.054	247.91	0.035	270.46	0.033

203	0.034	225.55	0.053	248.09	0.035	270.64	0.033
203.18	0.034	225.73	0.053	248.27	0.034	270.82	0.033
203.37	0.034	225.91	0.053	248.45	0.034	271	0.033
203.55	0.035	226.09	0.052	248.63	0.034	271.18	0.033
203.73	0.035	226.27	0.052	248.82	0.034	271.36	0.033
203.9	0.035	226.45	0.051	249	0.034	271.54	0.033
204.09	0.035	226.63	0.051	249.18	0.034	271.72	0.033
204.27	0.035	226.81	0.05	249.35	0.034	271.9	0.033
204.45	0.035	226.99	0.05	249.54	0.034	272.08	0.033
204.63	0.035	227.17	0.05	249.72	0.034	272.26	0.033
204.81	0.035	227.35	0.049	249.9	0.034	272.44	0.033
204.99	0.035	227.53	0.049	250.08	0.034	272.62	0.033
205.17	0.036	227.71	0.048	250.26	0.034	272.8	0.033
205.35	0.036	227.89	0.048	250.44	0.034	272.98	0.033
205.53	0.036	228.07	0.048	250.62	0.034	273.16	0.033
205.71	0.036	228.25	0.047	250.8	0.034	273.34	0.033
205.89	0.036	228.43	0.047	250.98	0.034	273.52	0.033
206.07	0.036	228.62	0.046	251.16	0.034	273.7	0.033
206.25	0.036	228.8	0.046	251.34	0.034	273.88	0.033
206.43	0.036	228.98	0.046	251.52	0.034	274.07	0.033
206.61	0.037	229.15	0.046	251.7	0.034	274.24	0.033
206.79	0.037	229.34	0.045	251.88	0.034	274.43	0.033
206.97	0.037	229.52	0.045	252.06	0.034	274.61	0.033
207.15	0.037	229.7	0.045	252.24	0.034	274.79	0.033
207.33	0.037	229.88	0.044	252.42	0.034	274.97	0.033
207.51	0.038	230.06	0.044	252.6	0.034	275.15	0.033
207.69	0.038	230.24	0.044	252.78	0.034	275.33	0.033
207.87	0.038	230.42	0.043	252.96	0.034	275.51	0.033
208.05	0.038	230.6	0.043	253.14	0.034	275.69	0.033
208.23	0.039	230.78	0.043	253.32	0.034	275.87	0.033
208.42	0.039	230.96	0.043	253.5	0.034	276.05	0.033
208.6	0.039	231.14	0.042	253.68	0.034	276.23	0.033
208.78	0.04	231.32	0.042	253.87	0.034	276.41	0.033
208.95	0.04	231.5	0.042	254.05	0.034	276.59	0.033
209.14	0.04	231.68	0.042	254.23	0.034	276.77	0.033
209.32	0.041	231.86	0.041	254.4	0.034	276.95	0.033
209.5	0.041	232.04	0.041	254.59	0.034	277.13	0.033
209.68	0.042	232.22	0.041	254.77	0.034	277.31	0.033
209.86	0.042	232.4	0.041	254.95	0.034	277.49	0.033
210.04	0.043	232.58	0.041	255.13	0.034	277.67	0.033
210.22	0.044	232.76	0.04	255.31	0.034	277.85	0.033
210.4	0.044	232.94	0.04	255.49	0.034	278.03	0.033
210.58	0.045	233.12	0.04	255.67	0.034	278.21	0.033
210.76	0.045	233.3	0.04	255.85	0.034	278.39	0.033
210.94	0.046	233.48	0.04	256.03	0.034	278.57	0.033
211.12	0.047	233.67	0.04	256.21	0.034	278.75	0.033

211.3	0.048	233.85	0.039	256.39	0.034	278.93	0.033
211.48	0.048	234.03	0.039	256.57	0.034	279.12	0.033
211.66	0.049	234.2	0.039	256.75	0.034	279.29	0.033
211.84	0.05	234.39	0.039	256.93	0.034	279.48	0.033
212.02	0.051	234.57	0.039	257.11	0.034	279.66	0.033
212.2	0.052	234.75	0.039	257.29	0.034	279.84	0.033
212.38	0.053	234.93	0.039	257.47	0.034	280.02	0.033
212.56	0.054	235.11	0.038	257.65	0.034	280.2	0.033
212.74	0.055	235.29	0.038	257.83	0.034	280.38	0.033
212.92	0.056	235.47	0.038	258.01	0.034	280.56	0.033
213.1	0.056	235.65	0.038	258.19	0.034	280.74	0.033
213.28	0.057	235.83	0.038	258.37	0.034	280.92	0.033
213.47	0.058	236.01	0.038	258.55	0.034	281.1	0.033
213.65	0.059	236.19	0.038	258.73	0.034	281.28	0.033
213.83	0.06	236.37	0.037	258.92	0.034	281.46	0.033
214	0.061	236.55	0.037	259.1	0.034	281.64	0.033
214.19	0.062	236.73	0.037	259.28	0.034	281.82	0.033
214.37	0.063	236.91	0.037	259.45	0.034	282	0.033
214.55	0.063	237.09	0.037	259.64	0.034	282.18	0.033
214.73	0.064	237.27	0.037	259.82	0.034	282.36	0.033
214.91	0.065	237.45	0.037	260	0.034	282.54	0.033
215.09	0.065	237.63	0.037	260.18	0.034	282.72	0.033
215.27	0.066	237.81	0.037	260.36	0.033	282.9	0.033
215.45	0.066	237.99	0.037	260.54	0.034	283.08	0.033
215.63	0.067	238.17	0.037	260.72	0.034	283.26	0.033
215.81	0.067	238.35	0.037	260.9	0.034	283.44	0.033
215.99	0.067	238.53	0.037	261.08	0.034	283.62	0.033
216.17	0.068	238.72	0.037	261.26	0.034	283.8	0.033
216.35	0.068	238.9	0.036	261.44	0.034	283.98	0.033
216.53	0.068	239.08	0.036	261.62	0.034	284.17	0.033
216.71	0.068	239.25	0.036	261.8	0.034	284.34	0.033
216.89	0.068	239.44	0.036	261.98	0.034	284.53	0.033
217.07	0.068	239.62	0.036	262.16	0.034	284.71	0.033
217.25	0.068	239.8	0.036	262.34	0.034	284.89	0.033
217.43	0.068	239.98	0.036	262.52	0.034	285.07	0.033
217.61	0.067	240.16	0.036	262.7	0.034	285.25	0.033
217.79	0.067	240.34	0.036	262.88	0.034	285.43	0.033
217.97	0.067	240.52	0.036	263.06	0.034	285.61	0.033

Tabla A9. Datos originales para calcular el porcentaje de forma β_2 de Ch-SIO a temperado alto y 5% de CB/SIO.

Temp. (°C)	Heat Flow (Normalized) (W/g)	Temp. (°C)	Heat Flow (Normalized) (W/g)	Temp. (°C)	Heat Flow (Normalized) (W/g)	Temp. (°C)	Heat Flow (Normalized) (W/g)
15.01	-0.448	20.86	-1.109	28.87	-2.33	37.83	-1.487
15.01	-0.449	20.93	-1.111	28.93	-2.353	37.92	-1.473
15.01	-0.449	20.99	-1.114	28.98	-2.376	38	-1.46
15.01	-0.449	21.05	-1.116	29.03	-2.399	38.08	-1.447
15.01	-0.449	21.12	-1.12	29.09	-2.422	38.2	-1.428
15.01	-0.45	21.21	-1.124	29.14	-2.446	38.28	-1.416
15.01	-0.45	21.28	-1.127	29.19	-2.47	38.36	-1.405
15.01	-0.451	21.34	-1.13	29.24	-2.494	38.44	-1.395
15.01	-0.451	21.41	-1.133	29.29	-2.518	38.52	-1.385
15.02	-0.452	21.47	-1.137	29.37	-2.555	38.6	-1.375
15.02	-0.452	21.53	-1.14	29.42	-2.579	38.68	-1.365
15.02	-0.453	21.6	-1.143	29.47	-2.604	38.76	-1.356
15.02	-0.453	21.66	-1.146	29.52	-2.629	38.83	-1.347
15.02	-0.453	21.72	-1.149	29.57	-2.654	38.91	-1.339
15.03	-0.454	21.82	-1.153	29.63	-2.679	39.02	-1.327
15.03	-0.454	21.88	-1.155	29.68	-2.704	39.1	-1.319
15.04	-0.455	21.95	-1.157	29.73	-2.729	39.18	-1.312
15.04	-0.456	22.01	-1.158	29.78	-2.755	39.25	-1.304
15.05	-0.457	22.08	-1.16	29.85	-2.793	39.33	-1.297
15.06	-0.459	22.14	-1.161	29.9	-2.819	39.4	-1.29
15.07	-0.461	22.2	-1.162	29.95	-2.845	39.48	-1.284
15.08	-0.464	22.27	-1.163	30	-2.87	39.55	-1.278
15.09	-0.466	22.33	-1.163	30.05	-2.896	39.63	-1.272
15.1	-0.47	22.43	-1.164	30.1	-2.922	39.74	-1.263
15.12	-0.473	22.49	-1.164	30.15	-2.948	39.81	-1.258
15.14	-0.477	22.56	-1.165	30.2	-2.974	39.88	-1.252
15.15	-0.482	22.62	-1.165	30.25	-2.999	39.96	-1.247
15.17	-0.488	22.69	-1.165	30.3	-3.025	40.03	-1.242
15.21	-0.497	22.75	-1.166	30.37	-3.064	40.1	-1.237
15.23	-0.504	22.82	-1.166	30.42	-3.09	40.17	-1.233
15.26	-0.511	22.88	-1.167	30.47	-3.116	40.25	-1.229
15.29	-0.52	22.95	-1.168	30.52	-3.141	40.32	-1.225
15.32	-0.528	23.01	-1.169	30.57	-3.167	40.43	-1.219
15.35	-0.538	23.11	-1.169	30.62	-3.192	40.5	-1.215
15.38	-0.547	23.18	-1.169	30.67	-3.218	40.57	-1.211
15.41	-0.558	23.24	-1.169	30.72	-3.243	40.64	-1.207
15.45	-0.568	23.31	-1.169	30.77	-3.268	40.71	-1.204
15.51	-0.586	23.37	-1.168	30.84	-3.304	40.78	-1.201
15.55	-0.597	23.44	-1.167	30.89	-3.329	40.85	-1.198
15.59	-0.609	23.5	-1.166	30.94	-3.353	40.92	-1.195
15.63	-0.621	23.57	-1.164	30.99	-3.377	40.99	-1.192
15.67	-0.633	23.64	-1.163	31.04	-3.401	41.1	-1.187

15.72	-0.646	23.74	-1.161	31.09	-3.424	41.17	-1.184
15.76	-0.658	23.8	-1.16	31.14	-3.448	41.24	-1.181
15.81	-0.67	23.87	-1.16	31.19	-3.47	41.31	-1.179
15.85	-0.682	23.93	-1.16	31.24	-3.493	41.38	-1.178
15.9	-0.694	24	-1.161	31.31	-3.526	41.44	-1.175
15.98	-0.712	24.06	-1.161	31.36	-3.548	41.51	-1.173
16.02	-0.723	24.13	-1.161	31.41	-3.569	41.58	-1.171
16.07	-0.734	24.2	-1.165	31.46	-3.59	41.65	-1.169
16.13	-0.746	24.26	-1.172	31.51	-3.61	41.72	-1.167
16.18	-0.756	24.36	-1.18	31.56	-3.63	41.82	-1.164
16.23	-0.767	24.42	-1.186	31.61	-3.649	41.89	-1.162
16.28	-0.777	24.49	-1.193	31.66	-3.667	41.96	-1.16
16.33	-0.787	24.55	-1.201	31.72	-3.685	42.03	-1.159
16.39	-0.797	24.62	-1.209	31.79	-3.711	42.1	-1.157
16.47	-0.811	24.68	-1.219	31.85	-3.728	42.17	-1.156
16.52	-0.82	24.74	-1.23	31.9	-3.745	42.24	-1.154
16.58	-0.829	24.81	-1.243	31.95	-3.761	42.3	-1.153
16.63	-0.837	24.87	-1.256	32	-3.777	42.37	-1.152
16.69	-0.845	24.96	-1.278	32.06	-3.792	42.48	-1.15
16.74	-0.853	25.02	-1.293	32.11	-3.807	42.54	-1.149
16.8	-0.861	25.08	-1.309	32.16	-3.821	42.61	-1.147
16.85	-0.869	25.14	-1.326	32.22	-3.834	42.68	-1.146
16.91	-0.876	25.2	-1.342	32.27	-3.847	42.75	-1.145
16.99	-0.886	25.26	-1.358	32.35	-3.865	42.82	-1.144
17.05	-0.893	25.32	-1.373	32.41	-3.875	42.88	-1.143
17.1	-0.9	25.38	-1.388	32.46	-3.883	42.95	-1.142
17.16	-0.906	25.44	-1.403	32.52	-3.89	43.02	-1.142
17.22	-0.912	25.49	-1.416	32.58	-3.896	43.12	-1.141
17.27	-0.918	25.58	-1.435	32.63	-3.901	43.19	-1.139
17.33	-0.924	25.64	-1.448	32.69	-3.903	43.26	-1.139
17.39	-0.93	25.7	-1.459	32.75	-3.902	43.33	-1.138
17.45	-0.935	25.76	-1.471	32.81	-3.899	43.39	-1.137
17.54	-0.943	25.81	-1.482	32.9	-3.888	43.46	-1.137
17.59	-0.948	25.87	-1.493	32.96	-3.877	43.53	-1.136
17.65	-0.953	25.93	-1.504	33.03	-3.862	43.6	-1.135
17.71	-0.958	25.99	-1.515	33.09	-3.841	43.66	-1.135
17.77	-0.963	26.05	-1.525	33.16	-3.815	43.77	-1.134
17.83	-0.968	26.13	-1.541	33.22	-3.782	43.83	-1.133
17.89	-0.973	26.19	-1.553	33.29	-3.741	43.9	-1.132
17.95	-0.977	26.25	-1.564	33.37	-3.692	43.97	-1.132
18.01	-0.981	26.31	-1.575	33.44	-3.631	44.04	-1.132
18.07	-0.986	26.37	-1.586	33.56	-3.518	44.1	-1.131
18.16	-0.993	26.43	-1.597	33.64	-3.425	44.17	-1.131
18.22	-0.997	26.48	-1.609	33.73	-3.32	44.24	-1.131
18.28	-1.001	26.54	-1.621	33.82	-3.203	44.31	-1.13
18.34	-1.005	26.6	-1.633	33.92	-3.079	44.37	-1.13

18.4	-1.01	26.69	-1.652	34.02	-2.955	44.47	-1.129
18.46	-1.013	26.75	-1.664	34.13	-2.836	44.54	-1.129
18.52	-1.017	26.8	-1.677	34.24	-2.729	44.61	-1.128
18.59	-1.021	26.86	-1.691	34.35	-2.635	44.68	-1.128
18.65	-1.024	26.92	-1.705	34.51	-2.519	44.74	-1.128
18.74	-1.03	26.98	-1.719	34.62	-2.454	44.81	-1.128
18.8	-1.033	27.04	-1.732	34.73	-2.395	44.88	-1.127
18.86	-1.036	27.09	-1.746	34.84	-2.34	44.94	-1.127
18.93	-1.039	27.15	-1.76	34.95	-2.289	45.01	-1.127
18.99	-1.043	27.24	-1.781	35.06	-2.241	45.11	-1.126
19.05	-1.046	27.3	-1.796	35.16	-2.197	45.18	-1.126
19.11	-1.049	27.35	-1.811	35.27	-2.155	45.25	-1.126
19.18	-1.052	27.41	-1.825	35.38	-2.116	45.31	-1.125
19.24	-1.055	27.47	-1.841	35.48	-2.08	45.38	-1.125
19.33	-1.059	27.52	-1.856	35.63	-2.028	45.45	-1.125
19.4	-1.062	27.58	-1.873	35.73	-1.996	45.52	-1.125
19.46	-1.064	27.64	-1.889	35.84	-1.965	45.58	-1.125
19.52	-1.067	27.69	-1.905	35.94	-1.936	45.65	-1.125
19.59	-1.069	27.75	-1.922	36.03	-1.908	45.75	-1.124
19.65	-1.072	27.84	-1.948	36.13	-1.88	45.82	-1.124
19.71	-1.075	27.89	-1.966	36.23	-1.853	45.88	-1.124
19.78	-1.077	27.95	-1.984	36.32	-1.827	45.95	-1.124
19.84	-1.08	28	-2.002	36.42	-1.802	46.02	-1.124
19.93	-1.083	28.06	-2.021	36.56	-1.765	46.08	-1.124
20	-1.084	28.12	-2.039	36.65	-1.741	46.15	-1.124
20.06	-1.086	28.17	-2.058	36.74	-1.717	46.22	-1.124
20.13	-1.088	28.22	-2.077	36.83	-1.695	46.29	-1.124
20.19	-1.09	28.28	-2.097	36.92	-1.673	46.38	-1.124
20.25	-1.092	28.36	-2.127	37.01	-1.652	46.45	-1.124
20.32	-1.094	28.42	-2.147	37.1	-1.631	46.52	-1.124
20.38	-1.096	28.47	-2.168	37.19	-1.612	46.58	-1.124
20.44	-1.097	28.53	-2.189	37.28	-1.593	46.65	-1.124
20.51	-1.099	28.58	-2.21	37.41	-1.566	46.72	-1.124
20.6	-1.102	28.63	-2.232	37.49	-1.549	46.78	-1.124
20.67	-1.104	28.69	-2.253	37.58	-1.533	46.85	-1.124
20.73	-1.105	28.74	-2.275	37.66	-1.517	46.92	-1.124
20.8	-1.107	28.79	-2.296	37.75	-1.501	46.98	-1.124

Tabla A10. Datos originales para calcular el porcentaje de forma β_2 de Ch-CNO a temperado bajo y 1% de CB/CNO.

Temp. (°C)	Heat Flow (Normalized) (W/g)	Temp. (°C)	Heat Flow (Normalized) (W/g)	Temp. (°C)	Heat Flow (Normalized) (W/g)	Temp. (°C)	Heat Flow (Normalized) (W/g)
15.02	0.017	20.9	-0.548	28.68	-2.001	38.03	-0.763
15.02	0.017	20.96	-0.55	28.73	-2.022	38.11	-0.756
15.02	0.016	21.03	-0.551	28.79	-2.043	38.22	-0.746
15.02	0.016	21.09	-0.553	28.84	-2.064	38.29	-0.74
15.02	0.015	21.16	-0.555	28.89	-2.084	38.37	-0.733
15.02	0.015	21.22	-0.558	28.97	-2.116	38.44	-0.727
15.02	0.015	21.28	-0.56	29.02	-2.137	38.52	-0.722
15.02	0.014	21.38	-0.564	29.08	-2.158	38.59	-0.716
15.02	0.014	21.44	-0.566	29.13	-2.18	38.66	-0.71
15.02	0.013	21.51	-0.569	29.18	-2.201	38.74	-0.705
15.02	0.013	21.57	-0.571	29.23	-2.223	38.81	-0.7
15.02	0.012	21.64	-0.573	29.29	-2.244	38.88	-0.695
15.03	0.012	21.7	-0.576	29.34	-2.265	38.99	-0.687
15.03	0.012	21.76	-0.578	29.39	-2.286	39.06	-0.683
15.03	0.012	21.83	-0.58	29.47	-2.317	39.13	-0.679
15.04	0.012	21.89	-0.583	29.52	-2.338	39.21	-0.674
15.04	0.012	21.96	-0.585	29.57	-2.358	39.28	-0.671
15.05	0.012	22.05	-0.589	29.62	-2.379	39.35	-0.667
15.06	0.013	22.12	-0.592	29.67	-2.4	39.42	-0.663
15.07	0.013	22.18	-0.595	29.73	-2.421	39.49	-0.659
15.08	0.013	22.24	-0.598	29.78	-2.442	39.56	-0.655
15.09	0.014	22.31	-0.602	29.83	-2.463	39.67	-0.651
15.1	0.014	22.37	-0.605	29.88	-2.484	39.74	-0.648
15.12	0.014	22.44	-0.609	29.93	-2.505	39.81	-0.644
15.13	0.014	22.5	-0.613	30.01	-2.536	39.88	-0.641
15.15	0.014	22.56	-0.619	30.06	-2.556	39.95	-0.638
15.17	0.014	22.66	-0.628	30.11	-2.576	40.02	-0.635
15.19	0.014	22.72	-0.635	30.17	-2.597	40.09	-0.632
15.21	0.014	22.78	-0.642	30.22	-2.617	40.16	-0.63
15.25	0.01	22.85	-0.65	30.27	-2.638	40.23	-0.627
15.28	0.006	22.91	-0.659	30.32	-2.658	40.34	-0.624
15.31	0.002	22.97	-0.667	30.37	-2.678	40.41	-0.622
15.34	-0.002	23.03	-0.676	30.42	-2.697	40.48	-0.619
15.37	-0.007	23.1	-0.685	30.5	-2.727	40.54	-0.617
15.4	-0.012	23.16	-0.694	30.55	-2.746	40.61	-0.615
15.44	-0.018	23.22	-0.703	30.61	-2.765	40.68	-0.613
15.48	-0.025	23.31	-0.716	30.66	-2.784	40.75	-0.611
15.51	-0.031	23.37	-0.724	30.71	-2.803	40.82	-0.61
15.57	-0.043	23.43	-0.732	30.76	-2.822	40.89	-0.608
15.62	-0.052	23.49	-0.741	30.82	-2.84	40.96	-0.606
15.66	-0.06	23.55	-0.749	30.87	-2.858	41.06	-0.604

15.7	-0.069	23.62	-0.757	30.92	-2.876	41.13	-0.602
15.75	-0.079	23.68	-0.765	31	-2.902	41.2	-0.6
15.79	-0.089	23.74	-0.774	31.05	-2.919	41.27	-0.599
15.84	-0.099	23.8	-0.782	31.11	-2.935	41.33	-0.598
15.89	-0.11	23.89	-0.795	31.16	-2.951	41.4	-0.597
15.94	-0.121	23.95	-0.803	31.21	-2.967	41.47	-0.595
15.99	-0.132	24.01	-0.811	31.27	-2.983	41.54	-0.594
16.06	-0.147	24.07	-0.82	31.32	-2.999	41.61	-0.593
16.12	-0.158	24.13	-0.828	31.37	-3.013	41.71	-0.591
16.17	-0.169	24.19	-0.837	31.43	-3.027	41.78	-0.59
16.22	-0.179	24.25	-0.846	31.48	-3.04	41.85	-0.589
16.27	-0.19	24.31	-0.855	31.56	-3.057	41.92	-0.588
16.32	-0.2	24.37	-0.864	31.62	-3.068	41.98	-0.587
16.38	-0.21	24.46	-0.877	31.67	-3.077	42.05	-0.586
16.43	-0.22	24.52	-0.886	31.73	-3.084	42.12	-0.585
16.48	-0.23	24.58	-0.895	31.79	-3.09	42.19	-0.584
16.57	-0.244	24.64	-0.905	31.84	-3.093	42.25	-0.583
16.62	-0.253	24.7	-0.915	31.9	-3.095	42.32	-0.582
16.68	-0.262	24.76	-0.924	31.96	-3.094	42.42	-0.582
16.73	-0.271	24.82	-0.935	32.02	-3.091	42.49	-0.581
16.79	-0.279	24.88	-0.944	32.11	-3.079	42.56	-0.58
16.84	-0.286	24.94	-0.954	32.17	-3.067	42.63	-0.58
16.9	-0.294	25	-0.965	32.23	-3.05	42.69	-0.578
16.95	-0.301	25.09	-0.98	32.3	-3.028	42.76	-0.578
17.01	-0.308	25.15	-0.991	32.37	-3	42.83	-0.577
17.09	-0.319	25.21	-1.001	32.43	-2.964	42.9	-0.577
17.15	-0.326	25.27	-1.012	32.5	-2.919	42.96	-0.576
17.21	-0.333	25.33	-1.023	32.58	-2.864	43.07	-0.576
17.26	-0.339	25.39	-1.034	32.65	-2.797	43.13	-0.576
17.32	-0.345	25.44	-1.046	32.73	-2.717	43.2	-0.575
17.38	-0.351	25.5	-1.057	32.86	-2.567	43.27	-0.575
17.43	-0.356	25.56	-1.069	32.95	-2.451	43.33	-0.574
17.49	-0.362	25.65	-1.088	33.05	-2.327	43.4	-0.573
17.55	-0.367	25.71	-1.099	33.15	-2.203	43.47	-0.573
17.61	-0.372	25.77	-1.111	33.25	-2.085	43.54	-0.573
17.7	-0.381	25.83	-1.124	33.36	-1.98	43.6	-0.572
17.76	-0.386	25.88	-1.137	33.47	-1.889	43.7	-0.572
17.82	-0.391	25.94	-1.15	33.58	-1.811	43.77	-0.572
17.87	-0.395	26	-1.163	33.69	-1.745	43.84	-0.571
17.94	-0.4	26.06	-1.176	33.85	-1.661	43.9	-0.571
17.99	-0.404	26.12	-1.189	33.96	-1.613	43.97	-0.571
18.05	-0.409	26.18	-1.203	34.07	-1.569	44.04	-0.571
18.11	-0.413	26.26	-1.224	34.18	-1.528	44.11	-0.571
18.18	-0.417	26.32	-1.238	34.28	-1.49	44.17	-0.571
18.27	-0.424	26.38	-1.252	34.39	-1.454	44.24	-0.57
18.33	-0.428	26.43	-1.266	34.49	-1.42	44.31	-0.57

18.39	-0.432	26.49	-1.28	34.59	-1.389	44.41	-0.569
18.45	-0.436	26.55	-1.295	34.69	-1.359	44.48	-0.569
18.51	-0.44	26.61	-1.31	34.84	-1.316	44.54	-0.569
18.57	-0.443	26.66	-1.325	34.94	-1.289	44.61	-0.569
18.63	-0.447	26.72	-1.34	35.04	-1.263	44.68	-0.569
18.69	-0.451	26.8	-1.364	35.14	-1.239	44.74	-0.569
18.76	-0.455	26.86	-1.38	35.23	-1.215	44.81	-0.569
18.82	-0.459	26.92	-1.396	35.32	-1.193	44.88	-0.569
18.91	-0.464	26.97	-1.412	35.42	-1.171	44.94	-0.569
18.97	-0.467	27.03	-1.429	35.51	-1.149	45.04	-0.568
19.03	-0.471	27.08	-1.445	35.6	-1.129	45.11	-0.568
19.1	-0.474	27.14	-1.462	35.69	-1.11	45.18	-0.568
19.16	-0.477	27.2	-1.479	35.83	-1.082	45.24	-0.568
19.22	-0.481	27.25	-1.496	35.92	-1.063	45.31	-0.568
19.28	-0.484	27.33	-1.522	36.01	-1.046	45.38	-0.568
19.35	-0.487	27.39	-1.54	36.09	-1.029	45.45	-0.568
19.41	-0.49	27.45	-1.557	36.18	-1.013	45.51	-0.568
19.5	-0.495	27.5	-1.575	36.27	-0.998	45.58	-0.568
19.57	-0.497	27.55	-1.593	36.35	-0.983	45.65	-0.568
19.63	-0.5	27.61	-1.611	36.44	-0.968	45.75	-0.568
19.69	-0.503	27.67	-1.629	36.52	-0.954	45.81	-0.568
19.75	-0.506	27.72	-1.648	36.65	-0.934	45.88	-0.568
19.82	-0.508	27.77	-1.667	36.73	-0.921	45.95	-0.568
19.88	-0.511	27.83	-1.686	36.81	-0.909	46.01	-0.568
19.94	-0.514	27.91	-1.715	36.89	-0.897	46.08	-0.568
20.01	-0.516	27.96	-1.733	36.98	-0.886	46.15	-0.568
20.1	-0.52	28.02	-1.752	37.06	-0.875	46.21	-0.568
20.17	-0.523	28.07	-1.771	37.14	-0.864	46.28	-0.568
20.23	-0.525	28.12	-1.79	37.22	-0.854	46.38	-0.568
20.29	-0.527	28.18	-1.809	37.3	-0.844	46.45	-0.567
20.36	-0.529	28.23	-1.83	37.37	-0.834	46.51	-0.567
20.42	-0.532	28.28	-1.849	37.49	-0.82	46.58	-0.567
20.48	-0.534	28.34	-1.869	37.57	-0.811	46.65	-0.567
20.55	-0.536	28.42	-1.9	37.65	-0.803	46.71	-0.567
20.61	-0.538	28.47	-1.92	37.72	-0.794	46.78	-0.567
20.68	-0.54	28.52	-1.94	37.8	-0.786	46.85	-0.567
20.77	-0.544	28.58	-1.96	37.88	-0.778	46.91	-0.567
20.84	-0.546	28.63	-1.98	37.95	-0.771	46.98	-0.567

Tabla A11. Datos originales para calcular los parámetros reológicos de Ch-CNO a temperado bajo y 1% de CB/CNO

Prueba:	TM-COCO 1% R1				
Resultado:	INT_50				
Interval and data points:	1	1			
Interval data:	Point No.	Shear Rate [1/s]	Shear Stress [Pa]	Viscosity [mPa·s]	Torque [µN·m]	Status
	1	50	122.32	2446.4	6496.8	
Resultado:	Pre-Shear 1				
Interval and data points:	1	0			
Interval data:	Point No.	Shear Rate	Shear Stress	Viscosity	Torque	Status
		[1/s]	[Pa]	[mPa·s]	[µN·m]	
Resultado:	Flow curve 1				
Interval and data points:	1	18			
Interval data:	Point No.	Shear Rate [1/s]	Shear Stress [Pa]	Viscosity [mPa·s]	Torque [µN·m]	Status
	1	2	30.48	15240	1618.9	Dy_auto
	2	4.82	38.704	8024.1	2055.7	Dy_auto
	3	7.65	45.567	5958.8	2420.2	Dy_auto
	4	10.5	51.847	4951.7	2753.7	Dy_auto
	5	13.3	57.796	4347.5	3069.7	Dy_auto
	6	16.1	63.473	3938.1	3371.2	Dy_auto
	7	18.9	68.975	3641.5	3663.4	Dy_auto
	8	21.8	74.311	3414.3	3946.8	Dy_auto
	9	24.6	79.53	3234.5	4224.1	Dy_auto
	10	27.4	84.646	3087.9	4495.7	Dy_auto
	11	30.2	89.648	2965	4761.4	Dy_auto
	12	33.1	94.543	2859.9	5021.4	Dy_auto
	13	35.9	99.325	2768.1	5275.4	Dy_auto
	14	38.7	104.05	2688.2	5526.2	Dy_auto
	15	41.5	108.72	2618	5774.6	Dy_auto
	16	44.4	113.39	2556.6	6022.6	Dy_auto
	17	47.2	118.03	2501.8	6268.7	Dy_auto
	18	50	122.63	2452.6	6513.1	Dy_auto
Interval and data points:	2	6			
Interval data:	Point No.	Shear Rate [1/s]	Shear Stress [Pa]	Viscosity [mPa·s]	Torque [µN·m]	Status
	1	50	122.65	2453.1	6514.4	Dy_auto
	2	50	122.64	2452.8	6513.6	Dy_auto
	3	50	122.6	2452	6511.5	Dy_auto
	4	50	122.53	2450.5	6507.7	Dy_auto
	5	50	122.46	2449.2	6504.2	Dy_auto

		6	50	122.39	2447.8	6500.5	Dy_auto

Interval and data points:		3	18				

Interval data:	Point No.	Shear Rate [1/s]	Shear Stress [Pa]	Viscosity [mPa·s]	Torque [µN·m]	Status
	1	50	122.32	2446.4	6496.8	Dy_auto
	2	47.2	117.71	2495.2	6252.1	Dy_auto
	3	44.4	113.02	2548.1	6002.7	Dy_auto
	4	41.5	108.28	2607.4	5751.2	Dy_auto
	5	38.7	103.49	2673.8	5496.8	Dy_auto
	6	35.9	98.66	2749.5	5240.1	Dy_auto
	7	33.1	93.776	2836.6	4980.7	Dy_auto
	8	30.2	88.837	2938.2	4718.4	Dy_auto
	9	27.4	83.841	3058.6	4453	Dy_auto
	10	24.6	78.785	3204.2	4184.5	Dy_auto
	11	21.8	73.638	3383.4	3911.1	Dy_auto
	12	18.9	68.398	3611.1	3632.8	Dy_auto
	13	16.1	63.018	3909.8	3347	Dy_auto
	14	13.3	57.466	4322.6	3052.2	Dy_auto
	15	10.5	51.69	4936.7	2745.4	Dy_auto
	16	7.65	45.541	5955.2	2418.8	Dy_auto
	17	4.82	38.803	8044.4	2060.9	Dy_auto
	18	2	30.637	15318	1627.2	Dy_auto

Resultado:	INT_2					

Interval and data points:		1	1			

Interval data:	Point No.	Shear Rate [1/s]	Shear Stress [Pa]	Viscosity [mPa·s]	Torque [µN·m]	Status
	1	2	30.637	15318	1627.2	

Resultado:	INT_5					

Interval and data points:		1	1			

Interval data:	Point No.	Shear Rate [1/s]	Shear Stress [Pa]	Viscosity [mPa·s]	Torque [µN·m]	Status
	1	5	39.29	7858.1	2086.8	

Resultado:	INT_10					

Interval and data points:		1	1			

Interval data:	Point No.	Shear Rate [1/s]	Shear Stress [Pa]	Viscosity [mPa·s]	Torque [µN·m]	Status
	1	10	50.741	5074.1	2695	

Resultado:	INT_20					

Interval and data points:		1	1			

Interval data:	Point No.	Shear Rate [1/s]	Shear Stress [Pa]	Viscosity [mPa·s]	Torque [µN·m]	Status
	1	20	70.404	3520.2	3739.3	

Resultado:	Regression Casson					

195

Interval and data points:		1	18			
Interval data:	Point No.	Shear Rate [1/s]	Shear Stress [Pa]	Viscosity [mPa·s]	Torque [µN·m]	Status
	1	50	122.19	2443.7		
	2	47.2	117.56	2492		
	3	44.4	112.9	2545.6		
	4	41.5	108.21	2605.5		
	5	38.7	103.47	2673.1		
	6	35.9	98.677	2750		
	7	33.1	93.834	2838.4		
	8	30.2	88.93	2941.3		
	9	27.4	83.956	3062.8		
	10	24.6	78.9	3208.8		
	11	21.8	73.748	3388.4		
	12	18.9	68.48	3615.4		
	13	16.1	63.069	3913		
	14	13.3	57.475	4323.3		
	15	10.5	51.636	4931.5		
	16	7.65	45.445	5942.7		
	17	4.82	38.681	8019.1		
	18	2	30.709	15355		
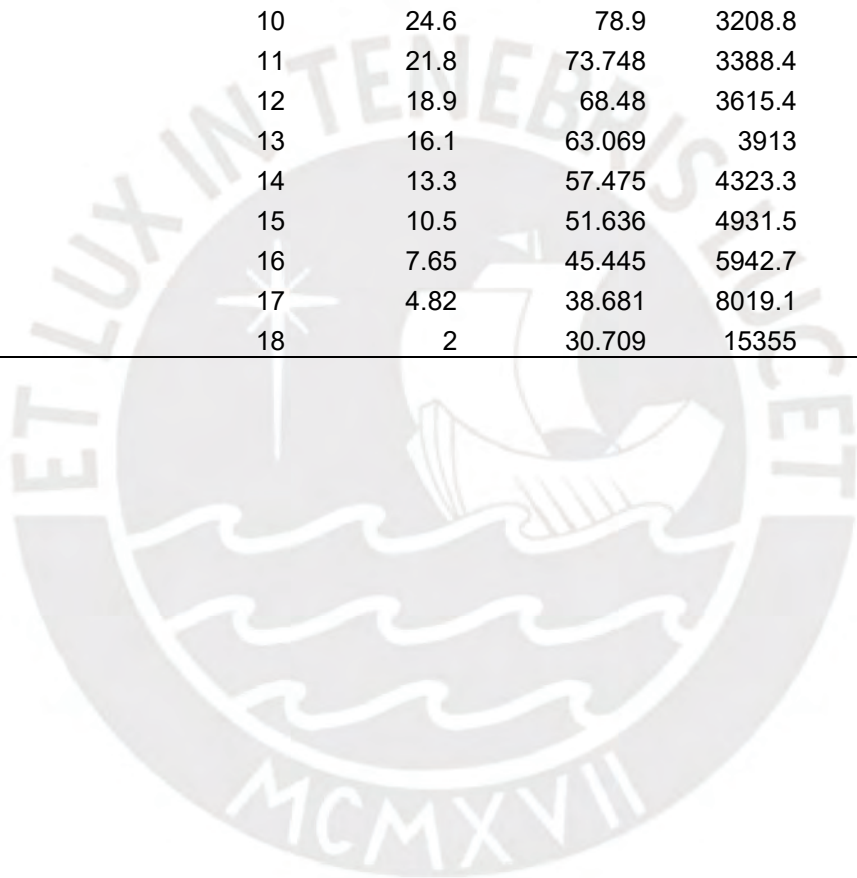
Tabla A12. Datos originales para calcular los parámetros reológicos de Ch-SIO a temperado alto y 5% de CB/SIO.

Project:	Choco, IOCCC2000	DESKTOP-1PDKJKN, 9/04/2022	2				
Prueba:	TA-SIO 1% R2					
Resultado:	Pre-Shear 1					
Interval and data points:	1	0				
Interval data:	Point No.	Shear Rate [1/s]	Shear Stress [Pa]	Viscosity [mPa·s]	Torque [µN·m]	Status
Resultado:	Flow curve 1					
Interval and data points:	1	18				
Interval data:	Point No.	Shear Rate [1/s]	Shear Stress [Pa]	Viscosity [mPa·s]	Torque [µN·m]	Status
	1	2	29.944	14972	1590.4	Dy_auto
	2	4.82	38.172	7913.6	2027.4	Dy_auto
	3	7.65	45.079	5895	2394.3	Dy_auto
	4	10.5	51.409	4909.9	2730.5	Dy_auto
	5	13.3	57.403	4317.9	3048.8	Dy_auto
	6	16.1	63.142	3917.6	3353.6	Dy_auto
	7	18.9	68.683	3626.1	3647.9	Dy_auto
	8	21.8	74.067	3403.1	3933.9	Dy_auto
	9	24.6	79.345	3227	4214.2	Dy_auto
	10	27.4	84.519	3083.3	4489	Dy_auto
	11	30.2	89.582	2962.8	4757.9	Dy_auto
	12	33.1	94.537	2859.7	5021.1	Dy_auto
	13	35.9	99.388	2769.8	5278.7	Dy_auto
	14	38.7	104.2	2692	5534.1	Dy_auto
	15	41.5	108.95	2623.5	5786.7	Dy_auto
	16	44.4	113.66	2562.5	6036.5	Dy_auto
	17	47.2	118.32	2508.1	6284.5	Dy_auto
	18	50	122.96	2459.2	6530.7	Dy_auto
Interval and data points:	2	6				
Interval data:	Point No.	Shear Rate [1/s]	Shear Stress [Pa]	Viscosity [mPa·s]	Torque [µN·m]	Status
	1	50	123	2459.9	6532.6	Dy_auto
	2	50	122.97	2459.5	6531.4	Dy_auto
	3	50	122.91	2458.3	6528.2	Dy_auto
	4	50	122.85	2456.9	6524.6	Dy_auto
	5	50	122.77	2455.3	6520.4	Dy_auto
	6	50	122.67	2453.4	6515.4	Dy_auto
Interval and data points:	3	18				
Interval data:	Point No.	Shear Rate [1/s]	Shear Stress [Pa]	Viscosity [mPa·s]	Torque [µN·m]	Status
	1	50	122.6	2451.9	6511.4	Dy_auto

	2	47.2	117.94	2500	6264.1	Dy_auto
	3	44.4	113.22	2552.6	6013.3	Dy_auto
	4	41.5	108.44	2611.2	5759.5	Dy_auto
	5	38.7	103.61	2676.9	5503.1	Dy_auto
	6	35.9	98.74	2751.8	5244.3	Dy_auto
	7	33.1	93.813	2837.8	4982.7	Dy_auto
	8	30.2	88.839	2938.2	4718.4	Dy_auto
	9	27.4	83.79	3056.7	4450.3	Dy_auto
	10	24.6	78.688	3200.2	4179.3	Dy_auto
	11	21.8	73.496	3376.8	3903.5	Dy_auto
	12	18.9	68.198	3600.5	3622.2	Dy_auto
	13	16.1	62.781	3895.2	3334.5	Dy_auto
	14	13.3	57.181	4301.2	3037	Dy_auto
	15	10.5	51.344	4903.6	2727	Dy_auto
	16	7.65	45.143	5903.2	2397.6	Dy_auto
	17	4.82	38.355	7951.5	2037.1	Dy_auto
	18	2	30.13	15065	1600.3	Dy_auto

Resultado:	INT_2					
Interval and data points:		1	1			
Interval data:	Point No.	Shear Rate [1/s]	Shear Stress [Pa]	Viscosity [mPa·s]	Torque [μN·m]	Status
	1	2	30.13	15065	1600.3	

Resultado:	INT_5					
Interval and data points:		1	1			
Interval data:	Point No.	Shear Rate [1/s]	Shear Stress [Pa]	Viscosity [mPa·s]	Torque [μN·m]	Status
	1	5	38.845	7769.1	2063.2	

Resultado:	INT_10					
Interval and data points:		1	1			
Interval data:	Point No.	Shear Rate [1/s]	Shear Stress [Pa]	Viscosity [mPa·s]	Torque [μN·m]	Status
	1	10	50.385	5038.5	2676.1	

Resultado:	INT_20					
Interval and data points:		1	1			
Interval data:	Point No.	Shear Rate [1/s]	Shear Stress [Pa]	Viscosity [mPa·s]	Torque [μN·m]	Status
	1	20	70.225	3511.2	3729.8	

Resultado:	Regression Casson					
Interval and data points:		1	18			
Interval data:	Point No.	Shear Rate [1/s]	Shear Stress [Pa]	Viscosity [mPa·s]	Torque [μN·m]	Status
	1	50	122.47	2449.5		
	2	47.2	117.81	2497.2		
	3	44.4	113.11	2550.1		

|			
4	41.5	108.37	2609.4
5	38.7	103.58	2676.1
6	35.9	98.75	2752
7	33.1	93.864	2839.3
8	30.2	88.916	2940.8
9	27.4	83.898	3060.6
10	24.6	78.797	3204.6
11	21.8	73.6	3381.6
12	18.9	68.286	3605.1
13	16.1	62.828	3898.1
14	13.3	57.187	4301.6
15	10.5	51.299	4899.3
16	7.65	45.056	5891.8
17	4.82	38.236	7926.8
18	2	30.198	15099

Tabla A13. Parámetros de textura de Ch-CON a temperado bajo y 1% de CB/CNO

TexturePro CT V1.8 Build 31   **Brookfield Engineering Labs. Inc.**

INFORME DATOS

Descripci·n Muestra

Nombre	COCO1%-TM-R1	Note:
Nombre de lote:	Chocolate CBE	
Ejemplo:	1	
Dimensiones:		
Forma:	Bloque	
Longitud:	115.00 mm	
Anchura:	50.00 mm	
Altura:	7.00 mm	

M®todo Test

Fecha:	20/05/2022		Hora:	10:24:12
Tipo de Test:	Compresi·n		Tpo.	0 s
Objetivo:	6.0 mm		Mismo	Exacto
Esperar t.:	3 s		Velocidad	1.00 mm/s
arga Activaci·n:	0.09 N		Fr. Muestreo:	20.00 points/sec
Vel. Test:	0.50 mm/s		Sonda:	TA9
elocidad Vuelta:	0.5 mm/s		Elemento:	TA-RT-KIT
Contador ciclos:	2.0		Celda Carga:	25000g
Target Type:	Distancia			

Resultados

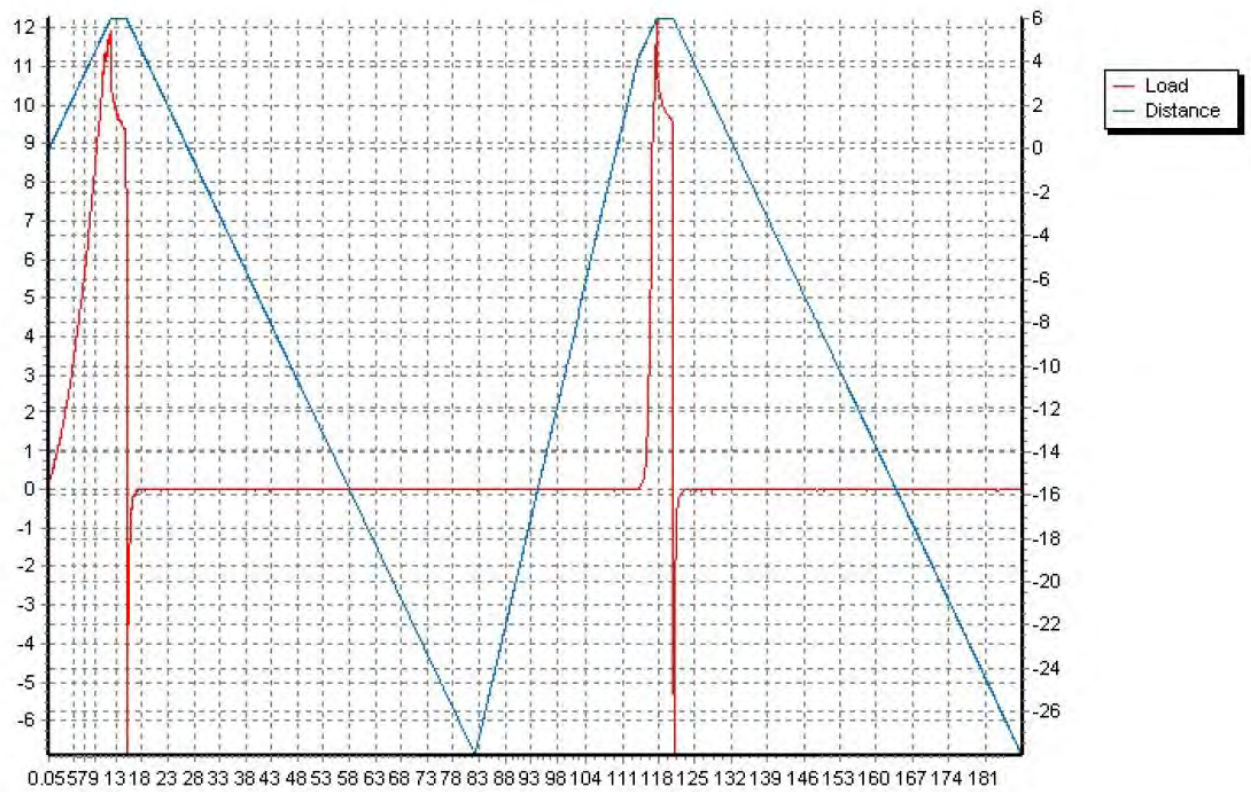|		
Ciclo 1 Dureza:	13.42	N
Deformaci·n seg¼n Dureza:	5.98	mm
%Deformaci·n seg¼n dureza:	5.20	%
Fuerza adhesividad:	5.90	N
Adhesividad:	0.00	J
Cantidad de Fracturas:	0.00	
	con 1% de sensibilidad de carga	
Fracturabilidad:	13.42	N
	con 1% de sensibilidad de carga	
Ciclo 2 Dureza:	14.24	N
Ciclo 1 Trabajo Dureza terminado:	0.01	J
Gomosidad:	2.54	N
Masticabilidad:	0.00	J
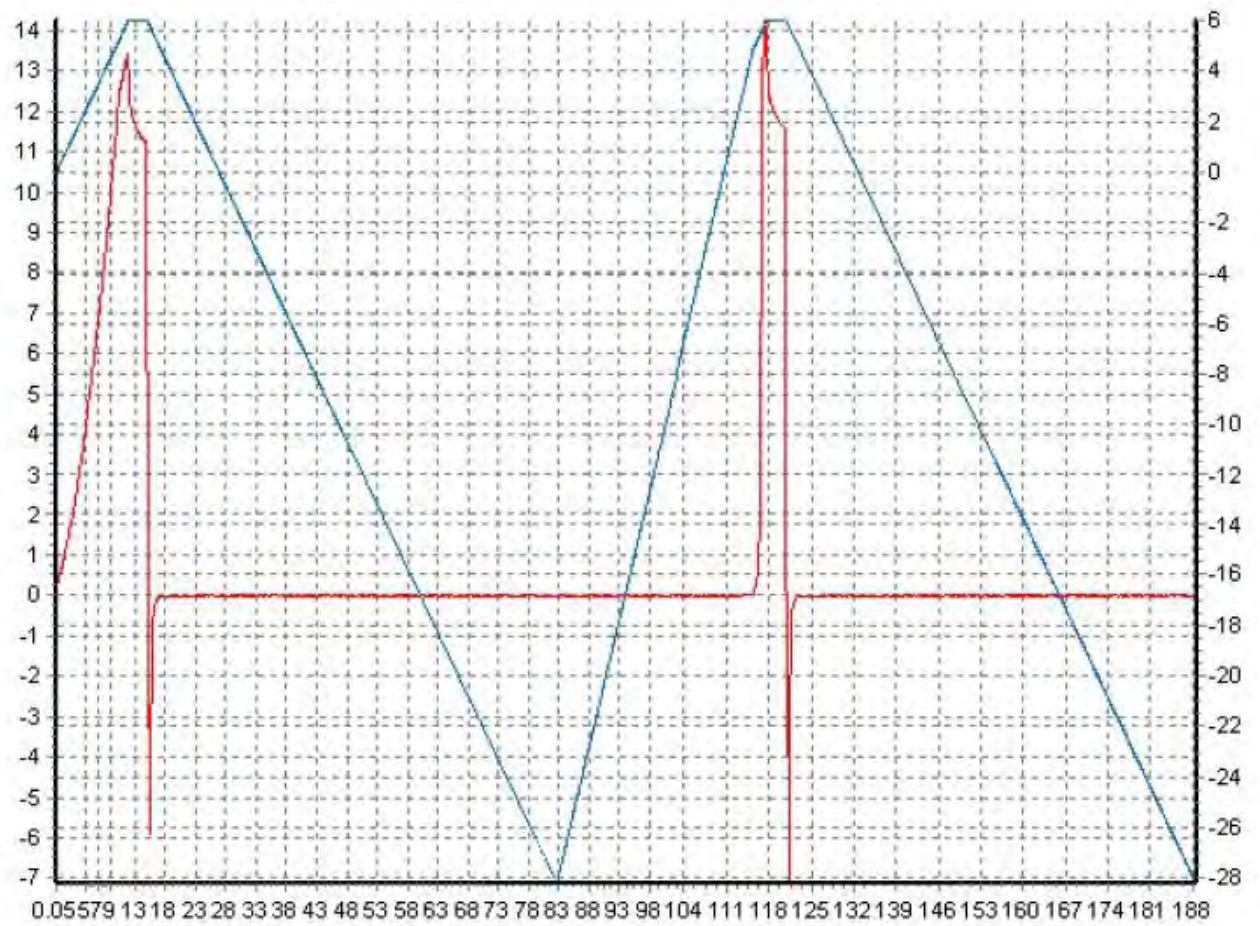
Figura A3. Textura de Ch-CON a temperado bajo y 1% de CB/CNO
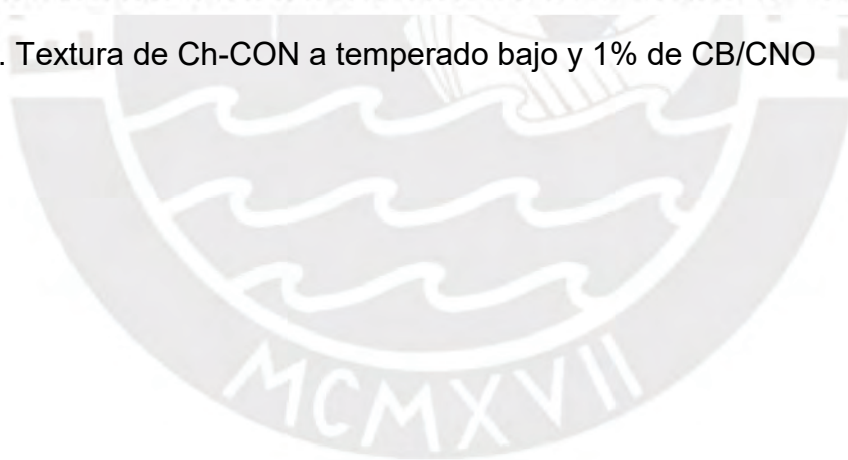
Tabla A14. Parámetros de textura de Ch-SIO a temperado alto y 5% de CB/SIO.

TexturePro CT V1.8 Build 31   **Brookfield Engineering Labs. Inc.**

<div align="center">INFORME DATOS</div>

<u>Descripci·n Muestra</u>

Nombre	SIO5%-TA-R1	Note:	
Nombre de lote:	Chocolate CBE		
Ejemplo:	1		
Dimensiones:			
Forma:	Bloque		
Longitud:	115.00	mm	
Anchura:	50.00	mm	
Altura:	7.00	mm	

<u>M®todo Test</u>

Fecha:	20/05/2022		Hora:	17:54:45	
Tipo de Test:	Compresi·n		Tpo.	0	s
Objetivo:	6.0	mm	Mismo	Exacto	
Esperar t.:	3	s	Velocidad	1.00	mm/s
arga Activaci·n:	0.09	N	Fr. Muestreo:	20.00	points/sec
Vel. Test:	0.50	mm/s	Sonda:	TA9	
elocidad Vuelta:	0.5	mm/s	Elemento:	TA-RT-KIT	
Contador ciclos:	2.0		Celda Carga:	25000g	
Target Type:	Distancia				

<u>Resultados</u>

Ciclo 1 Dureza:	11.92	N
Deformaci·n seg½n Dureza:	5.97	mm
%Deformaci·n seg½n dureza:	5.20	%
Fuerza adhesividad:	6.86	N
Adhesividad:	0.00	J
Cantidad de Fracturas:	4.00	
	con 1% de sensibilidad de carga	
Fracturabilidad:	10.98	N
	con 1% de sensibilidad de carga	
Ciclo 2 Dureza:	12.24	N
Ciclo 1 Trabajo Dureza terminado:	0.01	J
Gomosidad:	2.71	N
Masticabilidad:	0.00	J

Figura A4. Textura de Ch-SIO a temperado alto y 5% de CB/SIO.

Figura A5. Invitación como ponente internacional.